Report no.
UC SESM 75 - 6

STRUCTURES AND MATERIALS RESEARCH
Department of Civil Engineering

A NETWORK-TOPOLOGICAL APPROACH TO THE FINITE ELEMENT ANALYSIS OF PROGRESSIVE CRACK GROWTH IN CONCRETE MEMBERS

by

De Ngo

JUNE 1975

STRUCTURAL ENGINEERING LABORATORY
UNIVERSITY OF CALIFORNIA
BERKELEY, CALIFORNIA

Department of Civil Engineering
Division of Structural Engineering
and Structural Mechanics

A NETWORK-TOPOLOGICAL APPROACH TO THE FINITE ELEMENT ANALYSIS OF PROGRESSIVE CRACK GROWTH IN CONCRETE MEMBERS

by

De Ngo

Dissertation Committee

A. C. Scordelis

E. L. Wilson

Professors of Civil Engineering

L. O. Chua

Professor of Electrical Engineering

and Computer Sciences

University of California
Berkeley, California

June 1975

ABSTRACT

One of the major complexities in investigating the behavior of reinforced or prestressed concrete members is the problem of cracking in concrete. Analytical study of crack growth in concrete members becomes possible only with the advent of large capacity high speed digital computers and the finite element method of stress analysis. However, the disruption of continuity due to cracking presents a number of analytical difficulties. In order to simulate the cracking condition in a finite element model, either a crack has to be manually formed, or the property of a finite element has to be modified.

The objective of this thesis is to develop a computer technique which is capable of simulating crack growth by automatically generating crack-lines in the finite element model. A network-topological approach is proposed herein to facilitate such an analysis. A system concept is adopted in which the entire structure is treated as a structural network and the various structural elements are treated as the network components. Cracking in the concrete members is then viewed as merely a change in the structural network topology. Graph theoretic matrices are used in describing and recording the topology of the structural network as cracking progresses.

Through the graph representation of the Gaussian elimination method, the frontal technique is interpreted as a means of achieving near optimal ordering. With the aid of incidence matrices, the "Frontal Solution Method" developed by Irons is modified and implemented, thus alleviating the constraint in the node numbering normally required in most banded type of solution schemes.

By extending the "Link-At-A-Time" algorithm in network theory, a reanalysis procedure is developed within the framework of the frontal solution technique. Modifications of member properties as well as structural topology are possible. A proof of nonsingularity and positive-definiteness of the solution matrix is also presented.

A computer program is developed to carry out the frontal solution procedure, the crack growth procedure, and the modification procedure. The types of elements used in the program include a two-dimensional isoparametric element for plane stress, plane strain or axisymmetric analysis, a bar element, a bond element, and a link element. Therefore, any two-dimensional reinforced or prestressed concrete structure can be modeled and analyzed by the program. With the crack growth procedure, a predominant crack pattern can be obtained for a given loading condition.

Finally, a crack propagation hypothesis is proposed, which is based on the Griffith's theory and a network sensitivity function. However, no attempt is made to link the modification procedure and the crack propagation hypothesis directly to the crack growth procedure in the present work.

It is believed that the present research represents a new direction in the analytical investigation of complex composite structures where the effect due to crack interference must be duly considered. While many simplifications have been made either for the sake of convenience or for clarity in the development of such a research tool, they should not prevent any further refinement which is of practical importance.

TABLE OF CONTENTS

ABSTRACT		i
TABLE OF CONTENTS		iv
LIST OF FIGURES		viii
CHAPTER 1:	INTRODUCTION	1
1.1	Nature of the Problem	1
1.2	Some Previous Related Studies	5
1.3	Crack-Line vs. Crack-Zone Representation	12
1.4	A Conceptual Model	14
1.5	Need for a New Approach	18
1.5.1	Node Numbering	20
1.5.2	Structural Topology	22
1.5.3	Structural Modification and Reanalysis	22
1.5.4	Crack Propagation	22
1.5.5	A Proposed Approach	23
1.6	Objective and Scope	24
1.7	Notations	25
CHAPTER 2:	TOPOLOGY, GRAPH, NETWORK AND STRUCTURAL SYSTEM ANALYSIS	26
2.1	Structure Network and Topology	26
2.2	Some Graph Theoretic Matrices	28
2.2.1	Branch-Node Coincidence and Boolean Connectivity Matrices	28
2.2.2	Branch-Node and Branch-Mesh Indicence Matrices	35
2.2.3	Dual Graph and Adjacency Matrix	38

2.2.4	Node-Mesh Incidence Matrix	43
2.3	Structural Network with Changing Topology	43
CHAPTER 3:	FRONTAL SOLUTION TECHNIQUE	48
3.1	Gaussian Elimination and Its Peculiarity	48
3.1.1	Sparsity and Bandedness	50
3.1.2	Optimal Node Ordering	53
3.2	Graph Theoretic Approach	54
3.3	Frontal Solution Technique	67
3.4	Treatment of Displacement Boundary Conditions and Recovery of Reactions	73
CHAPTER 4:	ANALYSIS OF PROGRESSIVE CRACK GROWTH	85
4.1	Finite Element Model	85
4.1.1	Two-Dimensional Isoparametric Element	86
4.1.2	Triangular Element by Degeneration	87
4.1.3	Bar Element	87
4.1.4	Link Element	88
4.1.5	Bond Element	88
4.2	Simulation of Crack Growth	91
4.2.1	Crack Initiation	91
4.2.2	Crack Propagation	93
4.2.3	Crack Stabilization	94
4.3	General Crack Growth Procedure	94
4.4	Test of Crack Growth Capability	104
4.5	Treatment of Matrix Singularity due to Crack Growth	115

4.6	Interruption and Resumption of Solution Procedure	116
4.7	Example Problems	117
CHAPTER 5:	STRUCTURAL MODIFICATION AND REANALYSIS OF SOLUTION PROCEDURE	130
5.1	Cracking and Structural Modification	130
5.2	Modification of Structural Network	132
5.2.1	Fixed Topology	132
5.2.2	Changing Topology	133
5.3	Link-At-A-Time Algorithm and Its Dual	136
5.4	Modification Methods of Argyris and Roy	143
5.5	Extension of Link-At-A-Time Algorithm	155
5.6	A Proof of Nonsingularity and Positive-Definiteness	159
5.7	Construction of Choleski Decomposition from Frontal Solution	162
5.8	Program Input Requirements	164
5.9	Example Problems	166
5.10	Remarks on Efficiency	168
CHAPTER 6:	A CRACK PROPAGATION HYPOTHESIS	174
6.1	Fracture Mechanics and Concrete Research	174
6.2	Fracture Mechanics and Finite Element Analysis	178
6.2.1	Griffith, Irwin and Orowan	178
6.2.2	Dugdale, Barenblatt and Dvorak	184
6.2.3	Bueckner, Hayes and Williams	190
6.2.4	Finite Element Method in Fracture Mechanics	195

6.3	A Crack Propagation Hypothesis	207
6.4	A Network-Topological Consideration	209
6.4.1	Tellegen Theorem	209
6.4.2	A Network Sensitivity Function	212
6.5	A Model of Crack Tip Zone	217
6.6	A Parameter Study	219
CHAPTER 7:	SUMMARY AND CONCLUSION	222
7.1	Summary of the Present Work	222
7.2	Remark on the Network-Topological Approach	225
7.3	Conclusion	226
ACKNOWLEDGEMENTS		228
REFERENCES		230
APPENDICES		247
I.	Element Stiffness Matrices	247
II.	General Structure of the Computer Program NTAFEA	272
III.	Computer Program Input Description	275

LIST OF FIGURES

FIG. 1.1	A SIMPLE REINFORCED CONCRETE BEAM	2
FIG. 1.2	ILLUSTRATION OF CRACKING	2
FIG. 1.3	SECTION IN PURE BENDING	4
FIG. 1.4	SECTION IN COMBINED BENDING AND SHEAR	4
FIG. 1.5	FINITE ELEMENT CRACK REPRESENTATIONS	9
FIG. 1.6	A CONCEPTUAL MODEL	16
FIG. 1.7	A POSSIBLE CRACK PATTERN WITH RECTANGULAR ELEMENTS	17
FIG. 1.8	A POSSIBLE CRACK PATTERN WITH TRIANGULAR ELEMENTS	19
FIG. 1.9	NODE NUMBERING IN CRACKED AND UNCRACKED STRUCTURES	21
FIG. 2.1	SIMPLICAL COMPLEX AND COINCIDENCE MATRICES	29
FIG. 2.2	NODE CONNECTIVITY MATRICES	31
FIG. 2.3	A LINEAR GRAPH	37
FIG. 2.4	TRANSFORMATION DIAGRAM	39
FIG. 2.5	GRAPH AND DUAL GRAPH	41
FIG. 2.6	FINITE ELEMENT MESH AS A PLANAR GRAPH	42
FIG. 2.7	GRAPH REPRESENTATION OF AN UNCRACKED STRUCTURE	45
FIG. 2.8	GRAPH REPRESENTATION OF A CRACKED STRUCTURE	46
FIG. 2.9	GRAPH REPRESENTATION OF A CRACKED STRUCTURE WITH JOINT ELEMENT	47
FIG. 3.1	EFFECTS OF NODE ORDERING	52
FIG. 3.2	GRAPH REPRESENTATION OF MATRIX	55

FIG. 3.3	GRAPH REPRESENTATION OF SYMMETRIC MATRIX	58
FIG. 3.4	GRAPH REPRESENTATION OF ELIMINATION PROCESS	59
FIG. 3.5	BANDED ORDERED NETWORK	60
FIG. 3.6	DECOMPOSITION OF NETWORK	62
FIG. 3.7	NEAR-OPTIMAL ORDERED NETWORK	63
FIG. 3.8	NODE ORDERING FOR CRACKED STRUCTURE	64
FIG. 3.9	BRANCHED AND CRACKED STRUCTURES	66
FIG. 3.10	COEFFICIENTS INVOLVED IN THE ELIMINATION PROCESS	71
FIG. 3.11	ONE-DIMENSIONAL STORAGE SCHEME FOR UPPER TRIANGULAR MATRIX	71
FIG. 4.1	ISOPARAMETRIC QUADRILATERAL ELEMENT	89
FIG. 4.2	BAR ELEMENT	90
FIG. 4.3	LINK ELEMENT	90
FIG. 4.4	BOND ELEMENT	90
FIG. 4.5	A SIMPLIFIED FAILURE CRITERION	92
FIG. 4.6	CRACK GROWTH MODEL	95
FIG. 4.7	GENERAL TWO-DIMENSIONAL STRUCTURE	105
FIG. 4.8	NODES AND ELEMENTS INVOLVED WITH THE CRACKED NODE	105
FIG. 4.9	LOCAL NODE-MESH INCIDENCE ARRAY	106
FIG. 4.10	ILLUSTRATION OF CRACK-LINE GENERATION	106
FIG. 4.11	LOCAL ADJACENCY ARRAY	107
FIG. 4.12	DUAL GRAPH AND ITS POINTER ARRAY	107
FIG. 4.13	MODIFIED ADJACENCY RELATIONSHIP	108
FIG. 4.14	CONSTRUCTION OF SEPARATE CHAINS	108
FIG. 4.15	DEFINITION OF ISPLIT AND ANMAX	113

FIG. 4.16	CRACK GROWTH CAPABILITIES	114
FIG. 4.17	EXAMPLE A -- A SIMPLE RUPTURE TEST	119
FIG. 4.18	CRACK GROWTH OF EXAMPLE A	119
FIG. 4.19	CRITICAL LOAD LEVEL AT EACH CRACKING STAGE OF EXAMPLE A	120
FIG. 4.20	EXAMPLE B -- A CONCRETE BRACKET	122
FIG. 4.21	CRACK GROWTH OF EXAMPLE B	123
FIG. 4.22	EXAMPLE C -- A DOUBLY REINFORCED CONCRETE BEAM	125
FIG. 4.23	CRACK GROWTH OF EXAMPLE C	126
FIG. 4.24	EXAMPLE D -- A PRESTRESSED CONCRETE END BLOCK	128
FIG. 4.25	CRACK GROWTH OF EXAMPLE D	129
FIG. 5.1	MODIFICATION WITH FIXED TOPOLOGY	134
FIG. 5.2	MODIFICATION WITH CHANGING TOPOLOGY	135
FIG. 5.3	PARALLEL AND EQUIVALENT BRANCHES	137
FIG. 5.4	NODE COALESCING AND DISCOALESCING	142
FIG. 5.5	DECOUPLING OF NODAL UNKNOWNS IN A CONTINUUM	150
FIG. 5.6	DECOUPLING PROCESS BY LAT ALGORITHM	158
FIG. 5.7	MODIFICATION EXAMPLES E, F AND G	169
FIG. 5.8	MODIFICATION EXAMPLE H	170
FIG. 5.9	MODIFICATION EXAMPLE I	171
FIG. 6.1	MODES AND GEOMETRY OF CRACKS	183
FIG. 6.2	ACTUAL AND EFFECTIVE CRACK LENGTHS	185
FIG. 6.3	THE DUGDALE MODEL	186
FIG. 6.4	THE BARENBLATT MODEL	188
FIG. 6.5	THE DVORAK MODEL	189

FIG. 6.6	THE BUECKNER MODEL	194
FIG. 6.7	CRACK TIP COORDINATES AND J-INTEGRAL CONTOUR	204
FIG. 6.8	BYSKOV'S CRACKED ELEMENT	204
FIG. 6.9	INNER MESH USED IN THE ANALYSIS FOR ZERO ANGLE CRACKED SPECIMEN BY WALSH	205
FIG. 6.10	TRACEY'S SINGULARITY ELEMENT	206
FIG. 6.11	NETWORK N AND ADJOINT NETWORK $\hat{N}$	213
FIG. 6.12	MODEL OF CRACK TIP ZONE	218
FIG. 6.13	A SINGLE EDGE CRACKED PLATE FOR PARAMETER STUDY	220

CHAPTER 1 INTRODUCTION

1.1 Nature of the Problem

Concrete structural members, either reinforced or prestressed, are among the oldest and the most commonly employed construction elements. Their popularity and importance in the field of structural engineering have promoted much research in the hope of gaining a fuller understanding of their behavior. Unfortunately, due to the complex nature of the problem, research activities until recently have been largely confined to experimental investigations. Analytical studies became practical only when the availability of large capacity high speed digital computers revolutionalized the possible analytical techniques. The finite element method, for example, has proven to be an extremely powerful and versatile tool in stress analysis, and it has provided a new basis for the analytical studies of the structural behavior of concrete members.

The complexity of the problems associated with the concrete structural members can best be illustrated by a simple reinforced concrete beam shown in Fig.1.1. As the load P increases, and because of the well known fact that concrete is weak in tension, the beam will experience cracking and become highly indeterminate as depicted in Fig. 1.2. Within zone A where the shear force is zero,

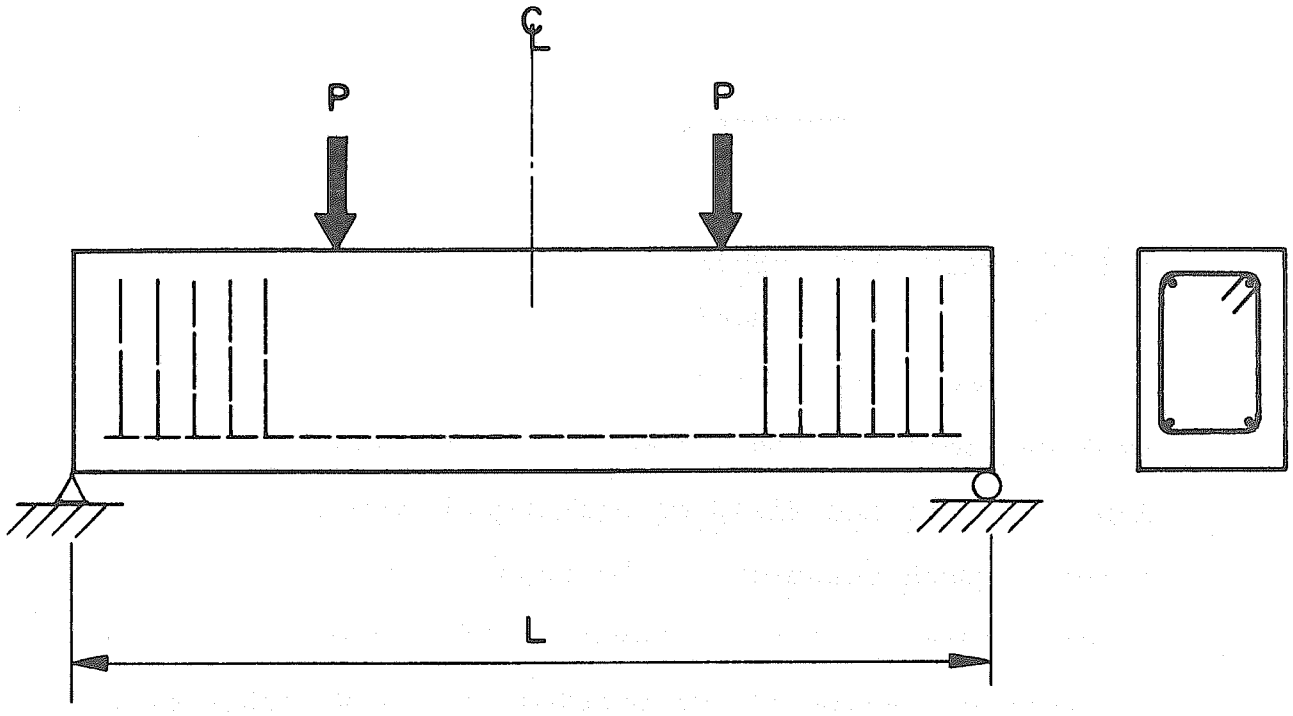

FIG. 1.1 A SIMPLE REINFORCED CONCRETE BEAM

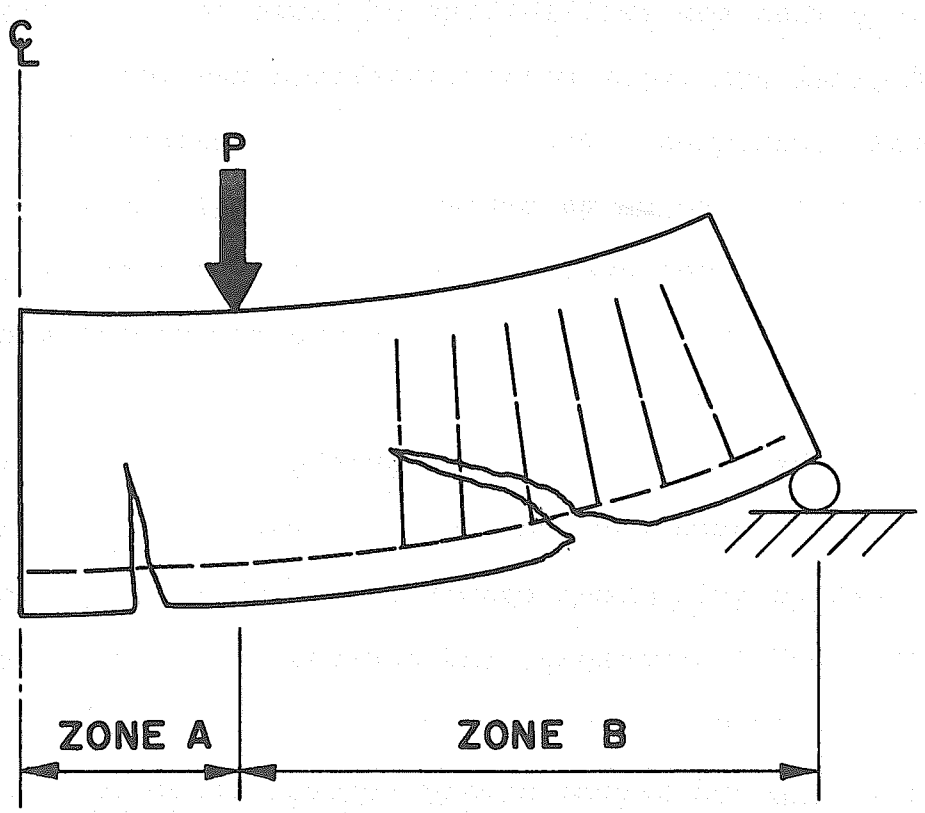

FIG. 1.2 ILLUSTRATION OF CRACKING

the reinforcement is subjected to a pull which produces a certain degree of bond slip, Fig. 1.3. Within zone B where there is a combination of shear and bending, the situation is no longer a simple one, Fig. 1.4. Besides the bond slip, dowel action comes into play. Stirrups will become more effective in carrying shear when the crack penetrates across them. The neutral axis of the beam is continuously shifting to adjust for the required T-C couple as progressive cracking develops. This makes the stresses in steel and concrete difficult to determine. Furthermore, forces due to aggregate interlock exist at the crack surfaces, even though this effect is usually neglected in most analyses because the magnitude and direction of these interlocking forces are not at all easy to assess.

The nonhomogeneous, nonlinear and time-dependent material properties of concrete multiply the analytical difficulties. The essentially biaxial state of stress in most of the concrete members requires new experimental evidence to support the selected constitutive relationship and failure criterion for concrete. All these factors, compounded and combined, would render the task of stress analysis by the conventional method of continuum mechanics virtually impossible.

Attention must also be given to the problem of stress concentration at the crack tips. Crack initia-

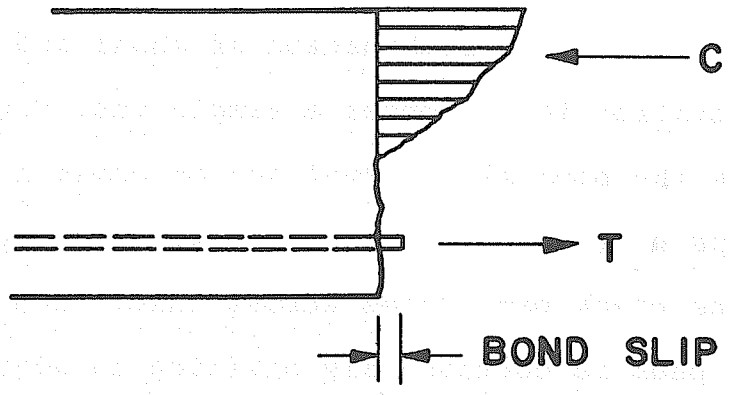

FIG. I.3 SECTION IN PURE BENDING

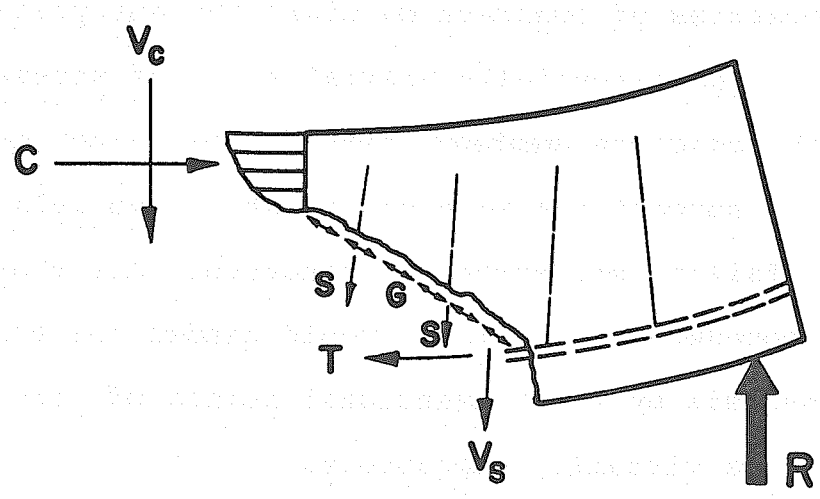

FIG. I.4 SECTION IN COMBINED BENDING AND SHEAR

tion, propagation and stabilization are three distinct processes and should be treated accordingly. However, the theory of fracture mechanics governing these three processes has only been recently extended to the study of concrete in a very limited manner.

When a prestressing force is introduced, either by pre-tensioning or post-tensioning, the basic nature of the problem still persists. Conceptually, prestressing can be conveniently thought of as a pattern of initial stresses having been superimposed on the ordinary reinforced concrete member. In this case, cracking is delayed until the initially compressed fiber reaches the critical tensile stress state, as the loading progresses.

It is beyond doubt that the nature of these problems is, indeed, a complex one. Nevertheless, a certain degree of success has been achieved in analyzing concrete structural members by means of finite element models. Some of these research investigations will be examined in the next section.

1.2 Some Previous Related Studies

Application of the finite element method to the analysis of concrete structures has been attempted ever since the method emerged. Wilson [1] in his thesis, which is one of the earliest treatises on finite element method, analyzed the effect of a vertical crack on the stresses and displacements in a gravity dam. The con-

cept of bi-modulus analysis was also introduced by Wilson in that thesis. Clough [2] conducted another series of extensive investigations on concrete dams with different loading and crack configurations. King [3] introduced material time-dependency into the finite element analysis. The time-dependency aspects of analysis were refined to include incremental construction, creep and temperature effects by Sandhu, Wilson and Raphael [4]. Problems such as the above related to plain concrete structures such as gravity dams can readily be treated by the finite element method of analysis. But when steel reinforcement is involved, and especially when progressive cracking is considered, other complications begin to appear.

Bresler and Bertero [5,6] employed axisymmetric finite elements to investigate stresses in a concentrically reinforced concrete cylinder, as a supplement to their experimental study. A similar method was used by Lutz, Gergely and Winter [7], where a special procedure was developed to account for bond slip. However, that procedure could only provide results for a known slip and presumed separation between concrete and steel.

Modelling of reinforced concrete beams to incorporate bond slip into the finite element analysis was first attempted by Ngo [8], where a physically dimensionless linkage element was developed to allow a certain degree

of relative movement between two adjacent nodes in two perpendicular directions. With this type of linkage element, together with some empirical stiffness values to simulate bonding between concrete and steel reinforcement, Ngo and Scordelis [9] carried out a series of linearly elastic analyses of simply supported reinforced concrete beams with predefined crack patterns. Ngo, Franklin and Scordelis [10] used the same approach to study the structural behavior of reinforced concrete beams with diagonal tension cracks. In that study, it was possible to examine the effects of stirrups, dowel actions, aggregate interlock and horizontal splitting along the reinforcement near support. Nilson [11, 12] extended the method to include non-linear material properties and a nonlinear bond-slip relationship for the analysis of concentrically as well as eccentrically loaded reinforced concrete members under incremental loads. The tracing of the crack propagation in Nilson's study was done by redefining the finite element mesh layout manually when the failure criterion was met at one or more points on the loaded member, and execution of the analysis was then re-started afresh from zero load and incrementally loaded up to next stage of failure. Houde, Youssef, Spokowski, Mufti and Mirza [13,14,15] have also employed a similar method to study cracking and bond failure. Murray [16] used a "rubber-like"

ring around the steel as a bond element in his analytical model to study crack formation. All these investigations, Ref. 8 to 16, regarded cracking as being represented by separating the nodal point where cracking was predicated to take place, hence producing a crack-line, Fig. 1.5a, in the finite element model. Loov [17] proposed a method of subdividing the finite element to adjust for inclined cracks, and introduced a crack of finite width with a "sensor element" at the crack tip to predict crack propagation, Fig. 1.5b.

In contrast to the crack-line approach, other investigators have employed a crack-zone type of representation, Fig. 1.5c, in which cracking is assumed to take place within a finite region of the structure. In terms of finite element analysis, this means that the element stiffness property is modified to reflect the failure of concrete strength in the direction perpendicular to a crack, whenever cracking has been predicted to occur in that element.

Isenberg and Adham [18] were the first ones to publish a mathematical model of stress-strain relations for a reinforced concrete element based on the properties of reinforcing steel, plain concrete, and slip in the bond between them. Nonlinearity due to material inelasticity and cracking was included in their finite element analysis. The idea of employing a finite element with composite concrete-steel material properties at

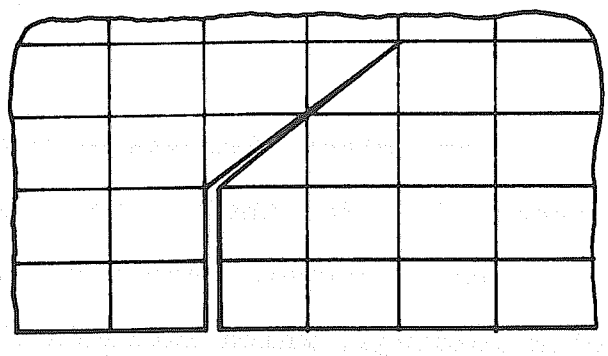

a) CRACK - LINE

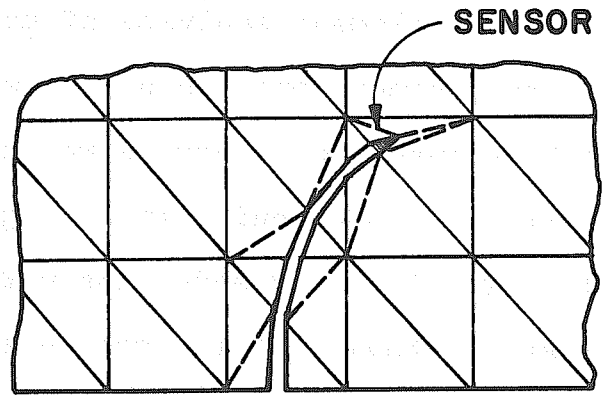

b) LINE - CRACK WITH FINITE WIDTH & SENSOR ELEMENT

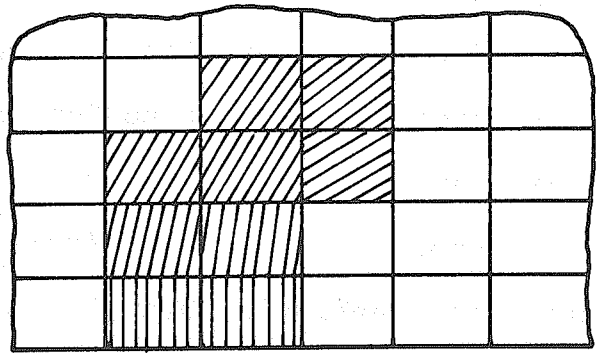

c) CRACK - ZONE

FIG. I.5 FINITE ELEMENT CRACK REPRESENTATIONS

uncracked, cracked and plastified stages was also developed by Cervenka [19] for the nonlinear incremental analysis of reinforced concrete panels under both monotonic and cyclic loadings, which included the closing and re-opening of cracks within the finite element. Valliappan and Nath [20] applied the "stress transfer" method to the finite element analysis of tensile crack propagation in reinforced concrete beams, where the limiting tensile strength of concrete was taken to be the failure criterion, but bond slip was ignored. Valliappan and Doolan [21] later extended the work to include the elasto-plastic behavior of the concrete and steel.

There is still another method of modelling reinforced concrete members. Selna [22,23] developed a one-dimensional layered system to study the time-dependent, creep, cracking and shrinkage effects on beams and frames. Franklin [24] used this type of layered beam system together with an approach similar to Cervanka's [19] to perform nonlinear analyses of reinforced concrete frames and panels. The study of shear wall-frame systems, using a method similar to Franklin's, has also been presented by Yuzugullu and Schnobrich [25].

The finite element analysis of prestressed concrete nuclear reactor vessels has been carried out by Rashid and Rockenhauser [26], Wahl and Kasiba [27]. Rashid has also attempted to take the effects of cracking, temperature changes, creep, as well as loading history and

ultimate strength of materials into consideration [28, 29]. Argyris et. al have presented a comprehensive study of the recent developments in the finite element analysis of prestressed concrete reactor vessels [30]. Transfer stress distribution was analyzed by Kripanarayanan and Meyers [31] for fully bonded wires in pretensioned concrete members. Post-tensioned highway bridges have been studied by Jofriet, McNeice and Csagoly [32]. A method of predicting the behavior of reinforced and prestressed concrete structures subject to cracking has been developed by Taylor, Romstad, Herrmann and Ramey [33], where an attempt was made to generate mesh layouts automatically to account for cracking.

Application of the finite element method for the analysis of reinforeced concrete plates and shells, with material nonlinearity and cracking effects, has been advanced by a number of investigators, such as Jofriet and McNeice [34], Bell and Elms [35, 36], and Scanlon [37]. The concept of layered finite element system was developed by Hand, Pecknold and Schnobrich [38] for plates and shallow shells of constant thickness. Lin [39] has developed a layered system for analyzing reinforced concrete slabs of arbitrary geometry and for free-form shells under dead loads and monotonically increasing live loads.

An excellent state-of-art paper has been presented recently (1972) by Scordelis [40] at a Specialty Con-

ference on Finite Elements Methods held in Canada. In that paper a comprehensive summary as well as the possible areas for future investigation was given for the application of the finite element analysis to reinforced concrete structures. A number of interesting related studies can also be found in the Proceedings of that Conference [41] where the subject of finite element analysis of concrete structures was one of the major topics.

1.3 Crack-Line vs. Crack-Zone

From reviewing the existing literature, it can be seen that the finite element method has become a powerful and feasible means of analysis, which helps considerably in the understanding of the behavior of various types of concrete structures. It can also be noted that most investigators prefer that crack-zone type of representation for the study of cracking in reinforced or prestressed concrete structures, and it is used almost exclusively for the analysis of reinforced concrete plates and shells. This choice is not at all difficult to understand. In this crack-zone type of approach, the finite element mesh layout need not be altered, and only the element stiffness matrix has to be modified to account for cracking. Thus the process is identical to the normal solution method for material nonlinearity problems. The justification for this approach seems to be based on the

fact that when fracture takes place within the concrete mass, the plane of failure is made up by a multitude of micro-cracks, rather than a clean-cut surface such as those exhibited in most metallic or ceramic materials. When the finite element size is small, as compared to the over-all structural dimensions, the crack-zone type of representation would indeed capture the gross structural behavior, without the tedious task of redefining the finite element mesh layout. But, on the other hand, one is immediately confronted with the problem of how small the crack-zone should be reduced in size in order to simulate a crack. From most of the published studies, the finite element mesh sizes are generally too coarse to represent a narrow band of failure zone, and consequently a large portion of the structure is pronounced as failed or yielded. Furthermore, this crack-zone type of representation tends to limit the ability of the finite element model in identifying the effect of cracking, bond slip and aggregate interlock, each individually and independently. Another latent difficulty is that when reversed loading, such as in the case of cyclic loads, is considered and cross cracking is allowed in each finite element, there is a possibility of total loss of the element stiffness if two crossing cracks happen to be orthogonal. This may lead to ill-conditioning of the structure stiffness matrix.

The crack-line type of representation also has its shortcomings. Again, there is the question of how fine the finite element mesh size should be in order to produce cracks that would closely simulate the cracking of the real structural members under real loading conditions. At any rate, the finite element model is an approximation at best. Nevertheless, the crack-line approach offers a good physical picture of the cracking condition, and at the same time, failure along a line or a plane, rather than a zone or a block, permits different added effects to be incorporated into the model and to be examined independently as demonstrated in Ref. 10. However, this seemingly simple process of producing a crack-line by introducing additional nodal degrees of freedom can complicate the analytical solution procedure considerably. The major part of the effort made in the present study is to overcome this analytical difficulty encountered in the finite element modelling of cracks by a crack-line type of representation.

1.4 A Conceptual Model

Suppose that cracking is literally taken to mean fracturing the structural solid into pieces, and the finite element model is nothing more than an assemblage of these small pieces of the structure, then a model to simulate cracking can be developed in the following manner:

a) Subdiving the solid into small elements, Fig. 1.6a;

b) Connecting the loose individual elements by the fictitious joint elements, Fig. 1.6b;

c) Simply eliminating the joint element to represent a crack, Fig.1.6c; or

d) Alternately modifying the stiffness of the joint element to account for a certain degree of bonding or interlocking between the adjacent elements, Fig. 1.6d.

A possible resulting crack pattern from such a model is shown in Fig. 1.7 for a simple reinforced concrete beam.

The impracticality of such a model is, of course, obvious. As compared to the ordinary finite element model, it can easily be found that:

a) The number of nodes is nearly doubled.

b) The number of elements is approximately increased by threefold.

c) The bandwidth of the structure stiffness matrix is approximately increased by 1-1/2 times.

d) The system is too flexible if the joint stiffness value is set too low.

e) The system becomes ill-conditioned if the joint stiffness value is set too high.

f) The crack pattern composed of only vertical and horizontal lines leaves much to be desired.

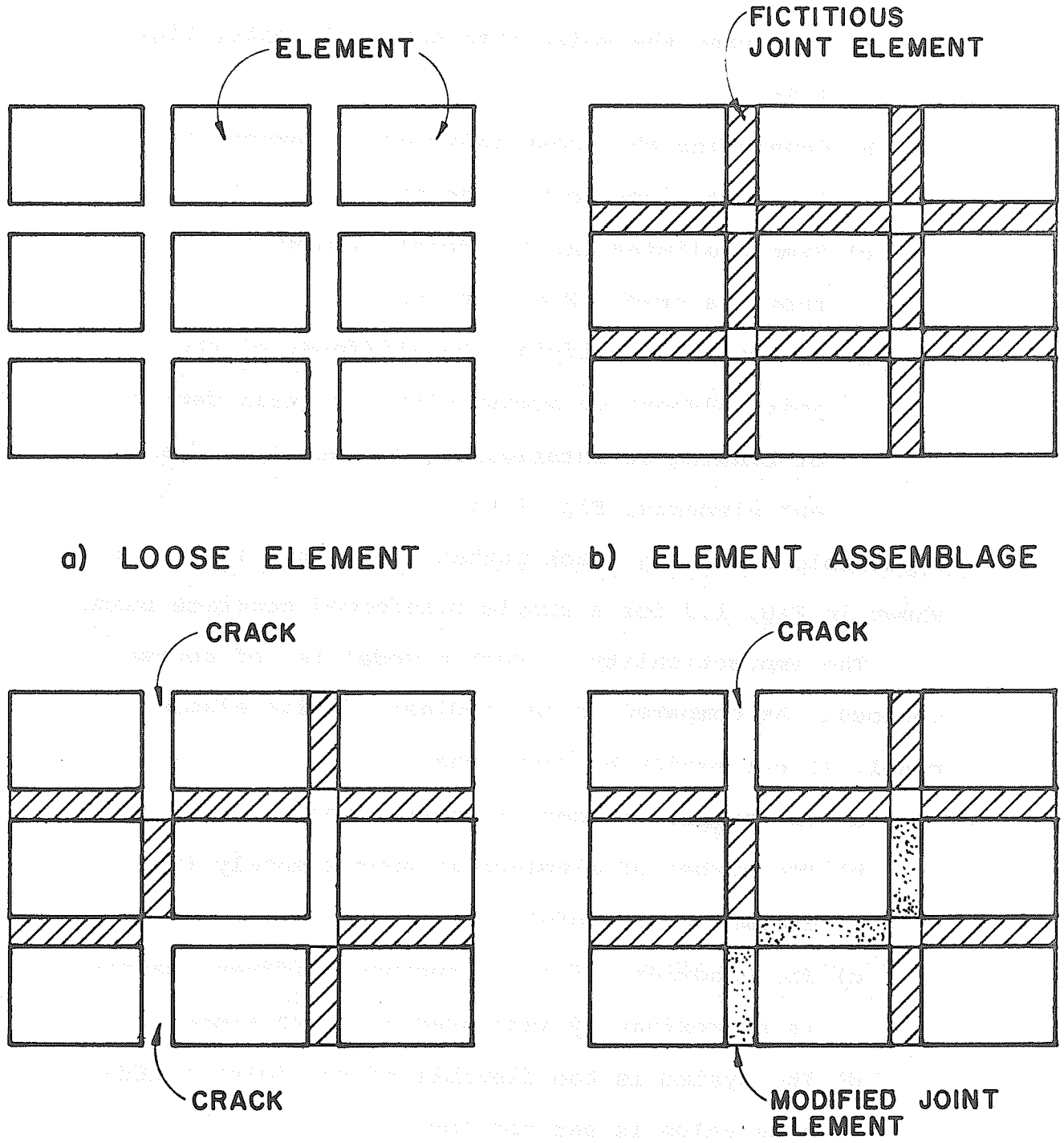

FIG. 1.6 A CONCEPTUAL MODEL

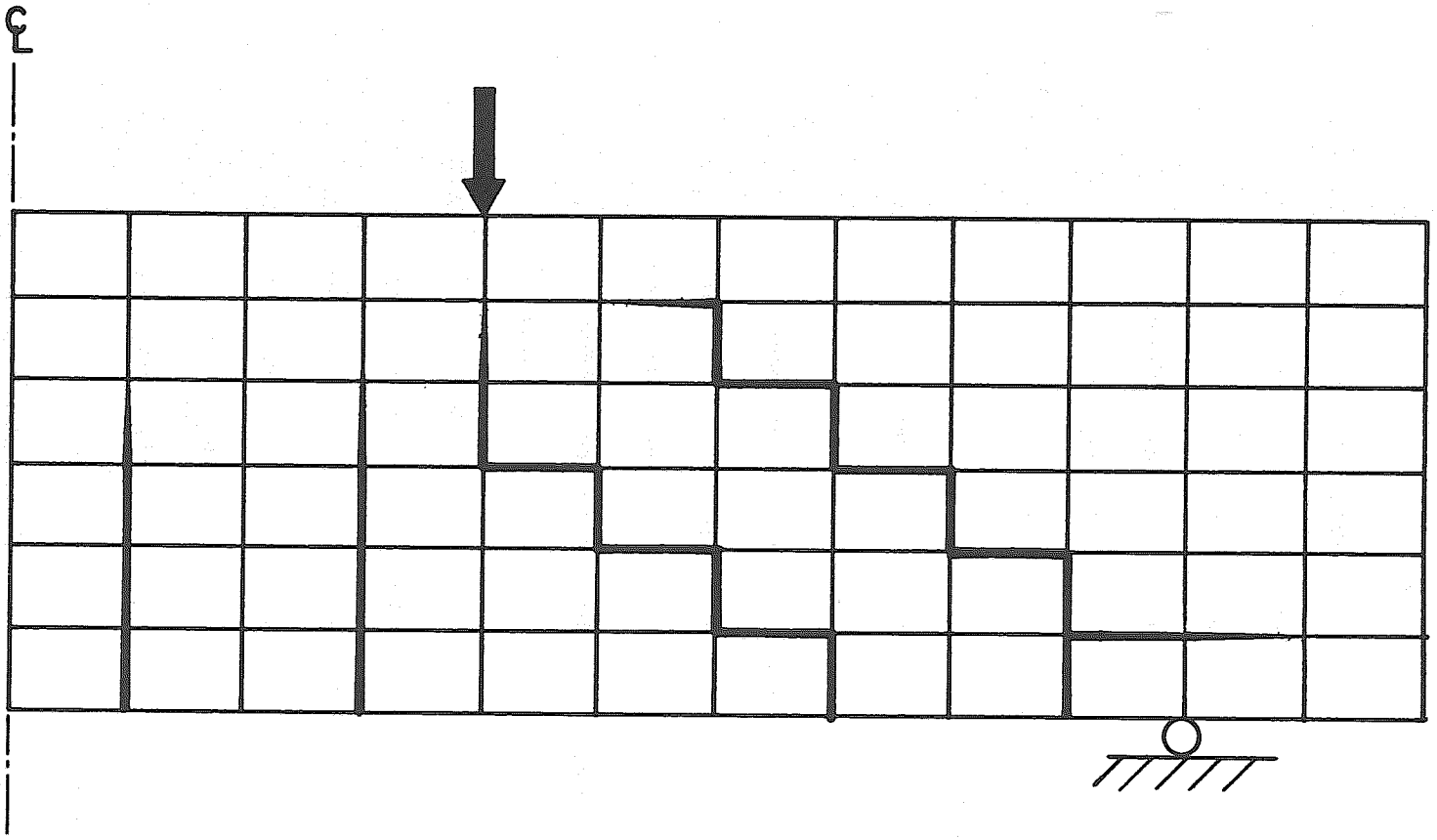

FIG. 1.7 A POSSIBLE CRACK PATTERN WITH RECTANGULAR ELEMENTS

However, despite all these shortcomings, this conceptual model emphasizes the very fundamental concept upon which a finite element model can be built to incorporate the crack-line type of representation. The remaining question will be how to incorporate such a conceptual model into a more amenable solution process, which is capable of exhibiting various special features such as bond slip, aggregate interlock and dowel action.

1.5 Need for a New Approach

Working directly with the conceptual model is seen to be rather cumbersome. While there is a distinctive advantage that no new nodes need to be introduced at any stage of cracking, the excessive number of nodal points and elements, plus the enlarged bandwidth, will demand an enormous increase in the solution effort. Another even more objectionable aspect of the model is that the stiffness of the joint element is very difficult to select. There is no a priori knowledge about the appropriate stiffness value which should be high enough to produce a minimum unwanted additional flexibility in the system, and yet low enough not to disturb the conditioning of the solution matrix. It is possible to improve the crack pattern, for instance, by employing triangular elements, Fig. 1.8. However, the increase in the number of nodes, the number of elements and the size of bandwidth will make the solution even more unfeasible.

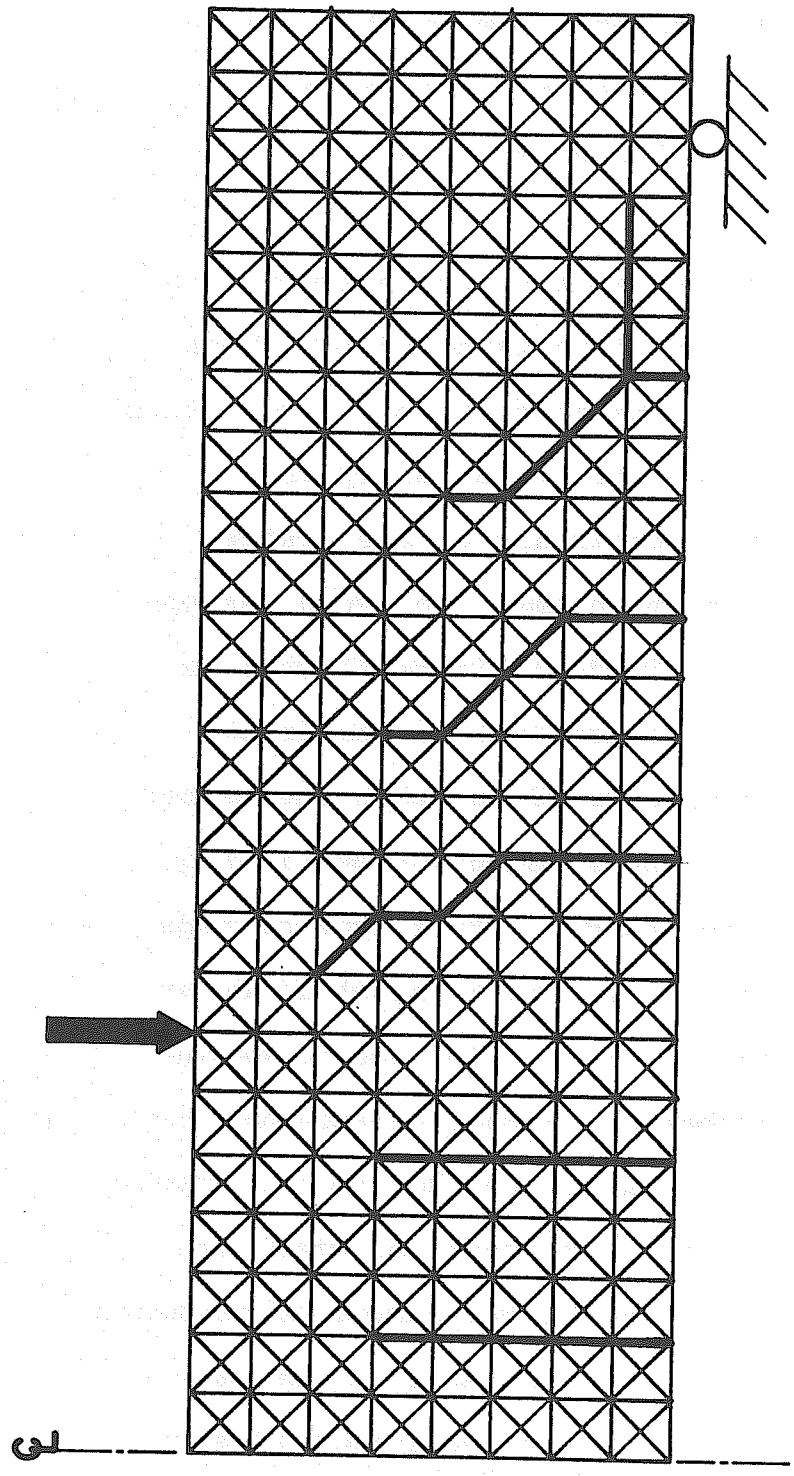

FIG. 18 A POSSIBLE CRACK PATTERN WITH TRIANGULAR ELEMENTS

In order to transform the present conceptual model into a feasible operational scheme, some of the fundamental properties of the finite element method of analysis require a more detailed examination.

1.5.1 Node Numbering

Node numbering in such a way that the bandwidth is kept to a minimum is of utmost importance and has been generally accepted as one of the inherent characteristics of the displacement method of structural analysis. This imposes a considerable constraint on the finite element analysis of cracking problems. To avoid assigning node numbers to every individual finite element in the conceptual model shown earlier, the conventional way of node numbering can be carried out when the member is uncracked. For example, the structure shown in Fig. 1.9a is well adapted to the banded matrix type of node numbering sequence. However, as soon as crack-lines are introduced into the structure, Fig. 1.9b, the nodes inevitably have to be re-numbered in order to achieve a minimum bandwidth. Moreover, while the horizontal crack increases the bandwidth by one, the vertical crack increases the bandwidth by as many as the number of elements that the crack runs across, which is three in the case shown in Fig. 1.9b. It would be very desirable if such a detrimental relationship between node numbering and bandwidth could be eliminated.

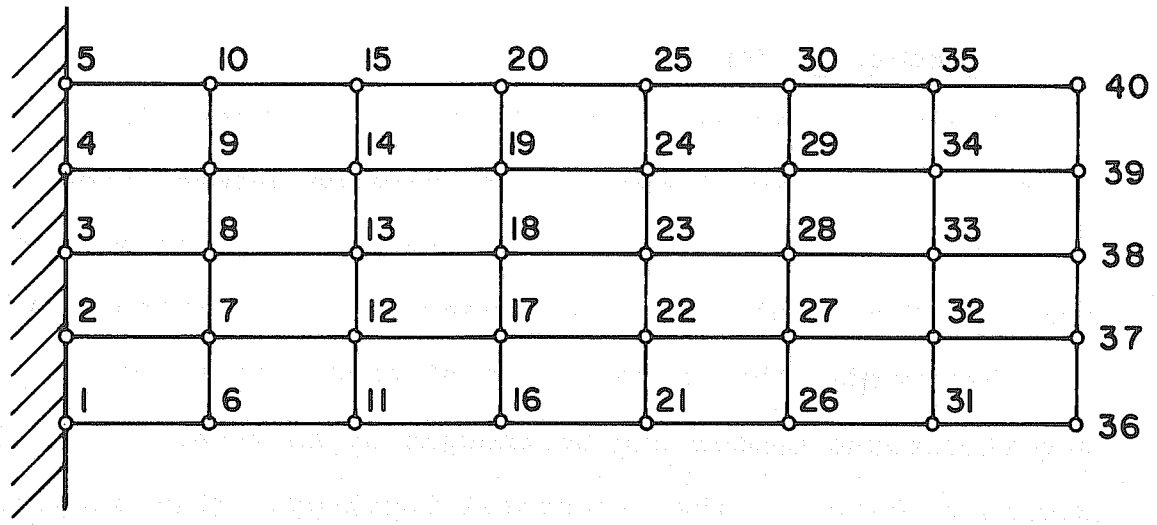

a) UNCRACKED

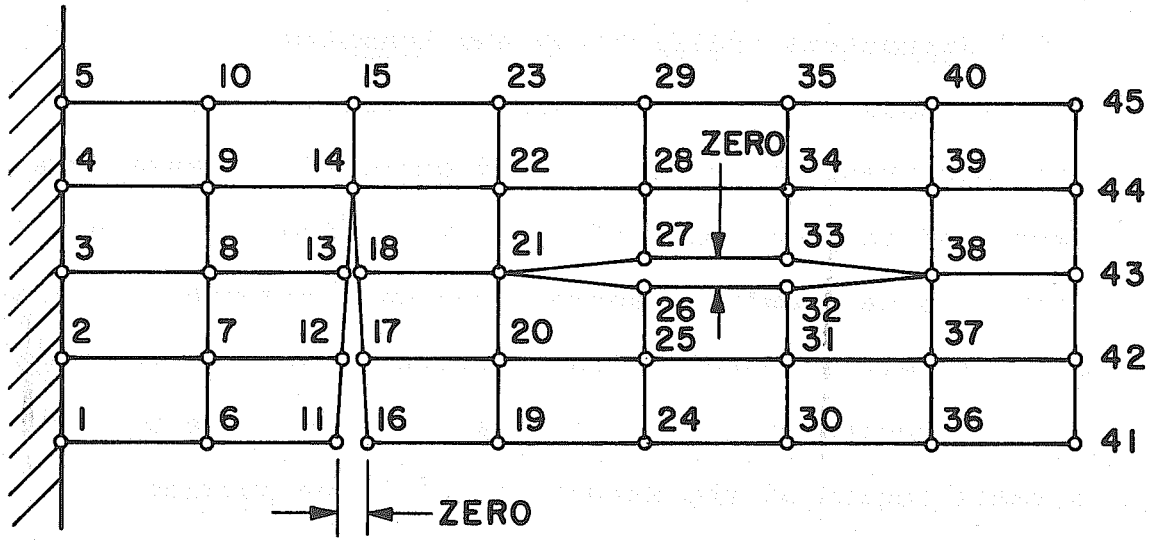

b) CRACKED

FIG. 1.9 NODE NUMBERING IN CRACKED AND UNCRACKED STRUCTURES

1.5.2 Structural Topology

A closer examination of the two structures, Fig.1. 9a and b, will reveal that the difference between them is merely in their structural topology, i.e., the manner that the finite elements are connected to one another. In other words, the introduction of crack-lines into any structural member can be thought of as merely inducing a change in the structural topology. This suggests that the topological aspect of structural analysis should play an important part in the study of progressive crack growth.

1.5.3 Structural Modification and Reanalysis

Methods of structural modification and reanalysis can conceivably be developed and employed to lessen the burden of computational effort. This direction of endeavor is particularly appropriate when cracking is viewed as merely a change in the structural network topology. Such a topological change generally takes place within a small region of the structure. A large portion of the structure remains unaffected as far as the topological and the mechanical properties are concerned. This fact suggests that the already formed and decomposed stiffness matrix can again be utilized to seek a new solution, if the original stiffness matrix can be properly modified to account for the changes encountered.

1.5.4 Crack Propagation

The proposed conceptual model only provides a means of accommodating cracks within a structural member. The condition and the manner which dictate where a crack should appear and when a crack should grow must be stipulated in order to properly simulate and study crack propagation. Almost all investigators employ a failure criterion, and cracking is declared for the portion of the structure where the condition of the failure criterion is met. Little effort has been made to study the problems of crack propagation in concrete from the fracture mechanics standpoint. Stress concentration at the crack tip is known to exist. It is also well known that fracture can occur at a much lower stress level in a notched specimen. All these facts deserve some recognition in the development of a finite element model for the study of progressive crack growth in concrete members.

1.5.5 A Proposed Approach

The various problems mentioned above form the core of the present study. To reconcile most of the difficulties, a new orientation of viewpoint is taken. The structure is treated as physical system represented by a network whose topological properties are given full recognition. Graph theoric matrices and some network theories can then be utilized. This methodology is collectively called "network-topological approach",

a term which has been coined by Fenves and Branin [42]. The fundamental concept of such an approach has been pioneered and advanced by scholars both in the United States and abroad in recent years.

1.6 Objective and Scope

An attempt will be made in this thesis to develop an operational scheme based upon the improvement of the conceptual model proposed earlier for the analytical studies of cracking in reinforced and prestressed concrete members. Discretization and simulation of the structural system are carried out by means of the finite element method where a computer can be utilized as a solution aid. A network-topological approach is suggested as a unified treatment for the various problems encountered in analyzing crack growth. It aims at supplementing the existing finite element method of analysis for the purpose of handling the problems associated with cracking.

The objective of the present study is threefold:

1) To develop a finite element model which is capable of automatically producing crack-lines to simulate progressive crack growth.
2) To show that the network-topological approach can be extended to include modification and re-analysis.
3) To postulate a hypothesis regarding crack

propagation in the spirit of fracture mechanics, based on a network sensitivity function.

A computer program is written to perform the necessary computations with examples to demonstrate its capabilities. However, no attempt is made at present to combine the structural modification procedure, the crack propagation hypothesis and the progressive growth calculation into a single general purpose computer program. This task is left for future investigations.

1.7 Notations

This thesis involves a number of different engineering disciplines. To avoid any unwarranted confusion in nomenclature, notations commonly used in a particular field of study will be followed, and will be defined when they first appear in the text, or when they assume a new meaning. No special symbol is adopted for matrix equations, since they should be self-evident from the context. Brackets for matrices and vectors are used only when they are deemed necessary for greater clarity. Greek letters generally denote a constant.

CHAPTER 2 TOPOLOGY, GRAPH, NETWORK AND STRUCTURAL SYSTEM ANALYSIS

2.1 Structural Network and Topology

A structural system can be considered as a physical network, and the connectivity of the structural elements can be depicted by a system graph G. Network analysis can be thought of as a practical application of algebraic topology beginning with Kron's application of topological theorems to the analysis of complex elastic networks.

Kron also coined the word "Diacoptics," or the "method of tearing" [43, 44, 45, 46]. However, it is Branin [47, 48, 49] who was responsible for making Kron's ideas of tearing and the network-topological method understandable to the engineering world. In addition, Roth [50, 51, 52] provided much of the topological foundation for Kron's Diacoptics as well as for the network analysis.

In the last two decades, many important contributions of the network-topological approach to the analysis of structural networks have been made. The pioneering work of Langefors [53,54], especially the use of coincidence matrices, is of fundamental importance. The topology underlying structural analysis has long been recognized by Baron [55]. Sammuelson [56,57] presented a thorough treatment of linear structural analysis by algebraic topology. Wiberg [58, 59, 60] used a similar method to study structural disection. The linear graph counterparts

of Sammuelson's and Wilberg's works are given by Fenves and Branin [42], and by Steward and Baty [61], respectively. System theory has been employed by Lind [62] and Wu [63]. Topological studies of structural stability and determinacy have been done by Henderson and Bickley [64], Morice [65], Henderson [66] and DiMaggio [67]. DiMaggio and Spiller [68] have also applied the network analysis to various types of structures. Henderson and Maunder [69], Maunder [70] employed the topological methods to the feasible selection of cycle bases in the flexibility method for the linear elastic analysis of skeletal structures. Oden and Neighbor [71] extended the network-topological formulation of the force method to the analysis of geometrically and materially nonlinear space frames. Oden [72, 73] has further carried out the topological consideration into the general theory of the finite element method. Additional references can be found in the Reference Section at the end of this thesis.

The term "network-topology", in the context of the present study, is a collective term which stands for the fundamental concept and methodology in the areas of algebraic topology, linear graph, network and system theories, that are useful in structural analysis, particularly with respect to the study of progressive crack growth. It is not the intention of the present study, however,

to produce a unified network-topological formulation or a system theory for structural analysis. Instead, advantage will be taken of the already well known and established theories in linear graphs, networks and systems to help solve the problems associated with progressive crack growth. Therefore, only the relevant network-topological concepts needed in the present study are presented here and in following chapters whenever it is deemed necessary.

2.2 Some Graph Theoretic Matrices

Network topologies can be conveniently described by graph theoretic matrices. Some of such matrices related to the present study are presented below, and their properties of interest are also discussed. A more complete discussion of graph theoretic matrices can be found in Ref. 74, 75 and 76.

2.2.1 Branch-Node Coincidence and Boolean Connectivity Matrices

Consider the system graph G which consists of non-oriented 1-complexes, Fig. 2.1a. Then G can be uniquely specified by a coincidence matrix M_1, suggested by Langefors [53]. The elements of the matrix M_1 are of order 1 and are known as coincidence numbers. Using the terms of node and branch in place of 0- and 1- simplex, respectively, the nodes of G are listed in a row, and the endpoints of the branches are listed in a column. A

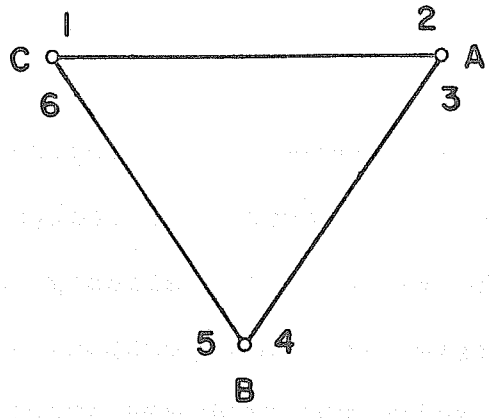

a) SIMPLICAL COMPLEX

	A	B	C
1	0	0	1
2	1	0	0
3	1	0	0
4	0	1	0
5	0	1	0
6	0	0	1

b) COINCIDENCE MATRIX M_1

	A	B	C
1,2	1	0	1
3,4	1	1	0
5,6	0	1	1

c) COINCIDENCE MATRIX H_1

FIG. 2.1 SIMPLICAL COMPLEX AND COINCIDENCE MATRICES (AFTER LANGEFORS)

coincidence number of 1 is assigned in each row under the node where the endpoint of each branch is coincident to that node, and all other entries are 0's, Fig. 2.1b. Another scheme can also be established where there is only one row for each branch and in each of such row 1's are placed in the columns of these nodes to which the branch is incident, Fig. 2.1c. The matrix so defined is called an unoriented incidence matrix H_1 by Langefors.

The graph in Fig. 2.1a can also be described in a third way. Let a branch represent the connectivity relationship between nodes, and an incidence number 1 is assigned whenever such a connectivity exists, a new coincidence matrix D_1 can then be constructed, Fig. 2.2a. Similarly, the connectivity of a node, or a group of nodes, to the rest of nodes in a graph can also be represented by a coincidence matrix B_1, Fig. 2.2b, a special case of which is the Boolean connectivity matrix referred to by Argyris and Roy [132-134]. Strictly speaking, D_1 and B_1 are quite different from M_1 and H_1 in nature. However such a differentiation is not necessary in the present study. Therefore, no distinction is made among them, and they are collectively referred to as coincidence matrices and denoted by M, unless otherwise specified.

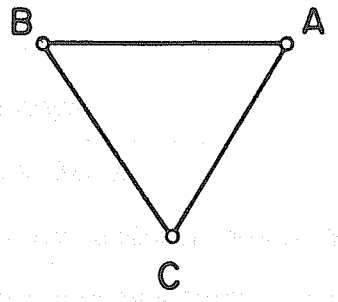

	A	B	C
A	0	1	1
B	1	0	1
C	1	1	0

a) COINCIDENCE MATRIX D_1

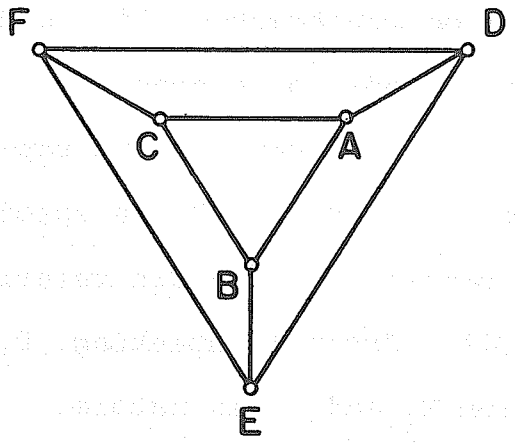

	A	B	C
D	1	0	0
E	0	1	0
F	0	0	1

b) COINCIDENCE MATRIX B_1

FIG. 2.2 NODE CONNECTIVITY MATRICES

Note that the coincidence matrix M consists of Boolean components, i.e., the entries are either 0's or 1's. Such a coincidence matrix can legitimately be considered as a Boolean Matrix [77]. However, unlike in the study of switching circuits, no special matrix operation is required in the present study. All rules of ordinary matrix algebra apply to matrix M. When the elements in M are treated as decimal instead of binary numbers, the matrix M possesses some properties which are noteworthy.

Property I: Defining the summation of the coincidence number in each row of matrix M as being the row sum r_s, and similarly, column sum c_s, it is obvious that

$$c_s \text{ of } M_1 = c_s \text{ of } H_1 = c_s \text{ of } B_1.$$

Furthermore, in the case of $r_s = 1$, such as in M_1, it can be easily verified that

$$M_1^t M_1 = D_{cs} \tag{2.1}$$

where D_{cs} is a diagonal matrix whose elements are the column sums c_s of the corresponding columns. This is simply a consequence of matrix product and the condition $r_s = 1$. Therefore, if the column sum c_s is also set to unity, $c_s = 1$, such as in the case of B_1, then according to Eq. 2.1,

$$B_1^t B_1 = I$$

In this light, the Boolean connectivity matrices b_i,

b_m and b_r employed by Argyris and Roy [132-134] can be regarded as conincidence matrices, because they all satisfy the conditions

$$r_s = 1$$

$$c_s = 1$$

and the orthonormal relationship

$$b_i^t b_i + b_m^t b_m + b_r^t b_r = I_n \tag{2.2}$$

clearly holds. The meaning of various matrices in Eq. 2.2 will be explained later in Chapter 5 where structural modification and realalysis are discussed.

Property II: Let coincidence matrix M satisfy the conditions

$$r_s = 1 \qquad c_s = 1 \tag{2.3}$$

and K be a square matrix, then

a) the pre-multiplication of K by M, MK, has the effect of interchanging the rows in K,

b) the post-multiplication of K by M^t, KM^t, has the effect of interchanging the columns in K,

c) and therefore, the triple product

$$M\ K\ M^t \tag{2.4}$$

will result in rearranging the elements in the matrix K in such a way that the rows and columns are interchanged according to the order specified by a non-zero entry in each row and column of the coincidence matrix M. This property has been

utilized to form the "Law of 3 x 3 partitioning" by Argyris and Roy [132]. It should also be noted that the conditions stated in Eq. 2.3 imply that M is a square matrix, and

$$M^t M = I = M M^t \tag{2.5}$$

Property III: If the conditions in Eq. 2.3 are altered to be

$$\begin{aligned} r_s &= 1 \\ c_s &\leq 1 \end{aligned} \tag{2.6}$$

This implies M is a rectangular matrix in which the number of columns c is greater than the number of rows r. Then

a) pre-multiplication of K by M means collection of rows in K according to the columns in M, where $c_s = 1$,

b) post-multiplication of K by M^t means collection of columns in K according to the rows in M^t, where $r_s = 1$,

c) and the triple product $M^t K M$ has the effect of dispersing the elements of K into a matrix of higher dimension, according to the order specified by the non-zero entries of M.

Property IV: If the column sum c_s is greater than or equal to 1, i,e.,

$$\begin{aligned} r_s &= 1 \\ c_s &\geq 1 \end{aligned} \tag{2.7}$$

then M is a rectangular matrix with $r > c$. The triple

product M^tKM compresses K into a matrix of smaller dimension, in which rows and columns of K are summed according to the non-zero entries in each column of M. This is the well known summation process and equivalent to the direct stiffness method which has been commonly used to form the total structural stiffness matrix from individual element stiffness matrices in the matrix method of structural analysis.

All these properties of the coincidence matrix M are rather elementary. They are re-iterated here because they have been used extensively by Argyris and Roy in their formulation of the structural modification method, they also help simplify some of the computational procedures developed in the present study once the essence of these properties is recognized. Furthermore, the employment of the coincidence matrix M, instead of the more conventional types of incidence matrix for the oriented graph (see next section) enables the direct adoption of the conventional element stiffness matrices without the necessity of modifying either the stiffness or the incidence matrix itself.

2.2.2 Branch-Node and Branch-Mesh Incidence Matrices

Most network theories make use of the oriented linear graph, rather than the unoriented one. A linear graph G, Fig. 2.3a, is oriented when its branches and meshes are assigned a sense of direction, Fig. 2.3b.

Thus distinction can be made whether a branch is positively or negatively incident to a node or a mesh. Consequently, the element of a branch-node incidence matrix A, Fig. 2.3c, associated with an oriented graph is defined as

$$a_{ij} = \begin{cases} +1 \\ -1 \\ 0 \end{cases} \quad \text{if } i^{th} \text{ branch is } \begin{cases} \text{positively} \\ \text{negatively} \\ \text{not} \end{cases} \quad \text{incident to the } j^{th} \text{ node}$$

and the element of a branch-mesh incidence matrix C, Fig. 2.3d, is given by

$$c_{ij} = \begin{cases} +1 \\ -1 \\ 0 \end{cases} \quad \text{if } i^{th} \text{ branch is } \begin{cases} \text{positively} \\ \text{negatively} \\ \text{not} \end{cases} \quad \text{incident to the } j^{th} \text{ mesh}$$

The algebraic structure related to a linear graph arises from the fact that it is possible to associate a set of mathematical objects such as vectors spaces to the nodes, the branches and the meshes of an oriented graph. This is equivalent to the construction of chain and cycle spaces in the case of algebraic topology. It can be shown that the incident matrices A^t and A, C and C^t play the roles of boundary operator ∂_o and coboundary operator δ_o, injective homomorphism j and prejective homomorphism j*, respectively [56, 57, 58]. Therefore, two exact sequences and their trans-

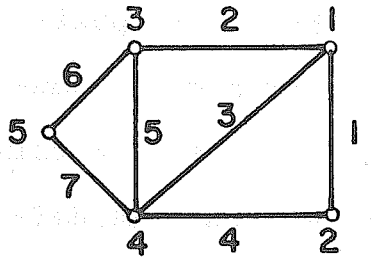

a) LINE GRAPH G

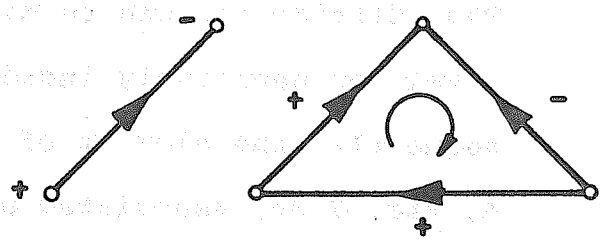

b) ORIENTED BRANCH & MESH

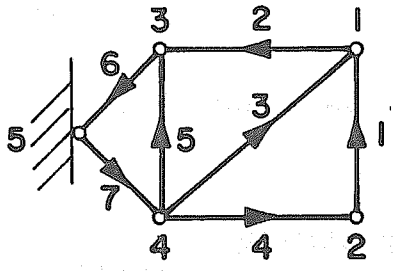

BRANCH \ NODE	1	2	3	4	5 (DATUM NODE COLUMN DELETED)
1	-1	1	0	0	0
2	1	0	-1	0	0
3	-1	0	0	1	0
4	0	-1	0	1	0
5	0	0	-1	1	0
6	0	0	1	0	-1
7	0	0	0	-1	1

c) BRANCH-NODE INCIDENCE MATRIX A

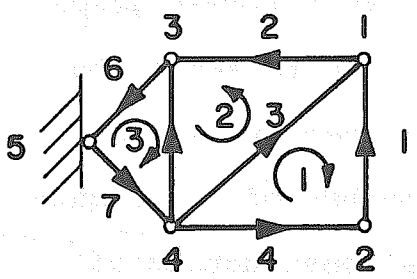

BRANCH \ MESH	1	2	3
1	-1	0	0
2	0	1	0
3	1	1	0
4	-1	0	0
5	0	-1	-1
6	0	0	-1
7	0	0	-1

d) BRANCH-MESH INCIDENCE MATRIX C

FIG. 2.3 A LINEAR GRAPH (AFTER FENVES & BRANIN)

formation can be constructed in terms of the matrices A and C, as presented by Fenves and Brain [42], Fig. 2. 4. It can further be shown that node and mesh analyses, or equivalently, displacement and force methods can be derived from the transformation diagram when the two isomorphisms F and K are prescribed [42, 47, 56]. Hence any system which can be cast into a network formulation will be handled in the same manner. However, when this type of network formulation is applied to structural systems, the conventional stiffness or flexibility matrix has to be modified. Fortunately, this problem is overcome in the present study by working with the coincidence matrices instead. But it is still crucial to note that two fundamental laws in network theory, namely, KCL and KVL or equivalently, the static and kinematic compatibility requirements in a structural network, can be conveniently expressed as

$$\begin{aligned} A^t\, p = 0 \quad \text{and/or} \quad p = C\, p' \\ C^t\, u = 0 \quad \text{and/or} \quad u = A\, u' \end{aligned} \tag{2.8}$$

and based upon which Tellegen's theorem is derived, as presented later in Chapter 6. The link-at-a-time algorithm discussed in Chapter 5 also makes use of the incidence matrices A and C.

2.2.3 Dual Graph and Adjacency Matrix

Given a topological graph G which is planar, unhinged and connected, it is possible to construct another

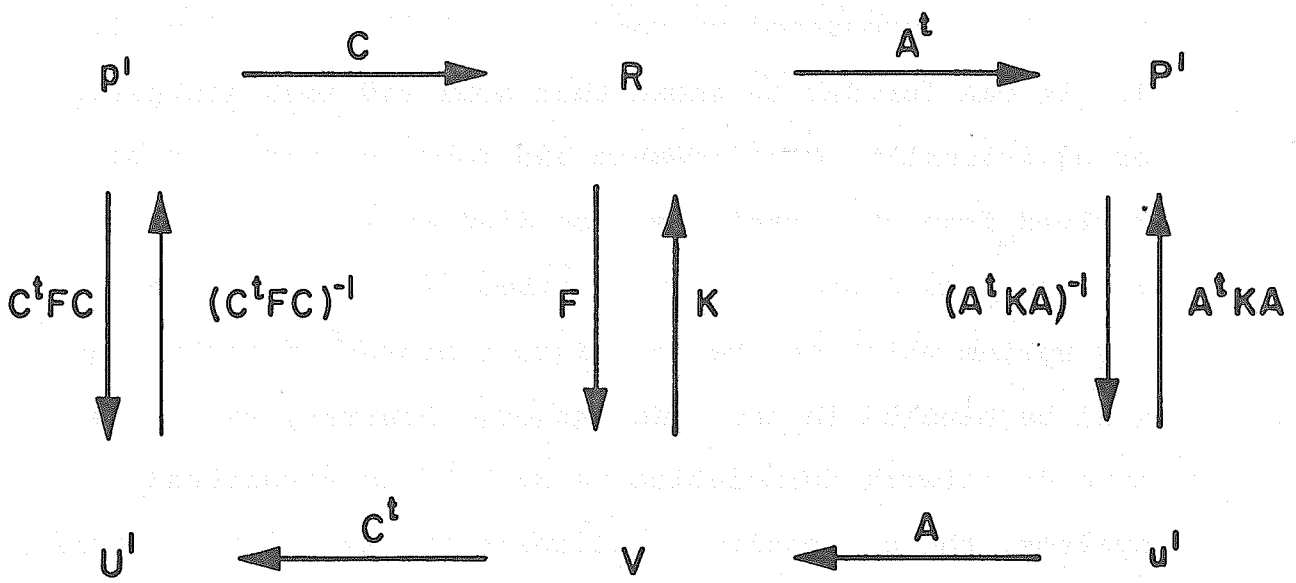

p' = MESH FORCE
P' = APPLIED BRANCH FORCE
u' = JOINT DISPLACEMENT
U' = APPLIED BRANCH DISTORTION
R = INDUCED MEMBER FORCE
V = INDUCED MEMBER DISTORTION
F = FLEXIBILITY MATRIX
K = STIFFNESS MATRIX

FIG. 2.4 TRANSFORMATION DIAGRAM (AFTER FENVES & BRANIN)

graph $\hat{G}$ [78] by

1) associating each node in G with a mesh in $\hat{G}$, including the outer mesh,
2) assigning a branch to connect two nodes in $\hat{G}$ whenever there is a common branch between the meshes in G.

The resulting graph $\hat{G}$, Fig. 2.5, is a dual of G, and is called a dual graph. Note that the dual graph $\hat{G}$ depicts the adjacency relationship of the meshes in G. Therefore, an adjacency matrix A can be constructed from the dual graph $\hat{G}$. Each element in the (i, j) position of the matrix A is equal to the number of edges incident with both vertex i and vertex j [79].

A given finite element mesh, such as the one shown in Fig. 2.6a, can be thought of as a planar graph and correspondingly a dual graph can be obtained, Fig. 2.6b. This dual graph furnishes a complete picture of how the two-dimensional finite elements are connected and are adjacent to each other. Since only the adjacency relationship is of real interest in the present study, two modifications can be made to the construction of dual graph.

1) The outer mesh in the original graph G is irrelevant here and therefore will be omitted.
2) The requirement of the graph G being planar will also be relaxed.

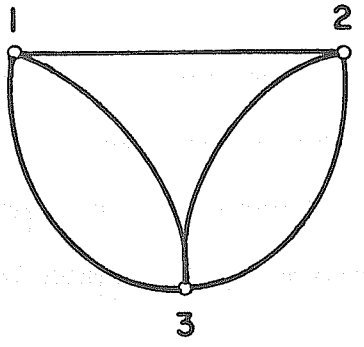

a) GRAPH G

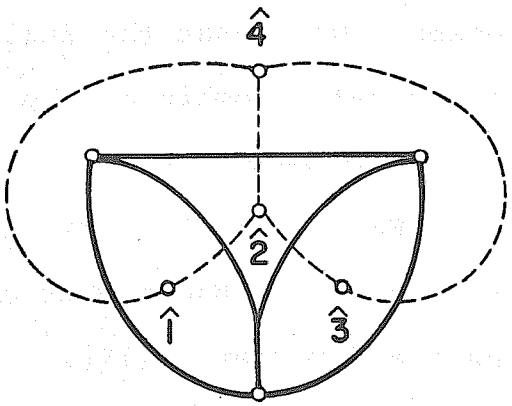

b) CONSTRUCTION STEP

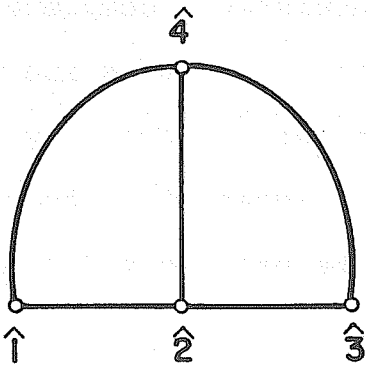

c) RESULTING DUAL GRAPH $\hat{G}$

FIG. 2.5 GRAPH AND DUAL GRAPH (AFTER DESOER AND KUH)

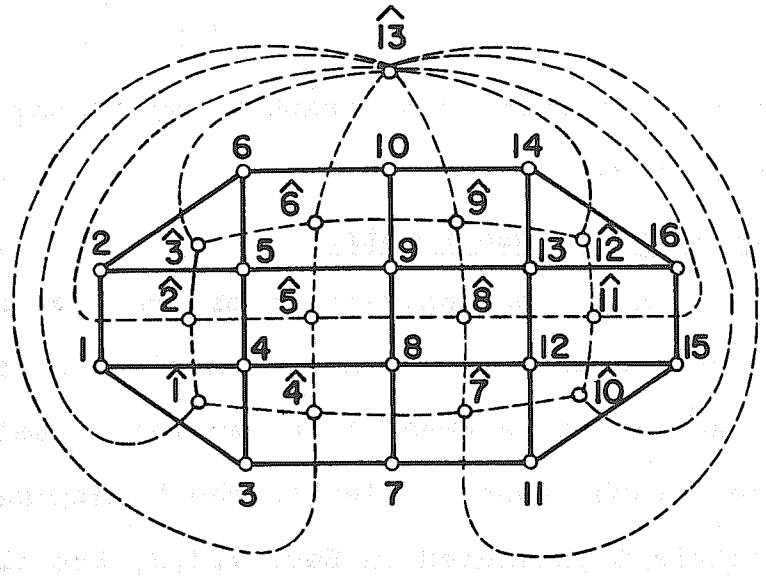

a) FINITE ELEMENT MESH

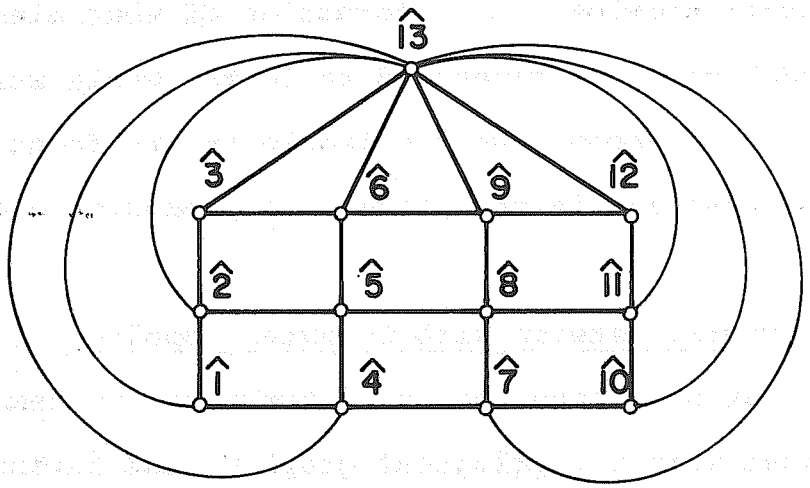

b) ITS DUAL GRAPH

FIG. 2.6 FINITE ELEMENT MESH AS A PLANAR GRAPH

Note that the resulting dual graph $\hat{G}$ may or may not be planar in this case.

2.2.4 Node-Mesh Incidence Matrix

To facilitate the analysis of progressive crack growth a novel node-mesh incidence matrix D is defined. Consider each finite element to be an individual mesh of a linear graph, then similar to the branch-mesh incidence matrix C presented in Sec. 2.2.2, the element of the node-mesh incidence matrix D is given by

$$d_{ij} = \begin{cases} 1 & \text{if i node is incident to j mesh.} \\ 0 & \text{if i node is not incident to j mesh.} \end{cases}$$

This matrix provides the information of what elements each nodal point is connected to in the whole structure. Therefore, it becomes very valuable in the frontal solution process and in the process of producing a crack-line.

2.3 Structural Network with Changing Topology

It has been seen that any structural system can be associated with a topological graph G, and furthermore, a dual graph $\hat{G}$ can also be obtained. This concept of casting the structural analysis into a network problem is particularly helpful in dealing with the problem of cracking in structures. Because, in a discretization analysis such as the finite element method, it is possible to view cracking as being merely a change in the

network topological graph, or equivalently, a change in the network dual graph, and all the graph theoretic matrices can be profitably employed in the various stages of the solution process.

Consider a portion of the structure idealized by finite element model in Fig. 2.7a. Omitting the outer mesh, its dual graph and adjacency matrix are shown in Fig. 2.7b and c. When a crack-line is introduced into the structure, Fig. 2.8a, the corresponding dual graph has one branch deleted, Fig. 2.8b, and its adjacency matrix is modified accordingly, Fig. 2.8c. If a joint element is inserted at the crack to simulate bonding or interlocking across the cracked surfaces, Fig. 2.9a, then the dual graph has one additional node and one additional branch, Fig. 2.9b, and the adjacency matrix is enlarged correspondingly, Fig. 2.9c. Using this vehicle, the ease in communicating with the computer should be apparent. It can also be observed that the adjacency matrix is symmetric and its row sum r_s is equal to the column sum c_s.

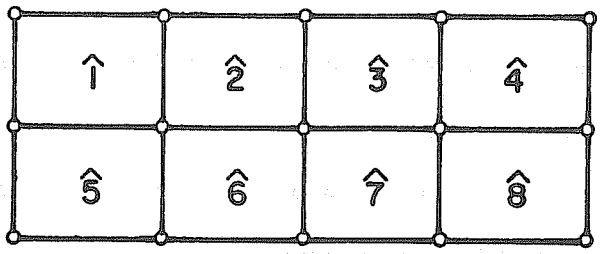

a) UNCRACKED STRUCTURE

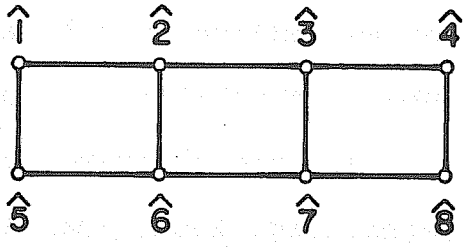

b) DUAL GRAPH

	1	2	3	4	5	6	7	8
1	1	1	0	0	1	0	0	0
2	1	1	1	0	0	1	0	0
3	0	1	1	1	0	0	1	0
4	0	0	1	1	0	0	0	1
5	1	0	0	0	1	1	0	0
6	0	1	0	0	1	0	1	0
7	0	0	1	0	0	1	1	1
8	0	0	0	1	0	0	1	1

b) ADJACENCY MATRIX

FIG. 2.7 GRAPH REPRESENTATION OF AN UNCRACKED STRUCTURE

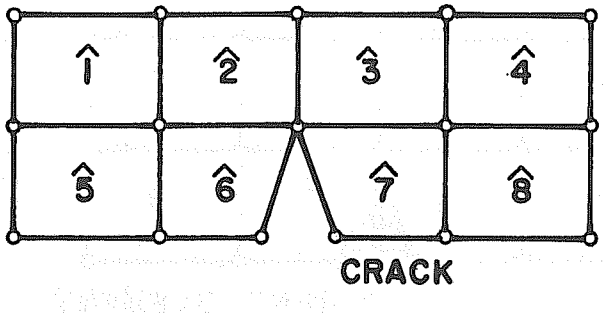

a) CRACKED STRUCTURE

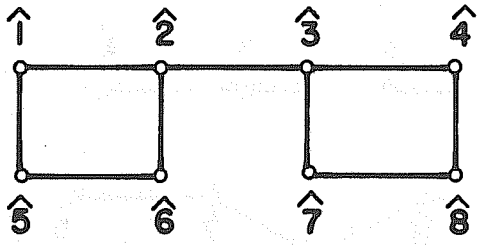

b) DUAL GRAPH

	1	2	3	4	5	6	7	8
1	1	1	0	0	1	0	0	0
2	1	1	1	0	0	1	0	0
3	0	1	1	1	0	0	1	0
4	0	0	1	1	0	0	0	1
5	1	0	0	0	1	1	0	0
6	0	1	0	0	1	1	0	0
7	0	0	1	0	0	0	1	1
8	0	0	0	1	0	0	1	1

c) ADJACENCY MATRIX

FIG. 2.8 GRAPH REPRESENTATION OF A CRACKED STRUCTURE

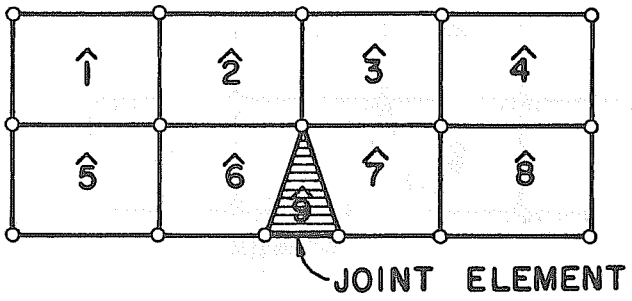

a) CRACKED STRUCTURE WITH JOINT ELEMENT

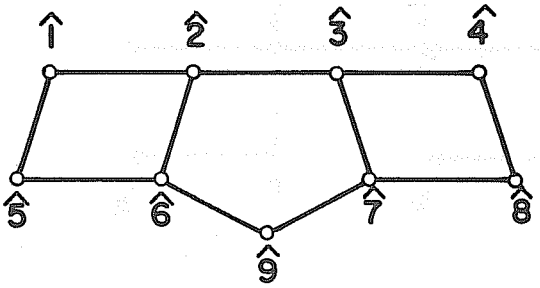

b) DUAL GRAPH

	1	2	3	4	5	6	7	8	9
1	1	1	0	0	1	0	0	0	0
2	1	1	1	0	0	1	0	0	0
3	0	1	1	1	0	0	1	0	0
4	0	0	1	1	0	0	0	1	0
5	1	0	0	0	1	1	0	0	0
6	0	1	0	0	1	1	0	0	1
7	0	0	1	0	0	0	1	1	1
8	0	0	0	1	0	0	1	1	0
9	0	0	0	0	0	1	1	0	1

c) ADJACENCY MATRIX

FIG. 2.9 GRAPH REPRESENTATION OF A CRACKED STRUCTURE WITH JOINT ELEMENT

CHAPTER 3 FRONTAL SOLUTION TECHNIQUE

3.1 Gaussian Elimination and Its Peculiarity

For a linear time-invariant steady-state system, the network equation can be simply described by a matrix equation

$$Y\,x = b \qquad (3.1)$$

where Y is a coefficient matrix, b the known input vector and x the unknown output vector to be determined. It has become clear to engineers today that direct methods of solutions are often preferred to iterative ones [80].

Almost all of the direct methods are based on the concept of triangular decomposition by equivalent transformation of matrices. In recent years, various schemes have been proposed to solve Eq. 3.1 for both structural and electrical network problems. Tocher [81] suggested a selective inversion. The Choleski Decomposition was used by Johnson [82] and Roy [133]. Sato and Tinney [83] carried out the decomposition in terms of elementary matrices. The use of "table of factors" was proposed by Tinney and Walker [84], and was extended to solve large scale structural problems by Jensen and Parks [85]. A LU decomposition, also known as Gaussian-Doolittle Method, was employed by Berry [86]. Melosh and Bamford [87] decomposed the coefficient matrix in a triple product of $LD^{-1}L^{t}$. Whestone [88] used a solution method

based on K-partitioning. The Crout reduction method has been efficiently programmed by Wiberg [89] and further improved by Mondkar and Powell [90]. And many improvements on the solution of banded matrices have been accomplished by Wilson and others [91, 92, 93]. Meyer [94] has summarized the recent advances in this general subject area.

The list of the solution methods may appear to be long. But by taking a closer examination, one can regard all these methods as being a judicious application of the over one and a half century old concept of Gaussian elimination. Elimination, decomposition and reduction are similar in theory. The difference among them is mainly in the sequence of operations. This is particularly true when the coefficient matrix Y is symmetric. For instance, the Crout reduction can be viewed as a scheme of recording the factors of decomposition in the lower triangular matrix L, and differs from the LU decomposition only in the manner of storing the diagonal terms. While the LU decomposition associates the diagonal terms with the upper triangular matrix U, Crout reduction associates the diagonal terms with L. The "table of factors" also bears a great similarity with Crout's method. When the diagonal terms are handled as an individual matrix, then a triple product LDU of the Choleski type can be formed. This triple product can

also assume the form of $LD^{-1}L^{t}$ as proposed by Melosh and Bamford [87]. When the K-partitioning reduces to the order of one, then it is identical to the Gaussian elimination procedure. Another interesting fact is that for a dense coefficient matrix, i.e., where the topological graph of a physical network is complete, it has been shown that no rational operation can take fewer steps for the solution than the Gaussian elimination [95].

3.1.1 Sparsity and Bandedness

Rarely, if ever, is a physical network so strongly connected that its topological graph is a complete graph. This is especially true for structural systems. Therefore, the resulting coefficient matrix Y in Eq. 3.1 is generally sparsely populated, and many efforts have been made to take advantage of this fact in solving such a system of equations. For structural systems, the banded matrix technique is commonly employed in the displacement method of analysis. The minimization of bandwidth is generally achieved by the proper selection of a node-numbering scheme. On the other hand, the topology of electrical networks does not lend itself easily to the banded matrix technique by node numbering. Instead, a so-called sparse matrix technique is often used, such as the ones proposed by Tinney and Walker [84], and by Berry [86].

It should be emphasized once more that both the

banded matrix technique and the sparse matrix technique aim at reducing the computational effort by recognizing the vast numbers of zero entries in the coefficient matrix, and any type of elimination procedure can be employed in both techniques. However, the two techniques are founded on somewhat different concepts: one deals mainly with the minimization of bandwidth and relies heavily on node numbering; the other concerns itself chiefly with the minimization of the number of new entries in the coefficient matrix during the elimination process and generally requires an elaborate bookkeeping scheme. This latter aspect is another peculiarity of the Gaussian elimination procedure, which is often overlooked by most structural analysts.

Consider the network shown in Fig. 3.1a, the system coefficient matrix will have the form of Fig. 3.1b, associated with the given node numbering. After the first row has been processed, the matrix Y has the form of Fig. 3.1c. It can be seen that all of the formerly zero entries are now filled. But if the network is given a different node numbering as shown in Fig. 31d, the resulting Y matrix has a different form as shown in Fig. 3. 1e, and no new non-zero entry is produced after the first row is processed as shown in Fig. 3.1f. These examples demonstrate how the node numbering or operation sequence will affect the matrix sparsity and the over-all

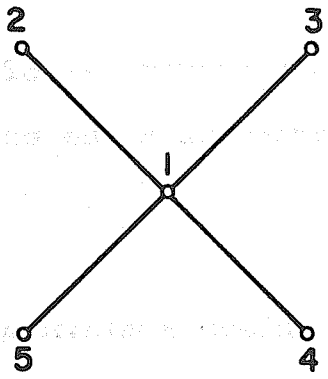

a) EXAMPLE NETWORK

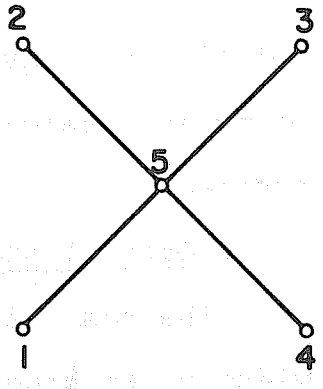

d) DIFFERENT NODE NUMBERING

$$Y = \begin{array}{c} \begin{array}{ccccc} 1 & 2 & 3 & 4 & 5 \end{array} \\ \begin{bmatrix} X & X & X & X & X \\ X & X & & & \\ X & & X & & \\ X & & & X & \\ X & & & & X \end{bmatrix} \end{array}$$

b) COEFFICIENT MATRIX

$$Y = \begin{array}{c} \begin{array}{ccccc} 1 & 2 & 3 & 4 & 5 \end{array} \\ \begin{bmatrix} X & & & & X \\ & X & & & X \\ & & X & & X \\ & & & X & X \\ X & X & X & X & X \end{bmatrix} \end{array}$$

e) COEFFICIENT MATRIX

$$Y' = \begin{bmatrix} D & X & X & X & X \\ & X & X & X & X \\ & X & X & X & X \\ & X & X & X & X \\ & X & X & X & X \end{bmatrix}$$

c) AFTER PROCESSING 1st ROW

$$Y' = \begin{bmatrix} D & & & & X \\ & X & & & X \\ & & X & & X \\ & & & X & X \\ & X & X & X & X \end{bmatrix}$$

f) AFTER PROCESSING 1st ROW

FIG. 3.1 EFFECTS OF NODE ORDERING (AFTER SATO & TINNEY)

solution process. Therefore, the node odering is of prime importance if the solution process is to be economized.

3.1.2 Optimal Node Ordering

The task of node numbering to achieve a minimum bandwidth or to create a minimum number of new entries can sometimes become frustrating even for an experienced analyst. Automatic node numbering algorithms to minimize the bandwidth have been presented by Rosen [96], Akyuz and Utku [97]. Some of the now commercially available structural analysis programs also have this feature built-in. However, the effort expended on minimizing the bandwidth may or may not be rewarding, because the banded matrix technique itself does not always represent an optimal solution. It can easily be shown that the zero entries within the band are rapidly filled [85, 98].

To preserve the sparsity as much as the topology of the network permits, a number of sparse matrix techniques have been developed by various authors [83, 84, 85,96]. In general, node re-numbering in the sparse matrix technique is more elaborate than in the banded matrix technique. It also involves the altering of the actual operation sequence, which no longer follows the natural order of the node numbers. This drastic departure from the banded matrix technique requires a more sophisticated book-keeping scheme.

For networks having a changing topology, the provision of an automatic node re-numbering or reordering capability within a computer program is certainly essential. But in the case of finite element analysis of cracking problems, minimum bandwidth may not be the optimal solution. Node re-ordering such as the one employed in the sparse matrix technique can be shown to be more efficient. To gain a better picture of the effect of re-ordering, graph representation again proves to be very helpful.

3.2 Graph Theoretic Approach

Given a square matrix Y of order n, whose elements are denoted by y_{ij}, an incidence matrix M, whose elements are m_{ij}, can be defined by [99]:

$$m_{ij} = \begin{cases} 0 & \text{if } y_{ij} = 0 \text{ or } i = j \\ 1 & \text{otherwise} \end{cases}$$

From this incidence matrix M, an oriented graph D, sometimes also called directed graph or digraph for short, can be constructed. An example is shown in Fig. 3.2. A few definitions and theorems are now presented to facilitate the discussion [100].

Definition 3.1: A square matrix Y or a digraph D is "incidence-symmetric" if the associated inicidence matrix M is symmetric.

A special class of incidence-symmetric matrices

$$Y = \begin{array}{c} \begin{matrix} V_1 & V_2 & V_3 & V_4 & V_5 & V_6 \end{matrix} \\ \begin{bmatrix} 11 & 0 & -3 & -4 & 11 & 0 \\ 0 & -1 & -1 & 0 & 0 & 0 \\ 0 & 0 & -1 & 0 & 0 & 1 \\ 3 & 5 & -1 & -1 & 2 & 2 \\ 3 & 2 & 0 & -1 & 3 & 1 \\ 0 & 0 & -2 & 0 & 0 & 3 \end{bmatrix} \end{array}$$

$$M = \begin{bmatrix} 0 & 0 & 1 & 1 & 1 & 0 \\ 0 & 0 & 1 & 0 & 0 & 0 \\ 0 & 0 & 0 & 0 & 0 & 1 \\ 1 & 1 & 1 & 0 & 1 & 1 \\ 1 & 1 & 0 & 1 & 0 & 1 \\ 0 & 0 & 1 & 0 & 0 & 0 \end{bmatrix}$$

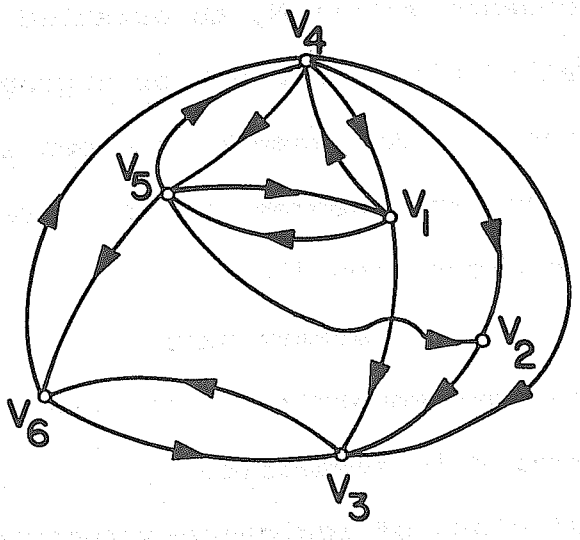

FIG. 3.2 GRAPH REPRESENTATION OF MATRIX (AFTER HARARY)

are the symmetric matrices Y, which are typical for all stiffness matrices dealt with in structural analysis. For this special class of incident-symmetric matrices, an unoriented graph G is sufficient to represent the symmetric matrix Y as shown in Fig. 3.3. This representation will be used exclusively in the present study.

Definition 3.2: The "valency" of a node (or a group of nodes) in a graph G is the number of new paths added among the remaining set of nodes as a result of the elimination of the node (or the group of nodes).

Definition 3.3: The "valency of an ordering" on a given subset of nodes of a graph G is the total number of new paths generated in the process of performing the node elimination in the order specified.

Lemma 3.1 [100]: There is a one-to-one correspondence between valency of a node of a given graph G and the number of new non-zero elements introduced into the associated incidence matrix by the Gaussian elimination of that variable, which is associated with the node, from the system of linear algebraic equations associated with the graph G.

Theorem 3.1 [99]: Upon elimination of x_i from the subsequent equations, the new graph G' of the

remaining system is contained in the graph $\tilde{G}$ obtained from G by:

1) Eliminating the point "i", and

2) Pair-wire connecting (by arcs) all points which were previously connected to "i".

Lemma 3.1 and Theorem 3.1 are quite similar in nature. Lemma 3.1 is due to Ogbuobiri , Tinney and Walker [100]. Theorem 3.1 is given by Parter [99]. Their formal proofs will not be repeated here, but they should be intuitively clear from the inspection of Fig. 3.1. Bree [101] has also presented a similar theorem. Based upon these theorems, graph representation of the Gaussian elimination can then be constructed. As an example, the matrix shown in Fig. 3.3 is reduced step by step in Fig. 3.4 where the heavy branches denote the newly created connecting arcs, or the valency, which correspond to the added entries denoted by C in the matrix. The implication of this elimination process can be further illustrated by the example presented by Jensen and Parks [85] for structural networks.

Consider the network given in Fig. 3.5a, the conventional node numbering scheme produces a banded matrix as shown in Fig. 3.5b. The number of valency of this particular ordering in this graph, i.e. , the total number of the newly created terms C with symmetry accounted for, is found to be eight. If a new order is taken,

1	2	3	4	5	6	7
X	X	X	0	0	X	0
	X	0	0	X	0	0
		X	0	0	0	0
			X	0	0	X
				X	0	X
					X	X
						X

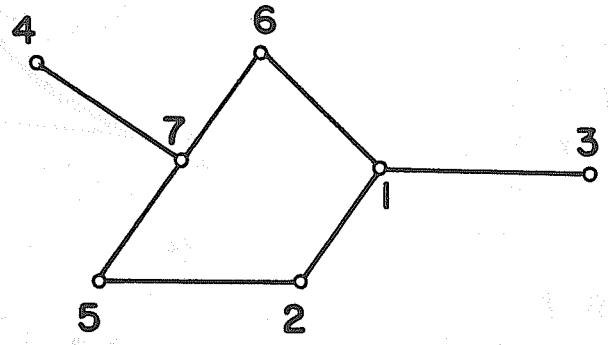

FIG. 3.3 GRAPH REPRESENTATION OF SYMMETRIC MATRIX (AFTER WHESTONE)

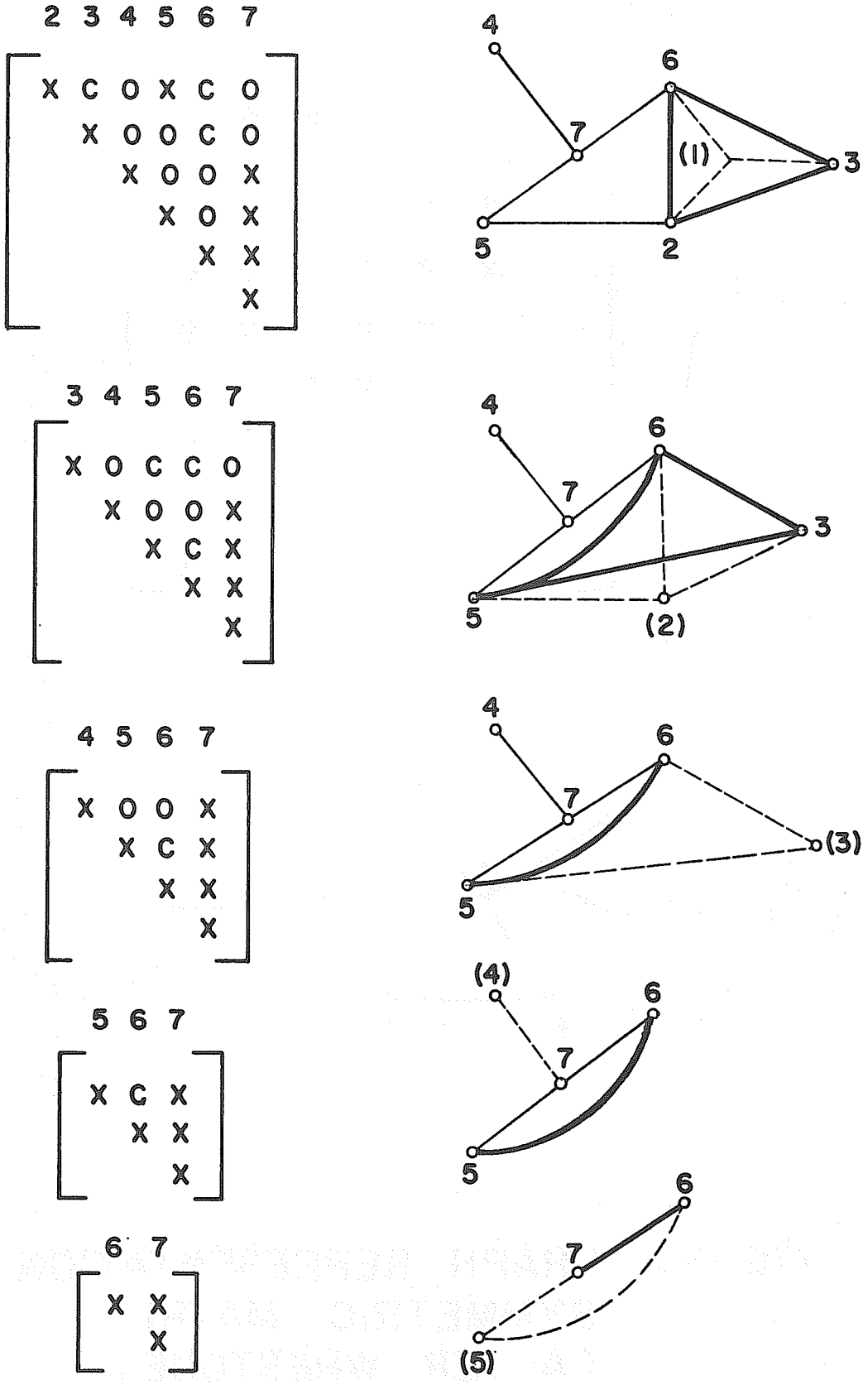

FIG. 3.4 GRAPH REPRESENTATION OF ELIMINATION PROCESS (AFTER WHESTONE)

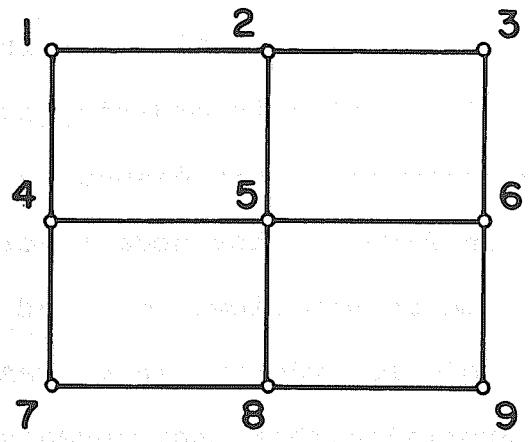

a) GIVEN NETWORK & NODE NUMBERING

1	2	3	4	5	6	7	8	9
X	X		X					
X	X	X	C	X				
	X	X	C	C	X			
X	C	C	X	X	C	X		
	X	C	X	X	X	C	X	
		X	C	X	X	C	C	X
			X	C	C	X	X	C
				X	C	X	X	X
					X	C	X	X

b) BANDED MATRIX

FIG. 3.5 BANDED ORDERED NETWORK (AFTER JENSEN & PARKS)

as shown in Fig. 3.6, the resulting matrix is shown in Fig. 3.7. The valency of this ordering is reduced to five. For large networks, this disparity will usually be much greater in favor of the node re-ordering scheme. This type of scheme is sometimes referred to as optimal or near-optimal node re-ordering in current literature, and it is not surprising that many researchers tackle the solution method for a system of linear equations with the graph theoretic or topological approach [99-109].

For the solution of the crack growth problem in structural system, saving on computational effort can further be realized by the graph theoretic approach. Take, for instance, the network in Fig. 3.8a to simulate a crack in the structure shown previously in Fig. 3.5a. The additional node has to assume the next higher number in sequence, 10 in the present example, because it is generally impractical to re-number all the nodes in the network. From the banded matrix solution standpoint, this inevitably results in an increase of bandwidth, which means more effort and storage are required, as it can be seen that the valency of this particular ordering is increased to eleven. On the other hand, a re-ordering shown in Fig. 3.8b produces only a valency of four, one valency less than the ordering of the previous case shown in Fig. 3.7. This is, indeed, a crucial point in

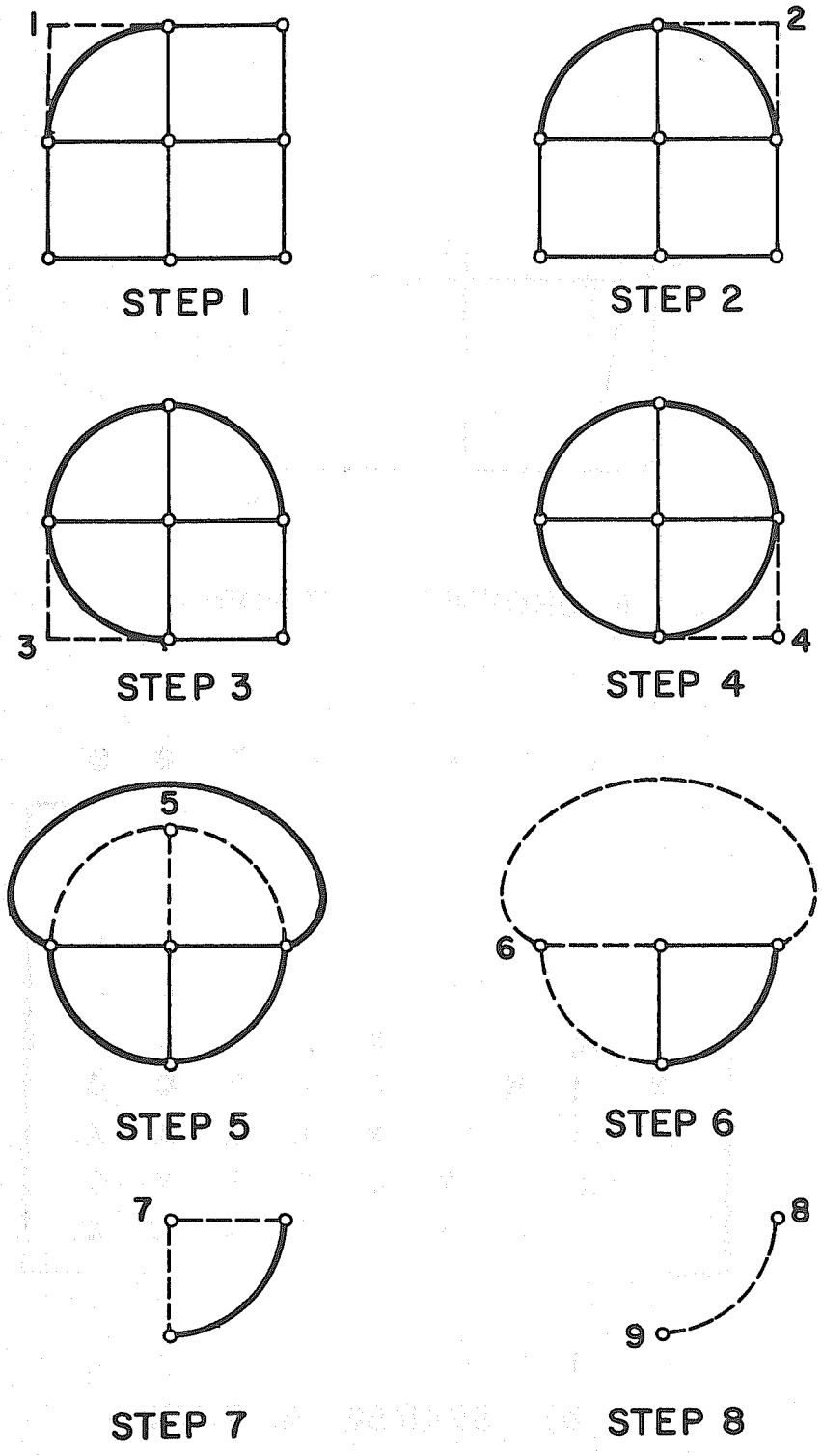

FIG. 3.6 DECOMPOSITION OF NETWORK (AFTER JENSEN & PARKS)

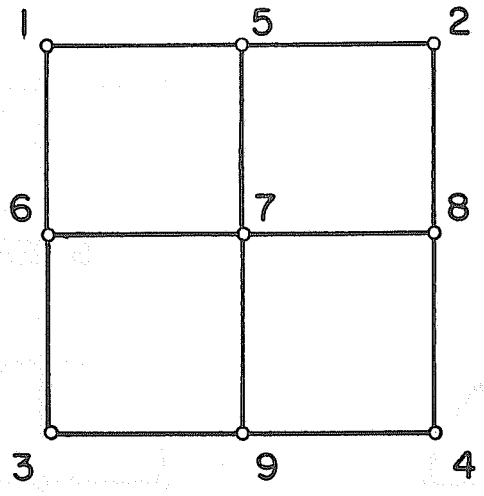

a) REORDERED NETWORK

1	2	3	4	5	6	7	8	9
X				X	X			
	X			X			X	
		X			X			X
			X				X	X
X	X			X	C	X	C	
X		X		C	X	X	C	C
				X	X	X	X	X
	X		X	C	C	X	X	C
		X	X		C	X	C	X

b) SPARSE MATRIX

FIG. 3.7 NEAR-OPTIMAL ORDERED NETWORK (AFTER JENSEN & PARKS)

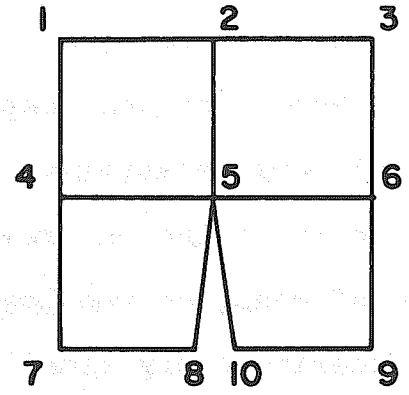

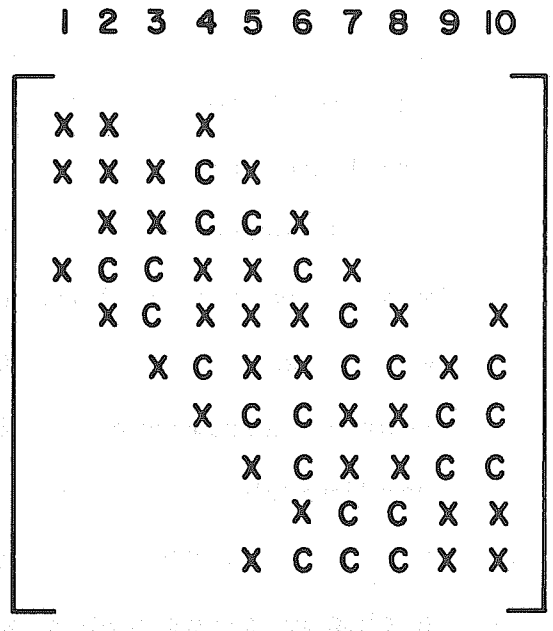

a) BANDED MATRIX TECHNIQUE

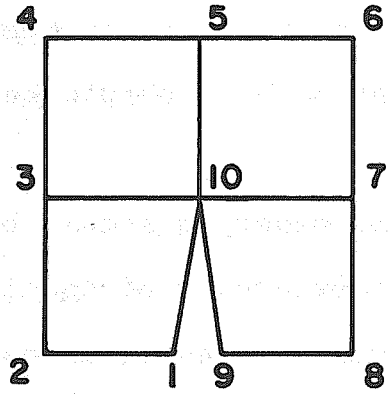

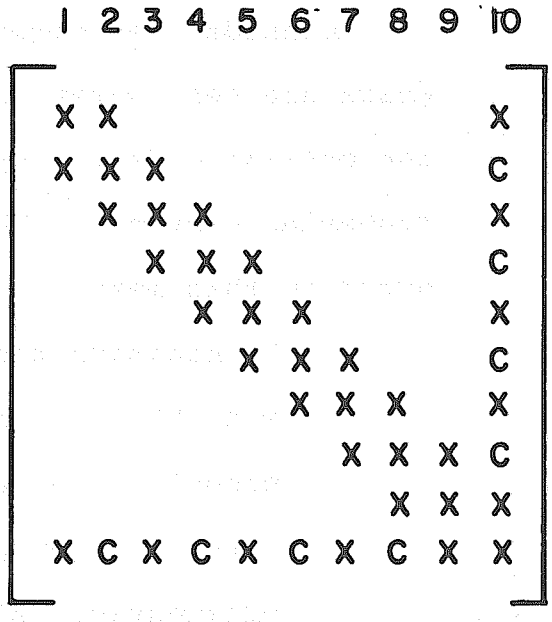

b) SPARSE MATRIX TECHNIQUE

FIG. 3.8 NODE ORDERING FOR CRACKED STRUCTURE

implementing a solution scheme for the analysis of crack growth.

A number of optimal ordering algorithms for the sparse matrix technique have been proposed for networks with fixed topology. Undoubtedly, all such algorithms require additional computer effort in searching and recording the variables. In the case of changing topology, the effort spent in the optimal ordering every time a change takes place may prove to be quite a burden. Fortunately, in most structural problems, the network is rather regular, and near-optimal ordering can generally be achieved by inspection.

Consider the structural networks shown in Fig. 3.9. which are very unfavorable to the banded matrix technique, the optimal ordering by inspection is indicated by the numbering sequence. Three important points should be noted in this method of ordering:

1) To minimize the valency, the ordering should be such that it creates a minimum number of "active nodes". A node becomes "active" when it is connected by a branch (or arc) to the node being eliminated. All the active nodes form an "active front" or "wave front".
2) The ordering process can be thought of as progressing mesh by mesh, as indicated by the mesh numbering.

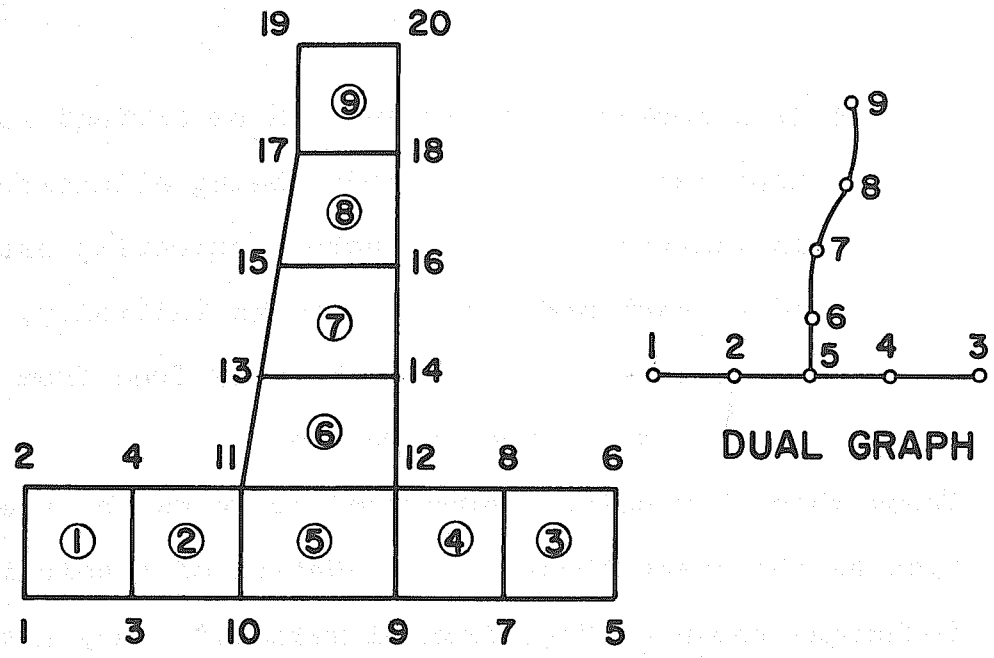

a) BRANCHED STRUCTURE

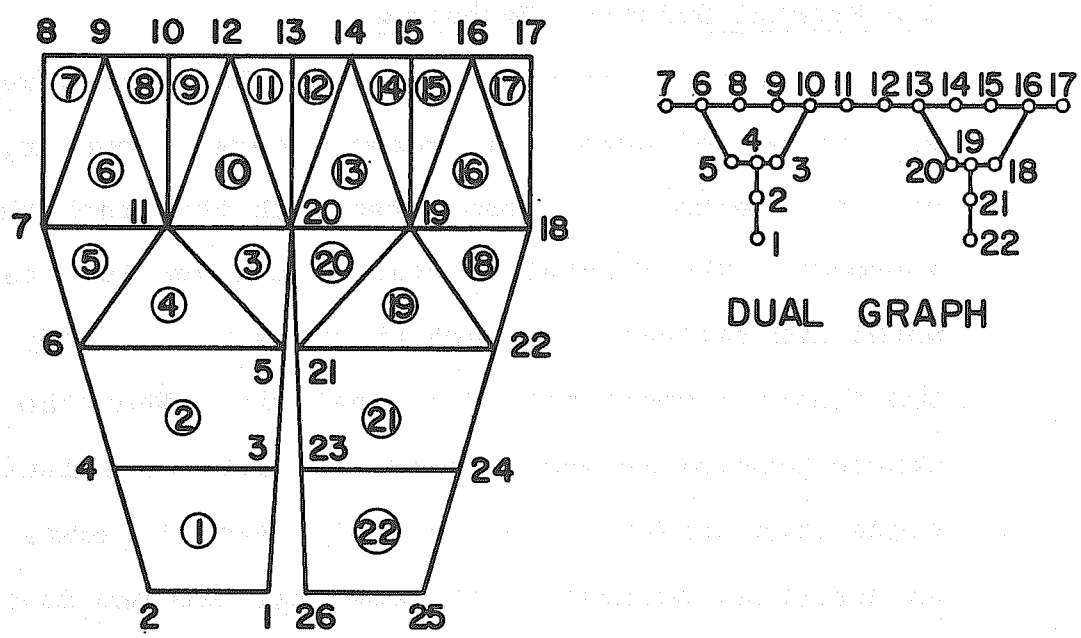

b) CRACKED STRUCTURE

FIG. 3.9 BRANCHED & CRACKED STRUCTURES

3) If a book-keeping scheme can be devised such that the ordering of nodes being eliminated is independent of the actual numbering assigned to each node in the network initially, the solution scheme will be totally free from the constraint of node numbering.

These three key points enumerated above can be viewed upon as the graph theoretic foundation of a solution technique known as "the frontal method." They also provide the prime motivation for adopting a frontal method as the basic solution algorithm in the present study.

3.3 Frontal Solution Technique

The frontal solution technique has been developed by a number of authors in recent years. However, seldom has this method been associated with the graph theoretic approach. The frontal solution technique is a rather novel and rational approach which is suited very well to the finite element method of analysis. When the crack growth problem is encountered, the frontal solution technique even appears to be the only feasible means for such an analysis, because as the computer program developed by Irons [98] has demonstrated, the solution can be completely independent of the node numbering assigned to the structure. In other words, the node numbers are merely node identification symbols, or nicknames as

they are so aptly called by Irons. Thus one can freely modify the topology at any stage of analysis by adding new node numbers anywhere in the structural network without the constraint imposed by bandwidth restriction.

To formulate the frontal solution technique, the first requirement is the description of the structural topology. This can be accomplished by the use of the adjacency matrix. Since each mesh is processed at a time, a pointer array can be established, and hence the ordering of the elimination sequence can also be made independent of the mesh or element numbering. The second requirement is the recording of the incidence relationship between the nodes and the branches or the meshes. Since each finite element is treated as a mesh, the node-mesh incidence provides all the incidence information required. Lastly, and perhaps most imortantly, a clear understanding of the Gaussian elimination process and a systematic method of tracking down the nodes and the valencies are required in order to dispense with the necessity of keeping a large two-dimensional array while working with matrices. An especially important characteristic of the frontal solution technique is that the order of the variables being eliminated is different from the order of the variables being picked up for processing.

Consider the set of equations resulting from the

displacement method of analysis

$$K\ u = P \tag{3.2}$$

where K is the structural stiffness matrix, u the unknown displacements, and P the known nodal loads. The equations obtained from eliminating the variable u_s, using equation e_s in Fig. 3.10, by Gaussian procedure are

$$k^*_{ij} = k_{ij} - \left[k_{sj} \frac{k_{is}}{k_{ss}} \right] \tag{3.3}$$

$$P^*_i = P_i - \left[P_s \frac{k_{is}}{k_{ss}} \right]$$

It was Irons [98] who noted that as long as the equation e_s is complete, i.e., all the contributions from the structural elements to the coefficients k_{is}, k_{sj}, k_{ss} and P_s have been fully accounted for, elimination of the variable u_s can be performed while the contributions to the rest of the coefficients k_{ij} and P_i may or may not have been fully summed. This important recognition of the Gaussian procedure holds the main key to the frontal solution technique. Also note that, due to symmetry of the stiffness matrix K, only the coefficients k_{sj} (j = 1, 2, ..., n) and P_s need by fully summed, because this will automatically imply k_{is} (i = 1,2,...,n) have been fully summed also. Furthermore, since only the upper triangular matrix is stored, the actual coefficients required to compute the quantities within

the brackets in Eq. 3.3 are

k_{is} $(i = 1,....,s)$,

k_{sj} $(j = 1,....,n)$, and

P_s

The coefficients to be modified are also confined to the upper triangular matrix and the column vector P. The various coefficients involved while processing the variable u_s are shown in Fig. 3.10.

All the coefficients k_{ij} and P_i involved in elimination process can be stored in a one-dimensional array within the computer. A scheme has been ingeniously devised by Irons to correlate the element k_{ij} in a matrix to the element k_q in a one-dimensional array. All matrix coefficients are stored columnwise as shown in Fig. 3. 11. This scheme has the advantage of being completely independent of the exact matrix size. Every location of the coefficient is conveniently determined by a Mathematical Statement Function NFUNC(I,J) in Irons' published computer program ZIPP [98].

$$NFUNC(I,J) = I + (J*(J-1))/2 \qquad (3.4)$$

This simple function turns out to be extremely useful. For instance, the location of a coefficient k_{sj} which is below the diagonal is given by NFUNC(J,S); the storage allocation required for the upper triangular matrix of order n x n is given by NFUNC(N,N); the head of each string of coefficients in a column j is given by NFUNC

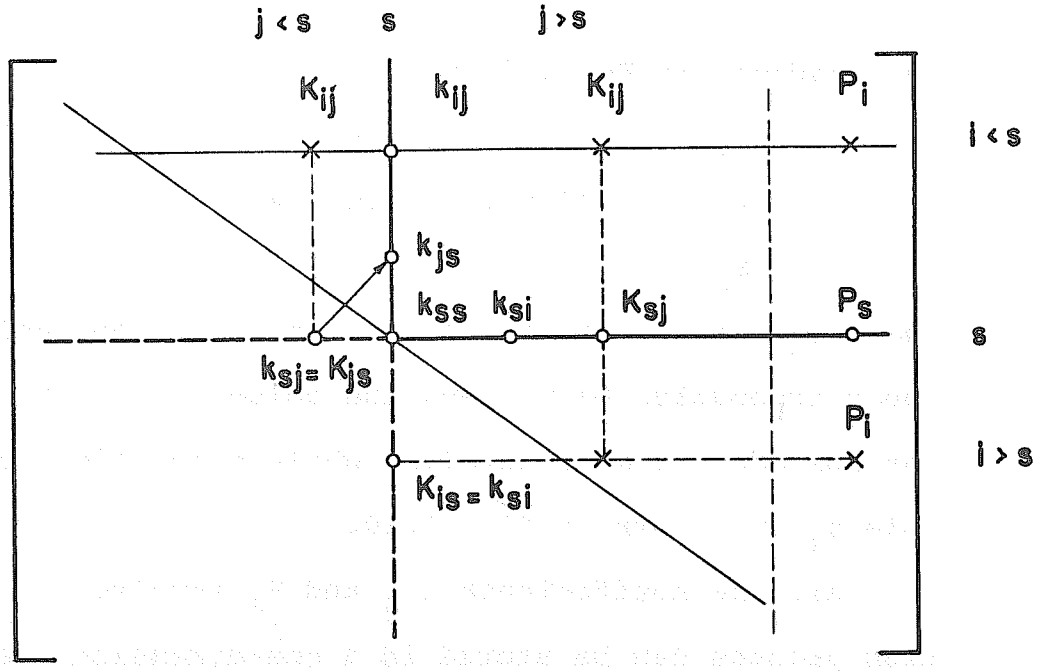

FIG. 3.10 COEFFICIENTS INVOLVED IN THE ELIMINATION PROCESS

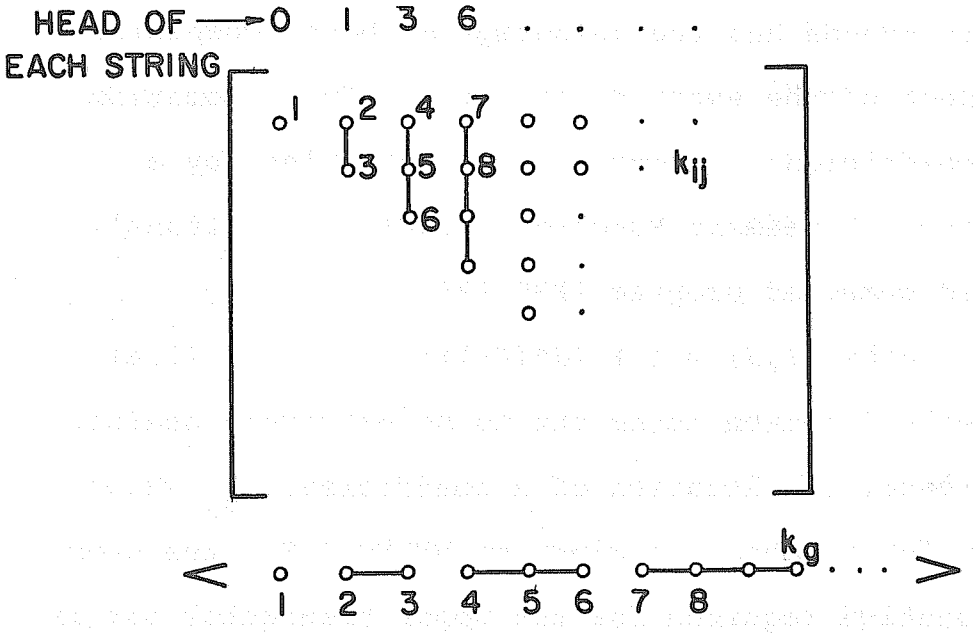

FIG. 3.11 ONE-DIMENSIONAL STORAGE SCHEME FOR UPPER TRIANGULAR MATRIX

(O,J), without the need of knowing the exact size of the matrix that the coefficients belong to.

Irons' program ZIPP, which is well documented and hence will not be repeated here, provides the foundation upon which the computer program developed in the present study is built. However, besides the alteration of input and output formats, several modifications to Irons' original program have been made:

1) The preprogram phase has been eliminated. The destination of each variable is assigned during the element stiffness assembling process instead of in the preprogram phase.
2) CODEST, a subroutine in ZIPP to interpret coded destinations, has been eliminated. Incidence numbers are used in place of the code.
3) Most of the major arrays are dynamically allocated. Therefore, the mathematical statement function NFUNC(I,J) in ZIPP is altered slightly and replaced by a new function

   LOCATE(I,J,K) = I + (J*(J-1))/2 + K

   where K is the starting location.
4) Multiple degrees of freedom per node are added.
5) Global loads are associated with nodal points rather than with individual elements. Therefore, no summing of load vectors is necessary. However, elements with an initial load such as in the

case of prestressing are also made possible.

6) Prescribed displacement boundary conditions are allowed and reactions are recovered.

7) The construction of the Choleski decomposition U^tU from the frontal solution technique has been made optional.

8) ECS (Extended Core Storage) and Disk File are used to serve as a two level I/O. Thus the time-consuming BACKSPACE-READ-BACKSPACE procedure is avoided.

9) To further save core storage space and to allow for partially format-free inputs, bit manipulation and string processing techniques are used, which necessitate the use of assembly language programming.

Some of these modifications will be discussed subsequently.

3.4 Treatment of Displacement Boundary Conditions and Recovery of Reactions

Simultaneous imposition of non-zero prescribed loads and displacements, and the recovery of reactions can be accomplished in various ways. The commonly employed method is to modify the load vector. Consider the set of equations shown in matrix form

$$\begin{bmatrix} K_{11} & K_{12} & K_{13} \\ K_{21} & K_{22} & K_{23} \\ K_{31} & K_{32} & K_{33} \end{bmatrix} \begin{bmatrix} u_1 \\ \bar{u}_2 \\ u_3 \end{bmatrix} = \begin{bmatrix} \bar{P}_1 \\ P_2 \\ \bar{P}_3 \end{bmatrix} \qquad (3.5)$$

adopting the notations of Melosh and Bamford [87] in which K_{ij} are stiffness coefficients; u_i and P_i are displacement and force components to be determined; and $\bar{u}_i$ and $\bar{P}_i$ are prescribed displacement and force components, respectively. If the values of reactions need not be computed, Eq. 3.5 can be simply rewritten in the form of

$$\begin{bmatrix} K_{11} & 0 & K_{13} \\ 0 & 1 & 0 \\ K_{31} & 0 & K_{33} \end{bmatrix} \begin{bmatrix} u_1 \\ \bar{u}_2 \\ u_3 \end{bmatrix} = \begin{bmatrix} \bar{P}_1 \\ 0 \\ \bar{P}_3 \end{bmatrix} + \begin{bmatrix} -K_{12} \\ 1 \\ -K_{32} \end{bmatrix} \bar{u}_2 \qquad (3.6)$$

Note that if $\bar{u}_2 = 0$, the equation and the terms associated with $\bar{u}_2$ are simply deleted without any modification to the load vector. When the values of reactions are desired, Eq. 3.5 can be modified as

$$\begin{bmatrix} K_{11} & 0 & K_{13} \\ K_{21} & -1 & K_{23} \\ K_{31} & 0 & K_{33} \end{bmatrix} \begin{bmatrix} u_1 \\ P_2 \\ u_3 \end{bmatrix} = \begin{bmatrix} \bar{P}_1 \\ 0 \\ \bar{P}_3 \end{bmatrix} + \begin{bmatrix} -K_{12} \\ -K_{22} \\ -K_{32} \end{bmatrix} \bar{u}_2 \qquad (3.7)$$

Alternately, Irons [98] and Wilson [90] have suggested a large coefficient, k^n say, be added to each of the

equations associated with a prescribed displacement. This procedure can be illustrated as follows, using Eq. 3.5 as an example:

$$\begin{bmatrix} K_{11} & K_{12} & K_{13} \\ K_{21} & (K_{22}+k^n) & K_{23} \\ K_{31} & K_{32} & K_{33} \end{bmatrix} \begin{bmatrix} u_1^* \\ x \\ u_3^* \end{bmatrix} = \begin{bmatrix} \bar{P}_1 \\ k^n \bar{u}_2 \\ \bar{P}_3 \end{bmatrix} \tag{3.8}$$

This will yield an x in the order of k^{-n}, and u_i with an error also in the order of k^{-n}. The reaction P can be obtained by comparing Eq. 3.8 with Eq. 3.7, i.e.,

$$K_{21}\, u_1 - P_2 + K_{33}\, u_3 = -K_{22}\, \bar{u}_2$$

$$K_{21}\, u_1^* + (K_{22} + k^n)\, x + K_{33}\, u_3^* = k^n\, \bar{u}_2$$

Since $u_1^* \simeq u_i$ for $k^n >> K_{ij}$

$$P_2 \simeq (K_{22} + k^n)\ (\bar{u}_2 - x) \tag{3.9}$$

However, in terms of the frontal solution technique, a method proposed by Melosh and Bamford [87] is much more natural and can be effectively incorporated into Irons' frontal solution program ZIPP for the treatment of displacement boundary conditions and to recover the reactions.

Instead of applying Gaussian elimination directly, as done by Irons, the stiffness matrix K of Eq. 3.2 is decomposed into a triple product by Melosh and Bamford

$$L\, D^{-1}\, L^t\, u = P$$

or in expanded form

$$\begin{bmatrix} L_{11} & 0 & 0 \\ L_{21} & L_{22}^t & 0 \\ L_{31} & L_{32} & L_{33} \end{bmatrix} \begin{bmatrix} D_{11}^{-1} & 0 & 0 \\ 0 & D_{22}^{-1} & 0 \\ 0 & 0 & D_{33}^{-1} \end{bmatrix} \begin{bmatrix} L_{11}^t & L_{21}^t & L_{31}^t \\ 0 & L_{22}^t & L_{32}^t \\ 0 & 0 & L_{33}^t \end{bmatrix} \begin{bmatrix} u_1 \\ u_2 \\ u_3 \end{bmatrix} = \begin{bmatrix} \bar{P}_1 \\ P_2 \\ \bar{P}_3 \end{bmatrix} \tag{3.10}$$

where L is a lower triangular matrix whose elements are given by

$$L_{ij} = K_{ij} - \sum_{h=1}^{i-1} \frac{L_{nj}\, L_{ni}}{L_{nn}} \quad ; \quad i \leq j$$

and D is a diagonal matrix whose elements D_{ii} are equal to the diagonal elements of L. The general solution procedure for this type of decomposition is to let

$$\begin{aligned} y &= D^{-1}\, L^t\, u \\ \text{and} \quad Ly &= P \qquad (3.11) \\ \text{or} \quad y &= L^{-1}\, P \end{aligned}$$

Since L is a triangular matrix, a "forward substitution" will yield y, and a "backward substitution" will

yield the required displacements u.

In order to avoid modifying the whole set of equations when prescribed displacements are encountered, such as in the cases of Eqs. 3.6 and 3.7, Melosh and Bamford recast Eq. 3.10 into

$$\begin{bmatrix} L_{11} & 0 & 0 \\ L_{21} & I & 0 \\ L_{31} & 0 & L_{33} \end{bmatrix} \begin{bmatrix} D_{11}^{-1} & 0 & 0 \\ 0 & D_{22}^{-1} & 0 \\ 0 & 0 & D_{33}^{-1} \end{bmatrix} \begin{bmatrix} L_{11}^{t} & L_{21}^{t} & L_{31}^{t} \\ 0 & K_{22}-L_{22}D_{11}^{-1}L_{21}^{t} & K_{23}-L_{21}D_{11}^{-1}L_{31}^{t} \\ 0 & 0 & K_{33}-L_{31}D_{11}^{-1}L_{31}^{t} \end{bmatrix} \begin{bmatrix} u_1 \\ \bar{u}_2 \\ u_3 \end{bmatrix}$$

$$= \begin{bmatrix} \bar{P}_1 \\ P_2 \\ \bar{P}_3 - (K_{33} - L_{31} D_{11}^{-1} L_{21}^{t})\ \bar{u}_2 \end{bmatrix} \qquad (3.12)$$

It can be seen that the equation preceding $\bar{u}_2$ is left undisturbed. This is an utmost crucial point in the frontal solution technique. A careful examination of Eq. 3.12 and the general procedure of treating the prescribed boundary conditions proposed by Melosh and Bamford suggests that transference to the Gaussian elimination process employed by Irons is quite plausible. The steps in the solution of Eq. 3.12 are recapitulated here.

1) Perform the decomposition of each row and distribution of its contribution to the following rows

of the stiffness matrix, until a row of the stiffness matrix associated with a particular prescribed displacement is reached.

2) At this particular instance, the data in core are

$$\begin{bmatrix} K_{22} - L_{21} D_{11}^{-1} L_{21}^{t} & K_{23} - L_{21} D_{11}^{-1} L_{31}^{t} \\ 0 & - L_{31} D_{11}^{-1} L_{31}^{t} \end{bmatrix} \tag{3.13}$$

The row vector $[\, K_{22} - L_{21} D_{11}^{-1} L_{21}^{t} \,,\, K_{33} - L_{21} D_{11}^{-1} L_{31}^{t} \,]$ is written out without further change.

3) Continue the decomposition of the remaining row to produce L_{33} .

4) Perform forward substitution, using the first set of decomposition rows one at a time until a constrained displacement is encountered. The available data in the core are

$$\begin{bmatrix} y_1 \\ -L_{21}\, y_1 \\ -L_{31}\, y_1 \end{bmatrix} \tag{3.14}$$

where $y_1 = L_{11}^{-1} \bar{P}_1$

5) When a constrained displacement is encountered, the reaction is given by the second row of Eq. 3.12 as modified by the inverse multplication, this is

$$\left[K_{22} - L_{21}D_{11}^{-1}L_{21}^{t} \;,\; K_{23} - L_{21}D_{11}^{-1}L_{31}^{t} \right] \begin{bmatrix} \bar{u}_2 \\ u_3 \end{bmatrix} = P_2 - L_{21}y_1 \tag{3.15}$$

The partitions on the left-hand side of Eq. 3.15 defining the contribution to following rows, and the contribution of prior rows on the right-hand side, $-L_{21}\ y$, can be written in an auxiliary storage. The boundary condition u_2 is read in to replace $-L_{21}\ y$, and the contribution of the restrained row to following rows is distributed.

6) Forward substitution of the remaining rows of the decomposition and boundary condition matrix, as in step 4 to produce

$$y_3 = L_{33}^{-1}\left[\bar{P}_3 - K_{32}\bar{u}_2 + L_{31}D_{11}^{-1}L_{21}^{t}\bar{u}_2 - L_{31}y_1 \right] \tag{3.16}$$

7) Perform backward substitutions in reverse order and operate on y_3 to yield

$$u_3 = \left[L_{33}^{t} \right]^{-1} D_{33}y_3 \tag{3.17}$$

8) When constrained rows of the decomposition are encountered, the $\bar{u}_2$, u_3 contribution to reactions (left-hand side of Eq. 3.15) are calculated and written on auxiliary storage.

9) The backward substitution continues to define the unknown u_1, with $\bar{u}_2$ and u_3 known,

$$u_1 = \left[L_{11}^{t} \right]^{-1} D_{11}\left[y_1 - L_{21}^{t}\bar{u}_2 - L_{31}^{t}u_3 \right] \tag{3.18}$$

10) The forward and backward contributions to the reaction are summed.

The steps outlined above suggest a way of treating the displacement boundary conditions to be incorporated into Irons' frontal solution program ZIPP. Using the original notation in Irons' paper, the Gaussian process employed by Irons to eliminate x_s, using equation e_s, is

$$C_{ij}^{*} = C_{ij} - \frac{C_{is}\, C_{sj}}{C_{ss}}$$
$$X_i^{*} = X_i - \frac{C_{is}\, X_s}{C_{ss}} \qquad (3.19)$$

for a set of equations

$$C\, x = X \qquad (3.20)$$

To see how the two solution methods are equivalent, expand the K matrix in Eq. 3.5 into triple product of $LD^{-1}L$

$$\begin{bmatrix} K_{11} & K_{12} & K_{13} \\ K_{21} & K_{22} & K_{23} \\ K_{31} & K_{32} & K_{33} \end{bmatrix} = \begin{bmatrix} L_{11} & 0 & 0 \\ L_{21} & L_{22} & 0 \\ L_{31} & L_{32} & L_{33} \end{bmatrix} \begin{bmatrix} D_{11}^{-1} & 0 & 0 \\ 0 & D_{22}^{-1} & 0 \\ 0 & 0 & D_{33}^{-1} \end{bmatrix} \begin{bmatrix} L_{11}^{t} & L_{21}^{t} & L_{31}^{t} \\ 0 & L_{22}^{t} & L_{32}^{t} \\ 0 & 0 & L_{33}^{t} \end{bmatrix} \qquad (3.21)$$

Carry out the multiplication to express K_{ij} in terms of $L_{ij}\, D_{ii}^{-1}\, L_{ij}^{t}$

$$K_{11} = L_{11}\, D_{11}^{-1}\, L_{11}^{t}$$
$$K_{12} = K_{21} = L_{11}\, D_{11}^{-1}\, L_{21}^{t}$$
$$K_{13} = K_{31} = L_{11}\, D_{11}^{-1}\, L_{31}^{t}$$
$$K_{22} = L_{21}\, D_{11}^{-1}\, L_{21}^{t} + L_{22}\, D_{22}^{-1}\, L_{22}^{t}$$

$$K_{23} = K_{32} = K_{21}\, D_{11}^{-1}\, L_{31} + L_{22}\, D_{22}^{-1}\, L_{32}^{t}$$
$$K_{33} = L_{31}\, D_{11}^{-1}\, L_{31}^{t} + L_{32}\, D_{22}^{-1}\, L_{32}^{t} + L_{33}\, D_{33}^{-1}\, L_{33}^{t}$$

(3.22)

Again, carry out the matrix multiplications in Eq. 3.12 to obtain

$$\begin{bmatrix} L_{11}\, D_{11}^{-1}\, L_{11}^{t} & L_{11}\, D_{11}^{-1}\, L_{21}^{t} & L_{11}\, D_{11}^{-1}\, L_{31}^{t} \\ L_{21}\, D_{11}^{-1}\, L_{11}^{t} & K_{22} & K_{23} \\ L_{31}\, D_{11}^{-1}\, L_{11}^{t} & K_{32} & K_{33} \end{bmatrix} \begin{bmatrix} u_1 \\ \bar{u}_2 \\ u_3 \end{bmatrix} = \begin{bmatrix} \bar{P}_1 \\ P_2 \\ \bar{P}_3 \end{bmatrix}$$

(3.23)

by comparing Eq. 3.23 with Eq. 3.22, it can be seen that Eq. 3.23 merely states that the first row and first column have been decomposed. Note that there exists the relationships

$$L_{ii}\, D_{ii}^{-1} = D_{ii}\, L_{ii}^{t} = I$$

and

$$L_{i1} = K_{i1} = K_{1j} = L_{1j} \qquad (3.24)$$

Perform the Gaussian elimination on Eq. 3.12 to obtain

$$\begin{bmatrix} L_{11} & L_{21}^{t} & L_{31}^{t} \\ 0 & K_{22} - L_{21} D_{11}^{-1} L_{21}^{t} & K_{23} - L_{21} D_{11}^{-1} L_{31}^{t} \\ 0 & K_{32} - L_{31} D_{11}^{-1} L_{21}^{t} & K_{33} - L_{31} D_{11}^{-1} L_{31}^{t} \end{bmatrix} \begin{bmatrix} u_1 \\ \bar{u}_2 \\ u_3 \end{bmatrix} = \begin{bmatrix} y_1 \\ P_2 - L_{21} y_1 \\ \bar{P}_3 - L_{31} y_1 \end{bmatrix}$$

(3.25)

where $y_1 = L_{11}^{-1}\, \bar{P}_1$. It should be clear that from Eq. 3.25

$$C_{ij} - \frac{C_{is}\, C_{sj}}{C_{ss}} = K_{ij} - L_{is}\, D_{ii}^{-1}\, L_{sj}$$

This identity indicates that the elimination procedure of Irons is equivalent to the "decomposition" procedure of Melosh and Bamford.

Since the second equation involves a known displacement, no decomposition is necessary. But it should be noted that, as pointed out by Melosh and Bamford, the term $-L_{21}\, y_1$ is the contribution from above $\bar{u}_2$ to P_2, and $(K_{22} - L_{21}D_{11}^{-1}L_{21}^{t} , K_{23} - L_{21}D_{11}^{-1}L_{31}^{t})$ are the contributions from below $\bar{u}_2$ to P_2. Therefore, they are stored as if a second equation, along with the first one.

The third row of Eq. 3.25 can be written as

$$(K_{32} - L_{31}D_{11}^{-1}L^{t})\ \bar{u}_2 + (K_{33} - L_{31}D_{11}^{-1}L_{31}^{t})\ u_3 = \bar{P}_3 - L_{31}y_1$$

or

$$(K_{33} - L_{31}D_{11}^{-1}L_{31}^{t})u_3 = \bar{P}_3 - L_{31}y_1 - (K_{32} - L_{31}D_{11}^{-1}L_{21}^{t})\ \bar{u}_2 \qquad (3.26)$$

where the right-hand side can immediately be recognized as being equal to $L_{33}\, y_3$ in Eq. 3.16. Now, u_3 can be readily obtained by

$$u_3 = [\ K_{33} - L_{31}D_{11}^{-1}L_{31}^{t}]^{-1} \left\{ \bar{P}_3 - L_{31}y_1 - (K_{32} - L_{31}D_{11}^{-1}L_{21}^{t})\ \bar{u}_2 \right\} \qquad (3.27)$$

which is equal to Eq. 3.17, if k_{33} is substituted by the quantity shown in Eq. 3.22 without the contribution of the $L_{32}\ D_{22}^{-1}\ L_{32}^{t}$ term.

The reaction P_2 is calculated from

$$[\, K_{22} - L_{21}D_{11}^{-1}L_{31}^{t}\,]\ \bar{u}_2 = P_2 + \{-L_{21}y_1\} - (K_{23} - L_{21}D_{11}^{-1}L_{31}^{t})\ u_3 \tag{3.28}$$

and u_1 from

$$[\, L_{31}^{t}\,]\ u_1 = \{y_1\} - (L_{21}^{t})\ \bar{u}_2 - (L_{31}^{t})\ u_3 \tag{3.29}$$

What should be observed is the striking similarity in pattern among Eqs. 3.27, 3.28 and 3.29. If the quantities within the curly brackets are stored as the right-hand side, called CONST, the quantities within the parentheses are the left-hand side coefficients being stored as C(I) , regardless whether or not the equation is associated with a known or unknown displacement, and the quantity in the square brackets is called PIVOT, then the simple backward substitution algorithm in ZIPP holds for all cases, namely,

```
      DO 10 I = N, M
      CONST = CONST - C(I)*U(I)          (3.30)
   10 CONTINUE
```

where N and M indicate the range of back substitution, C(I) and U(I) are the coefficients and the known displacements, respectively. To obtain the displacement component u_i , called ANSWER, it only needs to carry out

```
ANSWER = CONST/PIVOT                     (3.31)
```

If it is for a reaction, called REACT, for which the

displacement is prescribed

$$\text{ANSWER} = \bar{u}_2$$

and $$\text{REACT} = \text{ANSWER}*\text{PIVOT} - \text{CONST}$$

which should be evident from Eq. 3.28. Therefore, the procedure developed by Melosh and Bamford fits nicely into the program developed by Irons to handle prescribed boundary conditions and to recover reactions in a very straightforward manner, once the similarity and the equivalency between the two procedures are recognized.

CHAPTER 4 ANALYSIS OF PROGRESSIVE CRACK GROWTH

4.1 Finite Element Model

A number of finite element models have been constructed by various authors around the world for studies of reinforced and prestressed concrete structural systems, and some of these models have been mentioned in Sec. 1.2 of this thesis. For plane structures, the basic components of the finite element model generally consist of two-dimensional elements, one-dimensional bar elements, link elements and bond elements. The degrees of freedoms per node are limited to two in-plane displacement components. The two-dimensional finite element can be used to represent the concrete structure proper, and occasionally to represent the main steel reinforcement when shearing stress in the main steel reinforcement is of interest. The one-dimensional bar element can be used to represent the web reinforcement, prestressing strand, or main reinforcement, when only the uniaxial effect is to be simulated. The link or linkage element is physically dimensionless, but is capable of providing a structural connection between two nodal points, while at the same time permitting certain degrees of relative movement between them. Thus the link element can be used to model bonding between the concrete and the steel reinforcement, interlocking

across two cracked planes, or simply as a connecting device at discrete points in the structure. The bond element was originated from the study of jointed rock in the field of rock mechanics. It can be considered as an extension of the link element. Being physically dimensionless, it serves the same purpose as the link element, except that connection is distributed along a line rather than concentrated at a point. This added feature makes the bond element an ideal joint element in the conceptual model proposed earlier in Sec. 1.4.

The types of element employed in the present study will be described in the following sections.

4.1.1 Isoparametric Quadrilateral Element with 4 to 8 Nodes

The isoparametric two-dimensional quadrilateral element developed by Bathe, Ozdemir and Wilson [110] is shown in Fig. 4.1a, with its square mapping onto the "parent" element shown in Fig. 4.1b. Nodal points 1 to 4 are mandatory. Nodal points 5 to 8 may be included in any arbitrary manner to form the so-called "hierachical" elements. This higher order element, of course, produces better results. But at the same time, it requires more computational effort. This novel feature of being able to have a mid-node at any side offers added convenience in the gradation of mesh size within a particular layout. Formulation of the element stiffness is presented in Appendix I(a).

With this isoparametric element, plane stress, plane strain or axisymmetric analysis can be performed by simply specifying the corresponding constitutive relationship to be used.

4.1.2 Triangular Element by Degeneration

The isoparametric quadrilateral element developed by Bathe et al. can be degenerated to a constant strain triangular element if node 3 and node 4 are given the same coordinates, Fig. 4.1c. The assignment of the coordinates for node 4, however, is taken care of automatically in the present program. Therefore, plane stress, plane strain and axisymmetric constant strain triangular finite elements are made available in the manner as if they were ordinary triangular elements with three nodal points.

4.1.3 One-Dimensional Bar Elements

The one-dimensional axial bar or truss element is a very common type of structural element and its element stiffness matrix is well-known, Fig. 4.2. However, to be consistent with the present finite element development, the stiffness of a bar element having two or three nodal points is derived in a manner similar to the isoparametric element in Appendix I(b). In the present study, a bar element with only two nodal points is used, and initial stress is permitted in this type of element for the simulation of prestressing force.

4.1.4 Link Element

The link element was first published by Ngo and Scordelis [9] to simulate the effect of bonding and bond slip, Fig. 4.3. The basic concept is to derive an element whose stiffness characteristic is independent of its physical dimensions such as cross-sectional area and length. This is made possible by a direct appeal to the constitutive equation. A "spring constant" is assigned in place of the stress-strain relationship and hence neither the derivative of the shape functions nor the integration over the length of any particular direction is required. Formulation of this link element stiffness is reproduced in Appendix I(c).

4.1.5 Bond Element

Following the same basic concept of the link element, Goodman, Taylor and Brekke [111] later developed a joint element which assumes the shape of a line instead of a point, Fig. 4.4. While the link element can be considered to be a lumped stiffness element, the bond element is a distributed stiffness element along a straight line. Therefore, the spring constant assigned to bond element is on the basis of per unit length. Again, as for the bar element, its stiffness can be derived in a manner parallel to the isoparametric element, for a four or six node element as shown in Appendix I(d). Only the four-node element is used in the present study.

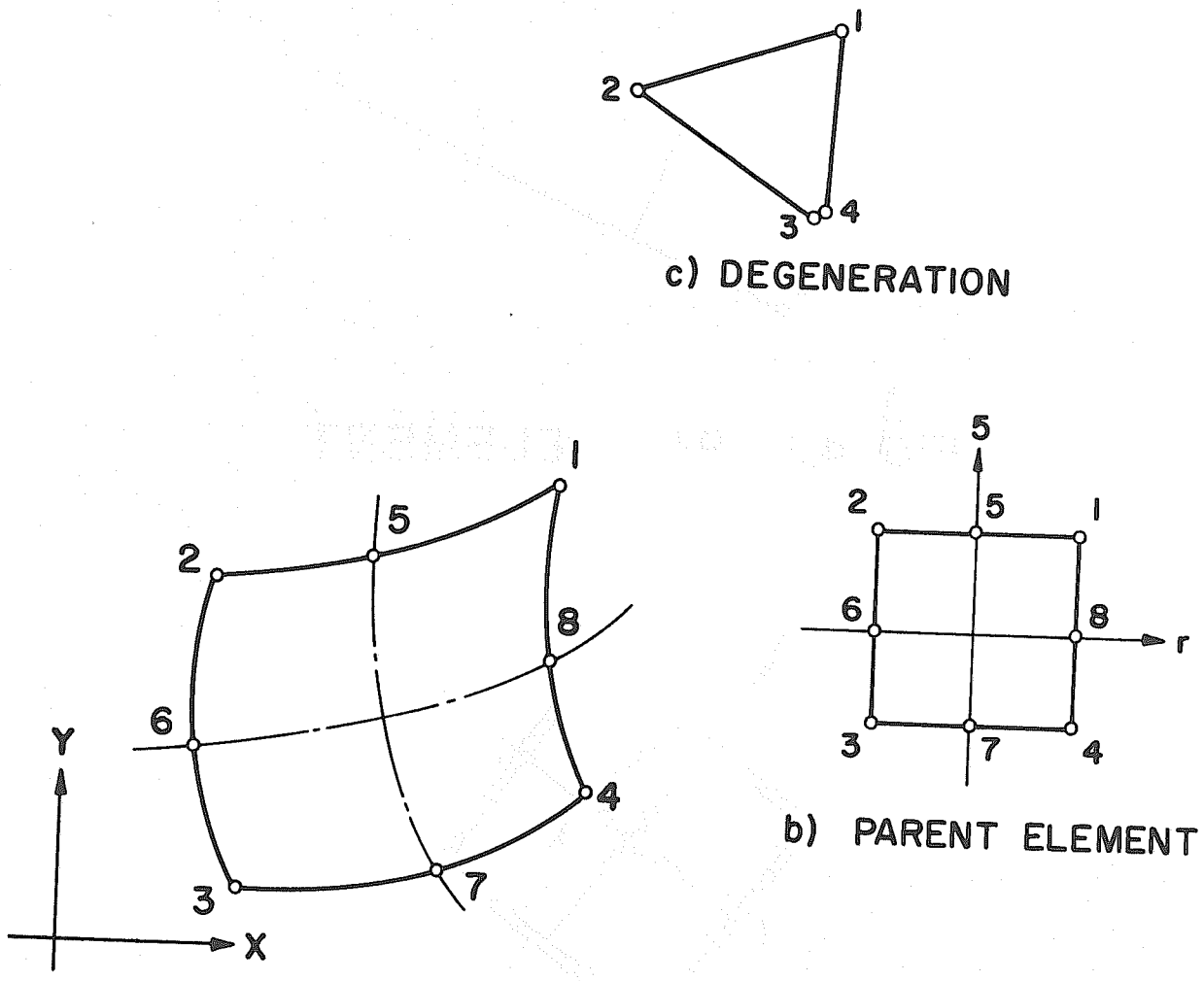

FIG. 4.1 ISOPARAMETRIC QUADRILATERAL ELEMENT

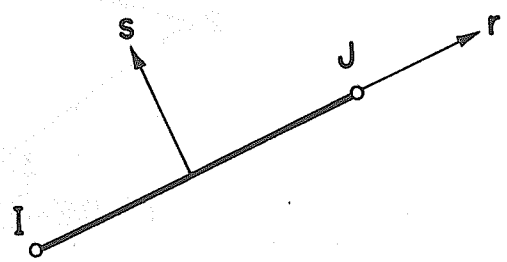

FIG. 4.2 BAR ELEMENT

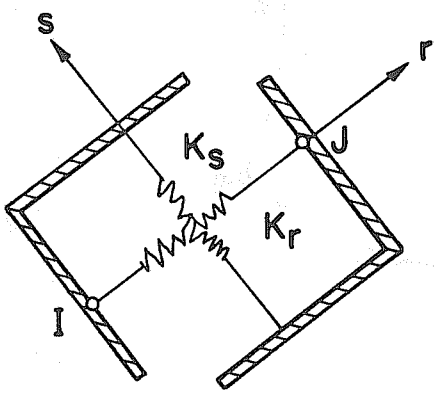

FIG. 4.3 LINK ELEMENT

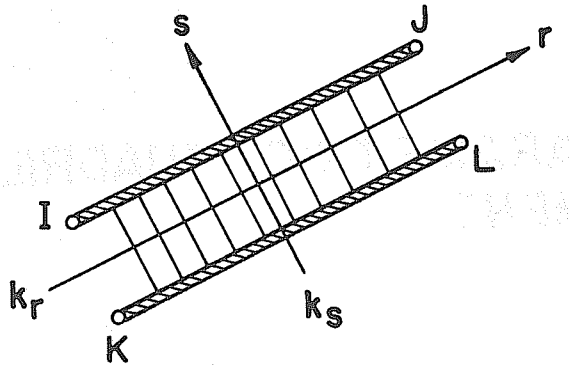

FIG. 4.4 BOND ELEMENT

4.2 Simulation of Crack Growth

As stated earlier, one of the main objectives in the present study is to develop a computer method which is capable of analyzing cracking problems by automatically introducing crack-lines into a two dimensional solid, using the finite element model. Therefore, some "ground rules" must first be laid. This involves the setting of the criteria for three major phases, namely, 1) crack initiation; 2) crack propagation; and 3) crack stabilization.

In what follows, a set of simplified rules is adopted for the sake of convenience in developing the "crack growth" procedure.

4.2.1 Crack Initiation

The prediction of where a crack will initiate is based on the conventional concept of failure criteria. Throughout the years, many failure criteria have been developed for concrete structures by various authors. See, for instance, a recent summary given by Argyris et al. [30] in connection with the finite element analysis of prestressed concrete reactor vessels.

For the present study, the simple failure criterion adopted is shown in Fig. 4.5. It offers simplicity in checking every point for potential crack initiation, once the principal stresses at every discrete point of the structure have been computed. If the principal

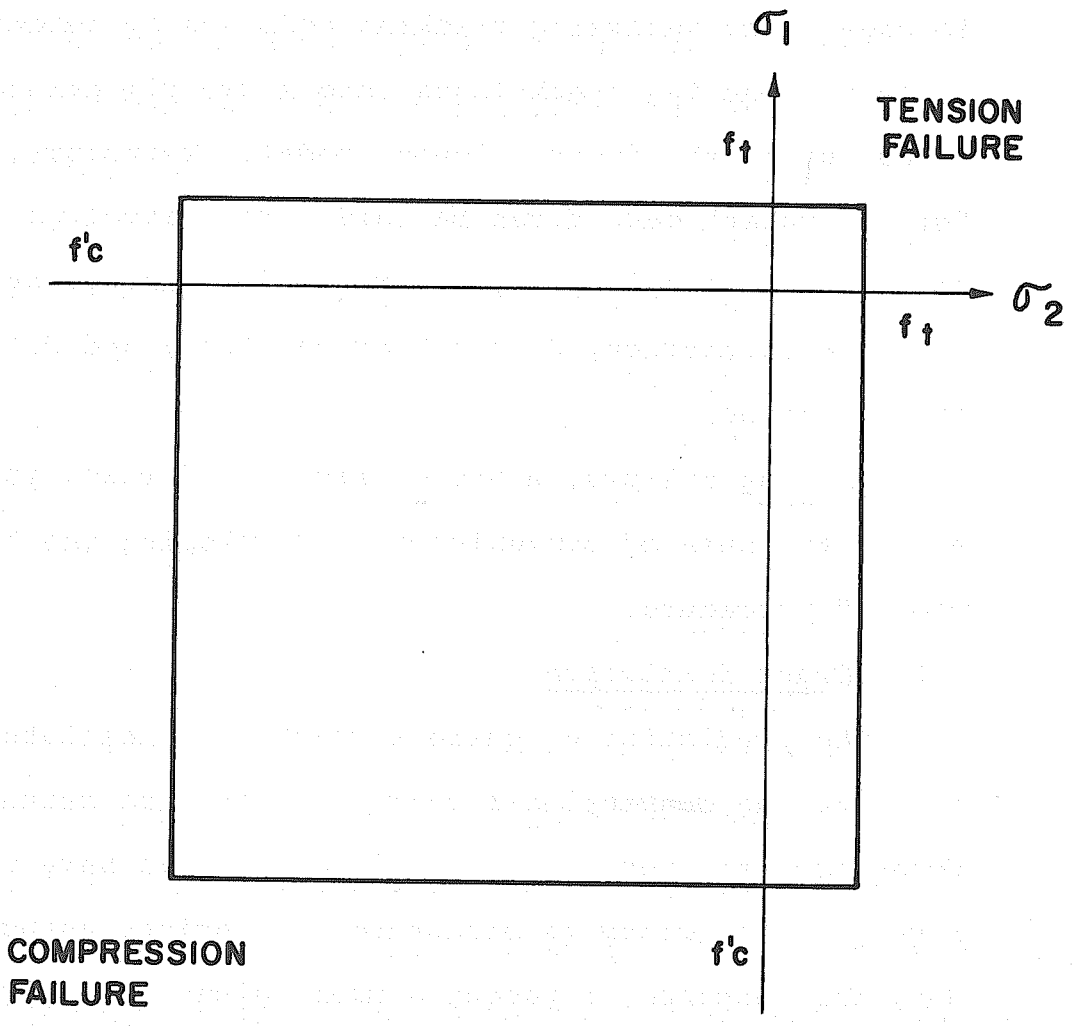

FIG. 4.5 A SIMPLIFIED FAILURE CRITERION

stress at a particular point meets the tensile failure criterion, then a crack is said to initiate at that point, which may be located anywhere in the two dimensional solid. If, on the other hand, a principal stress meets the compressive failure criterion, then the structure is declared failed in compression. No compressive fracture is investigated in the present study.

Note that the isoparametric element used in the present study is a higher order element. It can be expected that the stresses vary within the quadrilateral element itself. Therefore, it is possible to obtain a better stress gradient by first computing the stresses at each corner node of the quadrilateral elements, and then averaging all the stresses of those corners incident to a given nodal point. These averaged stresses are used to define the state of stress at that particular point. Clearly, the node-mesh incidence matrix devised earlier provides all the needed information for performing such an averaging process.

4.2.2 Crack Propagation

After a crack has been initiated, the structure is reanalyzed, which results in a new set of averaged nodal stresses, including the node at the crack tip, see Fig. 4.6a. The crack is assumed to propagate if the averaged nodal point stresses produce a highest maximum principal tensile stress that meets the failure criterion.

The direction of propagation is assumed to follow the path of the principal tensile stress trajectory.

It should be clear that the nodal point stresses at the crack tip are merely an indication of the "stress environment" around the crack tip, because no special provision is made to capture the stress singularity in the present model. Furthermore, the crack length and the crack orientation are dictated by the finite element mesh layout, as discussed previously in Sec. 1.4, with respect to the conceptual model. Possible paths for a crack to propagate are illustrated in Fig. 4.6b.

4.2.3 Crack Stabilization

Consequent to the crack propagation criterion stated above, a crack will be stabilized if the principal tensile stress at the crack tip falls below the critical level, or it will temporarily cease to grow when a higher principal stress level occurs at some other point in the structure. In the latter case, another crack will initiate or propagate instead. When the stresses at every point in the structure do not exceed or meet the failure criterion set forth, then the cracking configuration is considered to be stable under the given loading condition.

4.3 General Crack Growth Procedure

With the basic rules governing the crack initiation,

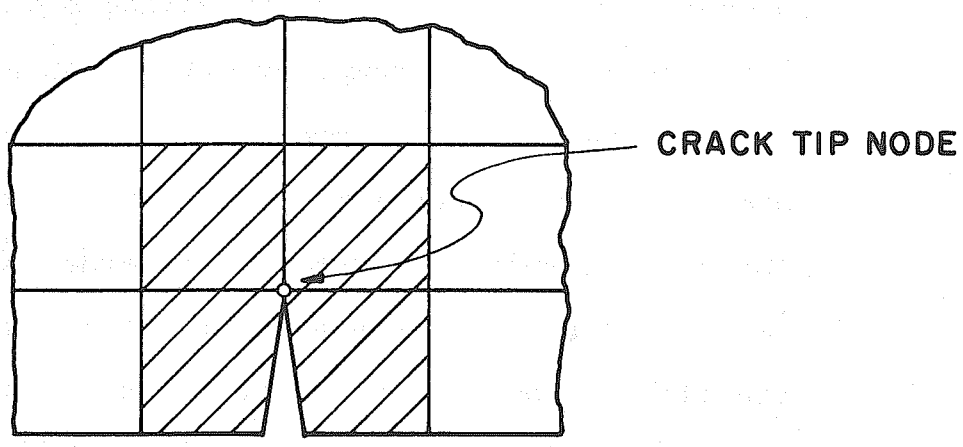

a) ELEMENTS CONTRIBUTING TO THE NODAL STRESSES TO BE AVERAGED AT CRACK TIP

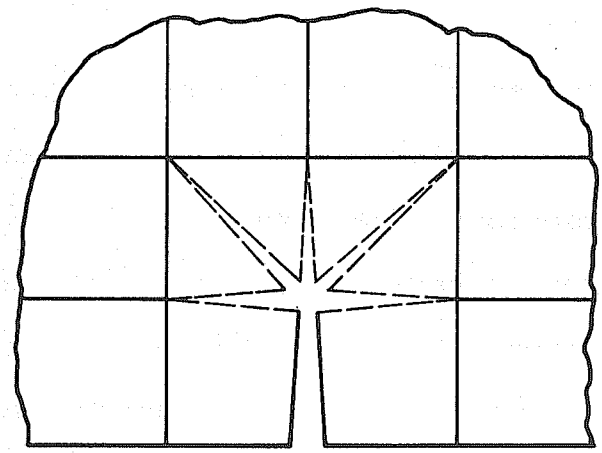

b) POSSIBLE CRACK PATHS

FIG. 4.6 CRACK GROWTH MODEL

propagation and stabilization having been set in the previous section, a computer method can now be developed for the crack growth procedure. Take, for example, the simplified two-dimensional structure shown in Fig. 4.7. The total structural system is regarded as composed of main structure represented by the two-dimensional finite elements and a substructure consisting of the bar and bond or link elements. Suppose that an initial solution by the frontal method has been carried out for a given loading condition, and it is expected that cracking, in the form of a crack-line, is going to develop. For the present, assume the crack growth is limited to the main structure only. The general procedure to generate a crack-line or to trace the crack growth is outlined as follows:

1) Average the stresses at each nodal point and compute the resulting principal stresses and angle defining their direction. Check the principal stresses against the failure criteria. The node with the highest principal stresses that meets the failure criterion is henceforth referred to as the cracked node, ISPLIT, Fig. 4.7, and the principal angle is defined as ANMAX, Fig. 4.8.
2) Execution of the program is terminated if no cracked node has been found, or if there is a failure in compression.

3) For the cracked node, ISPLIT, examine its status from the array (NOD) to see whether the cracked node is situated either at a prescribed force or displacement boundary point. If yes, execution is halted. If no, start to introduce a crack-line into the main structure proper by first setting a flag for the node ISPLIT in the (NDO) array and by checking whether the node has been the tip of a previous crack, If yes, set KRTIP=1.

4) From the node-mesh incidence array (NMI), locate the elements and the nodes which are directly involved with the cracked node ISPLIT, Fig. 4.8, and store them into (KELE) and (KNDE) arrays, respectively. The actual number of elements and nodes involved are denoted by NELE and NNDI.

5) Store the nodal points of each element in a two dimensional array (KNND), and construct the local node incidence number array (KICD)and local node-mesh incidence array (KNMD), Fig. 4.9. At the same time, store the corner nodes of each quadrilateral element into the (KQUD) array, Fig. 4.8. The total number of such nodes is indicated by NQUD. These corner nodes are included only for those elements which are:

   a) Not a boundary element (See Example C), or any element being excluded from the crack growth consideration.

b) Not an element having been previously cracked or bordering a crack-line, when KRTIP = 1. If NQUD = 0, it means that the cracked node is located within a totally fractured zone. Further cracking is possible only when a hinged connection exists at the cracked node, Fig. 4.16, which is indicated by NGAP $\geq$ 0 (See step 11 below). Note that a triangular element is not treated in the present crack growth procedure.

6) Rotate the node numbers of each element stored in the (KNND) array, so that the cracked node becomes the first node number in each element. The rotation count for each element is stored in the (KROT) array.

7) Store the elements indirectly affected by cracking into the (IELE) array and the total number of such elements, Fig. 4.10, is denoted by MELE. This defines the ultimate extent to which any topological change may occur due to cracking.

8) Treating the cracked node ISPLIT as being the origin, compute the angle to each corner node with respect to the cracked node, and store it into the (ANGL) array, Fig. 4.8.

9) Transfer the node status from (NOD) array to (INCD) array for all nodes affected by cracking.

10) Form the local adjacency array (KAJC) Fig. 4.11, as follows:

a) Obtain an element number from (KELE) array, Fig. 4.8.

b) Obtain the nodal point number of that element from the (KNND) array.

c) Check in the local node incidence array (KICD), Fig. 4.9, to see whether the incidence number of that node equals to 2. If no, skip that node. If yes, obtain the element numbers from the local node-mesh incidence matrix (KNMD), Fig. 4.9, of that node, and store them in the adjacency array (KAJC), Fig. 4.11.

11) Set the gap count NGAP to -2, and construct a pointer array (KDUA) for the dual graph, Fig. 4.12, directly from the adjacency array as follows:

a) Look for an empty slot in the (KDUA) array and check to see whether the corresponding row in the adjacency array (KJAC) has a single or double adjacency. If it is a single adjacency, signified by a 0 in the second column, then it is the head of the pointer array. If no such condition exists, i.e., the initial dual graph is a closed loop such as the one shown in Fig. 4.12, then simply pick an arbitrary element, say the J^{th} element in the (KELE) array.

b) Set IEL = JEL = KELE(J), as a start.

c) Obtain the row number I of the element number IEL in the (KELE) array.

d) Check in the I^{th} row of the (KAJC) array to see

if there is any positive number K which is not equal to JEL.

e) If yes, store K into KDUA(I) and reset JEL= IEL and IEL=K, at the same time, negate K in (KAJC) array and go back to step c) and repeat the procedure until all elements have been accounted for.

f) If no, set a large negative number in KDUA(I) and increment the gap count NGAP by 1, Then go back to step a).

g) After all elements have been processed, reset the large negative number, if any, in the (KDUA) array to zero, and all entries in (KJAC) array to positive numbers. Now NGAP indicates the number of gaps or discontinuities existing in the dual graph.

12) Determine the number of additional nodes to be created. In general, two new nodes are required if there is a substructure attached to the cracked node ISPLIT, otherwise, only one node is added to the total structure.

13) Create more additional nodes if there is more than two gaps existing in the dual graph, signified by NGAP>0. The number of extra new nodes required will be equal to NGAP. When NGAP≥0, it means that more

than one crack has reached the cracked node ISPLIT. Therefore, no determination of the crack orientation will be performed. Execution procedure jumps directly to step 18) below for the construction of separate chains. No new element is created in this case.

14) Detect the crack tip or tips as follows:
   a) Compute the crack orientation in accordance to the given principal angle ANMAX.
   b) Search through the angle array (ANGL) to see if there is any node which lies within 30° of the crack orientation. Any node which falls closest to the crack orientation within this 30° cone will be denoted as the crack tip.
   c) Flag the crack tip node in the (INCD) array.
   d) An error message will be given in no crack tip can be found.

15) Check if crack tip reaches the boundary of the structure, and record such a crack tip node in IBOUND or NBOUND. A boundary is characterized by a node incidence number of 2 or less.

16) Determine the number of elements to be added by checking in the local node incidence array (KICD) for each of the crack tip node:
   a) If the incidence number equals 2, that means no new element need by created. A crack-line is

formed by separating two adjacent elements along the element boundary. Negate the element number in each other's row of adjacency matrix (KAJC), Fig. 4.13.

b) If the incidence number equals 1, that means a quadrilateral has to be subdivided into two triangles to form a crack-line. Create a new element, say e, in Fig. 4.10 and 4.13. Store it in (KELE) and (IELE) arrays, and increment the counters NELE and MELI. Expand the dual graph and modify the adjacency relationship, Fig. 4.13. Update all the arrays involved.

17) Interchange the entries in each row of the adjacency matrix (KAJC), so that all positive entries appear on the first column.

18) Construct separate chains based on the adjacency array (KAJC), Fig. 4.14:

a) Initialize the (KDUA) array which now becomes the indicator for processed elements.

b) Check through the adjacency array (KAJC) for each unprocessed element to see if there is any severance which is indicated by a negative or zero entry.

c) If yes, store that element as a member of the chain and flag that element in the (KDUA) array

to indicate that it has been processed. Continue to build up the chain through the adjacency relationship, until next point of severance is encountered.

d) If no element remains to be processed, then the procedure for the construction of the chains is completed. Otherwise, start a new chain by repeating the construction procedure starting from step b.

19) Assign new node number to the elements belonging to each chain. One of the chains will retain the cracked node number, if there is no substructure attached to the cracked node.

20) If there is any quadrilateral being subdivided into triangles, formation of the triangular element node numbers must be made in accordance with its adjacent element. Using Fig. 4.10, as an illustration, the steps are:

a) From the adjacency array (KAJC), locate the element d which is connected to the newly created element e.

b) Similarily, locate the element c which is severed from the element e.

c) Since all node numbers have been rotated such that the cracked node is the first node number,

and all nodes have been numbered counterclockwise (I,J,K,L), it is necessary only to check the second node of element c to see if it is equal to the fourth node of element d.

d) If yes, the triangular element c assumes the node numbering I, K, L; and element e, I, J, K.

e) If no, then the opposite is true for the two elements c and e.

21) Assign the coordinates of the cracked node ISPLIT to all the newly created nodes.

22) Update all element data including rotation of the node numbers to their original order for all quadrilaterals, using the (KROT) array, and store them into ECS.

23) Update the original node status array (NOD), the original node-mesh incidence array (NMI), and the element pointer array (NXT) for next cycle of frontal solution.

24) If the crack tip has reached the boundary or reached another crack tip hence forming a hinged condition, then ISPLIT is set equal to that crack tip node and the procedure is repeated once again starting from step 3.

4.4 Tests of Crack Growth Capability

The steps outlined in the last section form the basic algorithm for the crack growth procedure which

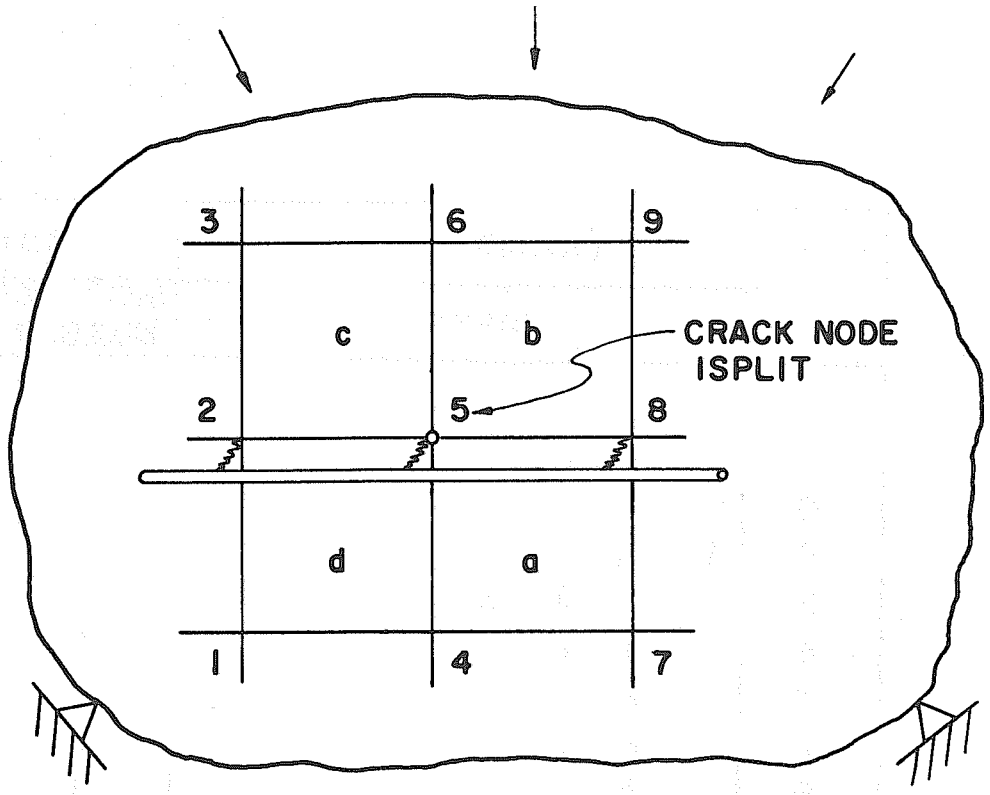

FIG. 4.7 GENERAL TWO-DIMENSIONAL STRUCTURE

(KELE)	ELEMENT INVOLVED	b	a	c	d				
(KNDE)	NODE INVOLVED	5	8	9	6	3	2	1	4	7
(KQUD)	CORNER NODE	8	9	6	3	2	1	4	7	
(ANGL)	ANGLE θ^0	0	45	90	135	180	225	270	315	

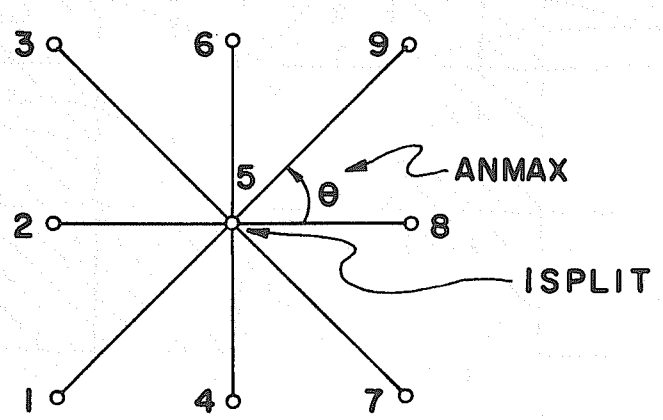

FIG. 4.8 NODES & ELEMENTS INVOLVED WITH THE CRACKED NODE

(KNMD)		(KICD)
NODE	MESH	INCIDENCE NUMBER
1	d	1
2	d, c	2
3	c	1
4	d, a	2
5	d, a, b, c	4
6	c, d	2
7	a	1
8	a, b	2
9	b	1

FIG. 4.9 LOCAL NODE-MESH INCIDENCE ARRAY

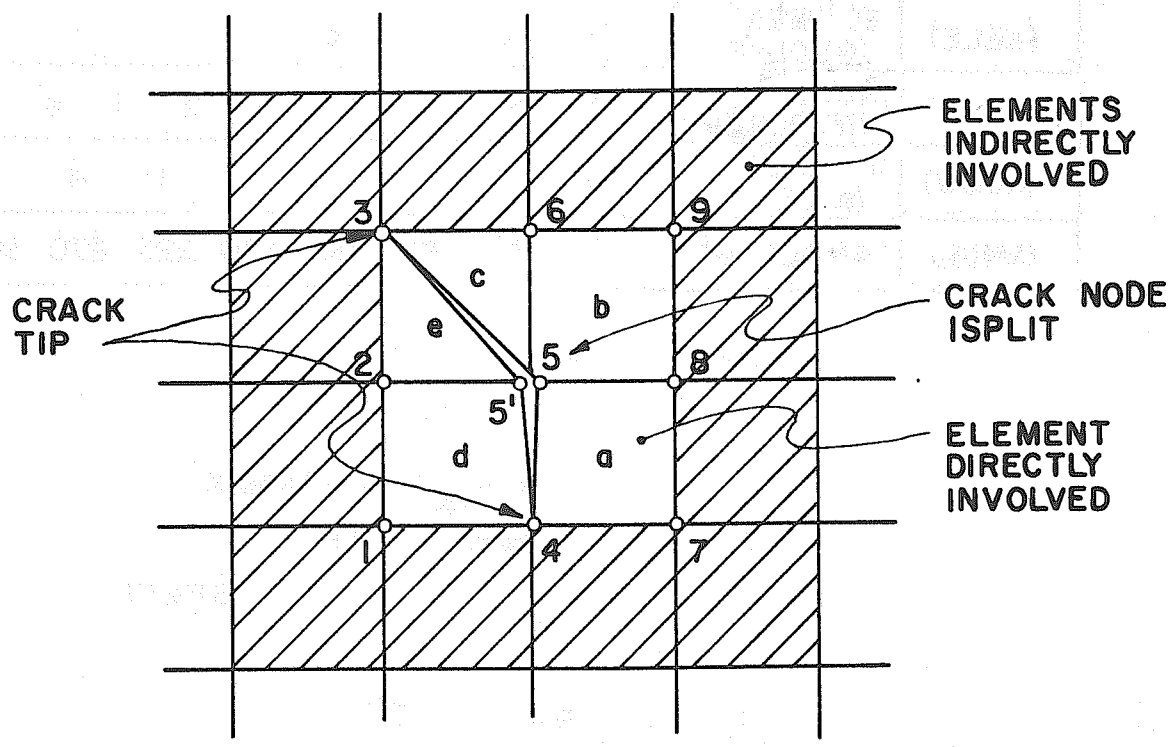

FIG. 4.10 ILLUSTRATION OF CRACK-LINE GENERATION

(KAJC)		
MESH	ADJACENT MESHES	
a	d	b
b	a	c
c	b	d
d	c	d

FIG. 4.11 LOCAL ADJACENCY ARRAY

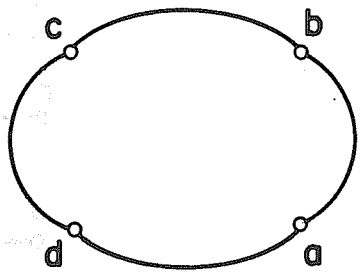

	a	b	c	d	
(KDUA)	b	c	d	a	

FIG. 4.12 DUAL GRAPH & ITS POINTER ARRAY

ADJACENCY ARRAY (KAJC)		
a	b	-d
b	a	c
c	b	-e
d	e	-a
e	-c	d

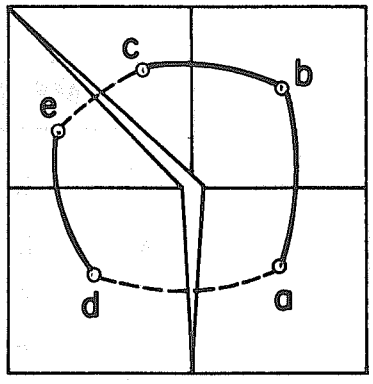

POINTER ARRAY (KDUA)

a	b	c	d	e
b	c	-e	-a	d

FIG. 4.13 MODIFIED ADJACENCY RELATIONSHIP

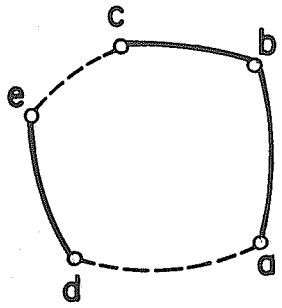

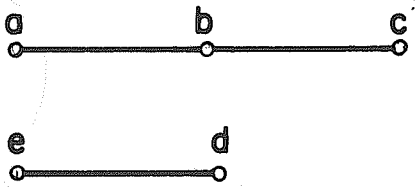

CHAIN ARRAY (KCHN)			
1	a	b	c
2	e	d	

FIG. 4.14 CONSTRUCTION OF SEPARATE CHAINS

has been programmed into a FORTRAN subroutine called CRACKPA. In reality, there are numerous crack growth patterns and configurations, depending on the structural layouts, finite element sizes and loading conditions. Therefore, it is desirable to examine the capability of the programmed crack growth procedure in developing crack-lines under differnt circumstances which conceivably can occur during a crack growth analysis. These kinds of tests can be easily accomplished here, because the subroutine CRACKPA has been so programmed that it depends only on two key parameters, the cracked node ISPLIT and the principal angle ANMAX. Instead of actually carrying out the frontal solution procedure and the stress averaging procedure, a simple driver routine can be written to read in specifically an ISPLIT and an ANMAX to simulate the desired cracking condition occuring on a given finite element mesh layout, Fig. 4.15. A few tests were performed and are described below:

a) Vertical Crack at Boundary. Common flexural cracks are initiated at the boundary. Figure 4.16a simulates such a condition, and Figure 4.16b shows that the vertical flexural crack continues to propagate. Because of the layout of the finite element mesh, the crack-line is generated along the element boundary, thus no new element is created.

b) Inclined Crack at Boundary. When flexural stress is

combined with shearing stress, an inclined crack often results. This is often observed in some beam experiments. Figures 4.16c and d show an inclined crack initiated at the boundary and continue to propagate. Note that because of the inclined crack path, quadrilateral elements are subdivided into triangles to accommodate the crack-line.

c) Vertical and Horizontal Cracks in the Interior. Cracks may also be initiated at an interior point of the structure, such as commonly seen in prestressed concrete and pull-out specimens. Figures 4.16e and f show how the vertical and horizontal interior cracks are handled by the crack growth procedure.

d) Inclined Cracks at Interior. Inclined cracks also frequently occur in the beam webs of laboratory test specimens. Limited by the layout of the finite element mesh, Figures 4.16g and h show how the inclined cracks at the interior point of a structure are accommodated.

e) Branching Cracks. In order to be able to obtain a better approximation of the crack growth patterns, propagation should be allowed to branch into the direction closely adherent to the predicted crack path. Figures 4.16i and j demonstrate two of such branching cracks. Branching in other directions is, of course, quite possible in the present crack growth

procedure to meet the actual cracking situation.

f) Separation of Substructure. In the study of reinforced and prestressed concrete members, cracks are commonly initiated at the point where reinforcement is attached to the concrete. In order to handle such situations, the computer program must be able to recognize this special problem of connectivity and properly assign extra new nodes to the structure. Certainly, no difficulty will be incurred if the topology of the structural network has been classified into main system and subsystems, for which separate subgraphs are envisioned. Therefore, the incidence member of each node consists of two classes: one for the graph of the main system and the other for the subsystem. Both numbers are stored in the node status array (NOD) which is constantly available for reference and updating. Figures 4.16k and l illustrate the separation of a substructure (e.g. reinforcement) when a crackline is introduced into the concrete. Note that the original node number is retained by the substructure, thus little is affected in the topology of the substructure, and two new nodes are assigned to the main structure, plus the creation of one additional element in this example.

g) Separation of Hinged Connection. Figure 4.16m shows

a hinged connection. This seemingly rare situation does occur when the cracking condition becomes more intensified. Using the concept of dual graph, gaps or discontinuities in the dual graph provide a means of detecting the hinged connection, as explained in previous section. The present crack growth procedure succeeds in recognizing and releasing the hinged connection, Fig. 4.16n. This capability is rather important, and will be demonstrated in the following cases.

h) Separation of Boundary Hinges. Boundary hinges are formed when the crack originally initiated at an interior point propagates outward and reaches the boundary. Figures 4.16o and q simulate this situation. Since both crack tips in these particular test examples reach the boundary, total severances of the structures result, Figs. 4.16p and r.

i) Separation of Crack Tip Hinge. Figure 4.16s shows a crack which is initiated at the boundary. Another interior crack is generated, Fig.4.16t, and reaches the tip of the boundary crack. Therefore, a crack tip hinge is formed, and subsequently released as shown in Fig. 4.16u. However, the other tip of the interior crack also reaches the boundary, which is also automatically released by the crack growth program. This results in fracturing the solid into two pieces, Fig. 4.16v.

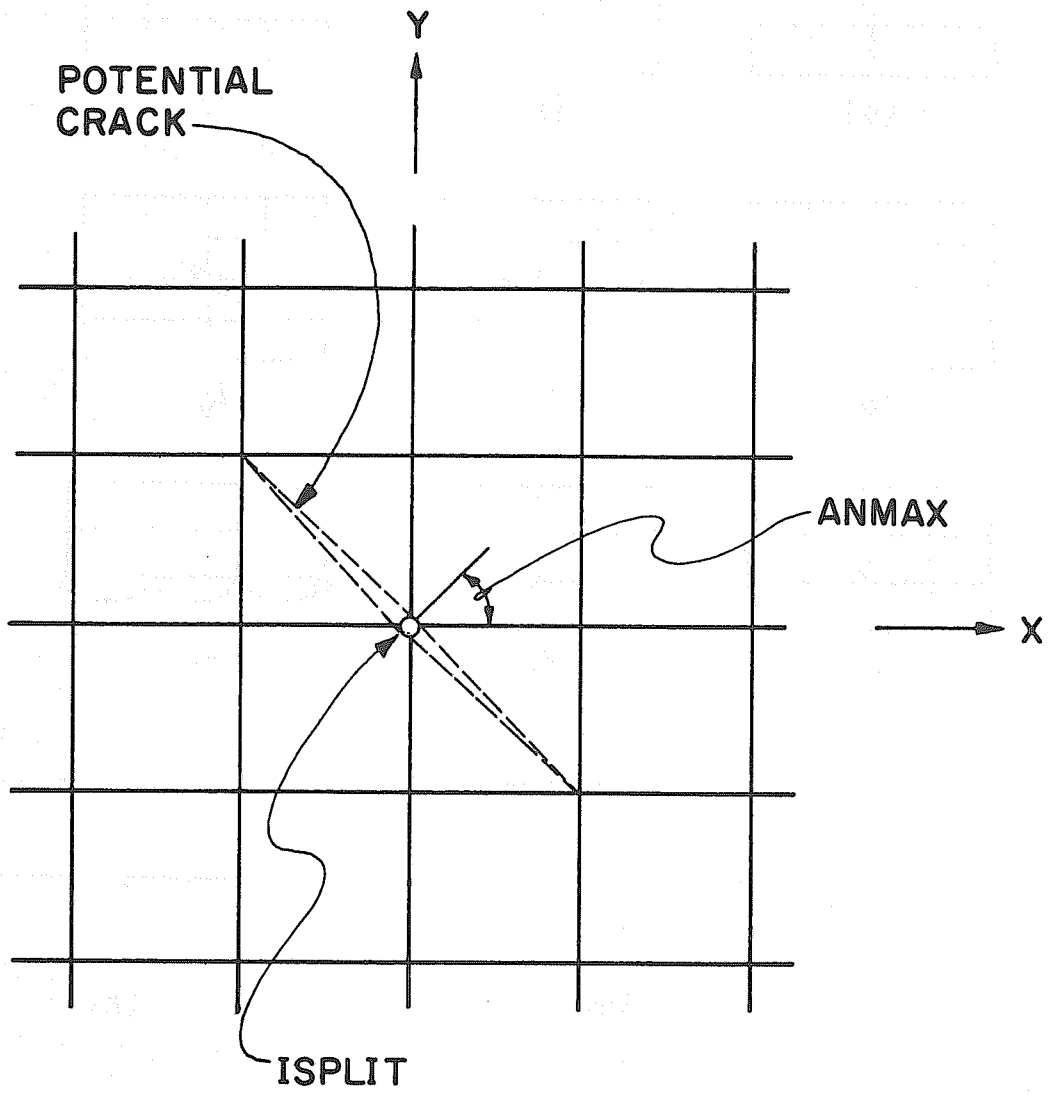

FIG. 4.15 DEFINITION OF ISPLIT AND ANMAX

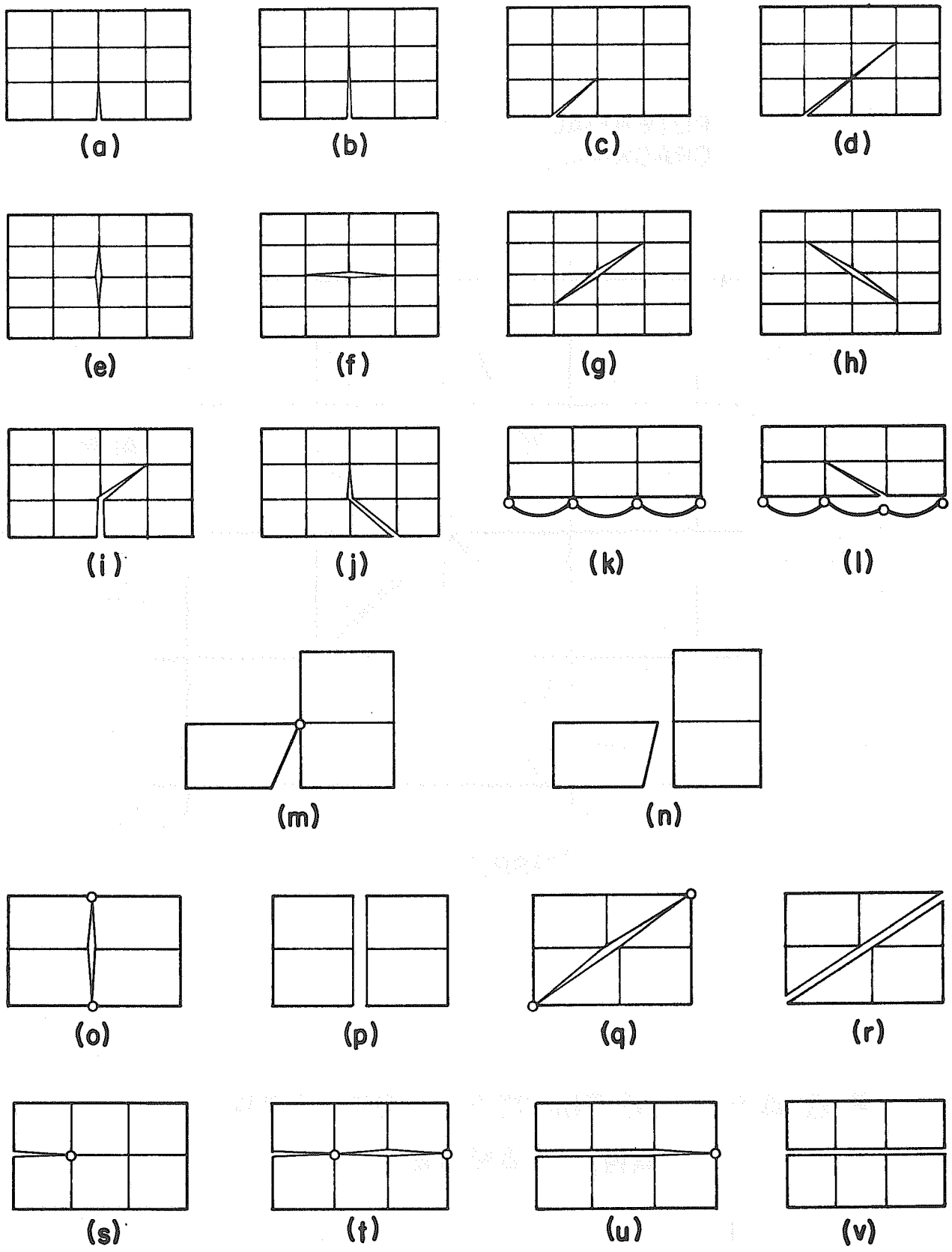

FIG. 4.16 CRACK GROWTH CAPABILITIES

4.5 Treatment of Matrix Singularity due to Crack Growth

The various test cases presented in the last section display the extent of the capabilities that can be processed by the crack growth procedure developed in the present study. At the same time, they point out a somewhat unusual problem that requires special treatment.

When bar elements are used to simulate steel reinforcement and their orientation happens to be parallel to the global axes, singularity in the structural stiffness matrix will result after a separation takes place, such as in the test case f (Figs. 4.16k and l) shown in the last section. Similarly, this ill-condition would occur in the situations of total severance or fracture, such as in the test cases g, h and i, (Figs. 4.16o to v) because of kinematic instability. In order to preserve the continuity in the execution of the crack growth procedure, a small stiffness in the order of 10^{-15} is automatically added to the variable at which equation singularity occurs during the frontal solution procedure. Physically, this means a minute grounded spring is attached to that node in the direction where the stiffness matrix becomes singular.

In most cases, the introduction of the small spring has no effect on the final results, because of the relatively low stiffness value and the physical configuration of the structure. Erroneous answers can happen

only in the case where the part being totally fractured or spalled out, is loaded. Fortunately, for reinforced and prestressed concrete members, the load carrying capacity is jointly shared by the concrete and the steel reinforcement. Therefore, a total loss of load carrying capacity without yielding of the steel reinforcement can be considered as an exceptionally rare occasion.

4.6 Interruption and Resumption of Solution Procedure

Even though much effort has been made to automate the progressive crack growth solution procedure, no claim has been made that the method will cover every possible cracking condition which may be encountered in every analysis. In fact, it has become evident that engineering judgement remains an essential part of the crack growth analysis. Therefore the need of human intervention must be anticipated. To this end, interruption and resumption of the program execution have been fully provided for.

In the present batch-processing computer system, interruption is done by halting the execution of the program and by printing a message to indicate further information and instructions needed to be input. These situations comprise the following:

a) Cracking occurs at or through a loaded point, or at a prescribed boundary point;

b) Cracking occurs at a totally fractured region; and

c) Crack tip cannot be located.

These constraints are inevitable consequences of the discretization and modelling of the structure in the finite element method. To avoid loss of intermediate results, output is printed at the end of each cycle of analysis. In addition, a "PUNCH MODE" has been made available so that any change in the data due to crack growth, such as the creation of new nodes and elements, together with their status with respect to cracking, can be output on cards which in turn can be used as input when the program execution resumes. Thus continuity of the solution process is preserved.

4.7 Example Problems

Several examples which have been analyzed with the present program are presented in this section to illustrate the versatility as well as the limitation of the crack growth procedure. Due to the many simplified assumptions used in developing the present model, no attempt is made here to compare the results with experimental values. But the ability of the method to capture the general trend and the predominant pattern of crack growth should be self-evident. The crack growths are shown by stage in a series of figures, and the location of the cracked node is indicated by an

arrow.

Example A: A Simple Modulus of Rupture Test.

A simple plain concrete specimen under a concentrated load at midspan is shown in Fig. 4.17. The sequence of crack growth from the analysis is shown in Fig. 4.18. It is of interest to note that diagonal cracks initiated prior to the vertical flexural crack. A perfect symmetrical crack pattern was obtained, as would be expected from the loading and geometrical configuration. Moreover, once the flexural crack develops, it continuously propagates upward until the top fiber experiences a compressive failure because the crack has almost penetrated through the entire cross-section. This is a typical phenomenon of a flexural repture test of a plain concrete specimen.

Due to the fact that a linear elastic analysis is performed at each stage of cracking, it is also possible to scale the stress intensity to obtain the critical load level at which crack will initiate or propagate at every stage of crack growth, Fig. 4.19. The critical load is seen to decline beyond the peak level once the vertical flexural crack has developed. This result offers a clear explanation why the crack growth is unstable in ordinary modulus of rupture tests.

Example B: A Concrete Bracket

The idealization of a concrete bracket and its steel

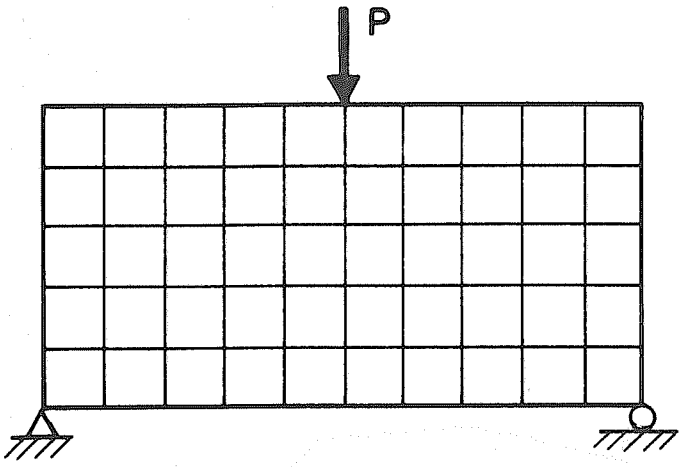

FIG. 4.17 EXAMPLE A - A SIMPLE RUPTURE TEST

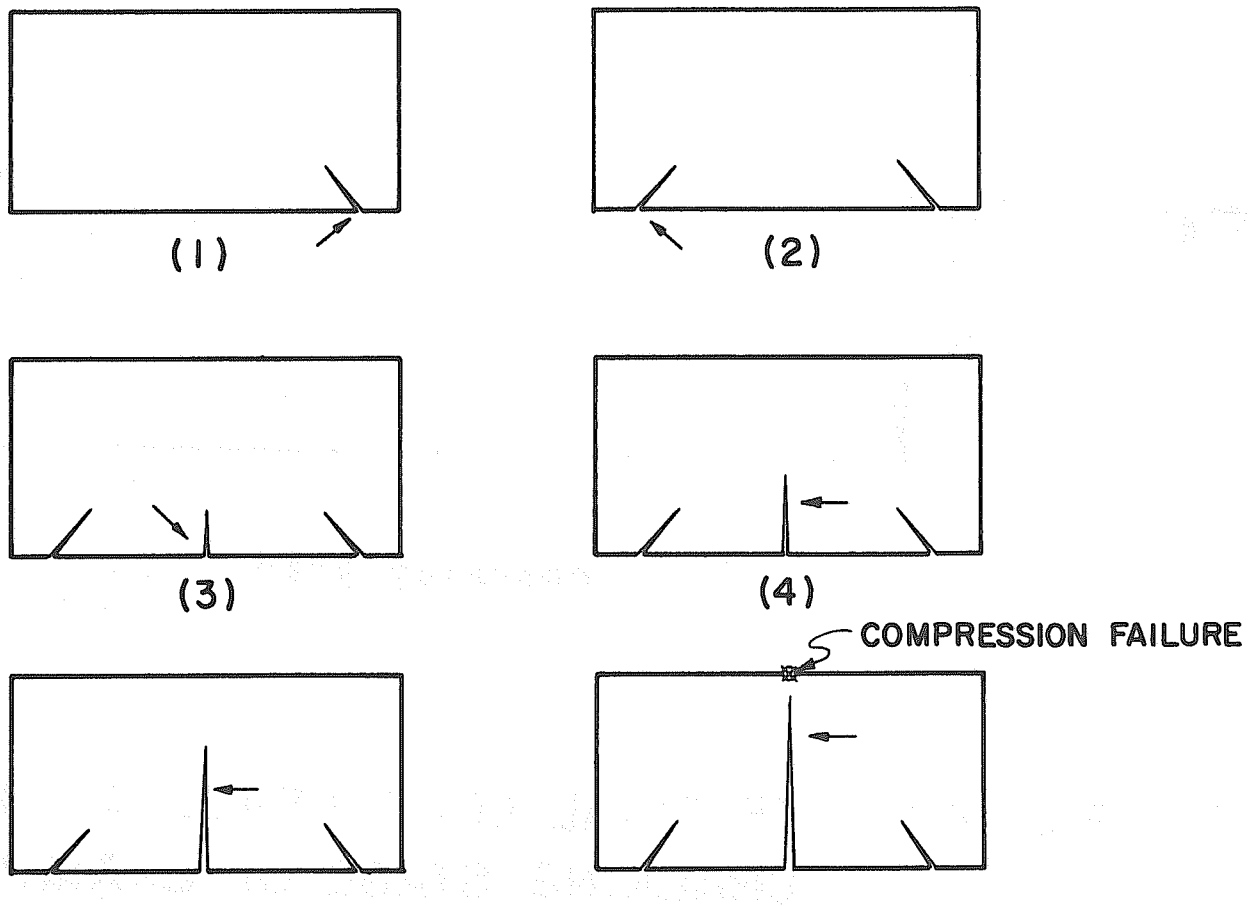

FIG. 4.18 CRACK GROWTH OF EXAMPLE A

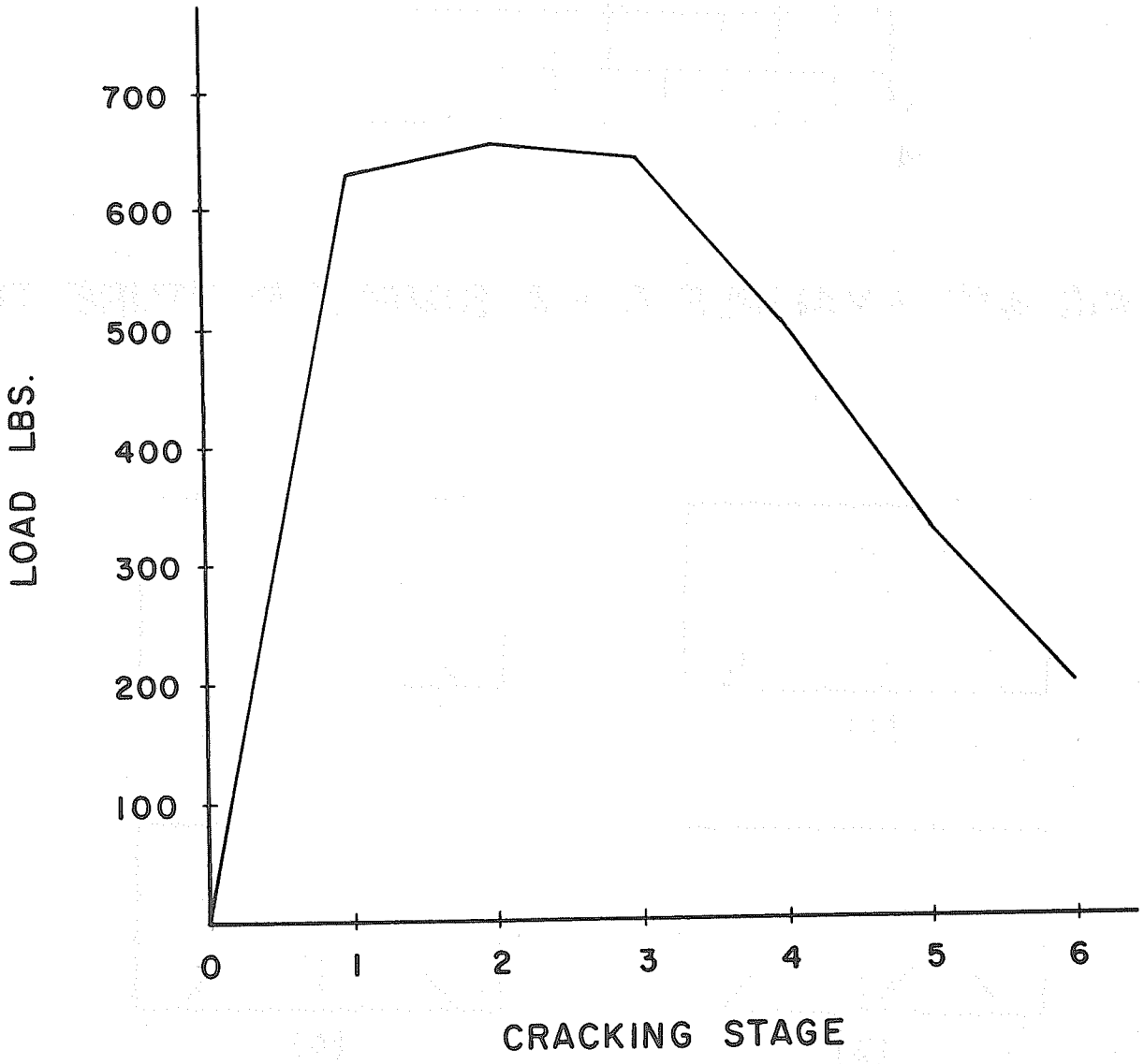

FIG. 4.19 CRITICAL LOAD LEVEL AT EACH CRACKING STAGE OF EXAMPLE A

reinforcement is shown in Fig. 4.20. The sequence of crack growth is shown in Fig.4.21. Note that the crack was initiated slightly away from the re-entrant angle where high stress concentration is predicted by the theory of elasticity. This deviation is probably due to the inherent characteristics of the finite element approximation and the averaged nodal stresses used. However, the over-all picture of the crack growth has not been hampered by this deficiency, and, certainly, is within limits of for the prediction of cracking in this reinforced concrete structure. The general behavior of the structure can be seen that after cracks have reached the steel level, the tensile force required to resist the external load is carried mostly by the steel reinforcement, which creates a situation similar to the pull-out test. Therefore, a vertical interior crack appears repeatedly, which further weakens the bond between the concrete and the steel. The structure finally fails by yielding of the horizontal steel reinforcement.

Example C: A Doubly Reinforced Concrete Beam

The doubly reinforced concrete beam specimen and its finite element model are shown in Fig. 4.22. Joint elements are introduced at the line of symmetry. This is an artifice which enables cracks to grow along prescribed displacement boundary line. The steel reinforcement is represented by bar elements which are directly

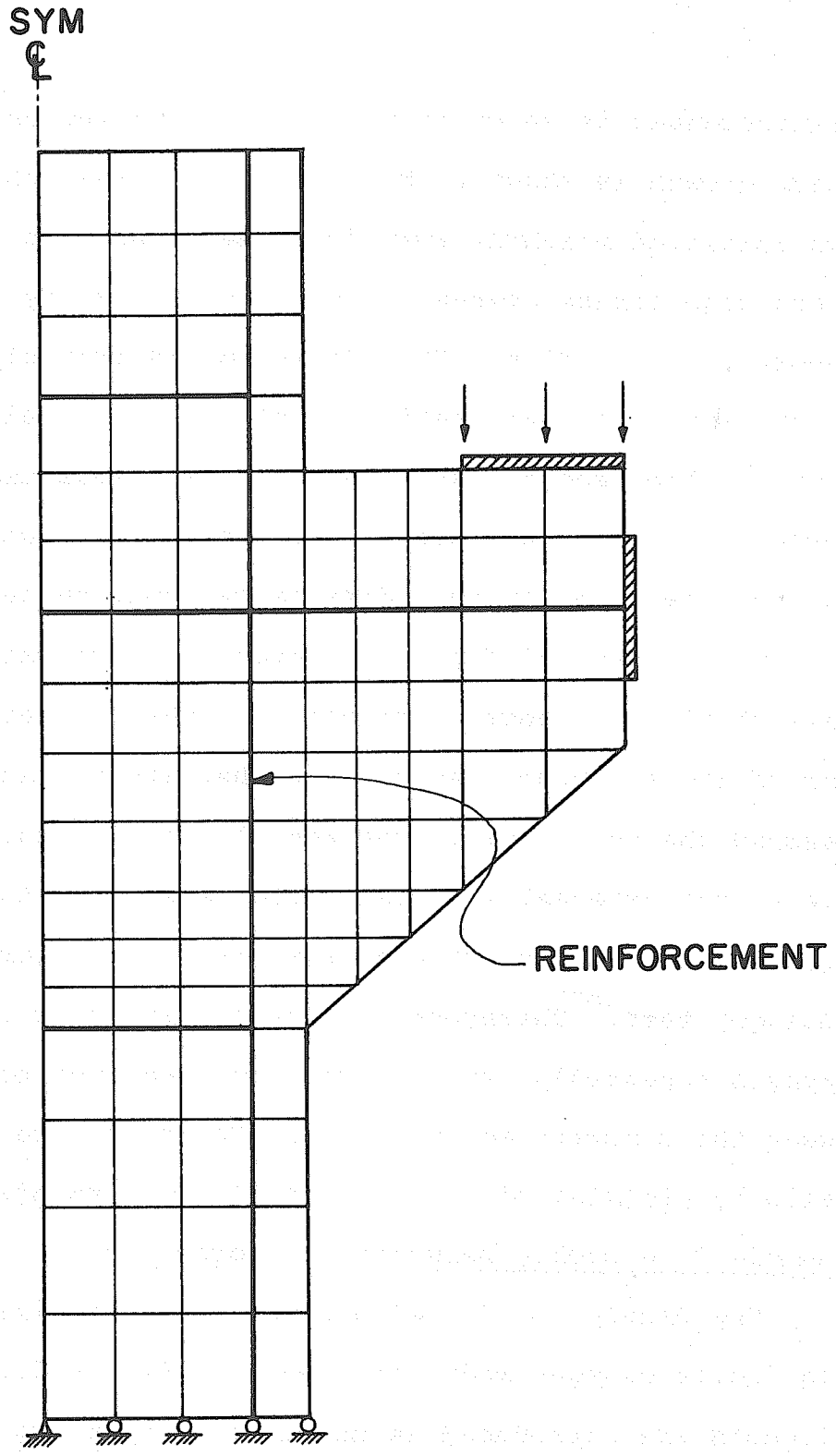

FIG. 4.20 EXAMPLE B - A CONCRETE BRACKET

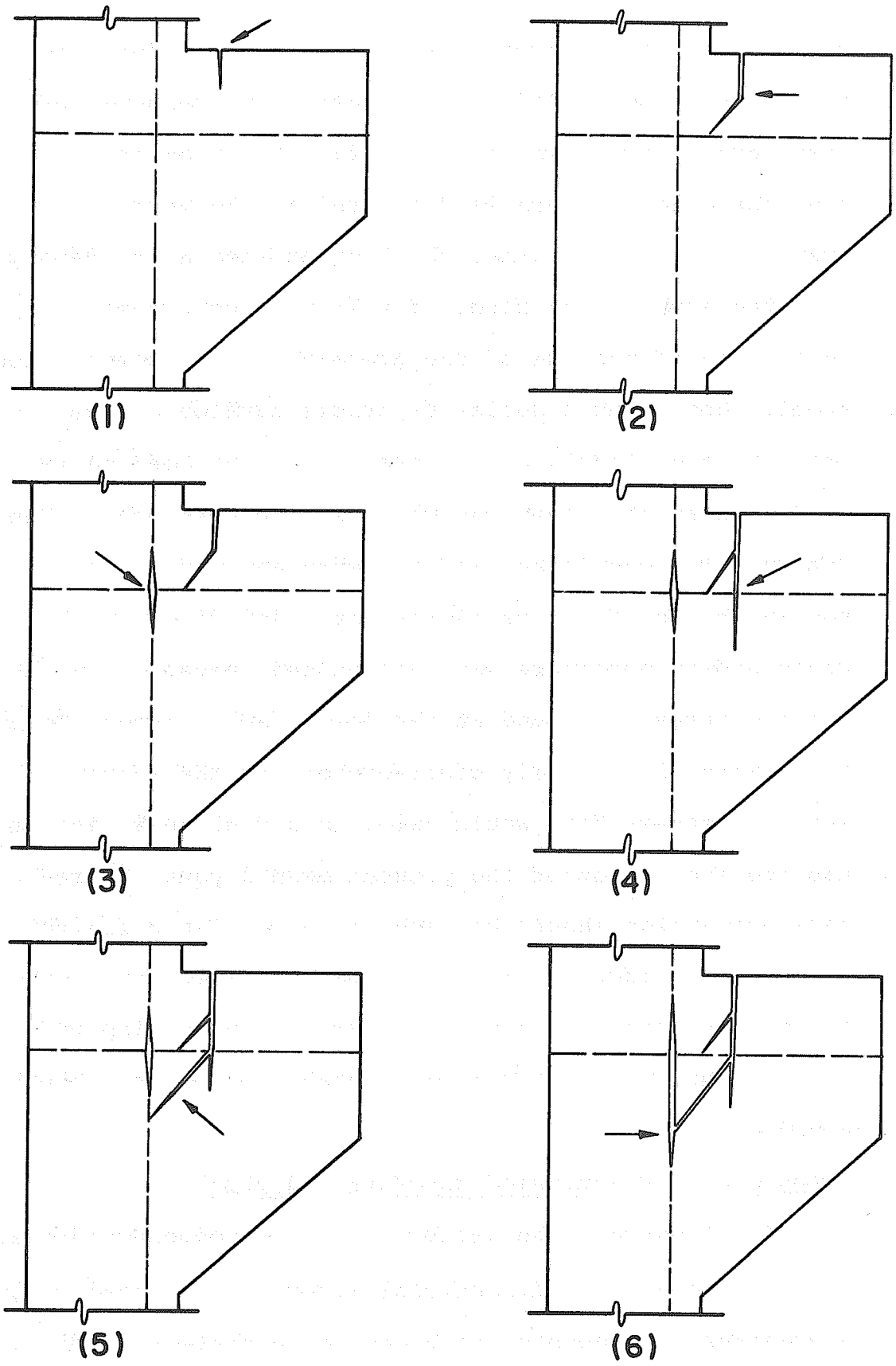

FIG. 4.21 CRACK GROWTH OF EXAMPLE B

connected to the concrete beam proper. Therefore, no bond slip is permitted in this case. The sequence of crack growth is shown in Fig. 4.23. It can be seen that the crack pattern is dominated by the vertical crack at the center line, which penetrates quite deeply into the compression zone. Equilibrium continues to be maintained because of the presence of the compression steel. Note that a series of cracks develop at the tension steel level, at the same time, the bonding is destroyed at the locations where such cracks occur. The internal T-C couple has shifted more and more to the top and bottom steel reinforcement. And finally, the crack growth procedure was interrupted, because a high tensile stress is found at the lower left corner. This fact, which is entirely contradictory to the actual state of stress that would exist in a real beam, indicates the limitation of the present mesh layout. Therefore precaution should be taken in selecting a finite element mesh layout. Had there been a finer mesh near the support reaction and some degree of bond slip permitted, this awkward situation probably could have been avoided.

Example D: A Prestressed Concrete End Block

To illustrate the capability of introducing initial stress into any two-dimensional structure for analysis, a prestressed concrete end block for a pretensioned

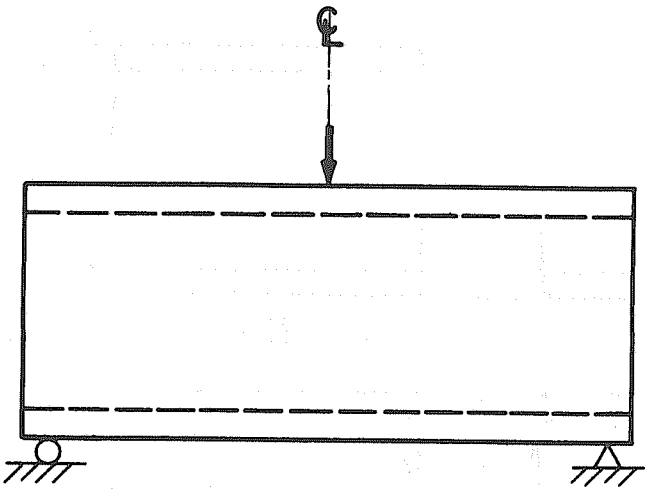

a) DOUBLY REINFORCED CONCRETE BEAM

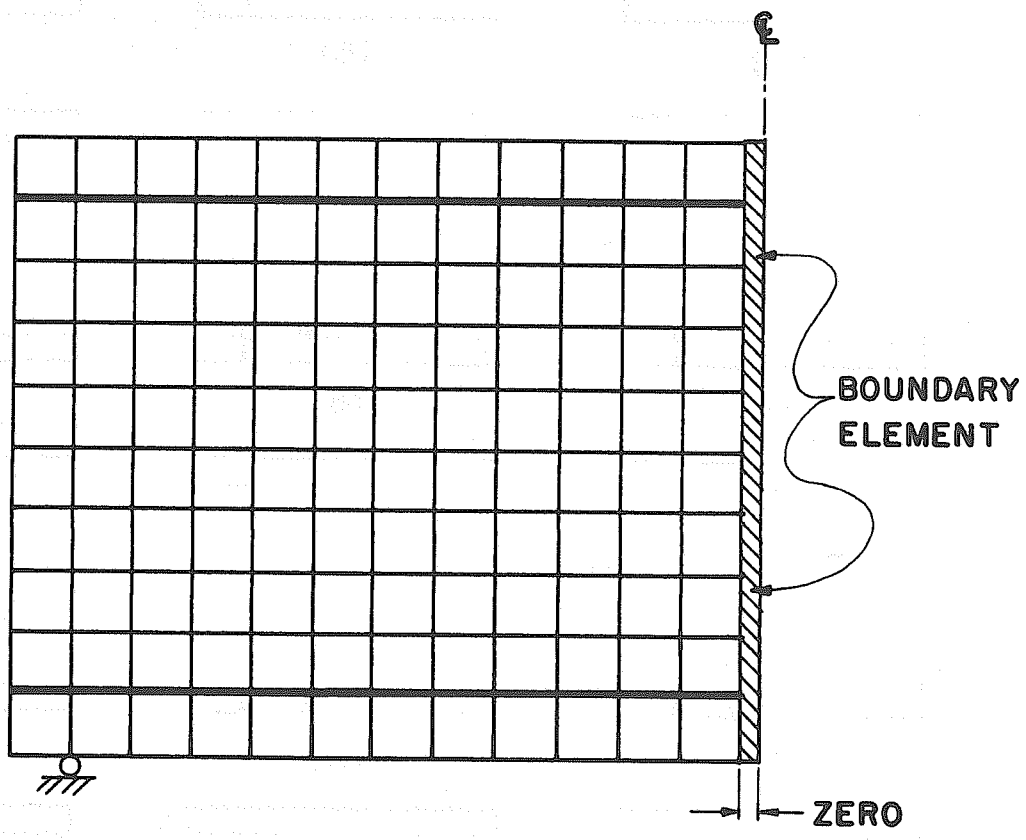

b) FINITE ELEMENT MODEL

FIG. 4.22 EXAMPLE C - A DOUBLY REINFORCED CONCRETE BEAM

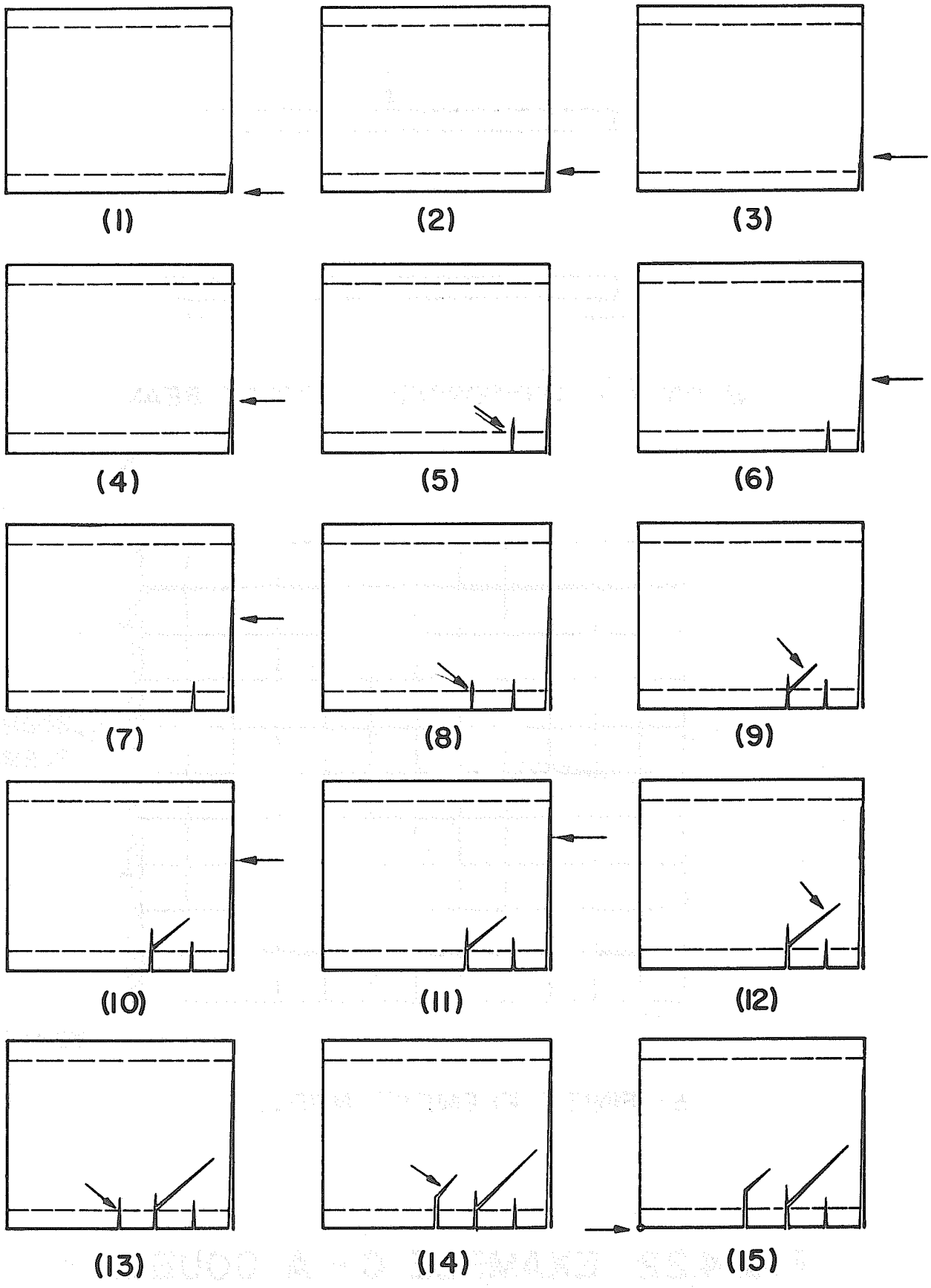

FIG. 4.23 CRACK GROWTH OF EXAMPLE C

beam is selected and shown in Fig. 4.24. Bond elements between the steel and concrete elements are provided for the purpose of obtaining a realistic transfer of the prestressing force from the steel to the concrete. The resulting crack growth patterns are shown in Fig. 4.25. As expected from tests in prestressed concrete end blocks, interior inclined shear cracks are developed and are accompanied by horizontal splitting.

The execution of the program was halted because another inclined crack, shown by dotted line in Fig. 4.25(6), was developed in an element being regarded as in the crack zone, since that element is adjacent to a horizontal crack line. This is, of course, an assumption artificially imposed in the crack growth procedure, which aims at providing an opportunity for checking and intervening should engineering judgement be deemed necessary. At this point, the engineer has the option of proceeding or suppressing the crack growth at that particular location, if further analysis is desired.

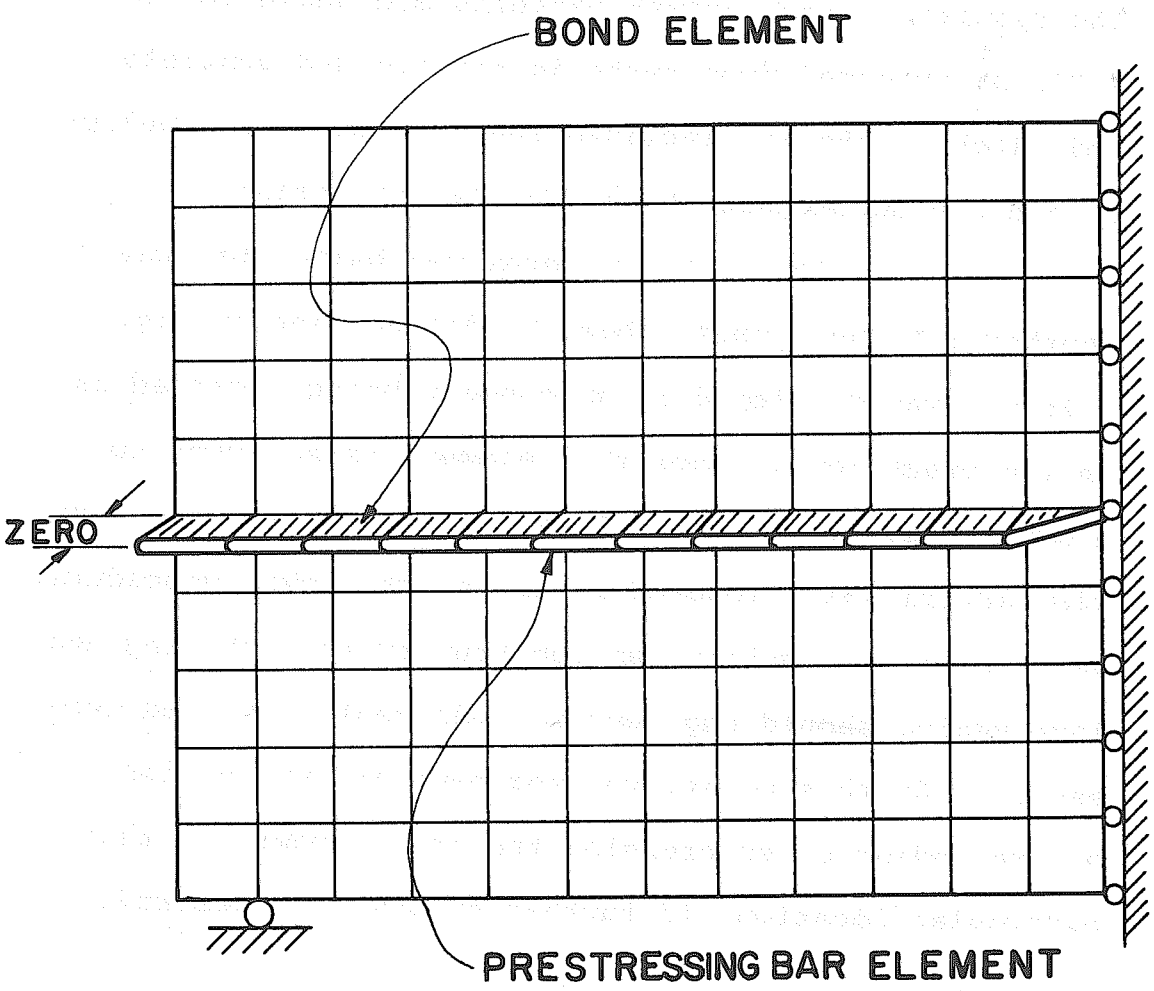

FIG. 4.24 EXAMPLE D - A PRESTRESSED CONCRETE END BLOCK

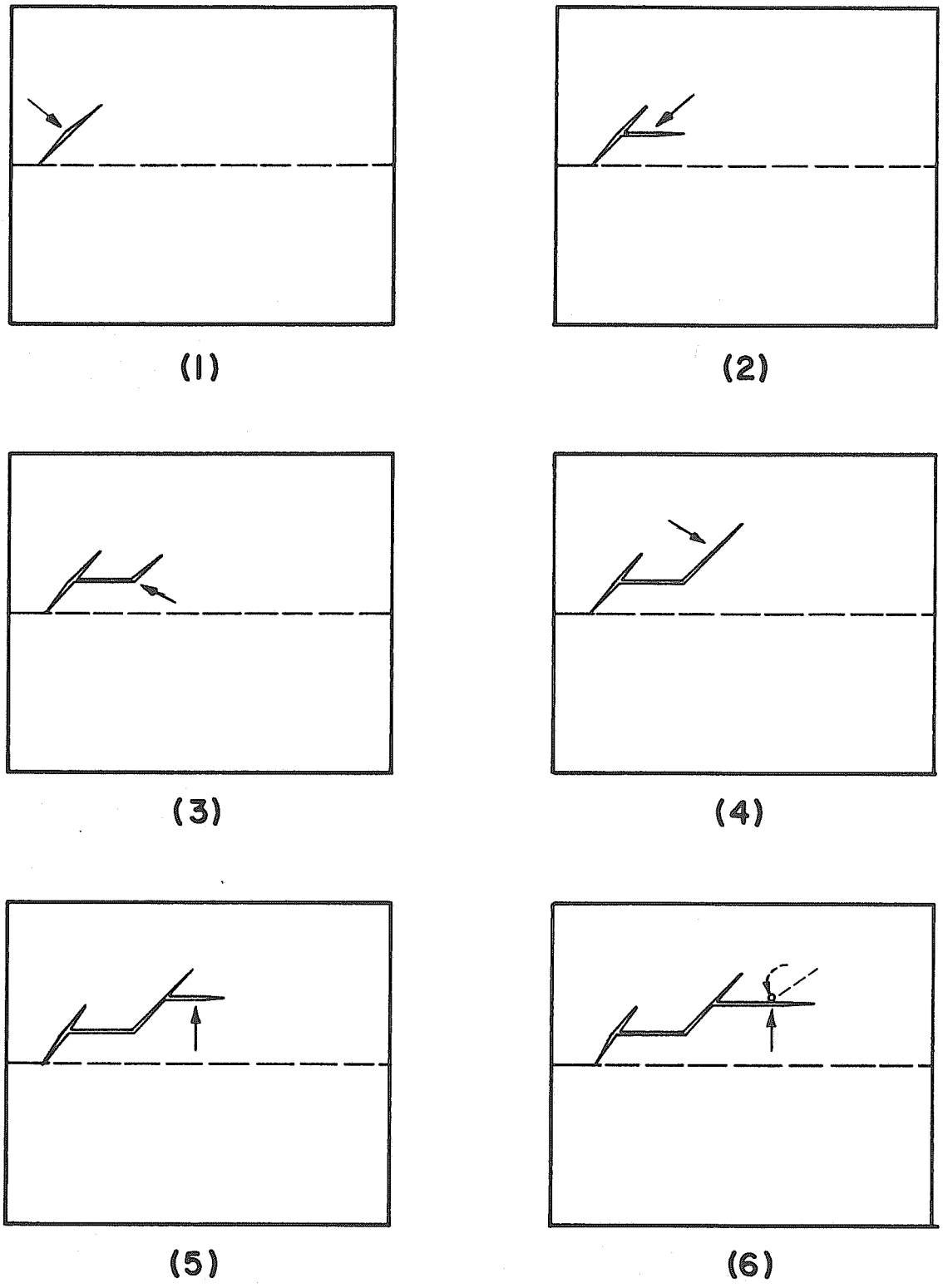

FIG. 4.25 CRACK GROWTH OF EXAMPLE D

CHAPTER 5 STRUCTURAL MODIFICATION AND REANALYSIS FOR CRACK GROWTH

5.1 Cracking and Structural Modification

It has been shown that cracking causes a change in the network topology. The structure is constantly being modified during the crack growth. Such a modification is very often confined to a small region of the structure at each stage of loading. In the analytical procedure presented in the previous chapter, the growth of a crack is treated individually, and it involves reanalysis of the entire structure each time a crack growth appears. This procedure is, of course, a time-consuming process. Therefore, in order to improve the efficiency of the procedure for crack growth analysis, an endeavour is made herein to develop a method which is aimed at reducing the computational effort during the reanalysis of the modified structure.

The basic nature of the structural modification for crack growth is common to all other structural modification problems, such as in cases of member properties alterations, cut-outs or add-ons, element yielding or plastification, optimization and redesign. The increasing use of high speed computers as a design aid, as well as an analytical tool, has further generated a wide-spread interest in efficient methods for the reanalysis of modified structures. The treatments

of structural modification can be classified into two main categories: the iterative method, and the direct method. Similar to the case of solving a set of linear algebraic equations, the iterative technique always encounters the difficulty of assuring the convergence, even though the method itself may prove to be advantageous in some instances. The direct method, on the other hand, produces a solution after a specified number of calculation steps. Thus, the pertinent question concerning the direct method again lies in the minimization of the total number of numerical operations.

In general, the direct method for reanalysis of modified structures is based on one of the following approaches:

1) compensation theorem [112, 113]
2) initial stress or strain methods [114-116]
3) parallel element concept [117-119]
4) perturbation method [120]
5) multiple configuration analysis [121, 122]
6) inverse matrix modification [123-127]
7) substructure analysis [128, 129]
8) mixed method [60, 89].

These headings should not be considered as a rigorous classification of the different approaches. In fact, there exist certain similarities in concept among them. A comprehensive comparison of some of the methods has

been presented by Kavlie and Powell [127]. Perhaps, it is safe to say, as concluded by Kavlie and Powell, that there is no single method of reanalysis which is superior in all cases. Therefore, the nature of any particular problem should be carefully examined before final judgment is made on the selection of a reanalysis procedure.

In what follows, a modification procedure based on a network theory is proposed. By realizing the topological implication of the general theory of modification, the procedure is not only carried out within the framework of the frontal solution technique, but it is also entirely consistent with the standard input used in structural analysis programs.

5.2 Modifications of Structural Networks

In order to visualize what is involved in the structural modification process, particularly with respect to the study of crack growth, a network-topological point of view again proves to be very helpful. Let the whole structural system be treated as a network. Then, modifications can take place under two conditions:

1) with fixed topology; and
2) with changing topology.

5.2.1 Fixed Topology

When the network topology is fixed, i.e., the number of nodes and branches remains unchanged; only the

branch characteristics are modified. This situation occurs when there is a change in the constitutive relationship, or in member geometry, or both, which results in a change of the element stiffness. Most of the crack-zone types of analysis fall into this category, Fig. 5.1. However, it should be noted that if the element stiffness is being reduced in the extreme, the element can be considered as being removed from the network, which in turn causes a change in the network topology.

5.2.2 Changing Topology

Another class of structural modifications involves a change in the network topology, in which the number of nodes and branches may increase or decrease. The introduction of crack-line into a structure inevitably changes the topology of the structural network. For the network shown in Fig. 5.2a, cracking may be simulated by splitting a node into two, which process may be termed "discoalescing," plus modifying some of the branch characteristics, Fig. 5.2b. Furthermore, new branches may be added between the two newly splitted nodes or connected to any pair of nodes in the network, for instance, to simulate interlocking, bonding, additional reinforcement, or constraints, as shown in Fig. 5.2b. Note that since all structures are represented as non-oriented graphs in the present study,

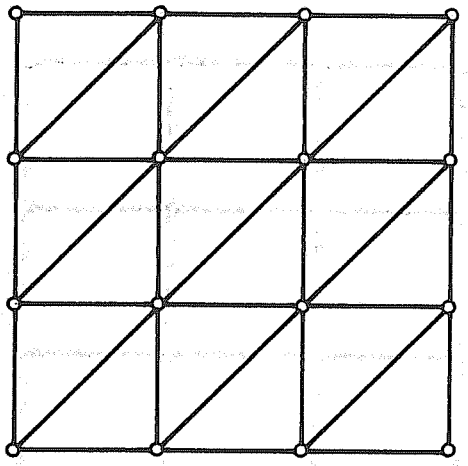

a) ORIGINAL STRUCTURAL NETWORK

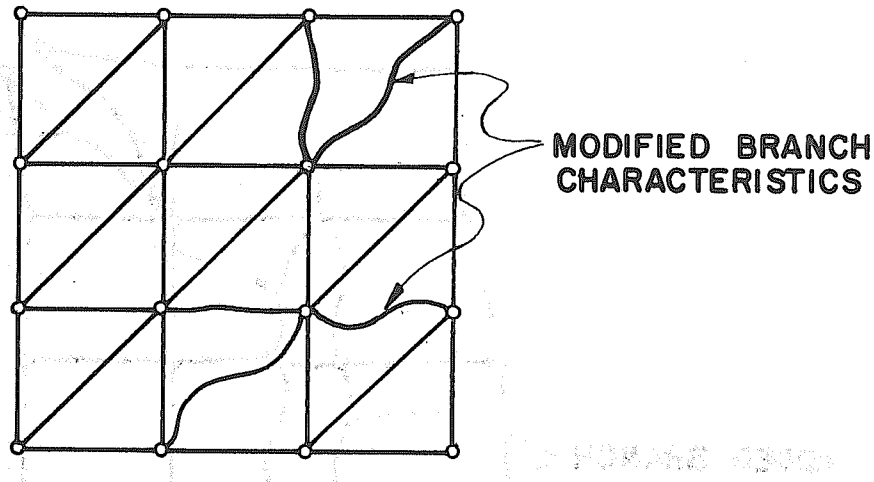

b) MODIFIED STRUCTURAL NETWORK

FIG. 5.1 MODIFICATIONS WITH FIXED TOPOLOGY

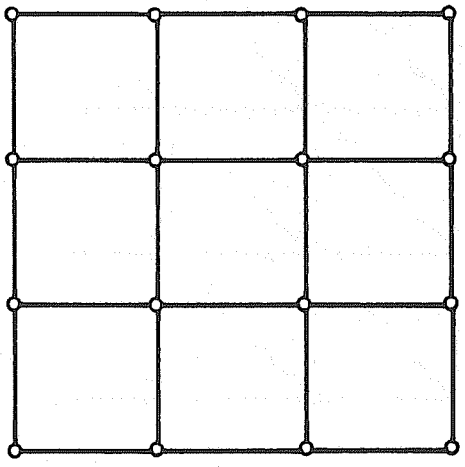

a) ORIGINAL STRUCTURAL NETWORK

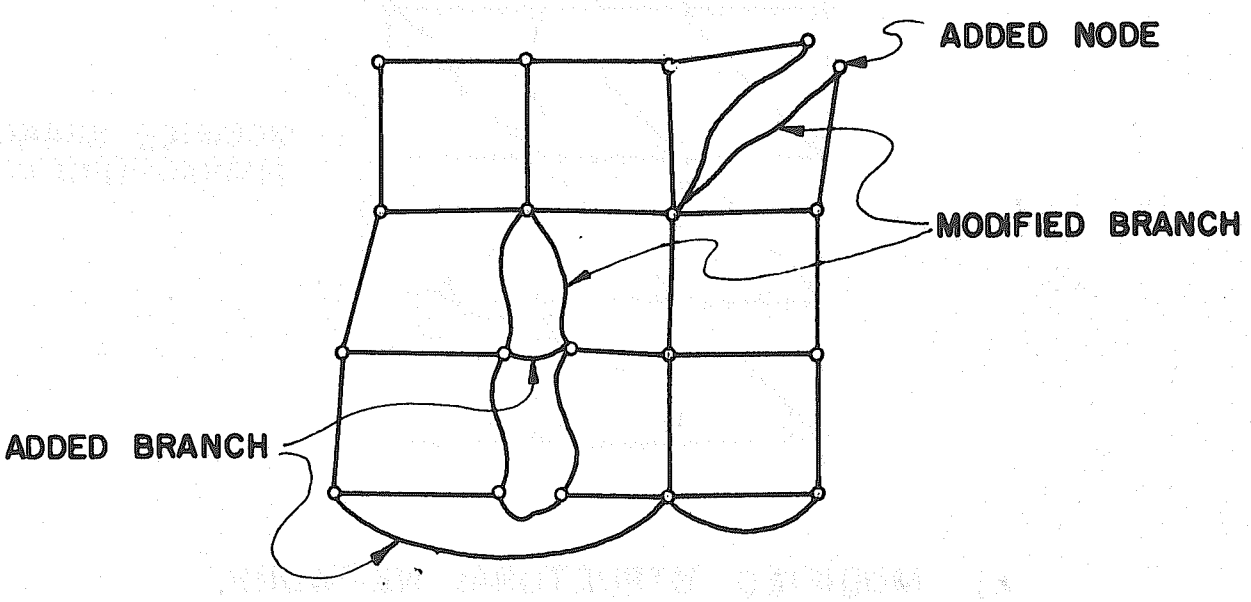

b) MODIFIED STRUCTURAL NETWORK

FIG. 5.2 MODIFICATION WITH CHANGING TOPOLOGY

multiple branches across any two nodes can be combined into a single branch, Fig. 5.3. This fact enables modification on any particular element to be accomplished by adding a parallel branch to account for the increase or decrease of the stiffness characteristics. In extreme cases, the element may be completely nullified or rigidified. Therefore, it can be seen that modification with changing topology constitutes a much broader and more important class of problems in structural modification than that associated with fixed topology.

5.3 Link-At-A-Time Algorithm and Its Dual

In electrical networks where each branch represents a scalar quantity, the LAT (link-at-a-time) algorithm provides a means of adding new branches, one at a time, to the original network without performing any additional inversion. This is accomplished by modifying the already computed inverse matrix at each time when a new branch, or link, is added to the network, hence without the necessity of resolving the whole new set of equations. The mathematical counterpart of this algorithm is the Sherman-Morrison (S-M) formula [130] which has been generalized to modification of inverse matrix by Householder. Thus it is also known as the Householder inverse matrix modification equation in matrix theory [131]. Several attempts have been made by various

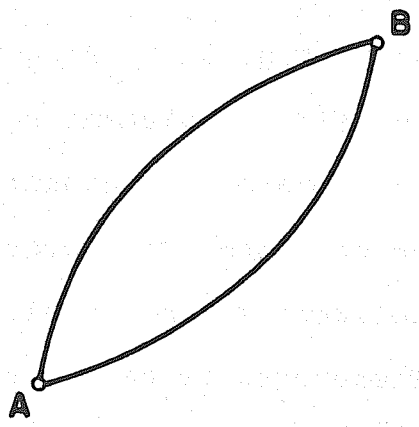

a) TWO PARALLEL BRANCHES

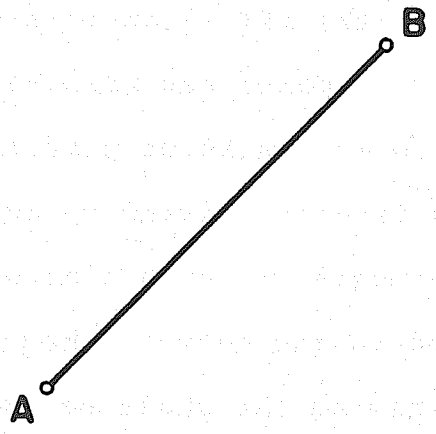

b) ONE EQUIVALENT BRANCH

FIG. 5.3 PARALLEL & EQUIVALENT BRANCHES

authors to apply the S-M formula, or the Householder equation with various degrees of success [124-127], and among them, the work of Argyris, Broulund, Roy, and Sharpf [125] holds the greatest promise. The Householder equation can be derived from different points of view. Householder generalized the S-M formulas from a heuristical approach [130]. Branin showed that it can be obtained from diacoptics using Kron's method of "tearing" [125]. Boesch gave an algebraic derivation of the equation in connection with electrical network theory [75]. Boesch's derivation is the only straightforward algebraic approach known to the writer, and offers a clear and simple insight into the Householder equation. Therefore, it is worthwhile to reproduce Boesch's derivation here for further discussion.

Suppose that matrix K, with K^{-1} being its known inverse, is perturbed by another matrix K_Δ. Assuming that K_Δ can be expressed as a triple product XkT, then:

$$(K + K_\Delta) = (K + XkT) = K(I + K^{-1}XkT)$$

Where I is a unit matrix let:

$$Q = K^{-1}X$$

$$H = kT$$

Then: $K(I + K^{-1}XkT) = K(I + QH)$.

Note that:

$$Q(I + HQ) = (I + QH)Q$$

Therefore:

$$(I + QH)^{-1}Q = Q(I + HQ)^{-1}$$

$$(I + QH)^{-1}QH = Q(I + HQ)^{-1}H$$

$$(I + QH)^{-1} + (I + QH)^{-1}QH = (I + QH)^{-1} + Q(I + HQ)^{-1}H$$

$$(I + QH)^{-1}(I + QH) = (I + QH)^{-1} + Q(I + HQ)^{-1}H$$

$$I = (I + QH)^{-1} + Q(I + HQ)^{-1}H$$

$$(I + QH)^{-1} = I - Q(I + HQ)^{-1}H$$

Make the corresponding substitution for Q and H

$$(I + K^{-1}XkT)^{-1} = I - K^{-1}X(I + kTK^{-1}X)^{-1}kT$$

$$[K^{-1}(K + XkT)]^{-1} = I - K^{-1}X[k(k^{-1} + TK^{-1}X)]^{-1}kT$$

$$(K + XkT)^{-1}K = I - K^{-1}X(k^{-1} + TK^{-1}X)^{-1}k^{-1}kT$$

and obtain

$$(K + XkT)^{-1} = K^{-1} - K^{-1}X(k^{-1} + TK^{-1}X)^{-1}TK^{-1} \qquad (5.1)$$

which is the LAT algorithm in matrix form. Clearly, if a link with a scalar value k is added to or deleted from a network whose coefficient matrix K is of the order n x n, then X and T can be interpreted as the branch-node incidence matrices A^T and A, whose order is n x 1 and 1 x n, respectively. Consequently, Eq. 5.1 can be put in the form

$$(K + A^tkA)^{-1} = K^{-1} - \frac{K^{-1}A^tAK^{-1}}{1/k + AK^{-1}A^t} \qquad (5.2)$$

where it can be seen that no inversion is necessary to obtain the new inverse matrix when a link is added or

deleted. This is the very essence of the LAT algorithm.

What must be observed in the derivation of Eq. 5.1 is that only two prerequisites are imposed:

1) There exists a K^{-1} for the coefficient matrix K; and

2) K_Δ can be decomposed into a triple product.

Another important point to be noted is that Eq. 5.1 is applicable as long as the network meets these two requirements, regardless whether the network graph is oriented or un-oriented. For most physical networks, the two prerequisites stated above can be fulfilled trivially.

Conversely, Boesch further shows that the dual of the LAT algorithm can be used to split a node in the network; and therefore, it is possible to increase the number of nodes in a network. In this case, the branch-mesh incidence matrix C takes the place of the branch-node incidence matrix A ; and F,f replace K,k , respectively. Obviously, F equals K^{-1}, and a mesh analysis is now performed, instead of a node anlaysis. The dual of the LAT algorithm can then be stated as:

$$(F + C^t f C)^{-1} = F^{-1} - F^{-1}C^t(f^{-1} + CF^{-1}C^t)^{-1}CF^{-1} \tag{5.3}$$

Again, if the rank of $(f^{-1} + CF^{-1}C^t)^{-1}$ is chosen to be one, then the new modified inverse matrix is simply given by:

$$(F + C^t f C)^{-1} = F^{-1} - \frac{F^{-1}C^t C F^{-1}}{1/f + CF^{-1}C^t} \qquad (5.4)$$

It is of interest to consider the topological interpretation of the dual LAT algorithm. If C is the branch-mesh matrix of a given network, with c being one of its rows and C_1 the remainder of C, then it is easily verified that C is not the branch-mesh matrix of the graph obtained by merely removing the branch corresponding to to the row c. Instead, it is obtained from removal of the branch by identifying its end nodes and deleting the created self loop, Fig. 5.4, [75]. This process is called "coalescing" the nodes. The reverse process, "discoalescing" the nodes, will then create a new node plus a new branch. By this process of coalescing or discoalescing, the size of a network can be continuously modified by deleting or adding new nodes and new branches.

Equations 5.2 and 5.4 are identical to the S-M formula, and Equations 5.1 and 5.3 are identical to the Householder equations. By this network-topological interpretation of the modification equations a clearer physical picture of how these formulas can be applied to the modification of structural networks is obtained. Indeed, the LAT algorithm and its dual have supplied much of the incentive to the network-topological approach taken in the present study. However, there are certain pitfalls in the practical application of the LAT algorithm.

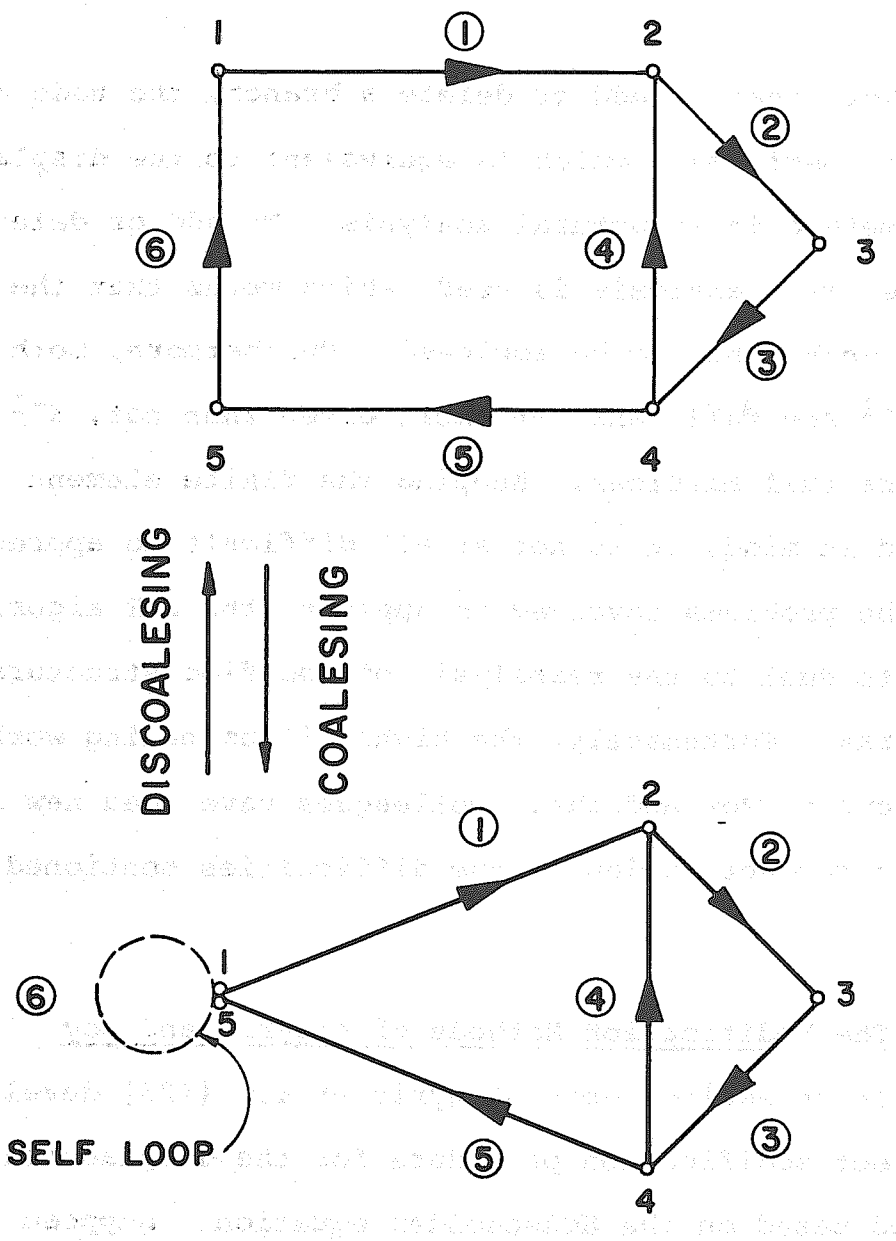

FIG. 5.4 NODE COALESCING AND DISCOALESCING

Note that to add or delete a branch, the node analysis is performed, which is equivalent to the displacement method in structural analysis. To add or delete a node, mesh analysis is used, which means that the force method has to be employed. Furthermore, both K^{-1} and F^{-1} are full rank, and more often than not, K^{-1} and F^{-1} are full matrices. Keeping the finite element method in mind, it is not at all difficult to appreciate all the problems involved in applying the LAT algorithm and its dual to the reanalysis of modified structural networks. Fortunately, the highly illuminating works of Argyris, Roy and their colleagues have shed new light on the reconciliation of the difficulties mentioned above.

5.4 The Modification Methods of Argyris and Roy

In an earlier work, Argyris et al. [125] developed a direct modification procedure for the displacement method based on the Householder equation. Suppose that in the well-known stiffness solution equation

$$K\, r = R$$

where K is the stiffness matrix, r the displacements, and R the applied loads, the matrix K is modified by K_Δ, then

$$(K + K_\Delta)(r + r_\Delta) = R$$

where r_Δ is the change in r due to K_Δ. By letting

$$K_\Delta = b^t k_\Delta b$$

where b is a coincidence or Boolean matrix with linearly independent rows, each of which contains all zeros except for one unit value located at the column associated with a change in K, the Householder equation assumes the form:

$$(K + b^t k_\Delta b)^{-1} = K^{-1} - K^{-1}b^t(k_\Delta^{-1} + bK^{-1}b^t)^{-1}bK^{-1}$$

Instead of solving directly for the modified inverse matrix, Argyris et al. computed the change in the displacement by

$$[(K + b^t k_\Delta b)^{-1}]R = [K^{-1} - K^{-1}b^t(k_\Delta^{-1} + bK^{-1}b^t)^{-1}bK^{-1}]R$$

$$r + r_\Delta = r - K^{-1}b^t\,(k_\Delta^{-1} + bK^{-1}b^t)^{-1}\,b\,r$$

$$\therefore \quad r_\Delta = -K^{-1}b^t\,(k_\Delta^{-1} + bK^{-1}b^t)^{-1}\,b\,r \qquad (5.5)$$

However, k_Δ^{-1} may not exist. Eq. 5.5 was rearranged to get

$$r_\Delta = -K^{-1}b^t\,[\,k_\Delta^{-1}(I + k_\Delta bK^{-1}b^t)\,]^{-1}\,b\,r$$

$$= -K^{-1}b^t(I + k_\Delta bK^{-1}b^t)^{-1}k_\Delta br \qquad (5.6)$$

Equation 5.6 can be further simplified by using the Choleski decomposition:

$$K = U^tU$$

$$K^{-1} = U^{-1}(U^t)^{-1} = U^{-1}U^{-t}$$

Let $Z = U^{-t}b^t$ to be obtained by forward-substitution, and

$$Q = bK^{-1}b = b\,U^{-1}\,U^{-t}\,b^t = Z^tZ$$

Then

$$r_\Delta = -U^{-1}U^{-t}b^t(I + k_\Delta Q)^{-1}k_\Delta br$$

$$= -U^{-1}Z[(Q^{-1} + k_\Delta)Q]^{-1}k_\Delta br$$

$$= -U^{-1}ZQ^{-1}(Q^{-1} + k_\Delta)^{-1}k_\Delta br \qquad (5.7)$$

This ingenious switch in strategy certainly makes the computation much more amenable. Note that no full inverse matrix is involved. Bearing in mind that U is triangular, and even though the inverse of a triangular matrix is also triangular, it is more convenient to let

$$r''' = ZQ^{-1}(Q^{-1} + k_\Delta)^{-1}k_\Delta br$$

The change in displacement r_Δ can then be obtained by back substitution

$$r_\Delta = -U^{-1}r'''$$

without the chore of actually inverting U and storing U^{-1}.

In their more recent work, Argyris and Roy [132-134] have developed a much more general treatment of structural modifications, which includes changing elements, adding degrees of freedom, removing degrees of freedom, and coupled combinations of all these three types of modifications, which are based on the "laws of 3 x 3 partitioned matrices", and the "Boolean separation of freedoms" [132]. Argyris and Roy were able to obtain not only an equation for modifications to elements, which is identical to Eq. 5.7 but also solutions for many other cases of modification as illustrated in their publications. Among all the examples, the most interesting of all is the "decoupling", as Roy called it [133, 134]. It is believed that, for the first time, adding new nodes to an existing structure has been made feasible. The method of Argyris and Roy truly provides a means of

treating problems in the structural modification with changing topology, which, obviously, is of great interest in the analysis of crack growth. For this reason, the computational procedure of the decoupling method proposed by Roy [133, 134] is summarized into the following steps:

1) In the displacement method of structural analysis, the system equation is written as

$$K\ r = R \tag{5.8}$$

where K is the global stiffness matrix, r the unknown displacements, and R the nodal point loads.

2) The stiffness matrix K is expressed through the symmetric transformation

$$K = a^t\ k\ a \tag{5.9}$$

where a is the Boolean connectivity matrix, and k the hyper-matrix of element stiffnesses with respect to global coordinates.

3) Decompose K into U^tU and solve for r.

4) The matrix K is partitioned into three distinct families:

(i) family i for U_i unmodified freedoms

(ii) family m for the U_m freedoms modified by element changes

(iii) family r for the U_r freedoms to be completely removed.

If F is defined as the inverse of K, $F = K^{-1}$, and the total degrees of freedom $n = n_i + n_m + n_r$, then

$$\begin{bmatrix} F_{rr} & F_{mr}^t & F_{ir}^t \\ F_{mr} & F_{mm} & F_{im}^t \\ F_{ir} & F_{im} & F_{ii} \end{bmatrix} \begin{bmatrix} K_{rr} & K_{mr}^t & K_{ir}^t \\ K_{mr} & K_{mm} & K_{im}^t \\ K_{ir} & K_{im} & K_{ii} \end{bmatrix} = \begin{bmatrix} I_r & 0 & 0 \\ 0 & I_m & 0 \\ 0 & 0 & I_i \end{bmatrix} \tag{5.10}$$

5) The submatrices of K are expressed in terms of F through a forward pass of Gaussian elimination. This 3 x 3 partitioning in Eq. 5.10 is thus reduced to

$$\begin{bmatrix} F_{rr} & F_{mr}^t & F_{ir}^t \\ 0 & V_{mm} & W_{im} \\ 0 & 0 & X_{ii} \end{bmatrix} \begin{bmatrix} K_{rr} & K_{mr}^t & K_{ir}^t \\ K_{mr} & K_{mm} & K_{im}^t \\ K_{ir} & K_{im} & K_{ii} \end{bmatrix} = \begin{bmatrix} I_r & 0 & 0 \\ -F_{mr}F_{rr}^{-1} & I_m & 0 \\ Y_{ir} & -W_{im}V_{mm}^{-1} & I_i \end{bmatrix} \tag{5.11}$$

where

$$V_{mm} = (F_{mm} - F_{mr}F_{rr}^{-1}F_{mr}^t)$$

$$W_{im} = (F_{im} - F_{ir}F_{rr}^{-1}F_{mr}^t)$$

$$X_{ii} = (F_{ii} - F_{ir}F_{rr}^{-1}F_{ir}^t - W_{im}V_{mn}^{-1}W_{im}^t)$$

and $Y_{ir} = W_{im}V_{mm}^{-1}F_{mr}F_{rr}^{-1} - F_{ir}F_{rr}^{-1}$.

6) The following relationships are obtained by a back substitution process through the last two rows of Eq. 5.11.

$$K_{ii}^{-1} = X_{ii}$$

$$K_{ii}^{-1}K_{im} = -W_{im}V_{mm}^{-1}$$

$$K_{ii}^{-1}K_{ir} = Y_{ir}$$

$$(K_{mr} - K_{im}^{t}K_{ii}^{-1}K_{ir}) = -V_{mm}F_{mr}F_{rr}^{-1}$$

$$(K_{mm} - K_{im}^{t}K_{ii}^{-1}K_{im}) = V_{mm}^{-1} \tag{5.12}$$

7) With the Boolean matrices $\tilde{b}_i$, $\tilde{b}_m$, $\tilde{b}_r$ for family i, m, r, respectively, the submatrices of F can be expressed as

$$F_{ii} = \tilde{b}_i\, F\, \tilde{b}_i^t \quad ; \quad F_{im} = \tilde{b}_i\, F\, \tilde{b}_m^t \quad ; \quad F_{ir} = \tilde{b}_i\, F\, \tilde{b}_i^t$$

$$F_{mm} = \tilde{b}_m\, F\, \tilde{b}_m^t \quad ; \quad F_{mr} = \tilde{b}_m\, F\, \tilde{b}_r^t \quad ; \quad F_{rr} = \tilde{b}_r\, F\, \tilde{b}_r^t \tag{5.13}$$

Note that $\tilde{b}_i^t\tilde{b}_i + \tilde{b}_m^t\tilde{b}_m + \tilde{b}_r^t\tilde{b}_r = I_n$.

8) Defining

$$Z_m = U^{-t}\tilde{b}_m^t$$

$$Z_r = U^{-t}\tilde{b}_r^t \tag{5.14}$$

the submatrices of F can alternately be obtained from

$$F_{mm} = Z_m^t Z_m \quad ; \quad F_{mr} = Z_m^t Z_r \quad ; \quad F_{rr} = Z_r^t Z_r \tag{5.15}$$

9) Correspondingly, the displacements r and loads R can be regrouped by the Boolean matrices as

$$R = \tilde{b}_i^t\, R_i + \tilde{b}_m^t\, R_m + \tilde{b}_r^t\, R_r$$

$$r = \tilde{b}_i^t\, r_i + \tilde{b}_m^t\, r_m + \tilde{b}_r^t\, r_r \tag{5.16}$$

where

$$R_i = \tilde{b}_i\, R \quad ; \quad R_m = \tilde{b}_m\, R \quad ; \quad R_r = \tilde{b}_r\, R$$

$$r_i = \tilde{b}_i\, r \quad ; \quad r_m = \tilde{b}_m\, r \quad ; \quad r_r = \tilde{b}_r\, r$$

10) The original system, Eq. 5.8 can now be written in partitioned form

$$\begin{bmatrix} K_{ii} & K_{im} & K_{ir} \\ K_{im}^t & K_{mm} & K_{mr} \\ K_{ir}^t & K_{mr} & K_{rr} \end{bmatrix} \begin{bmatrix} r_i \\ r_m \\ r_r \end{bmatrix} = \begin{bmatrix} R_i \\ R_m \\ R_r \end{bmatrix} \tag{5.17}$$

11) In the case of decoupling, there is no removal of freedom involved, and Eq. 5.17 reduces to

$$\begin{bmatrix} K_{ii} & K_{im} \\ K_{im}^t & K_{mm} \end{bmatrix} \begin{bmatrix} r_i \\ r_m \end{bmatrix} = \begin{bmatrix} R_i \\ R_m \end{bmatrix} \tag{5.18}$$

12) The family m is further expanded into a new family e to account for the newly created degrees of freedom, (see Fig. 5.5).

$$\begin{bmatrix} K_{ii} & \tilde{K}_{im} & K_{ie} \\ \tilde{K}_{im}^t & \tilde{K}_{mm} & K_{me} \\ K_{ie}^t & K_{me}^t & K_{ee} \end{bmatrix} \begin{bmatrix} \tilde{r}_i \\ \tilde{r}_m \\ r_e \end{bmatrix} = \begin{bmatrix} R_i \\ \tilde{R}_m \\ R_e \end{bmatrix} \tag{5.19}$$

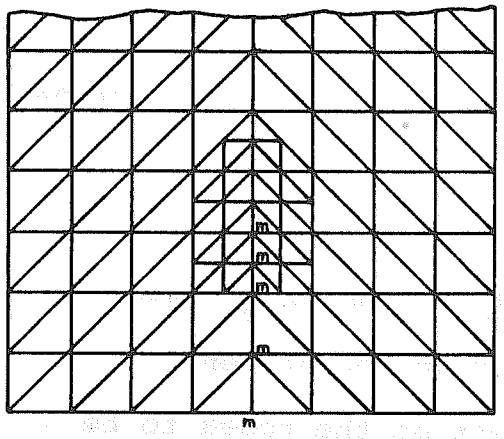

ORIGINAL CONTINUUM

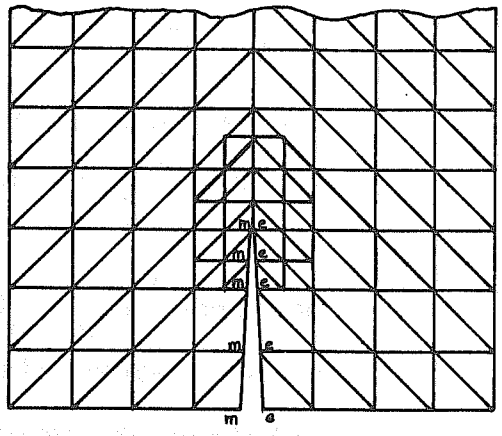

MODIFIED CONTINUUM

K_{ii}	K_{im}
$K_{im}^{\dagger}$	K_{mm}

RE-ORDERED CO-EFFICIENT MATRIX OF ORIGINAL CONTINUUM

K_{ii}	$\tilde{K}_{im}$	K_{ie}
$\tilde{K}_{im}^{\dagger}$	$\tilde{K}_{mm}$	K_{me}
$K_{ie}^{\dagger}$	$K_{me}^{\dagger}$	K_{ee}

RE-ORDERED CO-EFFICIENT MATRIX OF MODIFIED CONTINUUM

FIG. 5.5 DECOUPLING OF NODAL UNKNOWNS IN A CONTINUUM (AFTER ROY)

13) The following relationships are observed:

$$\begin{aligned} &\text{i)} && \text{In general, } n_e = n_m \text{ , with } K_{me} = 0 \\ &\text{ii)} && \tilde{K}_{im} + K_{ie} = K_{im} \\ &\text{iii)} && \tilde{K}_{mm} + K_{ee} = K_{mm} \\ &\text{iv)} && \tilde{R}_m = R_e = R_m \end{aligned} \qquad (5.20)$$

14) Matrices $\tilde{K}_{im}$, K_{ie} , $\tilde{K}_{mm}$, K_{me} , and K_{ee} have to be re-assembled from the branch or element matrices k which are incident at the nodes to be decoupled, i.e.,

$$\begin{aligned} K_{ie} &= \tilde{a}_i^t \; k \; \tilde{a}_e \\ \tilde{K}_{im} &= \tilde{a}_i^t \; k \; \tilde{a}_m \\ K_{me} &= \tilde{a}_m^t \; k \; \tilde{a}_e \\ \tilde{K}_{mm} &= \tilde{a}_m^t \; k \; \tilde{a}_m \\ K_{ee} &= \tilde{a}_e^t \; k \; \tilde{a}_e \end{aligned} \qquad (5.21)$$

where $\tilde{a}_i = a_i \tilde{b}_i^t$; $\tilde{a}_m = a_m \tilde{b}_m^t$; $\tilde{a}_e = a_e \tilde{b}_e^t$

15) Subtract Eq. 5.18 from Eq. 5.19 to obtain

$$\begin{bmatrix} K_{ii} & K_{im} & K_{ie} \\ K_{im}^t & \tilde{K}_{mm} & K_{me} \\ K_{ie}^t & K_{me}^t & K_{ee} \end{bmatrix} \begin{bmatrix} \tilde{r}_{\Delta i} \\ \tilde{r}_m \\ r_e \end{bmatrix} = \begin{bmatrix} K_{im} \; r_m \\ \tilde{R}_m - \tilde{K}_{im}^t \; r_i \\ R_e - K_{ie}^t \; r_i \end{bmatrix} \qquad (5.22)$$

where $\tilde{r}_{\Delta i} = r_i - r_i$

16) Solve for $\tilde{r}_{\Delta i}$ from the first row of Eq. 5.22,

$$\tilde{r}_{\Delta i} = K_{ii}^{-1} \left(K_{im} \; r_m - \tilde{K}_{im} \; \tilde{r}_m - K_{ie} \; r_e \right) \qquad (5.23)$$

17) Substitute $\tilde{r}_{\Delta i}$ back into Eq. 5.22 to obtain

$$\begin{bmatrix} (\tilde{K}_{mm} - \tilde{K}_{im}^t K_{ii}^{-1} \tilde{K}_{im}) & (K_{me} - \tilde{K}_{im}^t K_{ii}^{-1} K_{ie}) \\ (K_{me} - \tilde{K}_{im}^t K_{ii}^{-1} K_{ie})^t & (K_{ee} - K_{ie}^t K_{ii}^{-1} K_{ie}) \end{bmatrix} \begin{bmatrix} \tilde{r}_m \\ r_e \end{bmatrix} \tag{5.24}$$

$$= \begin{bmatrix} \tilde{R}_m - \tilde{K}_{im}^t (K_{ii}^{-1} K_{im} r_m + r_i) \\ R_e - K_{ie}^t (K_{ii}^{-1} K_{im} r_m + r_i) \end{bmatrix}$$

which can be abbreviated as

$$\begin{bmatrix} Y_{mm} & Y_{me} \\ Y_{me}^t & Y_{ee} \end{bmatrix} \begin{bmatrix} \tilde{r}_m \\ r_e \end{bmatrix} = \begin{bmatrix} P_m \\ P_e \end{bmatrix}$$

18) Make proper adjustments for the absence of family r in Eq. 5.12 and Eq. 5.11 to obtain

$$K_{ii}^{-1} K_{im} = - F_{im} F_{mm}^{-1} = - \tilde{b}_i U^{-1} Z_m F_{mm}^{-1}$$

$$K_{ii}^{-1} = F_{ii} - F_{im} F_{mm}^{-1} F_{im}^t \tag{5.25}$$
$$= \tilde{b}_i (K^{-1} - U^{-1} Z_m F_{mm}^{-1} Z_m^t U^{-t}) \tilde{b}_i^t$$

19) let

$$K_m = \tilde{b}_i^t K_{im}$$
$$T_m = U^{-1} K_m$$
$$K_e = \tilde{b}_i^t K_{ie}$$
$$T_e = U^{-1} K_e$$

and compute

$$
\begin{aligned}
X_{me} &= U_m^{-t} \quad (Z_m^t \quad T_e) \\
X_{mx} &= U_m^{-t} \quad (Z_m^t \quad T_m) \\
Y_{mm} &= \tilde{K}_{mm} - T_m^t T_m + X_{mx}^t X_{mx} \\
Y_{me} &= K_{me} - T_m^t T_e + X_{mx}^t X_{me} \\
Y_{ee} &= K_{ee} - T_e^t T_e + X_{me}^t X_{me}
\end{aligned}
\tag{5.26}
$$

20) Let $W_m = Z_m Q_{mm}^{-1} r_m = Z_m F_{mm}^{-1} r_m$

$\tilde{R}_m = R_m + \tilde{R}_\Delta = \tilde{b}_m R + \tilde{R}_\Delta$

where $\tilde{R}_\Delta$ is the change in applied load, if any, and compute

$$
\begin{aligned}
P_m &= \tilde{R}_m + T_m^t W_m - K_{mr}^t \\
P_e &= R_e + T_e^t W_m - K_{er}^t
\end{aligned}
\tag{5.27}
$$

21) Now the displacements of nodes being decoupled can be obtained from

$$
\begin{aligned}
r_e &= (Y_{ee} - V_{me}^t V_{me})^{-1} (P_e - V_{me}^t P_m') \\
\tilde{r}_m &= U_{mm}^{-1} (P_m' - V_{me} r_e)
\end{aligned}
\tag{5.28}
$$

where $P_m' = U_{mm}^{-t} P_m$, $V_{me} = U_{mm}^{-t} Y_{me}$ and $U_{mm}^{-1} U_{mm}^{-t} = Y_{mm}^{-1}$

22) The changes in displacement is obtained by substitution

$$
\tilde{r}_{\Delta i} = \tilde{b}_i U^{-1} \left\{ (Z_m F_{mm}^{-1} Z_m^t - I_m) \quad (T_e r_e + T_m \tilde{r}_m) - W_m \right\}
\tag{5.29}
$$

23) Recalling $\tilde{r}_i = \tilde{r}_{\Delta i} + r_i$, the final result of displacements $\tilde{r}$ due to decoupling are

$$\tilde{r} = \begin{bmatrix} \tilde{r}_i \\ \tilde{r}_m \\ r_e \end{bmatrix} \qquad (5.30)$$

Pursuing the decoupling procedure step by step is richly rewarding. In fact, the program SMIS by Wilson [135] has been extended by the writer to carry out the matrix algebra for the purpose of understanding Roy's decoupling procedure. It reveals that the topology of the structure, as expressed through the Boolean connectivity matrices a and b , plays a predominant role. The grouping of the variables into families i, m, r and e is accomplished by Boolean matrix transformations, Eqs. 5.13, 5.16, rather than physically reordering the equations. The stiffness matrices of all branches or elements incident to the nodes being decoupled have to be reformed, Eq. 5.21, according to the topological changes. The newly formed global stiffness matrix is then subtracted from the original one, Eq. 5.22. This can be interpreted as removing a portion of structure where decoupling occurs and replacing it by a new part with the decoupled nodes, Eq. 5.24. Again, as in the case of element modification in Eq. 5.7, the change in displacements is sought, Eq. 5.23. All these facets of the decoupling procedure suggest a new possibility of extending the LAT algorithm to handle the problem of node decoupling, which can be conveniently incorporated

into the frontal solution technique and perform structural modification in a much simpler way.

5.5 Extension of Link-At-A-Time Algorithm

Recall the derivation of LAT algorithm in Sec. 5.3. One of the prerequisites is the assumption of the existence of an inverse. This implies that the matrix K can be decomposed into U^tU and $K^{-1} = U^{-1}U^{-t}$. Suppose that K is concatenated to form

$$K = \begin{bmatrix} K & 0 \\ 0 & I_e \end{bmatrix} \tag{5.31}$$

where I_e is a unit submatrix to account for the newly created degrees of freedom. Clearly, it follows that

$$U = \begin{bmatrix} U & 0 \\ 0 & I_e \end{bmatrix} \tag{5.32}$$

and

$$\bar{U}^{-1} = \begin{bmatrix} U^{-1} & 0 \\ 0 & I_e \end{bmatrix} \tag{5.33}$$

whereby the original system has not been disturbed, and the inverse of $\bar{K}$ is readily obtainable. The next requirement to be fulfilled is the formation of a triple

product. This presents no difficulty if one recalls the properties of coincidence matrices, enumerated in Sec. 2.21. If the original system is to be modified or perturbed, the change $\bar{K}_\Delta$ in the global sense can be represented by

$$\bar{K}_\Delta = b^t \bar{k}_\Delta b \tag{5.34}$$

which simply means that the amount of change $\bar{k}_\Delta$ is dispersed throughout the entire system in a manner dictated by the coincidence or Boolean matrix b. Since the modification of any structure must be known ad init., the triple product can be constructed accordingly. Now Eq. 5.1 can be cast in the form of

$$(\bar{K} + b^t \bar{k}_\Delta b)^{-1} = \bar{K}^{-1} - \bar{K}^{-1} b^t (\bar{k}_\Delta^{-1} + b\bar{K}^{-1} b^t)^{-1} b\bar{K}^{-1} \tag{5.35}$$

and similarly Eq. 5.7 becomes

$$\bar{r}_\Delta = -\bar{U}^{-1} \bar{Z} \bar{Q}^{-1} (\bar{Q}^{-1} + \bar{k}_\Delta)^{-1} \bar{k}_\Delta b r \tag{5.36}$$

Therefore, the step in decoupling by LAT algorithm consists of:

1) Forming the stiffness matrix k_- of the branches or elements incident to the nodes to be decoupled, Fig. 5.6a.

2) Forming the stiffness matrix k_+ to account for the node decoupling. Fig. 5.6b.

3) Computing the total amount of change

$$\bar{k}_{\Delta} = k_{+} - k_{-} - I_{e}$$

4) Applying Eq. 5.33 to obtain the change in displacements r_{Δ}.

5) Summing the change in displacements r_{Δ} to the initial displacements to obtain final displacements $\bar{r}$

$$\bar{r} = r + r_{\Delta}$$

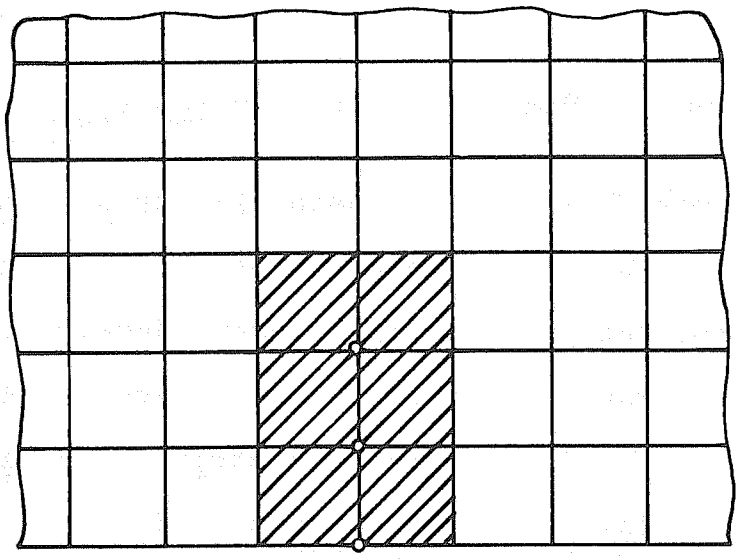

a) ELEMENT STIFFNESS k_- TO BE REMOVED

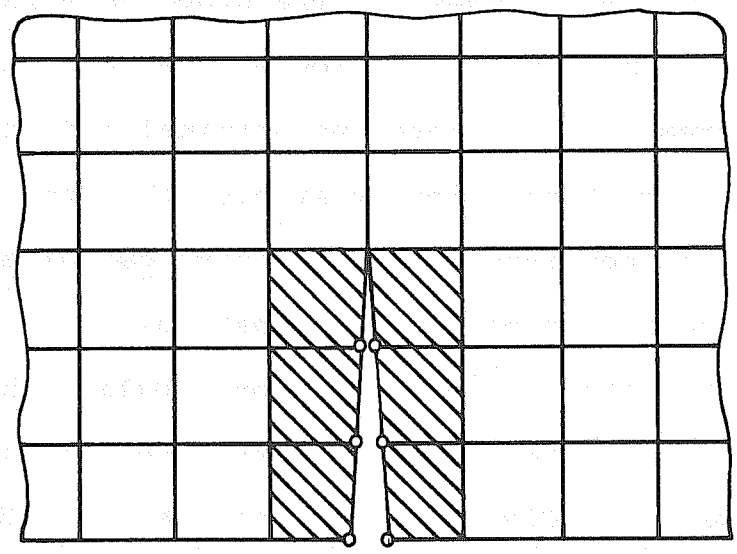

b) ELEMENT STIFFNESS k_+ TO BE ADDED

FIG. 5.6 DECOUPLING PROCESS BY LAT ALGORITHM

5.6 A Proof of Nonsingularity and Positive Definiteness

The possibility for nonsingularity of the matrix $(\bar{Q}^{-1} + \bar{k}_\Delta)$ in Eq. 5.33 becomes a particular concern, because the matrix $\bar{k}_\Delta$ in the present development is obtained in a rather unorthodox whay which involves subtraction of a unit diagonal submatrix. Argyris et al. [125] have claimed that the quantity $(I + k_\Delta b\ K^{-1}\ b^t)$ in Eq. 5.6 is nonsingular even when k_Δ is singular; and that $(Q^{-1} + k_\Delta)$ in Eq. 5.7 is positive definite, without giving the actual proof. An independent attempt is made by the writer here to assure the nonsingularity and positive definiteness in the proposed solution procedure by proving the following theorem:

Theorem 5.1 : If both the original and the modified structures are kinematically stable, then the quantity $(\bar{Q}^{-1} + \bar{k}_\Delta)$ is nonsingular and positive definite, regardless of whether or not $\bar{k}_\Delta$ is nonsingular.

To show that $(\bar{Q}^{-1} + \bar{k}_\Delta)$ is nonsingular, the following Lemma due to Lam [136] is first presented:

Lemma 5.1 : Given two matrices M and N . If (I + MN) is nonsingular, then (I + NM) is also nonsingular.

Proof : By contradiction, assume that

$(I + NM)$ is singular. Then

$\exists\ v \neq o\ ;\ \ni (I + NM)\ v = o$

$(NM)\ v = -v$

Let $M\ v = u$

$$M\ N\ u = M\ N\ (M\ v) = - Mv = - u$$

or $(I + MN)\ u = o$

But $u \neq o$

$(I + MN) = o$ 

$\therefore$ $(I + NM)$ is also nonsingular.

Since both the original structure and the modified structure are kinematically stable, which implies $\bar{K}$ and $(\bar{K} + \bar{K}_\Delta)$ are nonsingular, and there exists $\bar{K}^{-1}$ and $((\bar{K} + \bar{K}_\Delta)^{-1}$ Therefore,

$(\bar{K} + \bar{K}_\Delta) = (I + \bar{K}_\Delta \bar{K}^{-1})\ \bar{K}$ is nonsingular.

recall $\bar{K}_\Delta = b^t\ \bar{k}_\Delta b$ and $b\ b^t = I = b^t\ b$

and let $Y = \bar{k}_\Delta b$

then $(I + b^t\ Y\ \bar{K}^{-1})$ is nonsingular.

by lemma 5.1, $(I + Y\ \bar{K}^{-1}\ b^t)$ is also nonsingular.

Let $\bar{Q} = b\ \bar{K}^{-1} b^t$, which is nonsingular,

because it is possible to construct

$$(b\ \bar{K}^{-1}\ b^t)\ (b\ \bar{K}\ b^t) = I$$

Therefore, $\bar{Q}^{-1}$ exists.

Make substitution

$$(I + \bar{k}_\Delta\ b\ \bar{K}^{-1}\ b^t) = (\bar{Q}^{-1} + \bar{k}_\Delta)\ \bar{Q}$$

Clearly, $(\bar{Q}^{-1} + \bar{k}_\Delta)$ is nonsingular.

To show that $(\bar{Q}^{-1} + \bar{k}_\Delta)$ is also positive definite, one only needs to evoke the fact that the structural stiffness matrix is positive definite. Therefore $\bar{K}$ and $(\bar{K} + \bar{K}_\Delta)$ must be positive definite as in any other structure as long as they are kinematically stable. Then

$$(\bar{Q}^{-1} + \bar{k}_\Delta) = (b\ \bar{K}\ b^t + \bar{k}_\Delta)$$

$$= b\ \bar{K}\ b^t + b\ \bar{K}_\Delta b^t = b\ (\bar{K} + \bar{K}_\Delta)\ b^t.$$

By the definition of inner product

$$(\ y\ ,\ (\bar{K} + K_\Delta)\ y\ ) > 0$$

and $(\ A^t\ v\ ,\ u\ ) = (v\ ,\ Au)$

Let $y = b^t\ x$

$$(b^t\ x\ ,\ (\bar{K} + \bar{K}_\Delta)\ b^t\ x\ ) > 0$$

and $(\ x\ ,\ b\ (\bar{K} + \bar{K}_\Delta)\ b^t\ x\ ) > 0$

$\therefore$ $b\ (\bar{K} + \bar{K}_\Delta)\ b^t = (\bar{Q}^{-1} + \bar{k}_\Delta)$ is positive definite. Obviously, Theorem 5.1 holds true for all types of modification.

5.7 Construction of Choleski Decomposition from Frontal Solution

In order to implement the LAT algorithm, the Choleski decomposition U^tU is required. It was stated earlier in Sec. 3.1 that all methods of solving a system of linear equations can be regarded as being a judicious application of Gaussian elimination. An example of this has been illustrated in Sec. 3.4 where the $LD^{-1}L^t$ decomposition proposed by Melosh and Bamford is shown to be equivalent to the Gaussian elimination in the frontal technique developed by Iron. Consequently, one would expect that the Choleski decomposition U^tU could be obtained from the frontal solution. This is, indeed, the case, because the identity

$$LD^{-1}L^t = L\,(D^{-1/2})\,L^t = U^tU \qquad (5.34)$$

is trivial. The only remaining difficulty lies in the fact that in the frontal technique the order of variables being eliminated is entirely independent from the order of node numbering sequence. Therefore, a special computational scheme must be developed to recover matrix U of the Choleski decomposition for the reanalysis of modified structures. The method used in the present study consists of the following:

a) When the modification procedure is called for, storage allocation is made in the back substitution phase of the frontal solution proce-

dure.

b) Each row of the U matrix is formed in reversed order by dividing the entire equation by the square root of its diagonal term. This is equivalent to the multiplication of $(D^{-1/2})L^t$ in Eq. 5.34.

c) The resulting equation together with the active front are recorded in ECS.

d) The order of the variables being processed is recorded in an array (NIK), and the destination of the diagonal term in (VDS).

With these minor modifications to the frontal solution routine, the matrix U (in reversed order) of Choleski decomposition is readily made available for the reanalysis of the modified structure.

5.8 Program Input Requirements

Once the topological implication of the LAT algorithm and the properties of the coincidence matrix are recognized, together with the availability of matrix U , the implimentation of the modification procedure is rather simple from the user's standpoint. Two subroutines, MODIFIC and LATALGO, have been written for this purpose. No elaborate input data is required, since the main computer program developed in the present study is format free, except for those numerical data which can be expected in a repeated form, such as nodal point coordinates and element data. If modification of the structure is anticipated, the following simple commands will effectuate the reanalysis by the LAT algorithm:

a) SOLVE WITH MODIFICATION PROCEDURE

This command will cause the matrix U of the Choleski decomposition to be constructed during the back substitution phase of the frontal solution process.

b) STAGE i , NUMBER OF NODES INVOLVED = n

Value i is the identification number of the stage of modification, and n is the number of nodes involved in that stage of modification, which is needed for storage allocation.

c) ADD NODE

Supply nodal point data after this command, if there is a new node to be created in the structural

modification.

d) DELETE ELEMENT

Only the element number need be supplied. From this information the stiffness k_- is formed, see Fig. 5.6a.

c) ADD ELEMENT

Supply the element data from which stiffness k_+ will be constructed, see Fig. 5.6b.

Note that the coincidence matrix b in Eq. 5.31 is formed internally by the program. All the node and element data are input in the same format as in the original structure, and they are administrated by subroutine MODIFIC. However, different format is also allowed by specifying the new input data format at each command card. The LAT algorithm is then carried out in subroutine LATALGO. Multiple stages of modification are possible. But it should be kept in mind that each modification is made on the original structure, not on the last modified one. The "modification of modification" procedure proposed by Argyris and Roy [132 - 134] has not yet been included in the present program.

Once the displacements of the modified structure have been obtained, the normal process of computing the new element stresses or forces follows. And the program is ready for the execution of next stage of modification, or for another new problem.

5.9 Example Problems

As mentioned earlier in Sec. 5.4, the program SMIS (Symbolic Matrix Interpretive System) by Wilson [135] has been extended to carry out Roy's decoupling procedure. At the same time, it offers an independentcheck on the LAT algorithm. In fact, the SMIS program, with its capability of directly adding the element stiffness to form the total structure stiffness, has proven to be indispensable during the development of the modification procedure. The first three problems, Examples E, F and G, have been purposely devised as check cases which can be easily verified step by step with SMIS, or by hand calculation. Examples H and I aim at demonstrating the potential use in relation to the progressive crack growth analysis. All of the above examples were successfully analyzed.

Example E : Adding an Element

The original truss structure is shown on Fig. 5.7a. It is to be modified by adding another vertical member to the structure, Fig. 5.7b. Displacements of the two unrestrained nodes are given on the figures.

Example F : Discoalescing a Node

The lower node of the structure shown in Fig. 5.7a is to be split into two, hence the total degrees of freedom of the structure are increased by two due to such a modification. This situation is also a simulation of cracking at a node. Clearly, all truss members connected to that cracked node become unstressed, and the final results should be identical to a simple two-bar system, which can quickly be checked by statics, see Fig. 5.7c.

Example G : Deleting an element

A two-dimensional finite element is added to the truss system of Fig. 5.7a to serve as a diaphram, Fig. 5.7d. The modification procedure is used to obtain the resulting effect due to the removal of the diaphram. Obviously, the final displacements and bar forces should be identical to the case shown in Fig. 5.7a.

Example H : Double Cantilever Test

The double cantilever test, also known as trousers test, is often employed in the field of fracture mechanics to study the crack propagation phenomena. A simple specimen is shown in Fig. 5.8a. The cracking condition is shown in Fig. 5.8b. Furthermore, to illustrate the capability of the modification procedure in simultaneously introducing a new node and a new element, the effect of interlocking is simulated by the insertion of a bond or joint element at the crack, Fig. 5.8c.

Example I : Simulation of Crack Growth

Example I is a replica of Example A, in chapter 4, except that joint elements are introduced at the crack-lines to simulate the interlocking effect, and only half of the structure is considered because of symmetry. The stages of crack growth are identical to Example A Fig. 5.9a. Therefore, it is possible to examine the two different structural responses. The deflection at the point under the applied load is shown on Fig 5.9b for Example I and A , for the various stages of crack growth.

5.10 Remarks on Efficiency

The present modification procedure based on the LAT algorithm has been demonstrated to be feasible

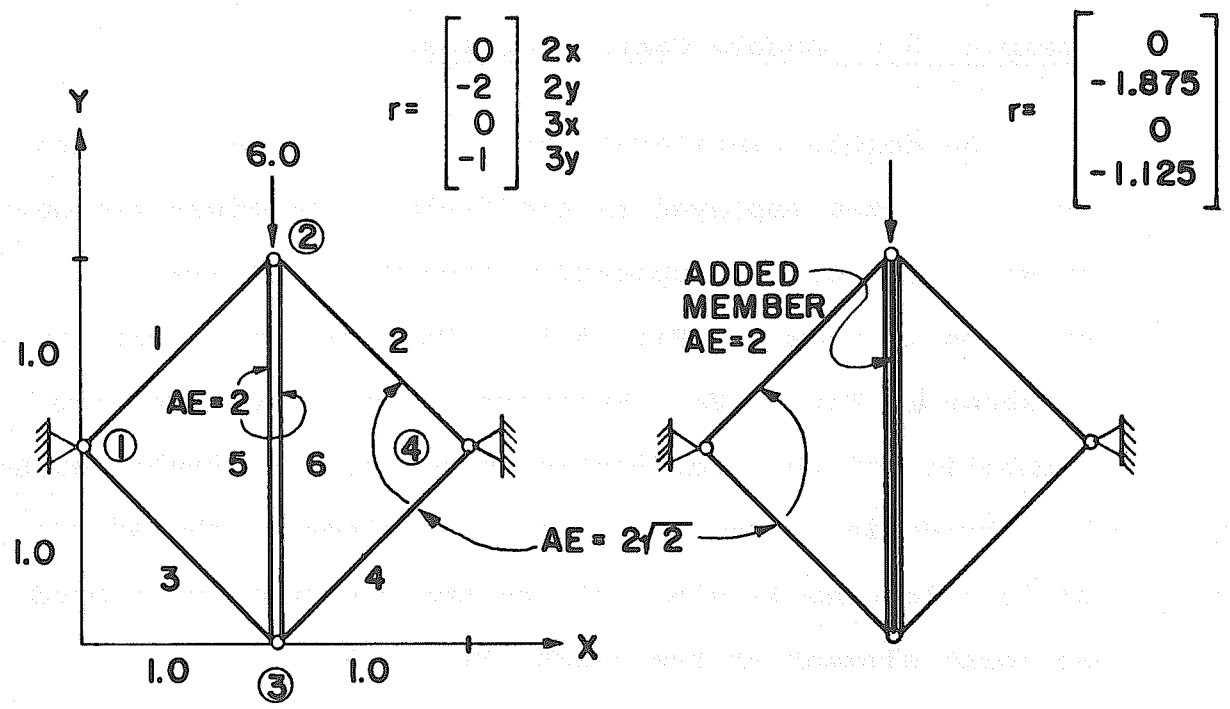

a) ORIGINAL TRUSS STRUCTURE

b) EXAMPLE E

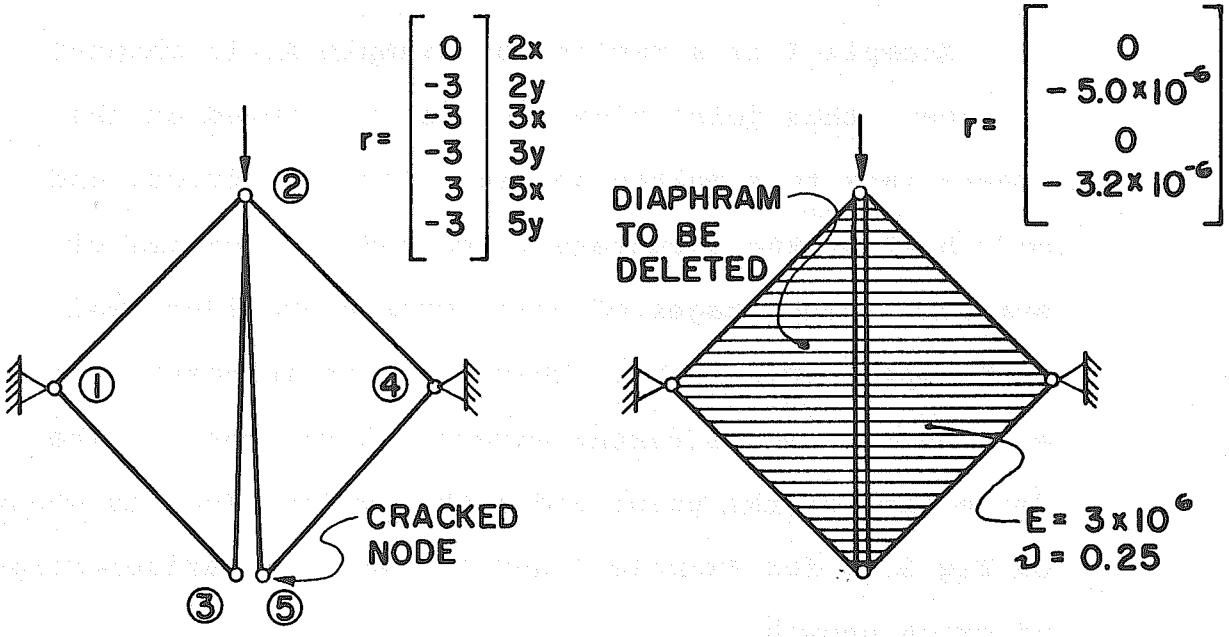

c) EXAMPLE F

d) EXAMPLE G

FIG. 5.7 MODIFICATION EXAMPLES E, F & G

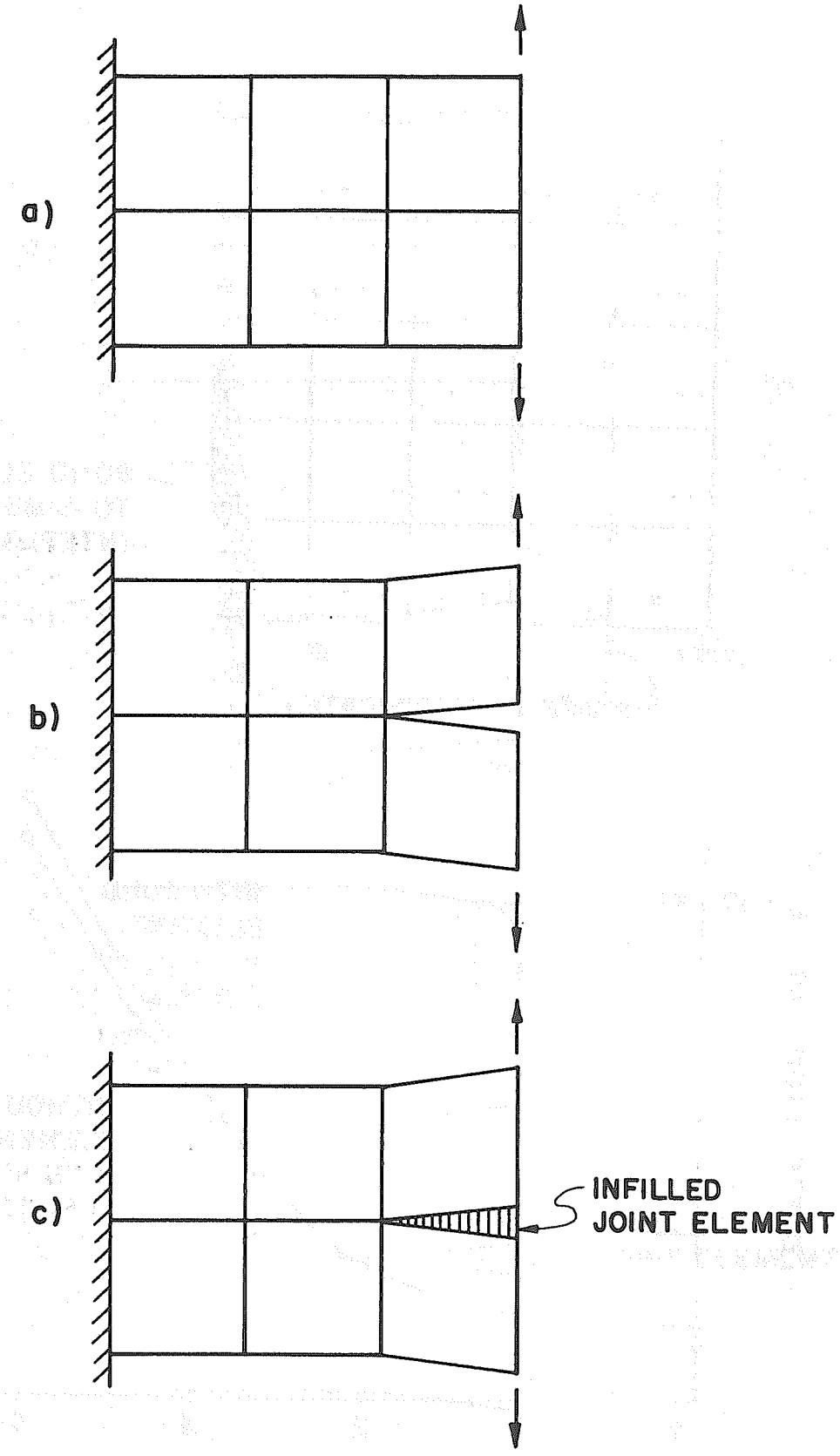

FIG. 5.8 MODIFICATION EXAMPLE H

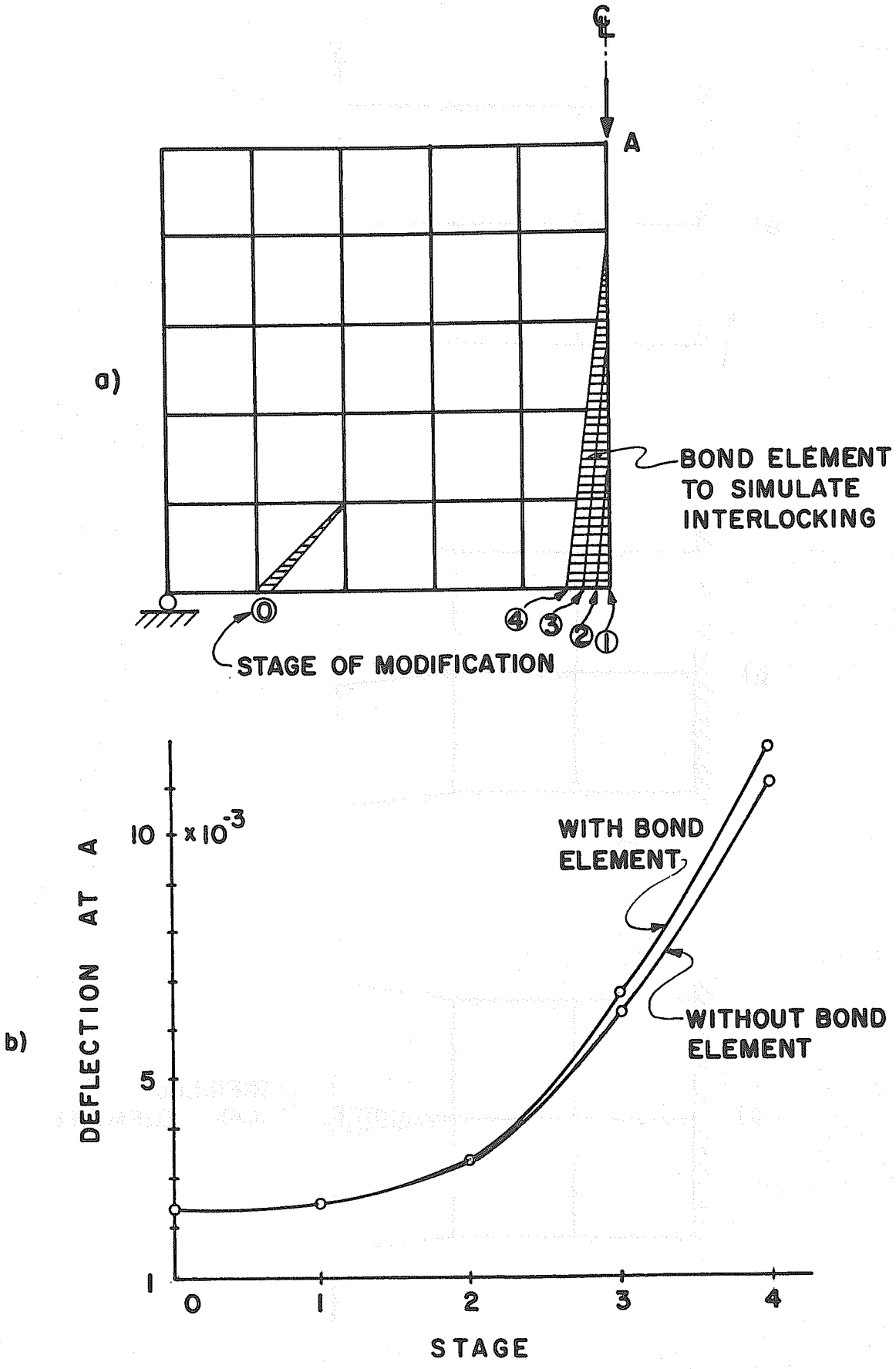

FIG. 5.9 MODIFICATION EXAMPLE I

within the framework of the frontal technique. Even though the evidence provided by the example problems in last section is not conclusive, it shows a strong possibility that the modification procedure can be fruitfully employed as a means of reducing the computational effort. Argyris et al. [125] gave an approximate operation count n by

$$n = NBn_c/2 + Nn_c^2/4 + 2n_c^3/3 \qquad (5.35)$$

where N is the total degrees of freedom, n_c the number of changed columns in the structure stiffness K , and B the half handwidth of K , which can be considered equivalent to the maximum active frontal size. The break-even point is approximately at $n_c = 0.75B$. However, it should be noted that the efficiency of the method depends on the location of the modification occuring in the structure stiffness K. If modification is in the lower portion of K, then a higher effeciency can be expected. This can be observed from Eq. 5.7 where the size of Z , consequently Q , is affected by the coincidence matrix b. Therefore, in Example E, F, and G no saving is possible, because the modification, signified by the matrix b, covers the full rank of the structure stiffness matrix K. But even so, the convenience offered by the modification procedure still cannot be overlooked.

When modification is confined to a small portion of the original structure, such as in Example I , time-saving can certainly be realized. For instance, the CP time required to analyze each case in Example I is 4.1 seconds; the total CP time required for solving stages 0 to 4 is 10.076 seconds, which averages to about 2 seconds per case. The reduction in time is approximately 50%. It is also of interest to examine the time required in each subroutine , as shown in the following table

Stage	Time , Sec.	Subroutine
0	1.559	FRONTAL
1	0.262	LATALGO
2	0.503	LATALGO
3	0.895	LATALGO
4	1.500	LATALGO

As the modification involves more and more nodes, hence the size of matrix Z grows bigger and bigger, the time consumed in LAT algorithm begins to approach the time required by the frontal solution process.

CHAPTER 6 A CRACK PROPAGATION HYPOTHESIS

6.1 Fracture Mechanics and Concrete Research

The conventional method of predicting crack propagation in concrete structural members is by means of a failure criterion, as presented previously in Sec. 4.2. This type of approach seems to be justifiable in the case where cracking is represented by a crack-zone. When a crack-line is introduced into a solid body, the employment of failure criteria to predict crack growth may require renewed evaluation. The effect of cracking in the latter case is centered at the crack tip where a stress singularity exists. The region surrounding the crack tip, known as the "process zone," is under such a complex state of stress that it demands special attention. Therefore, it appears that a fracture mechanics approach should be a logical alternative which deserves further exploration.

Fracture mechanics has been rapidly gaining prominence in many advanced levels of engineering design, such as for machines, ships, aircrafts and nuclear reactors. However, the application of fracture mechanics to concrete research is rather limited. This fact may be attributed to the following reasons:

1) Rarely, if ever, does only a simple single crack develop in a concrete structure. Multiple cracks would normally initiate and propagate, either simultaneously or successively within the same structure. On the other hand, the theories in fracture mechanics generally deal with a single individual crack under a particular loading condition.

2) Because of the interaction between steel and concrete in reinforced and prestressed concrete members, the "critical flaw size" in fracture mechanics does not assume a meaningful role.

3) The nonlinear, heterogeneous, time-dependent properties of concrete, and its composite action with steel reinforcement makes the fracture analysis an unwieldy task.

4) Even with the finite element method where stress and strain fields can be obtained with relative ease, the operational aspects such as node renumbering and mesh regeneration, and the integration and differentiation of the energy functions complicate the numerical procedure.

However, all these difficulties have not been a total deterrent. Some positive progress has been made in recent years, in attempts to apply fracture mechanics to the study of concrete structures. Kaplan [137] has calculated the critical strain energy release rates G_c for

three concrete mixes by the notch-bend method and applied them successfully in predicting beam strengths. Romualdi and Batson [138] used the critical strain release rate G_c and the critical stress intensity factor K_c to study the fracture arrest mechanism, and obtained theoretical results which indicated that the tensile cracking strength of concrete increases proportionally to the inverse square root of the reinforcement spacing. Glucklick [139] took a fracture mechanics approach to examine fracture in concrete and claimed that the strain energy was transformed almost entirely to surface energy and that the relatively high G_c in concrete was due to the increase of the microcracked zone and the heterogeneity of the material. He also found that G_c increases with cracked length in tensile fracture, but remains constant in compressive fracture. Bianchini, Kesler and Lott [140] suggested that the concept of fracture mechanics would be a logical extension to the theoretical and experimental works of Broms [141] who investigated the internal cracking in some simple reinforced concrete specimens, and proposed that double-cantilever specimen types could be used to simulate the internal cracking of the centrally reinforced concrete members used by Broms. Shah and McGarry [142] tried to relate notch sensitivity and critical crack length for concrete and mortar to Griffith's fracture criterion.

They found that the critical length for concrete and mortar is at least a few inches. Microcracks shorter than the critical length grow gradually and in a stable fashion, while cracks larger than critical length propagate spontaneously, for which the Griffith formula can be applicable. A macroscopic fracture criterion based on Griffith's theory and its modification by McClintock and Walsh [143] has been incorporated into a crack-zone type of finite element procedure by Sandhu and Huang [144, 145]. Their comparisons of the centerline deflections of some simple reinforced concrete beams with laboratory results indicate excellent agreement. Loov [17] suggested the use of a sensor element at the crack tip as a means of detecting crack propagation, Fig. 1.5. Rostam and Byskov [146] used the finite element method with "cracked elements" to analyze reinforced concrete beams. All these studies point toward the fact that the theory of fracture mechanics is indeed a potential means of investigating cracking in concrete structures.

In order to achieve a better understanding of how fracture mechanics can be fruitfully employed in conjunction with the finite element method, some fundamental concepts and the application of finite element method in fracture mechanics will be reviewed in the next section.

6.2 Fracture Mechanics and Finite Element Analysis

6.2.1 Griffith, Irwin and Orowan

The development of fracture mechanics is inevitably traced back to the paper by Griffith [147]. An excellent account of Griffith's work is given by Finnie and MacKenzie [148]. Essentially, Griffith took an energy approach to fracture prediction. Let the symbol U denote energy, then the basic concept is embodied in the relation

$$\frac{\partial U_{system}}{\partial a} = 0 \tag{6.1}$$

where a is the crack length, Fig. 6.1a, and the energy of the system is defined as

$$U_{system} = U_{loading} + U_{surface} \tag{6.2}$$

For an elliptical crack of length 2a, with zero semi-minor axis, through an infinite plate of unit thickness, so loaded that a uniform stress σ normal to the crack resulted, Griffith deduced that

$$U_{system} = -\frac{2\pi a^2\sigma^2}{E} + \frac{\pi a^2\sigma^2}{E} + 4a\gamma \tag{6.3}$$

$$= -\pi a^2\sigma^2 + 4a\gamma$$

where E is the Young's modulus, and γ, surface energy per unit area. By applying Eq. 6.1, the critical stress σ^* is obtained

$$\frac{\partial U_{system}}{\partial a} = \frac{\partial}{\partial a}\left(- \frac{\Pi a^2 \sigma^2}{E} + 4a\gamma \right) = 0$$

$$- \frac{2\Pi a\sigma^2}{E} + 4\gamma = 0$$

$$\frac{\Pi a\sigma^2}{E} = 2\gamma$$

or $$\sigma = \left(\frac{2E\gamma}{\Pi a} \right)^{\frac{1}{2}} = \sigma^* \quad \text{at critical state} \tag{6.4}$$

which is the well known Griffith formula. Any combination of stress and crack length which satisfies Eq. 6.4 will give a metastable equilibrium condition. In other words, when the critical stress level σ^* is attained, an infinitesmal increase in crack length will cause sufficient amount of energy released by the external loading and the stress field for creation of a fresh crack surface, with the applied load being kept constant. Therefore, the crack will start propagating.

There are, however, quantitative limitations to the Griffith formula, as discussed by Finnie and MacKenzie [148]. The question concerning the effects of loading on Griffith's fracture criterion has also been raised by Swedlow [149]. However, despite these uncertainties, Griffith's energy approach to fracture prediction is very useful, and there is experimental evidence to support the existence of a critical stress σ^* and even the type of law similar to Griffith's formula [150]. This very basic concept of Griffith has been modified and extended

by Irwin and Orowan to form the core of the present day approaches to fracture prediction.

Orowan [151, 152] pointed out that plastic deformation exists at the root of the crack. As the crack propagates, a new plastic zone is created while the previous plastic zone is being unloaded and left with some permanent deformation. Thus a surface layer of permanent plastic deformation is generated along the cracked surface. This process dissipates energy which may be calculated in proportion to the gain in crack surface. Therefore, Griffith's formula still stays valid if a dissipation energy is substituted for the surface energy. Irwin [153] postulated that one could define a surface energy characteristic of fracture which could be measured in a fracture test and defined a quantity, called "critical strain energy release rate," G_c where

G_c = the work required to create a unit increase in crack area by fracture

Irwin also designated the "strain energy release rate," sometimes referred to as "crack driving force," by

$$G = \frac{\partial U}{\partial A} = \frac{\partial U}{\partial (2ah)} \qquad (6.5)$$

where A is the crack surface which equals the plate thickness h times the crack length $2a$. Similar to Griffith's analysis, the stability of a crack is given by

$$G \begin{cases} < \\ = G_c \\ > \end{cases} \begin{array}{l} \text{stable} \\ \text{metastable} \\ \text{unstable, crack will propagate} \end{array} \qquad (6.6)$$

Irwin has also suggested [154] that if two different loading systems produce the same stress environment, then the influence on crack extension should be similar. This would indicate that the critical strain energy release rate G_c could be regarded as being a fundamental material property, similar to the Young's modulus E. This concept, though being not strictly correct, has turned out to be extremely useful when proper modification is made. Extensive applications of this concept in theoretical as well as experimental studies have been carried out by Irwin himself, and by many others in the field. of fracture mechanics.

An alternative to the energy approach is the so-called stress intensity factor approach. The elastic stresses near the tip of a sharp crack, Fig.6.1c, have an inverse square root singularity

$$\text{Mode I, II} : \quad \sigma_x = \frac{K_i}{(2\pi r)^{\frac{1}{2}}} f_{x,i}(\theta)$$

$$\sigma_y = \frac{K_i}{(2\pi r)^{\frac{1}{2}}} f_{y,i}(\theta)$$

$$\sigma_{xy} = \frac{K_i}{(2\pi r)^{\frac{1}{2}}} f_{xy}(\theta)$$

$$\sigma_z = \gamma\,(\sigma_x + \sigma_y) \quad \text{for plane strain}$$

$$\sigma_z = 0 \quad \text{for plane stress}$$

$$i = \text{I, II}$$

Mode III :

$$\sigma_{xy} = [\, K_{III}/(2\pi r)^{\frac{1}{2}} \,] \sin(\theta/2)$$

$$\sigma_{yz} = K_{III} \cos(\theta/2)$$

$$\sigma_x = \sigma_y = \sigma_z = \sigma_{xy} = 0$$

The parameters, K_I , K_{II} , K_{III} are called stress intensity factors for Mode I, II, and III respectively, Fig. 6.1b, they are independent of r and θ , but depend on the magnitude of loading and crack geometry. For instance, K_I equals to $\sigma_\infty(\pi a)^{\frac{1}{2}}$ for the case of a crack with length 2a in an infinite sheet under uniform stress σ_∞ , Fig. 6.1a. In the case of finite geometry such as narrow sheet, K_I can be expressed as $C\sigma_\infty\,(\pi a)^{\frac{1}{2}}$, where C is a correction factor made available from some handbooks. If the critical stress intensity factor under which failure occurs is denoted by K_c , and is a known material characteristic, then crack growth will result whenever K is equal to K_c , similar to the Griffith type of energy relationship. It was Irwin [155] who showed that the energy and stress intensity approaches

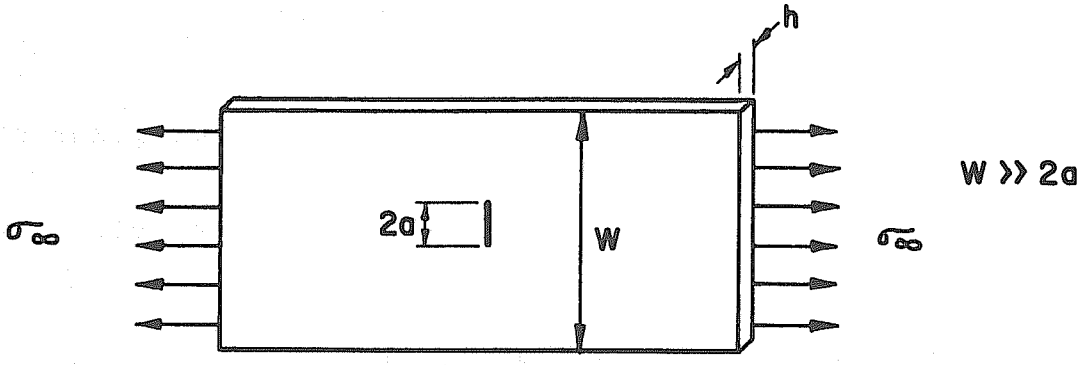

a) PLATE CONTAINING A THROUGH CRACK

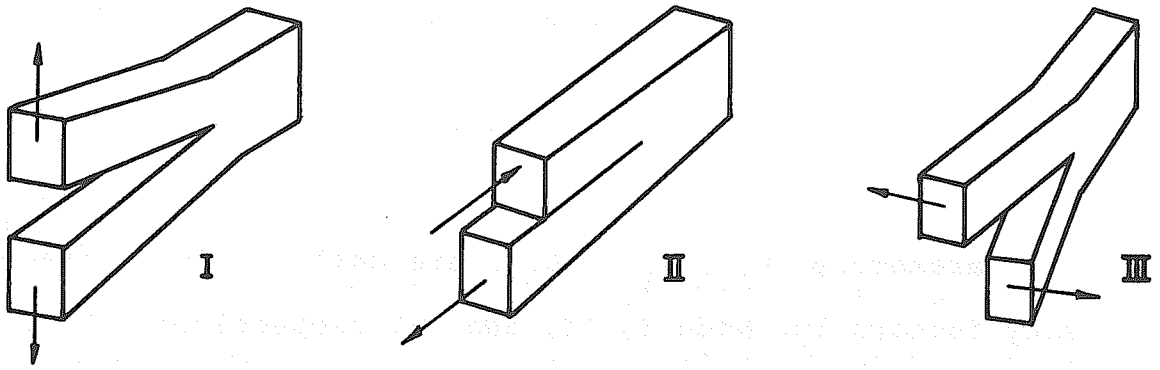

b) MODE OF CRACK DISPLACEMENT

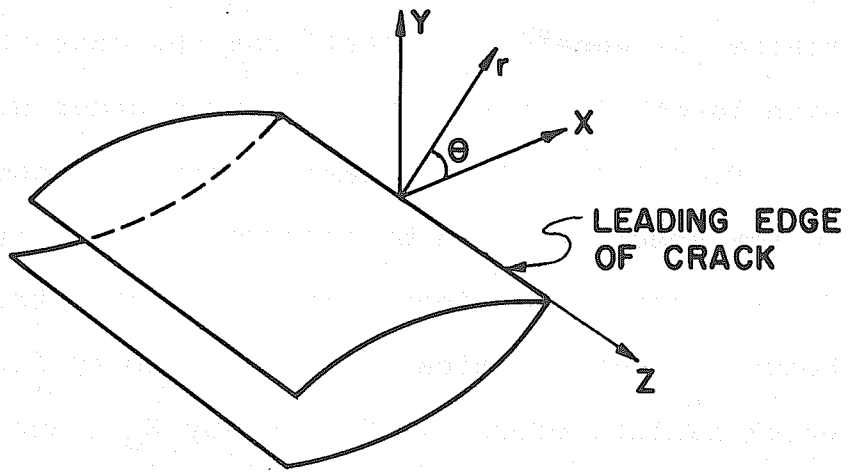

c) COORDINATE SYSTEM

FIG. 6.1 MODES AND GEOMETRY OF CRACKS

were equivalent in the fully linear elastic situation, i,e.,

$$K = (E\ G)^{\frac{1}{2}} \qquad \text{for plane strain,}$$

$$K = \left(\frac{E\ G}{1-\gamma^2}\right)^{\frac{1}{2}} \qquad \text{for plane stress.}$$

6.2.2 Dugdale, Barenblatt and Dvorak

Even though the crack surface may be stress free, localized stresses do exist at the root of the crack. The problem of plastic zone, as pointed out by Orowan, has been studied by Irwin [156] who represented the plastic zone as the shaded area shown in Fig. 6.2. The effective crack length becomes $2(c + r_y)$, where r_y is the radius of the plastic zone. With s_y being the yielding stress, r_y is approximately equal to $(1/2)(K_I/s_y)^2$ in the case of plane stress. Another method for estimating the plastic zone size for plane stress was given by Dugdale [157], and is often referred to as the Dugdale model, Fig. 6.3. He assumed that the plastic zone, instead of a circle, forms essentially as an extension of the crack, Fig. 6.3a. Dugdale reasoned that the stress intensity factors due to the applied loading and the "crack closing forces" should be equal and opposite so that the stress is finite at the end of the plastic zone. By superimposing the solutions for the two loadings shown in Fig. 6.3b and Fig. 6.3c, the plastic zone size s can then be obtained.

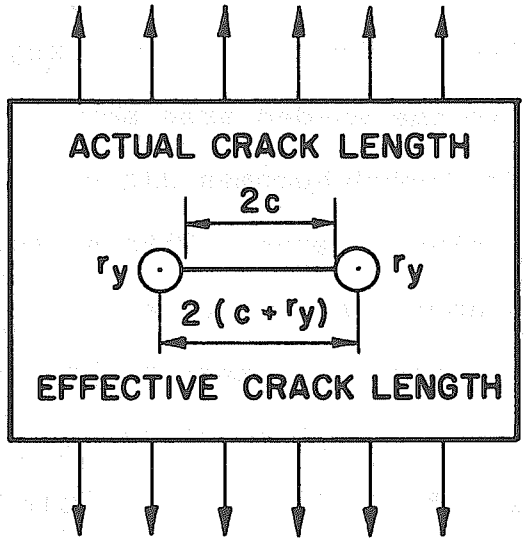

FIG. 6.2 ACTUAL & EFFECTIVE CRACK LENGTHS

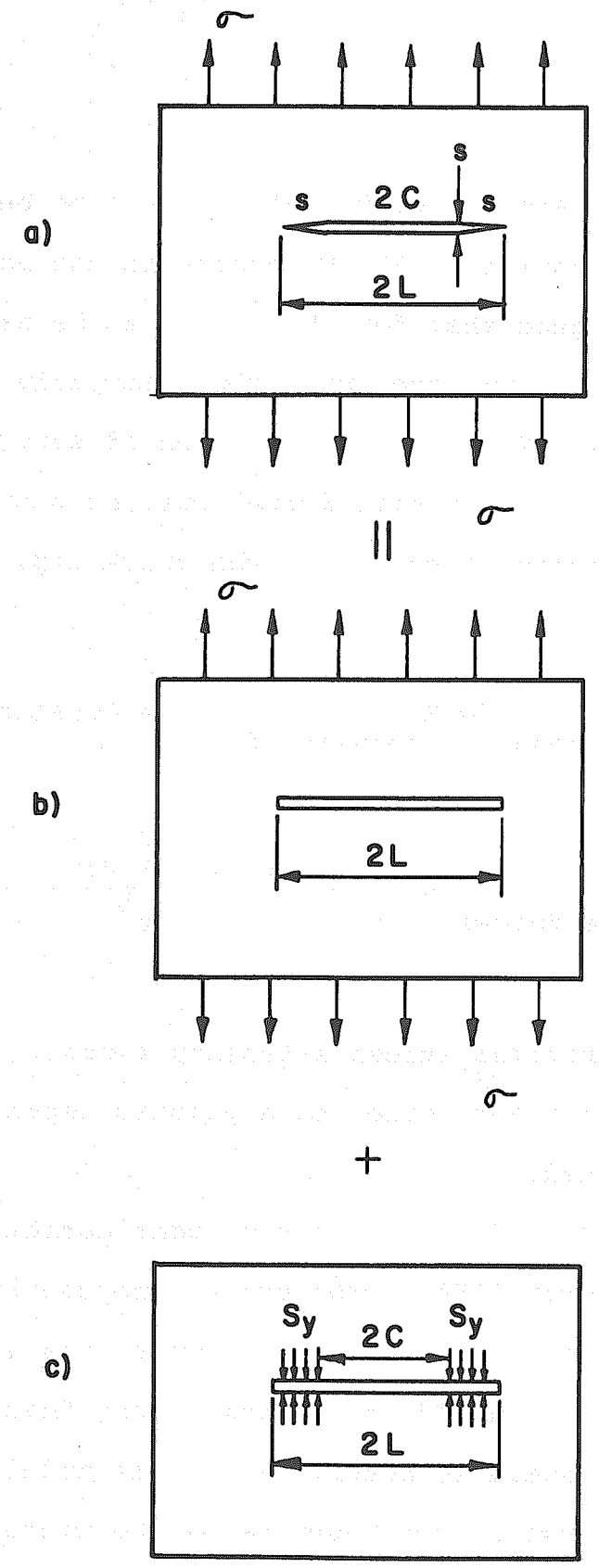

FIG. 6.3 THE DUGDALE MODEL

An approach similar to Dugdale's has also been advocated by Barenblatt [158] and others in the Soviet Union. It is argued that for the cracks to be at metastable equilibrium, they must close smoothly like a zipper, Fig. 6.4. Thus, the combination of stresses due to applied loads and cohesive forces must be such that there is no infinity of stress at the crack tip. It was deduced that

$$K_{\text{applied loads}} = K_{\text{cohesive forces}} = \text{Constant} = K_c \tag{6.7}$$

$$\text{with} \quad K_{\text{cohesive forces}} = -\sqrt{\frac{2}{\pi}} \int_0^d \frac{g(t)\, dt}{t^{\frac{1}{2}}} \tag{6.8}$$

and K_c is the critical stress intensity factor. Here, instead of plastic zone size s, a plastic intensity factor is obtained.

Another model of crack tip zone configuration was presented by Dvorak [159]. The crack zone consists of elastic and plastic parts, Fig. 6.5, where the stresses are transmitted by the "ductile links," and "material weakening" is assumed to occur. With this model, Dvorak was able to analyze in continuum terms the micro-mechanism of brittle fracture propagation in metals.

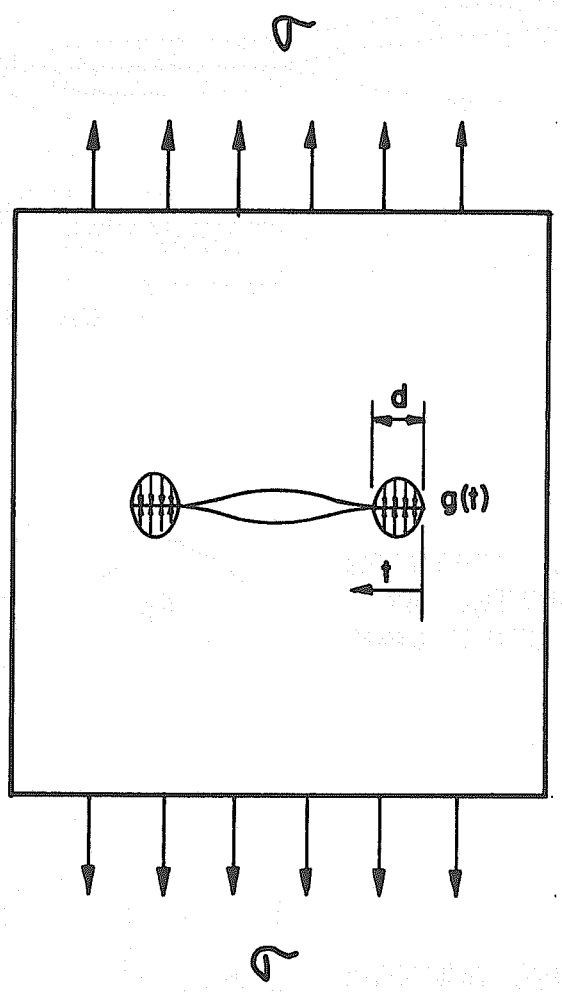

FIG. 6.4 THE BARENBLATT MODEL

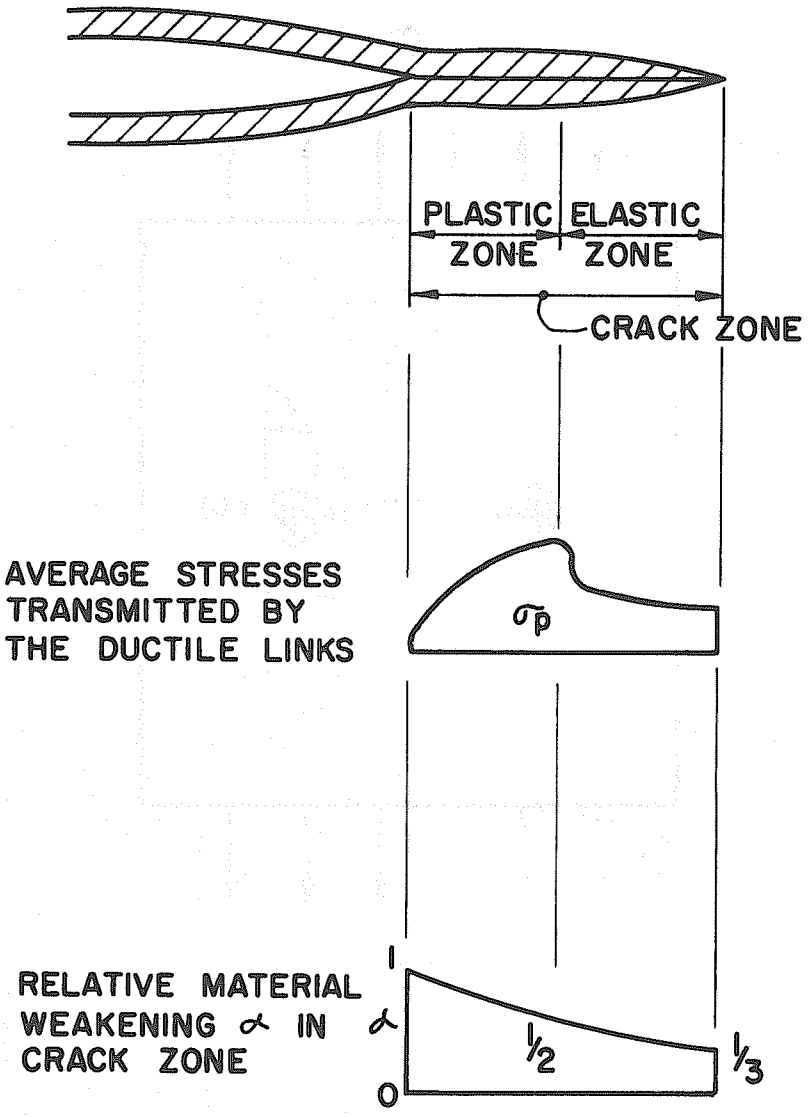

FIG. 6.5 THE DVORAK MODEL

6.2.3 Bueckner, Hayes and Williams

Following the energy approach of Griffith and Irwin, Bueckner [160] used the Clapeyron and Betti Theorems to develop the analysis of strain energy release rate for a cracked three-dimensional body of volume V, subject to body forces X, prescribed surface tractions T acting on surface S_1, and boundary displacements on surface S_2, Fig. 6.6a. The existing initial crack within the body, having the upper crack surface C_1 and lower surface C_2, is assumed to undergo a virtual crack extension resulting in new surfaces C_1' and C_2', under the same loading and displacement conditions, Fig. 6.6b. Denoting the initial cracking condition as being the "first state," and the condition with virtual crack extension being "second state," the stresses, strains, and displacement vectors for the first and second states are σ_{ik}, ε_{ik}, u and σ'_{ik}, ε'_{ik}, u' respectively. Bueckner further introduced a "sum state" and a "difference state" as

$$\text{sum state :} \quad \begin{aligned} \text{stresses} &= \sigma'_{ik} + \sigma_{ik} \\ \text{strains} &= \varepsilon'_{ik} + \varepsilon_{ik} \\ \text{displacements} &\quad v_s = u' + u \end{aligned}$$

Difference state : stresses = $\sigma'_{ik} - \sigma_{ik}$

strains = $\varepsilon'_{ik} - \varepsilon_{ik}$

displacements $v_d = u' - u$

The first state was then reinterpreted by Bueckner, which, for the sake of clarity, is called "virtual crack state" in this study, as represented in Fig. 6.6b.

Virtual crack State : The body V with the extended crack,
the body forces X,
The tractions T on S_1,
The prescribed displacements on S_2,
The tractions T^* on C'_1 and C'_2 (T^* is the traction required to close the crack surfaces C'_1 and C'_2),
The displacement u from first state.

The sum and difference states are found by using the corresponding interpretations, Fig 6.6c and 6.6d,

Sum State: The body V with extended crack,
The body forces 2X,
The tractions 2T on S_1,
The prescribed displacements on S_2,
No traction on C_1 and C_2,
The tractions T* on C_1' and C_2'.

Difference State: The body V with extended crack,
No body force,
No traction on S_1,
No prescribed displacement on S_2,
The tractions -T* on C_1' and C_2'.

With the energies associated with these three states, Bueckner was able to derive and conclude the following extremely useful relationships:

1) The strain energy of the difference state is all that counts for crack propagation.
2) Any reference state can be chosen, including the state of body V without any crack.
3) The traction T* resulting from the reference state and acting on $C_1' + C_1$ and $C_2' + C_2$ is responsible for crack propagation.
4) The strain energy of the difference state is then given by

$$U_d = -(1/2) \int_{C_1' + C_2'} v_d \cdot T^* \, ds \tag{6.9}$$

Hayes [161, 162] applied Bueckner's formulation to finite element analysis and arrived at an efficient and accurate method of determining stress intensity factors for cracked bodies of arbitrary shapes. Referring back to the Griffith-Irwin formula, Eq. 6.5, the strain energy release rate is then given by

$$G = \frac{\partial U_d}{\partial A} = \frac{-1}{2} \frac{\partial}{\partial A} \int_{C_1' + C_2'} v_d \cdot T^* \, ds \tag{6.10}$$

Schemes for automatically determining U_d and its derivative with respect to crack length have been devised by Hayes to obtain the stress intensity factors for several cracked plates which gave good agreement with known results. This method has also been adapted to give Dugdale model solutions for cracked arbitrary bodies by Hayes and Williams [163].

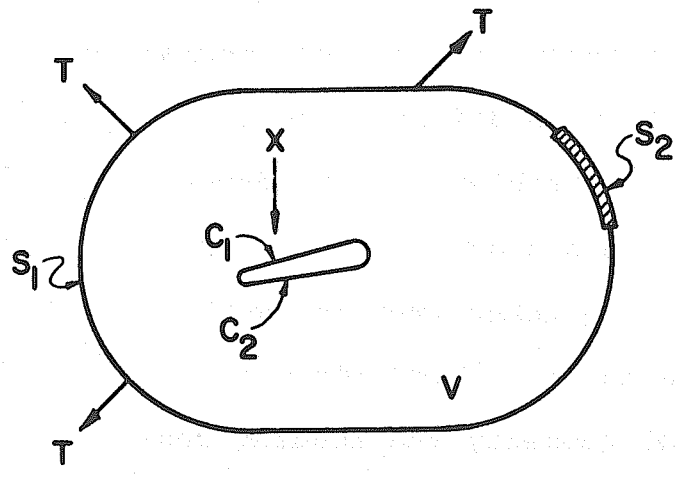

a) INITIAL OR REFERENCE STATE

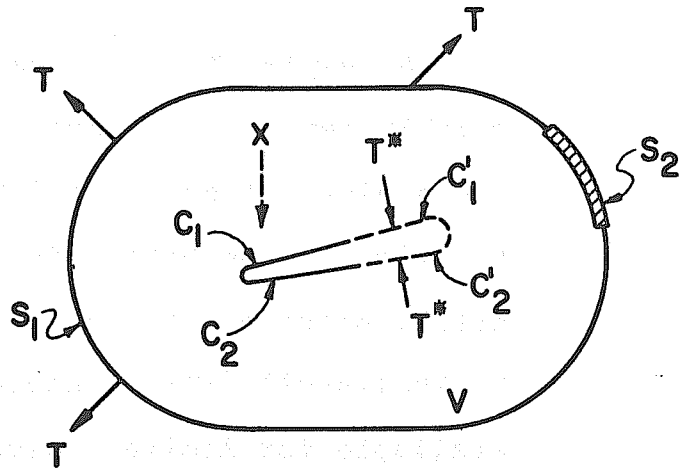

b) VITUAL CRACK STATE

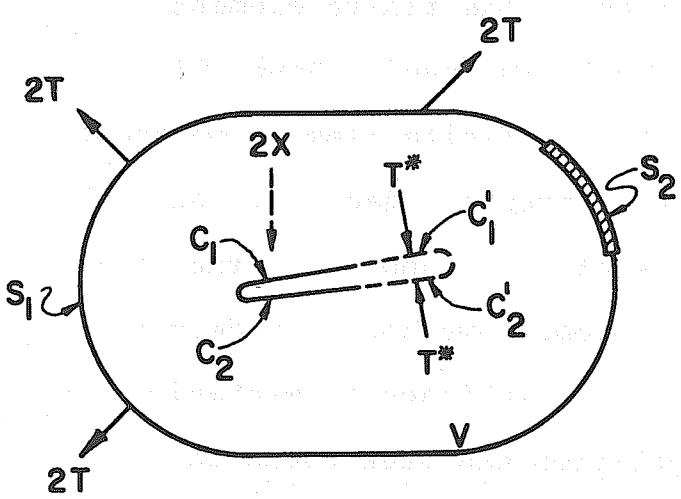

c) SUM STATE

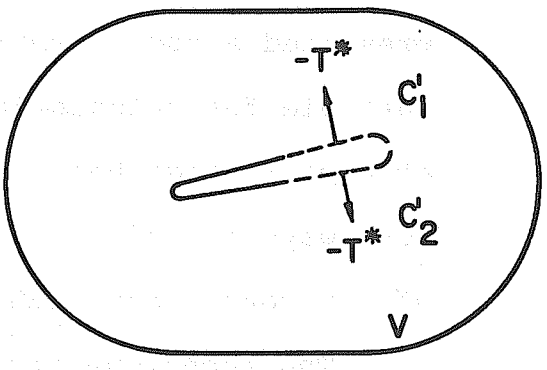

d) DIFFERENCE STATE

FIG. 6.6 THE BUECKNER MODEL

6.2.4 Finite Element Method in Fracture Mechanics

An exploration of the literature in fracture mechanics quickly reveals that one of the main difficulties in the analytical study of fracture problems is the determination of the stress fields in a cracked body. Very often, solutions for stresses are taken from the work of Muskhelishvili [164], where a number of solutions are available for limited cases of geometry and loading conditions. The versatility of the finite element method in stress analysis should logically find its rightful place in the domain of fracture mechanics. Indeed, there are a number of directions in which the finite element method has already been fruitfully employed. Rowe [165] presented a comprehensive review of finite element methods suitable for calculating stress intensity factors. An attempt is made here in this section to emphasize the various ways by which the finite element method is made use of, in connection with the studies in fracture mechanics.

The technique of extrapolation has been found to produce quite acceptable values for stress intensity factors K_I , by Chan, Tuba, and Wilson [166] in their earliest and most important contribution to the application of finite element method in fracture mechanics. Correlation of the nodal point displacements u_i^* is made with the well known crack tip displacement equations

$$u_i = \frac{K_I}{G} (r/2\pi)^{\frac{1}{2}} f_i(\theta,\nu) \qquad (6.11)$$

where G is the shearing modulus, ν is Poisson's ratio, r and θ are defined in Fig. 6.7. By substituting the nodal point displacements u_i^* at some point (r,θ) near the crack tip into Eq. 6.11, a quantity K_I^* can be calculated from

$$K_I^* = (2\pi/r)^{\frac{1}{2}} [GU_i^*/f_i(\theta, \nu)] \qquad (6.12)$$

The values of K_I^* can be plotted as a function of r for a fixed value of θ. Since the finite element displacements become inaccurate near the crack tip, an extrapolation technique was used to obtain the value of K_I^* at $r=0$, which should approximate the theoretical value of K_I. Nodal point stresses σ_{ij}^* could also be used in a similar manner to obtain the approximated value of K_I

$$\sigma_{ij} = \frac{K_I}{(2\pi r)^{\frac{1}{2}}} f_{ij}(\theta)$$

$$K_I^* = \frac{(2\pi r)^{\frac{1}{2}}}{f_{ij}(\theta)} \sigma_{ij}^*(r, \theta) \qquad (6.13)$$

$K_I^* \simeq K_I$ at $r = 0$; θ = constant.

Wilson and Thompson [168] used the same extrapolation technique for finding the stress intensity factors for cracked plates in bending.

The compliance method has been suggested by Dixon and Dukes [169]. The rate of change of stiffness with crack extension is related to the crack extension force G by

$$G = \tfrac{1}{2}P^2 \, (\partial\lambda/\partial A) \tag{6.14}$$

where P is the load, A is the crack size, λ is the compliance equal to the deflection Δ at loaded point divided by the load, $\lambda = \Delta/P$. In this approach, the small restricted region of high stress around crack tip is deemed to contribute little to the total deflection, thus the need of fine element mesh size can be eliminated. If λ is calculated for several crack lengths, a curve fitting by polynomials can be made, whereby $\partial\lambda/\partial A$ can be derived to obtain G. Watwood [170] published a variation of the compliance method. He used directly the energy release rate formula

$$G = \begin{matrix} + \\ - \end{matrix} \frac{\partial U}{\partial A} \tag{6.15}$$

where U is the strain energy stored in the system, A is the crack area, and + for constant loads, - for constant displacement.

The strain energy stored in an elastic body is

$$U = \tfrac{1}{2} \Sigma \; P_i \Delta_i \tag{6.16}$$

Therefore, $\partial U/\partial A$ can be obtained by calculating the strain energy for several crack lengths and by finding the rate of change. A similar method with linear-strain rectangular plane-stress elements was used by Mowbray [171] for a single edge crack specimen under uniform tension.

Utilization of Rice's J-integral [172] has also been suggested by Chan et al. [166]. Since the integral is path independent, any arbitrary path around the crack tip can be taken in the finite element layout to calculate the strain energy density W needed in

$$J = \int_{\Gamma} \left(W \, dy - T \, \frac{\partial u}{\partial x} \, ds \right) \tag{6.17}$$

where T is the traction vector defined according to the outward normal n along Γ, Fig. 6.7. The integral is evaluated in a counterclockwise sense starting at lower crack surface and continuing along Γ to the upper crack surface, by a numerical procedure. Leverenz [174] showed how this method can be extended for the analysis of a crack in a bi-material plate. Once J is determined, K_I is given by

$$K_I = \left[\frac{J\,E}{1-\gamma^2} \right]^{\frac{1}{2}} \quad \text{for plane strain cases.} \tag{6.18}$$

Chan [167] also suggested that instead of working with the numerical integration procedure, another useful relationship derived by Rice [173] can be used

$$J \equiv - \frac{dP}{d\ell} \tag{6.19}$$

where $- dP/d\ell$ denotes the rate of decrease of potential energy per unit thickness with respect to crack size, and can be approximated by

$$- \frac{dP}{d\ell} \simeq - \frac{\Delta W}{\Delta \ell} \tag{6.20}$$

where ΔW is the incremental work done. Therefore, by running a separate finite element analysis for crack lengths ℓ and $(\ell + \Delta\ell)$, Fig. 6.7, and calculating the work done in each case, W and $(W + \Delta W)$, respectively. Then J is simply obtained from

$$J \equiv - \frac{dP}{d\ell} \simeq - \frac{\Delta W}{\Delta \ell} = \frac{K_I^2 \,(1-\nu^2)}{E} \tag{6.21}$$

It has been found that this method of finding the stress intensity factor is very accurate, even when the element size around the crack tip is rather coarse.

What Chan has suggested bears a striking similarity to Irwin's energy release rate method used by Swanson [175].

$$G = \frac{dU}{dA} \simeq \frac{\Delta U}{\Delta A} \qquad (6.22)$$

$$K_I = \left(\frac{E\, G_I}{1 - \nu^2} \right)^{\frac{1}{2}} \qquad \text{(for plane strain)}$$

Stress intensity factors are obtained for a cracked two-layered cylinder. The strain energy U is computed for each element and summed over the entire body. This procedure, identical to Chan's, requires two computer runs in order to obtain $\Delta U/\Delta A$. Good results have also been obtained by Swanson with a relatively coarse mesh.

Practical application of Bueckner's formulation has been carried out by Hayes and Williams [161 - 163], as presented earlier in Sec. 6.2.3. Hayes [162] points out that Bueckner's formulation is a special case of Rice's formulation, and that the use of Bueckner approach can be regarded as evaluating Rice's J-integral, but in a much simpler way. It is only necessary to determine first the stresses that act on the surface where the crack is to appear. Then by introducing the crack and applying these stresses in reversed directions at the newly cracked surfaces with all other tractions, body forces and prescribed displacements set to zero, then the work done is

calculated. In the finite element method, all tractions are applied as nodal point loads. Therefore, the integral of Eq. 6.9 is simply the sum of the work done by each nodal point force acting through its own displacement. Expressing this work as a function of crack length and by differentiation, the required strain energy release rate is obtained.

Instead of using the Bueckner formulation, Walsh [176] calculated what he called the "unit distortion field" from the inner mesh, Fig. 6.9. The stresses which correspond to a unit value of K_I are computed from

$$\sigma = K_I \, r^{-\frac{1}{2}} \, f(\theta) \tag{6.23}$$

and applied as external loads to the inner mesh. This inner mesh is the entire specimen. An elastic analysis is carried out for the required specimen loading, from which the distortions near the crack tip, termed "computed distortion field," are obtained. The value of K_I is then calculated to give the best fit between the computed distortion field and K_I times the unit distortion field. This method can be extended to include material orthotropy.

Construction of a special crack tip singularity element has been done by Byskov [177] who made use of the complex stress functions of Muckhelishvili [164]. Byskov's cracked element is an equilateral triangle with

four nodes and the crack emanating from a corner, Fig. 6.8a. This cracked element can then be assembled with other constant strain triangles for the solution of cracked plates, Fig. 6.8b, which can produce a stress intensity factor agreeing within 3-4% of the known reference value. However, non-monotonous convergence was observed in that study. The lack of compatability between the cracked and uncracked elements is responsible partly for this behavior. Tracey [178] presented another triangular element which embodies the inverse square root singularity near a crack tip. The well-known Westergaard-Irwin [179] formulation for near-crack-tip stress and displacement distributions was used. The triangular element actually is a constrained quadrilateral element such that two of the nodes have the same physical coordinates and has a square map into the "parent" element, Fig. 6.10a. The mesh configuration consists of a whole ring of triangular elements around the crack tip, which are joined in the radial direction with quadrilateral isoparametric elements, Fig. 6.10b. The displacement functions are so chosen that the singularity is completely embedded while displacement compatability on inter-element boundaries is assured. Good results can be obtained from a relatively coarse mesh.

More advanced aspects of nonlinear finite element analysis of stresses and strains, which includes elasto-plastic material properties have been carried out

extensively by Swedlow and his co-workers [180 - 184]. Contributions in this area have also been made by Tuba [185], Wells [186], Levy, Marcal, Ostergren and Rice [187 -]90], among others. Recently, Levy, Marcal, and Rice [191] summarized the progress in the development of finite element methods for three-dimensional elastic-plastic stress analysis in fracture mechanics.

As remarked by Rowe [165], the linear elastic two-dimensional situation seems to be well established for practical application of finite element methods to fracture analysis, and the energy method appears to be the most expedient. Elasto-plastic analysis, particularly for three-dimensional cases, are more complex and costly. At any rate, the usefulness of the finite element method as an analytical tool in fracture mechanics is clearly unreputable.

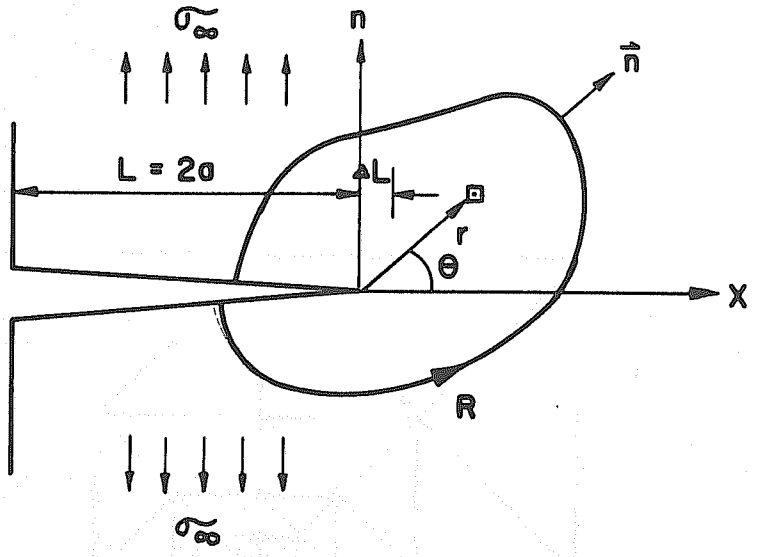

FIG. 6.7 CRACK TIP COORDINATES & J-INTEGRAL CONTOUR

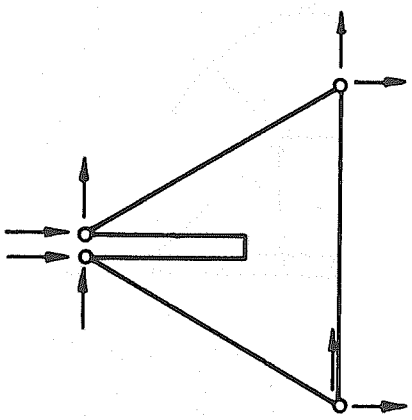

a) CRACKED TRIANGLE

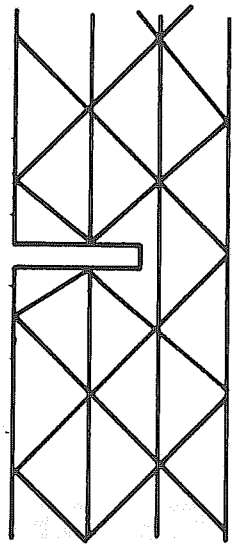

b) CRACKED PLATE

FIG. 6.8 BYSKOV'S CRACKED ELEMENT

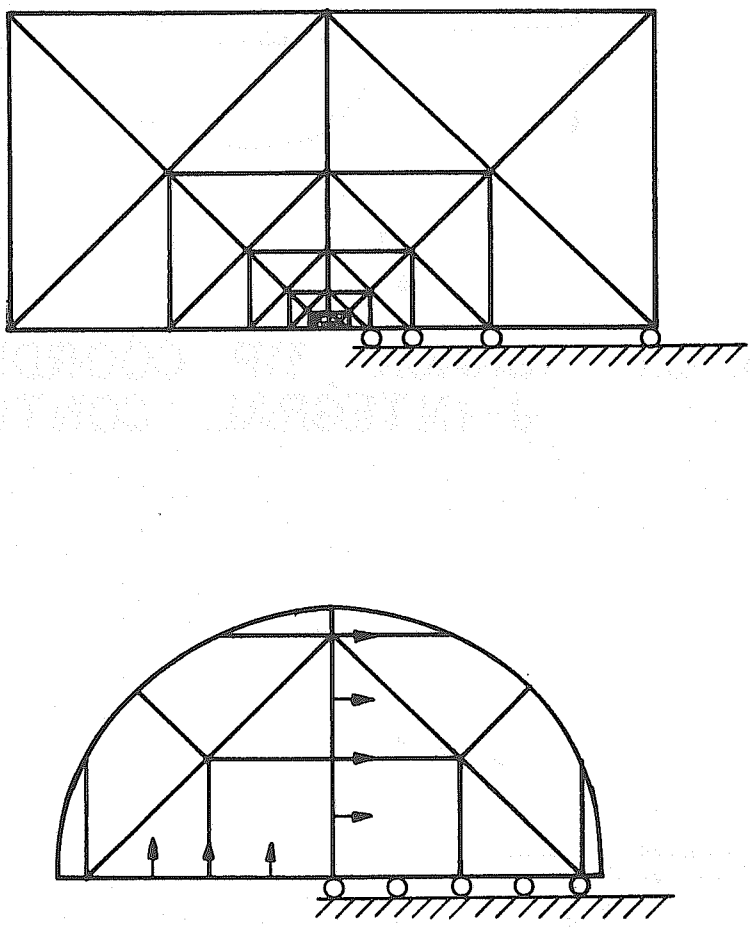

FIG. 6.9 INNER MESH USED IN THE ANALYSIS FOR ZERO ANGLE CRACKED SPECIMEN BY WALSH

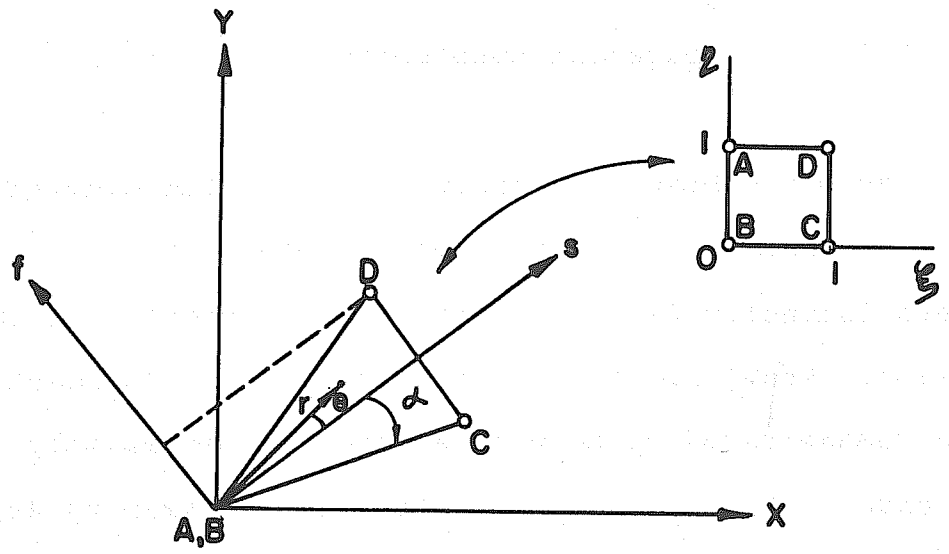

a) NEAR TIP TRIANGLE - SQUARE MAP

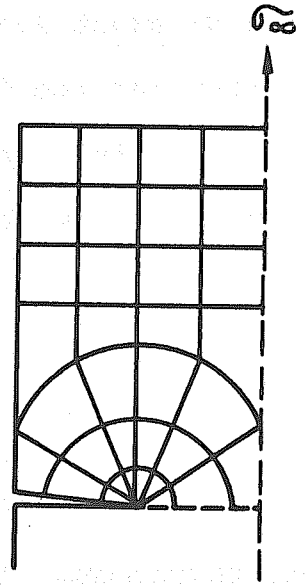

b) MESH LAYOUT FOR CRACKED PLATE

FIG. 6.10 TRACEY'S SINGULARITY ELEMENT

6.3 A Crack Propagation Hypothesis

Various schemes for applying the finite element method to obtain the strain energy release rate G or the stress intensity factor K have been presented in the last section. Among all the schemes, the energy approach has been demonstrated to be very attractive, especially in the case of Bueckner's formulation as utilized by Hayes and Williams [161 - 163]. However, to calculate the strain energy release rate G, a minimum of two strain energy values, U_{ℓ} and $U_{\ell+\Delta\ell}$, have to be computed; one at crack length ℓ and one at crack length $(\ell+\Delta\ell)$. This involves forming and inverting the total structural stiffness matrix at least twice, plus a numerical procedure to differentiate the energy U with respect to crack surface area A

$$G \simeq \frac{\Delta U}{\Delta A} = \frac{U_{\ell+\Delta\ell} - U_{\ell}}{h\ (\Delta\ell)} \qquad (6.24)$$

where h is the plate thickness. This procedure may prove to be overly laborious if the energy release rate G is to be incorporated into the finite element analysis of concrete structures. In order to provide a simpler method for approximating the strain energy release rate G, so that it can be more feasibly incorporated into a finite element analysis in an automatic fashion, a hypothesis is boldly postulated herein.

Let k be a parameter space and assume both U and A are continuous in k, then G can be written as

$$G = \frac{dU}{dA} = \frac{dU}{dk}\frac{dk}{dA} \tag{6.25}$$

However, there is no a priori evidence to support such a continuity condition. On the other hand, if the parameter k is taken to be an element stiffness, then the energy U is certainly a function of k. Intuitively, k can also be related to crack surface A in some way. But, instead of trying to resolve this dilemma, the following hypothesis is postulated:

Hypothesis : An energy release rate G^* is defined to be

$$G^* \equiv f(\alpha , s) \tag{6.26}$$

where α is an emperical constant and $s = (dU/dk)$ is defined as network sensitivity. Crack growth is then determined by the conditions

$$G^* \begin{cases} < & \text{stable} \\ = G_c & \text{metastable} \\ > & \text{unstable, propagates} \end{cases} \tag{6.27}$$

6.4 A Network-Topological Consideration

The motivation behind the hypothesis proposed above is that the quantity $\partial U/\partial k$, known as "network sensitivity," is relatively easy to compute.

The relative sensitivity or simply the sensitivity of a network function T , with respect to a parameter x, denoted by S_x^T is defined by Chua as [76].

$$S_x^T = \frac{\partial T}{\partial x} \qquad \frac{x}{T} = \frac{\partial T/T}{\partial x/x} = \frac{\partial \ell n T}{\partial \ell n x} \tag{6.29}$$

A number of methods are available for the determination of the sensitivity S , and among them, the adjoint network method appears to be well suited for automatic computer analysis [76, 192-196]. The adjoint method relies heavily on the Tellegen theorem. Therefore, for the sake of continuity in presentation, Telegen's theorem will be proved, using the graph theoretic matrices and the notations of Fenves and Branin [142].

6.4.1 Tellegen Theorem

Recall the equilibrium and continuity conditions stated in terms of the branch-node incidence matrix A in Eq. 2.8

$$\text{Equilibrium} \qquad A^t p = 0 \tag{6.30a}$$

$$\text{Continuity} \qquad A u' = u \tag{6.30b}$$

where, as defined previously,

p = total branch force vector

u = total branch distortion vector

u' = joint displacement vector

these conditions of Eqs. 6.30a and b must hold true for any structural network and are called invariant relationships in structural analysis by Baron [55].

Consider a network N and its adjoint network $\hat{N}$ having the same topology, i.e., $A = \hat{A}$, where the symbol " ^ " signifies adjoint quantities. The following relationships must also be true

$$\hat{A}^t \hat{p} = 0 \tag{6.31a}$$

$$\hat{A}\, \hat{u}' = \hat{u} \tag{6.31b}$$

if the branch distortions u of the original network N are multiplied by the branch forces $\hat{P}$ of the adjoint network $\hat{N}$, then one has the relationship

$$u^t \hat{p} = (A\, u')^t\, \hat{p} = (u')^t\, A^t\, \hat{p} = (u')^t\, (\hat{A}^t\, \hat{p}) = 0 \tag{6.32a}$$

Similarly, if the branch forces p of the original network N are multiplied by the branch displacements

$\hat{u}$ of the adjoint network $\hat{N}$, the product also vanishes,

$$p^t \hat{u}' = p^t(\hat{A}\ \hat{u}') = p^t A\ \hat{u}' = (A^t p)^t \hat{u}' = 0 \tag{6.32b}$$

Eqs. 6.32a and b are known as Tellegen's theorem, and are usually written in the following forms.

$$\sum_{i=1}^{b} u_i \hat{p}_i = 0 \tag{6.33a}$$

$$\sum_{i=1}^{b} p_i \hat{u}_i = 0 \tag{6.33b}$$

where b is the total number of the branches in the network N or $\hat{N}$. Note that networks N and $\hat{N}$ are only required to have the same topology, but not necessarily the same branch characteristics. Furthermore, Tellegen's theorem is only predicated upon the equilibrium and continuity conditions; thus, it is valid for all linear, nonlinear, time-invariant and time-variant networks.

6.4.2 A Network Sensitivity Function

A network sensitivity function $S(N,T,x)$ can now be derived by the adjoint network method. Again, let network N and its adjoint network $\hat{N}$ have the same topology, and the pairs of network variables p and u, $\hat{p}$ and $\hat{u}$ associate with network N and adjoint network $\hat{N}$, respectively. The number of nodes n and the number of branches b in network N are equal to those of the adjoint network $\hat{N}$.

To obtain, for instance, a very simple case of sensitivity, assume that the network function T represents the response u_{b-1} in branch h_{b-1} and the parameter x represents the branch characteristic k_b of branch h_b, Fig. 6.11, then the network sensitivity can be written as

$$S = \frac{\partial u_{b-1}}{\partial k_b} \tag{6.34}$$

Tellegen's theorem asserts that

$$\sum_{i=1}^{b-2} p_i \hat{u}_i + p_{b-1} \hat{u}_{b-1} + p_b \hat{u}_b = 0 \tag{6.35a}$$

$$\sum_{i=1}^{b-2} u_i \hat{p}_i + u_{b-1} \hat{p}_{b-1} + u_b \hat{p}_b = 0 \tag{6.35b}$$

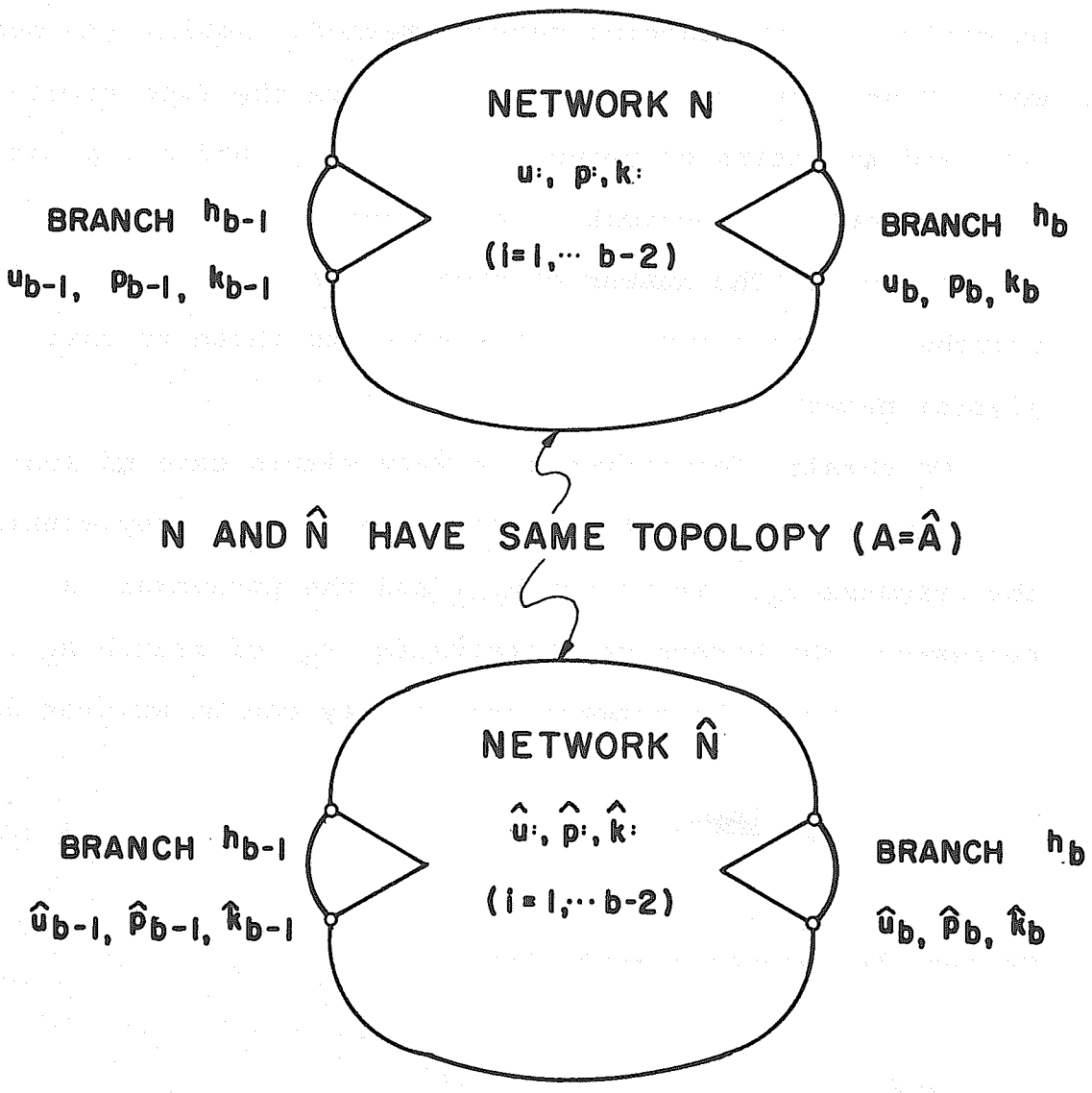

FIG. 6.11 NETWORK N & ADJOINT NETWORK $\hat{N}$

When the branch value k_b in network N is perturbed, it results in a variation of values Δp_i and Δu_i. Since Tellegen's theorem is independent of branch values, it still remains valid and can be written as

$$\sum_{i=1}^{b-2} (p_i + \Delta p_i)\hat{u}_i + (p_{b-1}+\Delta p_{b-1})\hat{u}_{b-1} + (p_b+\Delta p_b)\hat{u}_b = 0 \qquad (6.36a)$$

$$\sum_{i=1}^{b-2} (u_i + \Delta u_i)\hat{p}_i + (u_{b-1}+\Delta u_{b-1})\hat{p}_{b-1} + (u_b+\Delta u_b)\hat{p}_b = 0 \qquad (6.36b)$$

Subtract Eqs. 6.35 from Eqs. 6.36 to obtain

$$\sum_{i=1}^{b-2} \Delta p_i \hat{u}_i + \Delta p_{b-1}\hat{u}_{b-1} + \Delta p_b \hat{u}_b = 0 \qquad (6.37a)$$

$$\sum_{i=1}^{b-2} \Delta u_i \hat{p}_i + \Delta u_{b-1}\hat{p}_{b-1} + \Delta u_b \hat{p}_b = 0 \qquad (6.37b)$$

Subtract Eq. 6.37b from Eq. 6.37a to obtain

$$\sum_{i=1}^{b-2} (\Delta p_i\hat{u}_i - \Delta u_i\hat{p}_i) + (\Delta p_{b-1}\hat{u}_{b-1} - \Delta u_{b-1}\hat{p}_{b-1}) + (\Delta p_b\hat{u}_b - \Delta u_b\hat{p}_b) = 0 \qquad (6.38)$$

If the network variables u_i and p_i are related by

$$p_i = k_i u_i \qquad (i=1, \ldots, b) \tag{6.39}$$

which implies

$$(p_i + \Delta p_i) = (k_i + \Delta k_i)(u_i + \Delta u_i)$$

or

$$\Delta p_i = k_i \Delta u_i + \Delta k_i u_i + \Delta k_i \Delta u_i \tag{6.40}$$

For the purpose of obtaining first order approximation to the sensitivity, the higher order terms $\Delta k_i \Delta u_i$ can be neglected. Furthermore, by keeping p_{b-1} constant, i.e., $\Delta p_{b-1} = 0$, Eq. 6.40 is substituted into Eq. 6.38 to obtain

$$\sum_{i=1}^{b-2} (k_i \hat{u}_i - \hat{p}_i)\Delta u_i + \sum_{i=1}^{b-2} \Delta k_i u_i \hat{u}_i - \Delta u_{b-1} \hat{p}_{b-1} \tag{6.41}$$

$$+ (k_b \hat{u}_b - \hat{p}_b)\Delta u_b + \Delta k_b u_b \hat{u}_b = 0 \tag{6.41}$$

Note that branch characteristics k_i (i=1,....,b-2) are unperturbed, therefore,

$$\Delta k_i = 0 \quad ; \quad \forall\ i=1,\ldots,\ b-2 \tag{6.42}$$

Thus far the branch characteristics in the adjoint network $\hat{N}$ have not been specified. If the variables $\hat{u}_i$ and $\hat{p}_i$ are so chosen that

$$\hat{p}_i = k_i \hat{u}_i \quad ; \quad \forall\ i=1,\ldots,\ b-2$$

which means that the adjoint network $\hat{N}$ is identical to the original network N (this is true only for resistive networks). Then Eq. 6.41 reduces to

$$- \Delta u_{b-1} \hat{p}_{b-1} + \Delta k_b u_b \hat{u}_b = 0$$

or

$$\frac{\Delta u_{b-1}}{\Delta k_b} = \frac{u_b \hat{u}_b}{\hat{p}_{b-1}} \tag{6.43}$$

If the driving force p_{b-1} in the adjoint network $\hat{N}$ is selected to be unity, then the first order network sensitivity S, for the change in the response u_{b-1} with respect to a change in k_b, is given by

$$S = \frac{\Delta u_{b-1}}{\Delta k_b} = u_b \hat{u}_b \tag{6.44}$$

The implication of Eqs. 6.43 and 6.44 is that the rate of change of response in branch i with respect to the change of the characteristic in branch j can be obtained by simply applying a branch force p_i at branch i in the adjoint network, and dividing the product of the two branch distorsions $u_j \hat{u}_j$ by $\hat{p}_i$. Since the adjoint network is identical to the original network, the solution effort required is merely a forward and a backward substitution of an additional load vector, and no additional inversion or decomposition is necessary.

6.5 A Model of Crack Tip Zone

In order to utilize the crack propagation hypothesis proposed in Sec. 6.3, a model for the crack tip zone is now constructed and shown in Fig. 6.12. It "pictorially" portrays the models of Dugdale, Barenblatt and Dvorak, in the sense that there is an elastic-plastic zone extended from the crack tip, and there is a set of forces acting at that zone. This particular zone is represented by an infilled bond element to transmit the stresses across the crack. Fig. 6.12b, in a spirit similar to the "ductile links' used by Dvorak [159], or the "distributed line spring" used by Rice and Levy [190], With a proper choice of the infilled element stiffness, it is possible to obtain the traction value T^* such as that required in the model of Bueckner, Hayes and Williams. By virtue of the finite element method, the infilled bond element can also be conveniently treated as a single link element, Fig. 6.12c, where the localized distributed traction T^* is lumped into a nodal force P^*, and the distributed stiffness is lumped into an equivalent link element stiffness denoted by k. Then ∂U_d in Eq. 6.10 can be written as

$$\partial U_d = \partial(\frac{1}{2} P^* u) = \partial U \qquad (6.45)$$

and from Eqs. 6.26 and 6.44 $G^* = f(\alpha, s)$

where S is obtained from $u\hat{u}/P^*$.

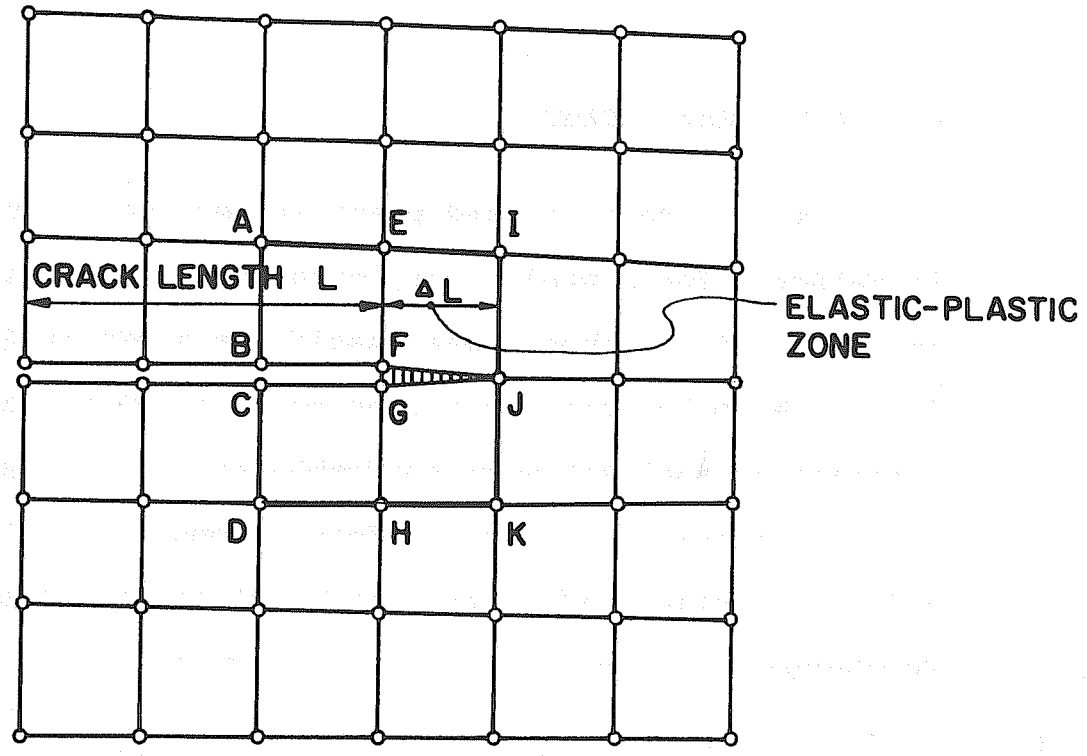

a) CRACK TIP ZONE

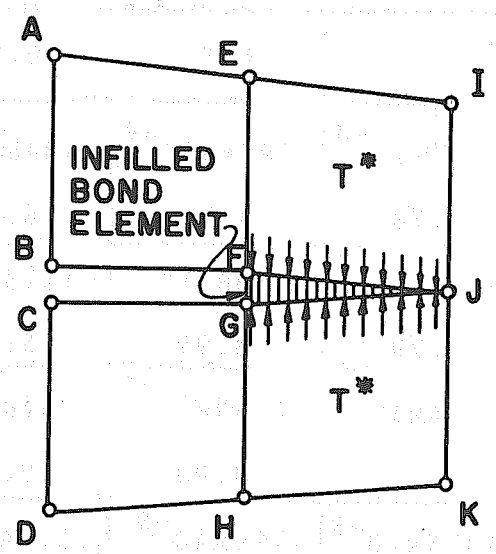

b) DISTRIBUTED LOCALIZED FORCES

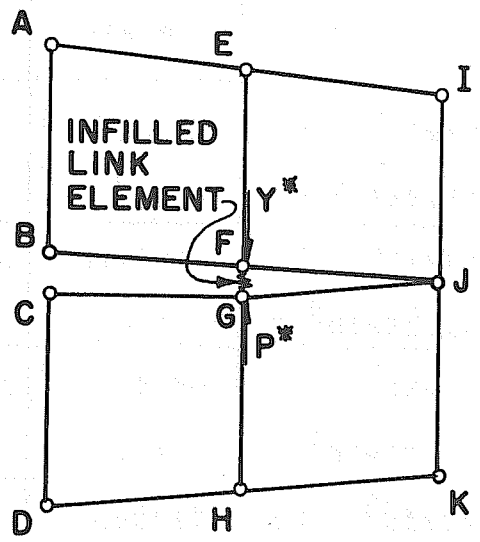

c) LUMPED NODAL FORCES

FIG. 6.12 MODEL OF CRACK TIP ZONE

6.6 A Parameter Study

A single edge cracked plate subject to uniform tension is selected for a preliminary parameter study, Fig. 6.13a, and its finite element idealization is shown in Fig. 6.13b. With the crack tip zone model shown in Fig. 6.12, a series of analyses were performed to obtain the network sensitivity S, for different combinations of crack and width ratio, a/d, and spring stiffness constant k. Furthermore, a simple function is assumed

$$G' = f(\alpha, s) = \alpha \cdot s \qquad (6.47)$$

some of the results are presented in the table below. It is

a/d		0.416	0.458	0.5	0.54	0.58
$k=3\times10^5$	S	$.6134\times10^{-5}$	$.8746\times10^{-5}$	$.1267\times10^{-4}$	$.1874\times10^{-4}$	$.2848\times10^{-4}$
$\alpha=2.2\times10^5$	G'	1.3	1.9	2.78	4.1	6.2
$k=3\times10^6$	S	$.2697\times10^{-5}$	$.3761\times10^{-5}$	$.5307\times10^{-5}$	$.7608\times10^{-5}$	$.1113\times10^{-4}$
$\alpha=5.25\times10^5$	G'	1.4	1.97	2.78	3.99	5.82
$k=3\times10^7$	S	$.6469\times10^{-7}$	$.8927\times10^{-7}$	$.1244\times10^{-6}$	$.1759\times10^{-6}$	$.2530\times10^{-6}$
$\alpha=2.23\times10^7$	G'	1.42	1.98	2.77	3.90	5.6
$k=3\times10^8$	S	$.7170\times10^{-9}$	$.9884\times10^{-9}$	$.1375\times10^{-8}$	$.194\times10^{-8}$	$.2784\times10^{-8}$
$\alpha=2.0\times10^9$	G'	1.54	1.97	2.75	3.88	5.56
Hayes, $K_I/\sigma\sqrt{\pi a}$		2.09	2.38	2.68	3.05	3.52

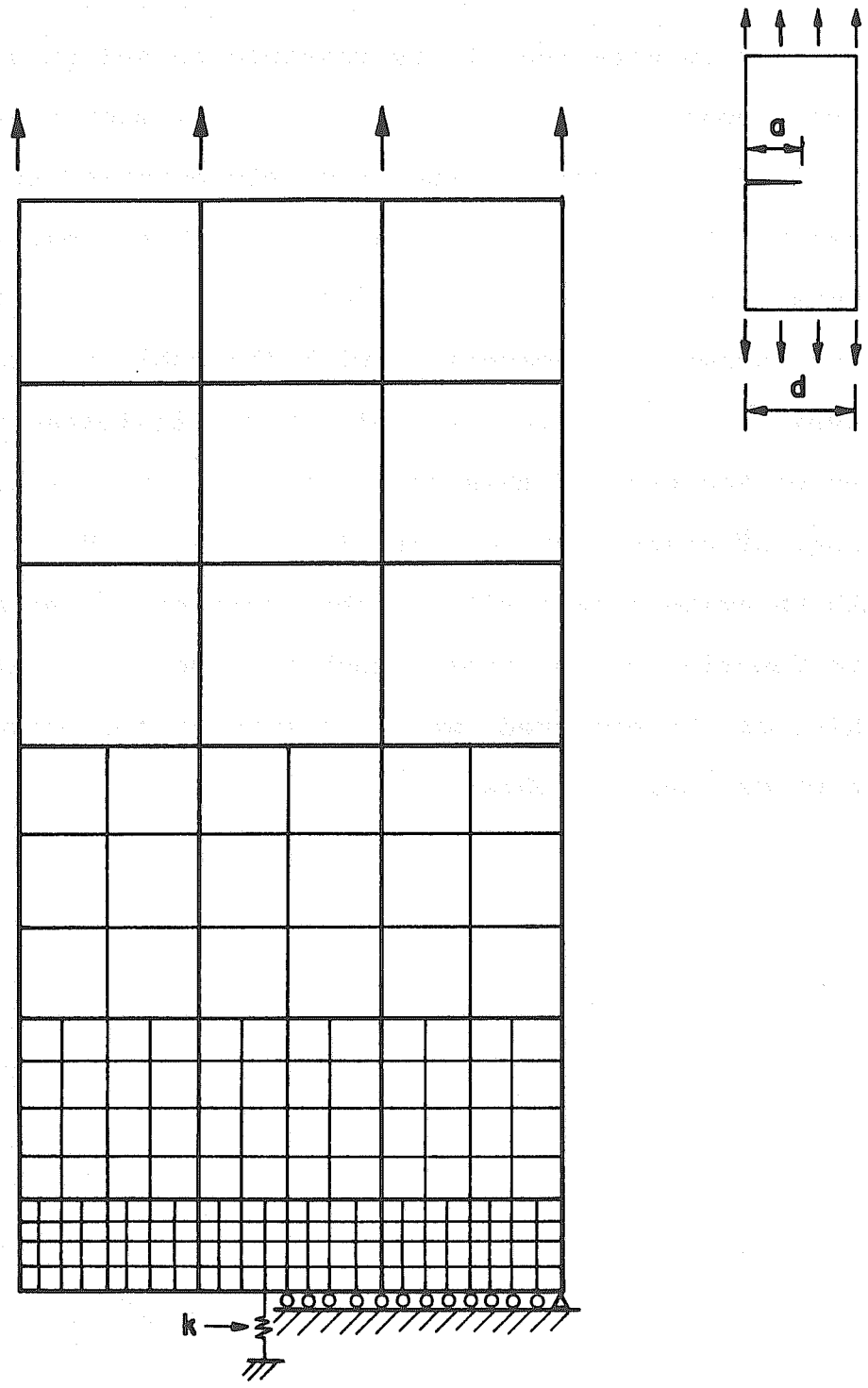

FIG. 6.13 A SINGLE EDGE CRACKED PLATE FOR PARAMETER STUDY

interesting to note that it is possible to select an arbitrary constant α for each k value, such that the valve $G' = \alpha \cdot s$ remains approximately constant at each a/d ratio. This encouraging fact seems to suggest that the network sensitivity is a fundamental parameter in terms of crack growth. A comparison with the published valves by Hayes [162] shown in the table above, indicates the degree of accuracy of this approximation. Full satisfaction, of course, can not be claimed here. But it should be evident that with further refinement, an appropriate function can be chosen such that more accurate G' value can be achieved, which in turn can be converted to proper unit to obtain G^*.

CHAPTER 7 SUMMARY AND CONCLUSION

7.1 Summary of the Present Work

Ever since the first publication on the subject by Ngo and Scordelis, interest has increased rapidly and progress has been made in the application of finite element method to study the behavior of reinforced and prestressed concrete structures where the problem of crack- is of particular concern. However, due to the many analytical difficulties involved, most researchers have chosen to represent cracking by a crack-zone rather than by individual crack-lines. In this thesis, an effort has been made to introduce crack-line automatically into the finite element model. To this end, some of the analytical difficulties were overcome. A broad over-all view of the subject was taken from the network-topological standpoint.

In Chapter 1, the nature of the problem was stated. Literature on the subject was reviewed, with the aim of showing how the cracking problem has been treated in the finite element method of analysis. A conceptual model was then proposed and the problems associated with the conceptual model were enumerated. These problems include the node numbering, the structural topology, the structural modification, and the crack propagation. The network-topological approach was proposed as being the unified treatment needed, both from the philosophical

and the methodological standpoint, to solve these problems.

In Chapter 2, the basic concept of structural network and topology was introduced. Some rudimentary graph theoretic matrices were given. It should be noted that the terms topology, graph, network and system were used interchangably, because a fine distinction among them was not necessary in the present work.

In Chapter 3, sparsity and bandedness were discussed. Graph theoretic interpretation of the Gaussian elimination was given, from which it was shown that the band type solution technique is not optimal, especially with respect to the problem of progressive crack growth. From this graph theoretic interpretation, the frontal solution technique was considered to be a means of achieving optimal ordering. The program ZIPP developed by Irons further shows that the usual node numbering scheme has no bearing on the solution procedure. Instead, the topology of the structure, expressed through the incidence matrices, plays a predominant role. Treatment of prescribed boundary conditions and recovery of reactions were made possible by adopting the method of Melosh and Bamford, once the equivalency between the elimination method of Irons and the decomposition method of Melosh and Bamford was demonstrated. Therefore, the frontal solution method becomes a feasible technique in the

present study.

In Chapter 4, the finite element model and the method of simulating crack growth were described. Each crack growth was viewed as a local change in the structural topology. Therefore, by examining the local incidence relationship expressed through graph theoretic matrices, it was possible to construct a crack-line automatically to accomodate any conceivable crack growth. The capability of the crack growth subroutine was illustrated with test cases. Some examples were also offered to show how predominant crack growth patterns can be obtained. Even though the cracking criteria as well as the crack geometry was restricted due to the simplified assumptions in modelling, satisfactory progressive crack growth analysis could still be achieved.

In Chapter 5, a method for structural modification was developed, which is based on the Link-At-A-Time algorithm in network theory. The computational aspect of the LAT algorithm was related to a method proposed by Argyris and his colleagues. Inspired by the work of Roy and Argyris, the LAT algorithm was extended to include the analysis of node discoalescing or decoupling. Again, through the graph theoretic interpretation, the modification can be implemented in such a way that it is entirely consistent with normal process of the direct stiffness analysis. The method of constructing the

Choleski decomposition from the frontal solution was also presented, which makes the computation procedure of the LAT algorithm feasible. A theorem concerning the nonsingularity and positive definiteness of the solution matrix was proposed and proved. Examples were used to illustrate the potential of the modification procedure in a progressive crack growth analysis.

In Chapter 6, an attempt was made to examine the relevant aspects of fracture mechanics, with the emphasis on how the finite element method could be employed as a solution aid. Among all the approaches, the energy method of Bueckner, as utilized by Hayes and Williams, appears to be promising. However, there is computational inconvenience even with this method when automatic crack growth analysis is to be achieved. Therefore, a hypothesis was postulated, which makes use of the network sensitivity function obtained from the adjoint network method. Tellegen's theorem, from which the adjoint network method is derived, was stated and proved in terms of the structural network incidence matrices given by Fenves and Branin. The preliminary results obtained by using this approach were found to be encouraging.

7.2 Remarks on the Network-Topological Approach

It is not the aim of this thesis to show the inter-transferrence of different physical systems, even though this aspect has proven itself naturally, Neither is the

purpose of this thesis to advocate a general structural system theory based upon the network-topological theorems. The network-topology, in the context of the present study, is a collective term which stands for a concept and metholology drawing from algebraic topology, linear graph, network and system theories which are useful in the solution of progressive crack growth. However, it would be a mistake if the network-topology is merely taken as a semantic difference from the conventional concept of matrix structural analysis, or merely a pedagogical experience.

In retrorespect, the network-topological approach employed in the present study, rudimentary as it is, still represents a unique method which makes the progressive crack growth analysis possible and feasible. Needless to say, much refinement is possible and necessary in order to perfect such an analytical tool.

7.3 Conclusion

This research represents another phase of the continuous effort, not only at the University of California, but also in this country and around the world, in the search for better understanding of the behavior of concrete structural members. The introduction of the crack-line concept into the finite element analysis has certain distinctive advantages of its own, such as being able to predict a well defined crack pattern, crack width, and

concrete-reinforcement interaction. The network-topology approach has been shown to be an invaluable aid in tracking and describing the crack, and provides the basic computational algorithm. The approach also finds application in the solution of simultaneous equations, structural modifications, and in the area of fracture mechanics.

It is believed that this research has created a new approach for the study of concrete structures, whether they are plain, reinforced or prestressed. The importance of the ability to predict and to control cracking in concrete structures, such as dams, bridges, highrise buildings, reactor vessels, or even pavements can not be overemphasized. It is hoped that this thesis will generate further imputus for study in this direction.

ACKNOWLEDGMENTS

The author wishes to express his deepest appreciation to the thesis supervisor, Prof. A. C. Scordelis, for his patient guidance and unfailing support during the course of the present research. The author is also grateful to the members of the thesis committee, Prof. E. L. Wilson and Prof. L. O. Chua, for reviewing and commenting on the thesis, and for the computer programs and references made available to the author. Computer facilities have been generously provided by the Computer Center of the University of California, Berkeley.

Many scholars and practitioners in the U. S. as well as from abroad have enthusiastically offered useful information and suggestions throughout the years. To all of them, the author wishes to convey his sincere gratitude, especially to Prof. F. Boasch, Prof. R. A. Rohrer, Prof. A. Samuelsson, Prof. I. Finnie, Prof. T. Y. Lam, Dr. F. H. Branin, Dr. J. R. Roy. Dr. N. E. Wiberg, Dr. S. K. Chan and Dr. C. S. Chan.

The author is also much indebted to the management of T. Y. Lin International, San Francisco, which has been very generous and understanding in providing an opportunity for the completion of the writing of this thesis.

A very special thanks goes to his good friend, Mr. A. K. Chou, who has not only been more than willing

in lending a helping hand whenever needed, but who also always cheerfully accepted the unsolicited honor of being the first audience of whatever theory or result, joy or grief that the author happened to possess.

To his parents, Mr. and Mrs. Ngo Van, parents-in-law, Mr. and Mrs. Tran Phao, and god-parents, Mr. and Mrs. Mok Chi Piu, the author wishes to express his deepest gratitude and highest respect for their warm encouragement and kind support. And lastly, but not the least, the author would like to thank his wife, Li-Cheing. It takes a superb lady to be the wife of such a long-time graduate student who became known as an "academic bum."

REFERENCES

1. Wilson, E. L., Finite Element Analysis of Two Dimensional Structures," Structures and Materials Research Report No. 63-2, Department of Civil Engineering, University of California, Berkeley, June 1963.

2. Clough, R. W., "The Stress Distribution of Norfork Dam," Structures and Materials Research Report, Series 100, Issue 19, Institute of Engineering Research, University of California, Berkeley, March 1962, 98 pp.

3. King, I. P., "Finite Element Analysis of Two-Dimensional Time-Dependent Stress Problems," Structures and Materials Research Report No. 65-1, Department of Civil Engineering, University of California, Berkeley, 1965.

4. Sandhu, R. S., Wilson, E. L., and Raphael, J. M., "Two-Dimensional Stress Analysis with Incremental Construction and Creep," SESM Report No. 67-34, University of California, Berkeley, December 1967, 50 pp.

5. Bresler, B., and Bertero, V., "Influence of Load History on Cracking in Reinforced Concrete," Report to California Division of Highways, Department of Civil Engineering, Division of Structural Engineering and Structural Mechanics, University of California, Berkeley, August 1966, 20 pp.

6. Bresler, B., and Bertero, V., "Behavior of Reinforced Concrete Under Repeated Load," J. Str. Div., ASCE, Vol, 94, No. ST6, June 1968, pp. 1567-1592.

7. Lutz, L. A., Gergely, P., and Winter, G., "The Mechanics of Bond and Slip of Deformed Reinforcing Bars in Concrete," Structural Engineering Report No. 324, Cornell University, August 1966, 300 pp.

8. Ngo, D., " A Study of Cracked Reinforced Concrete Beams by Finite Element Method," Graduate Student Research Report No. 216, Division of Structural Engineering and Structural Mechanics, University of California, Berkeley, 1965, 78 pp.

9. Ngo, D., and Scordelis., A. C., "Finite Element Analysis of Reinforced Concrete Beams," J. ACI, Vol. 64, No. 3, March 1967, pp. 152-163.

10. Ngo, D., Franklin, H. A., and Scordelis, A. D., "Finite Element Study of Reinforced Concrete Beams with Diagonal Tension Cracks," UC SESM Report No. 70-19, University of California, Berkeley, December 1970, 88 pp.

11. Nilson, A. H., "Finite Element Analysis of Reinforced Concrete," Ph.D. Dissertation, Division of Structural Engineering and Structural Mechanics, University of California, Berkeley, March 1967, 192 pp.

12. Nilson, A. H., "Nonlinear Analysis of Reinforced Concrete by the Finite Element Method," J. ACI, Vol. 65, No. 9, September 1968, pp. 757-766.

13. Mufti, A. A., Mirza, M. S., McCutcheon, J. O., and Houde, J., "A Study of the Behavior of Reinforced Concrete Elements Using Finite Elements," Structural Concrete Series No. 70-5, McGill University, Montreal, September 1971.

14. Youssef, A. A. R., McCutcheon, J. O., Mufti, A. A., and Mirza, M.S., "Inelastic Analysis of Plates and Slabs Using Finite Elements," Structural Concrete Series No. 70-1, McGill University, Montreal, March 1971.

15. Spokowski, R. W., "Finite Element Analysis of Reinforced Concrete Members," M.Eng. Thesis, Department of Civil Engineering, Montreal, May 1972.

16. Murray, K., "Theoretical and Experimental Analysis of Crack Formation in Reinforced Concrete," Ph.D Dissertation, Civil Engineering, Virginia Polytechnic Institute, October 1968, 102 pp.

17. Loov, R. E., "The Determination of Stresses and Deformations of Reinforced Concrete After Cracking," Structure, Solid Mechanics and Engineering Design, Part 2, Proceedings of the Southampton 1969 Civil Engineering Materials Conference, Edited by Te'eni, M., Wiley-Interscience, London, 1971, pp. 1257-1261.

18. Isenberg, J., and Adham, S., "Analysis of Orthotropic Reinforced Concrete Structures," J. Str. Div., ASCE, Vol. 96, No. ST12, December 1970, pp. 2607-2624.

19. Cervanka, V., "Inelastic Finite Element Analysis of Reinforced Concrete Panels Under In-Plane Loads," Ph.D. Dissertation, Department of Civil Engineering, University of Colorado, Boulder, 1970, 241 pp.

20. Valliappan, S., and Nath, P., "Tensile Crack Propagation in Reinforced Concrete Beams --- Finite Element Technique," Paper for International Conference on Shear, Torsion, and Bond in Reinforced and Prestressed Concrete, Coimbatore, India, 14-17 January, 1969.

21. Valliappan, S., and Doolan, T. F., "Nonlinear Stress Analysis of Reinforced Concrete," J. Str. Div., ASCE, Vol. 98, No. ST4, April 1972, pp. 885-898.

22. Selna, L. G., "Time-Dependent Behavior of Reinforced Concrete Structures," Structures and Materials Research, SESM Report no. 67-19, University of California, Berkeley, August 1967.

23. Selna, L. G., "Creep, Cracking, and Shrinkage in Concrete Frame Structures," J. Str. Div., ASCE, Vol. 95, No. ST12, December 1969.

24. Franklin, H. A., "Non-Linear Analysis of Reinforced Concrete Frames and Panels," Structures and Materials Research, SESM Report No. 70-5, University of California, Berkeley, March 1970, 259 pp.

25. Yuzugullu, O., and Schnobrich, W. C., "Finite Element Approach for the Prediction of Inelastic Behavior of Shear Wall-Frame Systems," Structural Research Series No. 386, Department of Civil Engineering, University of Illinois, August 1972.

26. Rashid, Y. R., and Rockenhauser, W., "Pressure Vessel Analysis by Finite Element Techniques," Conference on Prestressed Concrete Pressure Vessels, March 1967, The Institute of Civil Engineers, London, 1968.

27. Wahl, H. W., and Kasiba, R. J., "Design and Construction Aspects of Large Prestressed Concrete (PWR) Containment Vessels," J. ACI, Vol. 66, No. 5, May 1969.

28. Rashid, Y. R., "Ultimate Strength Analysis of Prestressed Concrete Pressure Vessels," Nuclear Engineering Design, Vol. 7, 1968, pp. 334.

29. Rashid, Y. R., "Analysis of Prestressed Concrete Nuclear Reactor Structures," unpublished notes presented at the Conference on Prestressed Concrete Nuclear Reactor Structures, University of California, Berkeley, March 1968, 63 pp.

30. Argyris, J. H., Faust, G., Szimmat, Warnke, E. P., and Willam, K. J., "Recent Developments in the Finite Element Analysis of Prestressed Concrete Reactor Vessels," ISD Report No. 151, Stuttgart, 1973.

31. Kripanarayanan, K. M., and Meyers, B. L., "Transfer Stress Distribution of Fully Bonded Pretensioned Wires Using the Finite Element Method," Proceeding of the Specialty Conference on Finite Element Method in Civil Engineering, June 1 and 2, 1972, Montreal, Quebec, Canada, pp. 729-744.

32. Jorfriet, J. C., McNeice, G. M., and Csagoly, P., "Analysis of Post-Tensioned Highway Bridges with Circular Voids," Proceeding of the Specialty Conference on Finite Element Method in Civil Engineering, June 1 and 2, Montreal, Quebec, Canada, pp. 869-891.

33. Taylor, M. A., Romstad, K. M., Herrmann, L. R., and Ramey, M. R., "A Finite Element Computer Program for the Prediction of the Behavior of Reinforced and Prestressed Concrete Structures Subject to Cracking," CR72.019, Department of Civil Engineering, University of California, Davis, June 1972, 110 pp.

34. Jofriet, J. C., and McNeice, G. M., "Finite Element Analysis of Reinforced Concrete Slabs," J. Str. Div., ASCE, Vol. 97, No. ST3, March 1971.

35. Bell, J. C., " A Complete Analysis of Reinforced Concrete Slabs and Shells," Ph.D. Dissertation, Department of Civing Engineering, University of Canterbury, Christchurch, New Zealand, 1970, 299 pp.

36. Bell, J, C., and Elms, D., " Partially Cracked Finite Elements," J. Str. Div., ASCE, Vol 97, No. ST7, July 1971.

37. Scanlon, A., "Time Dependent Deflection of Reinforced Concrete Slabs," Ph.D. Dissertation, Department of Civil Engineering, University of Alberta, Edmonton, Canada, December 1971.

38. Hand, F. P., Pecknold, D. A., and Schnobrich, W. C., "A Layered Finite Element Nonlinear Analysis of Reinforced Concrete Plates and Shells," Structural Research Series, No. 389, Department of Civil Engineering, Univeristy of Illinois, August 1972.

39. Lin, C. S., "Nonlinear Analysis of Reinforced Concrete Slabs and Shells," Structures and Materials Research, Report No. UC SESM 73-7, Department of Civil Engineering, University of California, Berkeley, April 1973, 161 pp.

40. Scordelis, A. C., "Finite Element Analysis of Reinforced Concrete Structures," Proceeding of the Specialty Conference on Finite Element Method in Civil Engineering, June 1 and 2, 1972, Montreal, Quebec, Canada, pp. 71-114.

41. McCutcheon, J. O., Mirza, M. S., and Mufti, A. A., Editors, "Proceeding of the Specialty Conference on Finite Element Method in Civil Engineering," Montreal, Quebec, Canada, June 1 and 2, 1972, 1254 pp.

42. Fenves, S. J., and Branin, F. H., "Network-Topological Formulation of Structural Analysis," J. Str. Div., ASCE, Vol. 89, No. ST4, August 1963, pp. 483-514.

43. Kron. G., "Tensorial Analysis and Equivalent Circuits of Elastic Structures," J. Franklin Institute, Vol. 238, No. 6, December 1944, pp. 399-442.

44. Kron, G., "A Set of Principles to Interconnect the Solutions of Physical Systems," J. Applied Physics, Vol. 24, 1953, pp. 965-980.

45. Kron, G., "A Method to Solve Very Large Physical Systems in Easy Stages," Proceedings, Insititue of Radio Engineers, Vol. 42, 1954, pp. 680-686.

46. Kron, G., "Solving Highly Complex Elastic Structures in Easy Stages," J. Applied Mechanics, Vol. 22, ASME, June 1955, pp. 235-244.

47. Branin, F. H., "Machine Analysis of Networks and Its Applications," TR 00.855, Development Laboratory, Data Systems Division, International Business Machines Corporation, Poughkeepsie, New York, March 30, 1962, 129 pp.

48. Branin, F. H., "The Algebraic-Topological Basis for Network Analogies and the Vector Calculus," TR 00.1495, Systems Development Division, International Business Machines Corporation, Poughkeepsie, New York, July 25, 1966, 66 pp.

49. Branin, F. H., "Computer Methods for Network Analysis," Proceedings of the IEEE, Vol. 55, No. 11, November 1967, pp. 1787-1801.

50. Roth, J. P., "An Application of Algebraic Topology to Numerical Analysis: On the Existence of a Solution to the Network Problem," Proceedings, National Academy of Science, Vol. 41, 1955, pp. 518-521.

51. Roth, J. P., "The Validity of Kron's Method of Tearing," Proceedings, National Academy of Science, Vol. 41, 1955, pp. 599-600.

52. Roth, J. P., "An Application of Algebraic Topology: Kron's Method of Tearing," Quarterly of Applied Mathematics, Vol. 17, No. 1, April 1959, pp. 1-24.

53. Langefors, B., "Algebraic Topology Applied to Network Problems," SAAB TN43, Saab Aircraft Co., Linkoping, July 1, 1959, 37 pp.

54. Langefors, B., "Algebraic Topology for Elastic Networks," SAAB TN49, Saab Aircraft Co., Linkoping, April 1, 1961, 52 pp.

55. Baron, F., "Logic and Topology of Structural Analysis," Report No. 62-63, Structures and Materials Research, Department of Civil Engineering, University of California, Berkeley, May 1962, 38 pp.

56. Samuelsson, A., "Linear Analysis of Frame Structures by Use of Algebraic Topology," Dissertation, Chalmers University of Technology, Gothenburg, 1962, 115 pp.

57. Samuelsson, A., "Conceptual Frame Analysis," Chalmers University of Technology, Gothenburg, 1963, 17 pp.

58. Wiberg, N. E., "Diacoptics and Codiacoptics, Two Dual Mixed Methods for Analyzing Elastic Structures," Publication 67:8, Department of Structural Mechanics, Chalmers University of Technology, Gothenburg, 1967, 92 pp.

59. Wiberg, N.E., "System Analysis with Mixed Variables," Publication 73:1, Department of Structural Mechanics, Chalmers University of Technology, Gothenburg, 1973.

60. Wiberg, N. E., "System Analysis in Structural Mechanics, by Use of Mixed Force and Displacement Variables," Dissertation, Department of Structural Mechanics, Chalmers University of Technology, Gothenburg, 1970.

61. Stewart, K. L., and Baty, J., " Dissection of Structures," J. Str. Div., ASCE, Vol. 93, No ST5, October 1967, pp. 217-232.

62. Lind, N. C., "Analysis of Structures by System Theory," J. Str. Div., ASCE, Vol. 88, No ST2, April 1972, pp. 1-22.

63. Wu, T. S., "Structural Analysis by System Theory," Development in Theoretical and Applied Mechanics, Vol. 2, Proceedings of the Second Southeastern Conference on Theoretical and Applied Mechanics, Pergamon Press, London, 1965, pp. 605-628.

64. Henderson, J. C. de C., and Bickley, W. G., "Statical Indeterminancy of a Structure," Aircraft Engineering, Vol. 27, December 1955, pp. 400-402.

65. Morice, P. B., "Linear Structural Analysis," Thames and Hudson, London, 1959, pp. 48-59.

66. Henderson, J. C. de C., "Topological Aspects of Structural Linear Analysis," Aircraft Engineering, Vol. 32, May 1960, pp. 137-141.

67. DiMaggio, F. L., "Statical Determinancy and Stability of Structures," J. Str. Div., ASCE, Vol. 89, No. ST3, June 1963, pp. 63-75.

68. DiMaggio, F. L., and Spillers, W. R., "Network Analysis of Structures," J. Eng. Mech. Div., ASCE, Vol. 91, No. EM3, June 1965, pp. 169-188.

69. Henderson, J. C. de C., and Maunder, E. A. W., "A Problem in Applied Topology : on the Selection of Cycles for the Flexibility Analysis of Skeletal Structures," J. Institute of Mathematical Applications, Vol. 5, 1969, pp. 254-269.

70. Maunder, E. A. W., "Topological and Linear Analysis of Skeletal Structures," Ph.D. Dissertation, Imperial College, England, 1971.

71. Oden, J. T., and Neighbors, A., "Network-Topological Formulation of Analysis of Geometrically and Materially Non-Linear Space Frames," International Conference on Space Structures, Department of Civil Engineering, University of Surrey, 1966, 12 pp.

72. Oden, J. T., "A General Theory of Finite Elements, I. Topological Considerations," Int. J. Numerical Methods in Engineering, Vol. 1, 1969, pp. 205-221.

73. Oden, J. T., "A General Theory of Finite Elements, II. Applications," Int. J. Numerical Methods in Engineering, Vol. 1, 1969, pp. 247-259.

74. Seshu, S., and Reed, M. S., "Linear Graphs and Networks," Addison-Wesley Co., Massachusetts, 1962.

75. Boasch, F., "Notes on Network Analysis," Department of Electrical Engineering and Computer Sciences, University of California, Berkeley, 1969.

76. Chua, L. O., "Foundation of Circuit Theory: Linear and Nonlinear," Department of Electrical Engineering and Computer Sciences, University of California, Berkeley, 1971.

77. Flegg, H. G., "Boolean Algebra and Its Application, Including Boolean Matrix Algebra," John Wiley & Sons, Inc., New York, 1964, 261 pp.

78. Desoer, C. A., and Kuh, E. S., "Basic Circuit Theory," McGraw-Hill, New York, 1968.

79. Busacker, R. G., and Saaty, T. L., "Finite Graphs and Networks: An Introduction with Applications," McGraw-Hill, New York, 1965, 294 pp.

80. Spiller, W. R., "Techniques for Analysis of Large Structures," J. Str. Div., ASCE, Vol. 94, No. ST11, November 1968, pp. 2521-2534.

81. Tocher, J. L., "Selective Inverse of Stiffnes Matrices," J. Str. Div., ASCE, Vol. 92, No. ST1, February 1966, pp. 75-88.

82. Johnson, C. P., "The Analysis of Thin Shell by a Finite Element Procedure," Structural Engineering Laboratory Report No. 67-22, University of California, Berkeley, 1967.

83. Sato, N., and Tinney, W. F., "Techniques for Exploiting the Sparsity of the Network Admittance Matrix," IEEE Trans., Power Apparatus and Systems, Vol. 82, December 1963, pp. 944-950.

84. Tinney, W. F., and Walker, J. W., "Direct Solution of Sparse Network Equations by Optimally Ordered Triangular Factorization," Proc. IEEE, Vol. 55, November 1967, pp. 1801-1809.

85. Jensen, H. G., and Parks, G. A., "Efficient Solution for Linear Matrix Equations," J. Str. Div., ASCE, Vol. 96, No. ST1, January 1970, pp. 49-64.

86. Berry. R. D., "An Optimal Ordering of Electronic Circuit Equations for a Sparse Matrix Solution," IEEE Trans. On Circuit Theory, Vol. CT-18, No. 1, January 1971, pp. 40-50.

87. Melosh, R. J., and Bamford, R. M., "Efficient Solution of Load-Deflection Equations," J. Str. Div., ASCE, Vol. 95, No. ST4, April 1969, pp. 661-675.

88. Whetstone, W. D., "Computer Analysis of Large Linear Frames," J. Str. Div., ASCE, Vol. 95, No. ST11, November 1969, pp. 2401-2417

89. Wiberg, N. E., Discussion of "Efficient Reanalysis of Modified Structures," by Kavlie, D., and Powell, G. H., J. Str. Div., ASCE, Vol. 97, No. ST10, October 1971, pp. 2612-2619.

90. Bathe, K. J., Wilson, E. L., Peterson, F. E., "SAP IV--A Structural Analysis Program for Static and Dynamic Response of Linear Systems," Report No. EERC 73-11, April 1974, College of Engineering, University of California, Berkeley, California, pp. 1-59.

91. Mondkar, D. P., and Powell, G. H., "Towards Optimal In-Core Equation Solving," Computer and Structures, Vol. 4, Pergamon Press, 1974, pp. 531-548.

92. Wilson, E. L., Bathe, K. J., Doherty, W. P., "Direct Solution of Large Systems of Linear Equations," Computer and Structures, Vol. 4, 1974, pp. 363-372.

93. Williams, F. W., "Rapid Reduction of Banded Stiffness Matrices," J. Str. Div., ASCE, Vol. 99, No. ST5, May 1973, pp. 967-972.

94. Meyer, C., "Solutions of Linear Equations--State-of-the-Art," J. Str. Div., ASCE, Vol. 99, No. ST7, July 1973, pp. 1507-1526.

95. Klyuyev, V. V., and Kokovkin-Scherbak, N. I., "On the Minimization of the Number of Arithmetic Operations for the Solution of Linear Algebraic Systems of Equation," Technical Report CS24, Computer Science Department, Stanford University, Stanford, California, 1965.

96. Rosen, R., "Matrix Bandwidth Minimization," Proceedings, 1968 ACM National Conference, pp. 585-595.

97. Akyuz, F. A., and Utku, S., "An Automatic Node-Relabeling Scheme for Bandwidth Minimization of Stiffness Matrices," J. AIAA, Vol. 6, No. 4, April 1968.

98. Irons, B. M., "A Frontal Solution Program for Finite Element Analysis," Int. J. Numerical Methods in Engineering, Vol. 2, 1970, pp. 5-32.

99. Parter, S., "The Use of Linear Graphs in Gauss Eliminations," SIAM Rev., Vol. 3, 1961, pp. 119-130.

100. Ogbuobiri , E. C., Tinney, W. F., and Walker, J. W., "Sparsity-Directed Decomposition for Gaussian Elimination on Matrices," Bonneville Power Administration, Portland, Oregon, 1969.

101. Bree, D. Jr., " Some Remarks on the Application of Graph Theory to the Solution of Sparse System of Linear Equations," Thesis, Department of Mathematics, Princeton University, N. J., May 1965, 15 pp.

102. Spillers, W. R., "On Diacoptics: Tearing of an Arbitrary System," Quarterly of Applied Mathematics, Vol. 23, No. 2, July 1965, pp. 188-190.

103. Spillers, W. R., and Hickerson, N., "Optimal Elimination for Sparse Symmetric Systems as a Graph Problem," Quarterly of Applied Mathematics, Vol. 26, 1968, pp. 425-432.

104. Coates, C. L., "Flow-Graph Solutions of Linear Algebraic Equations," IRE Transactions on Circuit Theory, Vol. CT-6, June 1959, pp. 170-187.

105. Steward, D. V., "Partitioning and Tearing Systems of Equations," J. SIAM, Numerical Analysis, Series B, Vol. 2, No. 2, 1965, pp. 345.

106. Steward, D. V., "On an Approach to Techniques of the Analysis of the Structure of Large Systems of Equations," SIAM Rev., Vol. 4, 1962, pp. 321-342.

107. Harary, F., " A Graph Theoretic Method for the Complete Reduction of Matrix with a View toward Finding Its Eigenvalues," J. Mathematics and Physics, Vol. 38, 1959, pp. 104-111.

108. Harary, F., "A Graph Theoretic Approach to Matrix Inversion by Partitioning," Numer. Math., Vol. 4, 1962, pp. 128-135.

109. Harary, F., "Graph Theory and Electrical Networks," IRE Trnas., Circuit Theory, CT6, 1959, pp. 95-109.

110. Bathe, K. J., Ozdemir, H., and Wilson, E. L., "Static and Dynamic Geometric and Material Nonlinear Analysis," SESM Report No. 74-4, Department of Civil Engineering, University of California, Berkeley, 1974.

111. Goodman, R. E., Taylor, R. L., and Brekke, T. L., "A Model for the Mechanics of Jointed Rock," J. Soil Mech, and Found. Div., ASCE, Vol. 94, No. SM3, May 1968, pp. 637-659.

112. Michielsen, H. F., and Dijk, A., "Structural Modifications in Redundant Structures," J. Aeronautical Sciences, Vol. 20, No. 4, April 1953, pp. 286.

113. MacNeal, R. H., "Application of the Compensation Theorem to the Modification of Redundant Structures," J. Aeronautical Sciences, Vol. 20, No. 10, October 1953, pp. 726-727.

114. Argyris, J. H., "The Matrix Analysis of Structures with Cutouts and Modifications," Proceedings, Ninth International Congress of Applied Mechanics, 1956, pp. 131-142.

115. Argyris, J. H., and Kelsey, S., "Initial Strains in the Matrix Force Method of Structural Analysis," J. Royal Aeronautical Society, Vol. 64, No. 596, August 1960.

116. Argyris, J. H., Kelsey, S., and Grzedzielski, A. L. M., "The Discussion on the Initial Strain Concept," J. Royal Aeronautical Society, Vol. 65, February 1961, pp. 127-137.

117. Cicala, P., "Effect of Cut-Outs in Semimonocoque Structures," J. Aeronautical Sciences, Vol, 15, No. 3, March 1948, pp. 171.

118. Grzedzielski, A. L. M., "Note on Some Applications of the Matrix Force Method of Structural Analysis," J. Royal Aeronautical Society, Vol. 64, No. 594, August 1960, pp. 354-357.

119. Sobieszczanski, J., "Matrix Algorithm for Structural Modification Based Upon the Parallel Element Concept," J. AIAA, Vol. 1, No. 11, November 1969, pp. 2132-2139.

120. Sobieszczanski, J., "Structural Modification by Perturbations Method," J. Str. Div., ASCE. Vol. 94, No. ST12, December 1968, pp. 2799-2816.

121. Melosh, R. J., and Luik, R., "Multiple Configuration Analysis of Structures," J. Str. Div., ASCE, Vol. 94, No. ST11, November 1968, pp. 2581-2595.

122. Melosh, R. J., and Luik, R., "Approximate Multiple Configuration Analysis and Allocation for Least Weight Structural Design," AFFPL-TR-67-59, Wright-Patterson Air Force Base, Ohio, April 1967.

123. Kosko, E., "Effect of Local Modifications in Redundant Structures," J. Aeronautical Sciences, Vol. 21, No. 3, March 1954, pp. 206-207.

124. Sack, R. L., Carpenter, W., and Hatch, G., "Modification of Elements in the Displacement Method," J. AIAA, Vol. 5, No. 9, September 1967, pp. 1708-1710.

125. Argyris, J. H., Bronlund, O. E., Roy, J. R., and Scharpf, D. W., "A Direct Modification Procedure for the Displacement Method," J. AIAA, Vol. 9, September, 1971, pp. 1861-1894.

126. Kirsch, U., and Rubinstein, M. F., "Reanalysis for Limited Structural Design Mofifications," J. Eng. Mech. Div., ASCE, Vol. 98, No. EM1, February 1972, pp. 61-70.

127. Kavlie, D., and Powell, G. H., "Efficient Reanalysis of Modified Structures," J. Str. Div., ASCE, Vol. 97, No. ST1. January 1971, pp. 377-392.

128. Rubinstein, M. F., "Combined Analysis by Substructures and Recursion." J. Str. Div., ASCE, Vol. 93, No. ST2 April 1967, pp. 231-235.

129. Rosen, R., and Rubinstein, M. F., "Substructure Analysis by Matrix Decomposition," J. Str. Div., ASCE, Vol. 93, No. ST3, March 1970, pp. 663-670.

130. Householder, A. S., "A Survey of Some Closed Methods for Inverting Matrices," J. SIAM, Vol. 5, No. 3, September 1957, pp. 155-169.

131. Householder, A. S., "The Theory of Matrices in Numerical Analysis," Blaisdell Publication Co., New York, 1964.

132. Argyris, J. H., and Roy, J. R., "General Treatment of Structural Modifications," J. Str. Div., ASCE, Vol. 98, No. ST2, February 1972, pp. 465-492.

133. Roy, J. R., "Allgemeine Modifikationsverfahren fur die lineare und nichtlineare Berechnung von Tragwerken und Kontinua mit der Matrizenverschiebungsmethode," D. Eng. Dissertation, University of Stuttgart, Stuttgart, Germany, 1971.

134. Roy, J. R., "General Modifications of Large Sets of Sparse Linear Equations," Paper Delivered at the NATO Conference on Decomposition, Cambridge, U. K., July 1972.

135. Wilson, E. L., "SMIS--Symbolic Matrix Interpretive System," Report No. UC SESM 73-3, Department of Civil Engineering, University of California, Berkeley, January 1973.

136. Lam, T. Y., Private communication, Department of Mathematics, University of California, Berkeley, 1973.

137. Kaplan, M. F., "Crack Propagation and the Fracture of Concrete," J. ACI, Vol. 58, No. 5, November 1961, pp. 591-610.

138. Romualdi, J. P., and Batson, G. B., "Mechanics of Crack Arrest in Concrete," J. Eng. Mech. Div., ASCE, Vol. 89, No. EM3, June 1963, pp. 147-168.

139. Gluckich, J., "Fracture of Plain Concrete," J. Eng. Mech. Div., ASCE, Vol. 89, No, EM6, December 1963, pp. 127-138.

140. Bianchini, A. C., Lesler, C. E., and Lott, J. L., "Cracking of Reinforced Concrete Under External Load," ACI Publication SP-20, 1968, pp. 73-85.

141. Broms, B. B., "Mechanism of Tension Cracking in Reinforced Concrete Members--Phase II," Report No. 311, Department of Structural Engineering, Cornell University, June 1963.

142. Shah, S. P., and McGarry, F. J., "Griffith Fracture Criterion and Concrete," J. Eng. Mech. Div., ASCE, Vol. 97, No. EM6, December 1971, pp. 1663-1676, see also closure, Vol. 99, No. EM2, April 1973, pp. 412.

143. McClintock. F. A., and Walsh, J.B., "Friction on Griffith Cracks in Rocks Under Pressure," Proceedings, Fourth U. S. Cong. App. Mech., 1962, pp. 1015-1021.

144. Sandhu, R.S., and Huang, S. W., "Application of Griffith's Theory to Analysis of Progressive Fracture," Paper accepted for publication in International Journal of Fracture, 1974.

145. Huang, S. W., "Finite Element Analysis of Fracture Propagation in Two-Dimensional Elastic Solid," Ph.D. Dissertation, Ohio State University, 1972.

146. Rostem, S., and Byskow, E., "Cracks in Concrete Structures--A Fracture Mechanics Approach," Structural Research Laboratory, Technical University of Denmark, Report No. R34 1973, 18 pp.

147. Griffith, A. A., "The Phenomena of Rupture and Flow in Solids," Philosophical Transactions, Royal Society of London, Series A, Vol. 221, 1920, pp. 163-198.

148. Finnie, I., and Mackenzie, A. C., "An Introduction to the Mechanics of Fracture," College of Engineering, University of California, Berkeley, 1973.

149. Swedlow, J. L., "On Griffith's Theory of Fracture," Int. J. Fracture Mechanics, Vol. 1, No. 3, September 1965, pp. 210-216.

150. Low, J. R. Jr., "The Relation of Microstructure to Brittle Fracture," ASTM Symposium on Behavior of Materials at Low Temperature, American Socity of Metals, Cleveland, Ohio, 1953, pp. 163.

151. Orowan, E., "Fundamentals of Brittle Behavior of Metals," Fatigue and Fracture of Metals, MIT Symposium, June 1950, John Wiley and Sons, Inc., New York, 1950.

152. Orowan, E., "Energy Criteria of Fracture," Welding Journal, Research Supplement, March 1955.

153. Irwin, G. R., "Fracture Dynamics, Fracturing of Metals," American Society of Metals, Cleveland, Ohio, 1948.

154. Irwin, G. R., "Fracture Mechanics, First Symposium on Naval Structural Mechanics," Stanford University, August 1958.

155. Irwin, G. R., "Analysis of Stresses and Strains Near the End of a Crack Traversing a Plate," J. App. Mech. Trans., ASME, Vol. 79, 1957, pp. 361-364.

156. Irwin, G. R., Proc., Sagamore Res. Ord, Materials, 1960, pp. 63.

157. Dugdale, D. S., "Yielding of Steel Sheets Containing Slits," J. Mech. Phys. Solids, Vol. 8, 1960, pp. 100-104.

158. Barenblatt, G. I., "The Mathematical Theory of Equilibrium Cracks in Brittle Fracture," Advances in Applied Mechanics, Academic Press, 1962, pp. 55-129.

159. Dvorak, G. J., "A Model of Brittle Fracture Propagation, Part I--Continuum Aspects," Engineering Fracture Mechanics, Vol. 3, No. 4, December 1971, pp. 351-379.

160. Bueckner, H. F., "The Propagation of Cracks and the Energy of Elastic Deformation," Trans., ASME, Vol. 80, 1958, pp. 1225-1230.

161. Hayes, D. J., "A Practical Application of Bueckner's Formulation for Determining Stress Intensity Factors for Cracked Bodies," Int. J. Fracture Mechanics, Vol. 8, No. 2, June 1972, pp. 157-165.

162. Hayes, D. J., "Some Applications of Elastic Plastic Analysis of Fracture Mechanics," Ph.D. Dissertation, Imperial College of Science and Technology, Mechanical Engineering Department, London, October 1970, 429 pp.

163. Hayes, D. J., and Williams, J. G., "A Practical Method for Determining Dugdale Model Solution for Cracked Bodies of Arbitrary Shape," Int. J. Fracture Mechanics, Vol. 8, No. 3, September 1972, pp. 239-256.

164. Muckhelishvili, N. J., "Some Basic Problems in the Mathematical Theory of Elasticity," (J. R. M. Radok, Trans.), 4th Ed., Noordhoff, Groningen, Holland, 1963.

165. Rowe, G. H., "Matrix Displacement Methods in Fracture Mechanics Analysis of Reactor Vessels," Nuclear Engineering and Design, Vol. 29, No. 1, 1972, pp. 251-263.

166. Chan, S. K., Tuba, I. S., and Wilson, W. K., "On the Finite Element Method in Linear Fracture Mechanics," Engineering Fracture Mechanics, Vol. 2, No. 1, July 1970, pp. 1-17.

167. Chan, S. K., private communication, Westinghouse Research Laboratory, Pittsburg, PA., June 1971.

168. Wilson, W. K., and Thompson, D. G., "On the Finite Element Method for Calculating Stress Intensity Factors for Cracked Plates in Bending," Engineering Fracture Mechanics, Vol. 3, No. 2, August 1971, pp. 97-102.

169. Dixon, J. R., and Dukes, T. P., "Analysis of Ship Structures by the Finite Element Method; Part II, The Use of the Finite Element Method in Fracture Mechanics," Proceedings of the ISD/ISSC Symposium on Finite Element Techniques, University of Stuttgart, Germany, June 10-12, 1969, pp. 62-98.

170. Watwood, V. B. Jr., "The Finite Element Method for Prediction of Crack Behavior," Nuclear Engineering and Design, Vol. 11, 1963, pp. 323.

171. Mowbray, D. F., "A Note on the Finite Element Method in Linear Fracture Mechanics," Engineering Fracture Mechanics, Vol. 2, No. 2, November 1970, pp. 173-176.

172. Rice, J. R., "A Path Independent Integral and the Approximate Analysis of Strain Concentration by Notches and Cracks," Trans., ASME, J. Applied Mechanics, Vol. 35, 1968, pp. 379.

173. Rice, J. R., "Mathematical Analysis in the Mechanics of Fracture," in "Fracture--An Advanced Treatise II," ed., Liebowitz, Academic Press, New York, 1968.

174. Leverenz, R. K., "A Finite Element Stress Analysis of a Crack in a Bi-Material Plate," Int. J. Fracture Mechanics, Vol. 8, No. 3, September 1972, pp. 311-324.

175. Swanson, S. R., "Finite Element Solutions for a Cracked Two-Layered Elastic Cylinder," Engineering Fracture Mechanics, Vol, 3, No. 3, October 1971, pp. 283-289.

176. Walsh, P. F., "Linear Fracture Mechanics Solutions for Zero and Right Angle Notches," Division of Building Research Technical Paper (Second Series) No. 2, Commonwealth Scientific and Industrial Research Organization, Australia, 1974, pp. 1-16.

177. Byskov, E., "The Calculation of Stress Intensity Factors Using Finite Element Method with Cracked Elements," Int. J. Fracture Mechanics, Vol. 6, No. 2, June 1970, pp. 159-167.

178. Tracey, D. M., "Finite Element for Determination of Crack Tip Elastic Stress Intensity Factors," Engineering Fracture Mechanics, Vol. 3, No. 3, October 1971, pp. 255-265.

179. Paris, P. C., and Sih, G. C. M., "Stress Analysis of Cracks," Fracture Toughness Testing and Its Applications, ASTM, Special Technical Publication No. 381, 1965, pp. 30-83.

180. Swedlow, J. L., Yang, A. H., and Williams, M. L., "Elasto-Plastic Stresses and Strains in a Cracked Plate," Proceedings, First International Conference on Fracture, Sendai, 1965, Vol. 1, 1966, pp. 259.

181. Swedlow, J. L., "Initial Comparisons Between Experiment and Theory of the Strain Fields in a Cracked Copper Plate," Int. J. Fracture Mechanics, Vol. 5, No. 1, March 1969, pp. 25-31.

182. Swedlow, J. L., "Elasto-Plastic Cracked Plates in Plane Strain," Int. J. Fracture Mechanics, Vol. 5, No. 1, March 1969, pp. 33-44.

183. Underwood, J. H., Swedlow, J. L., and Kendall, D. P., "Experiemntal and Analytical Strains in an Edge-Cracked Sheet," Engineering Fracture Mechanics, Vol. 2, No. 3, May 1971, pp. 183-196.

184. Jones, D. P., and Swedlow, J. L., "Bending of an Elasto-Plastic Cracked Plate, Including the Effects of Crack Closure," Department of Mechanical Engineering, Carnegie-Mellon University, 1972.

185. Tuba, I. S., "Comments on the Classical Elastic-Plastic Analysis for Fracture Mechanics Studies," Int. J. Fracture Mechanics, Vol. 6, No. 1, 1970, pp. 61.

186. Wells, A. A., "Crack Opening Displacements from Elastic-Plastic Analyses of Externally Notched Tension Bars," Engineering Fracture Mechanics, Vol. 1, No. 3, April 1969, pp. 399-410.

187. Ostergren, W., "Small Scale Yielding Near a Crack in Plane Strain: A Finite Element Analysis," M. S. Thesis at Brown University, February 1969.

188. Levy. N., Marcal, P.V., Ostergren, W., and Rice, J., "Small Scale Yielding Near a Crack in Plane Strain: A Finite Element Analysis," Int. J. Fracture Mechanics, Vol. 8, No. 2, 1971, pp. 143.

189. Levy, N., "Application of the Finite Element Method to Large-Scale Elastic-Plastic Problems of Fracture Mechanics," Ph. D. Dissertation at Brown University, June 1970.

190. Rice, J. R., and Levy, N., "The Part-Through Surface Crack in an Elastic Plate," Technical Report NASA NGL 40-002-080/3, Division of Engineering, Brown University, September 1970, 28 pp.

191. Levy, N., Marcal, P. V., and Rice, J., "Progress in Three-Dimensional Elastic-Plastic Stress Analysis for Fracture Mechanics," Nuclear Engineering and Design, Vol. 17, No. 1, August 1971, pp. 64-75.

192. Director, S. W., "Automated Network Design: Principles and Techniques," Ph. D. Dissertation in Electrical Engineering, University of California, Berkeley, September, 1968, 266 pp.

193. Rohrer, R. A., "Fully Automated Network Design by Digital Computer: Preliminary Consideration," Proceedings, IEEE, Vol. 55, No. 11. November 1967, pp. 1929-1939.

194. Director, S. W., and Rohrer, R. A., "The Generalized Adjoint Network and Network Sensitivities," Trans. on Circuit Theory, IEEE, Vol. CT-16, No. 3. August 1969, pp. 318-323.

195. Director, S. W., and Rohrer, R. A., "Automated Network Design--The Frequency-Domain Case," Trans. on Circuit Theory, IEEE, Vol. CT-16, No. 3, August 1960, pp. 330-337.

196. Director, S. W., and Rohrer, R. A., "On the Design of Resistance n-Port Networks by Digital Computer," Trans. on Circuit Theory, Vol. CT-16, No. 3, August 1969, pp. 337-346.

APPENDIX I

ELEMENT STIFFNESS MATRICES

I (a) Isoparametric Quadrilateral Element with 4 to 8 Nodal Points [110]

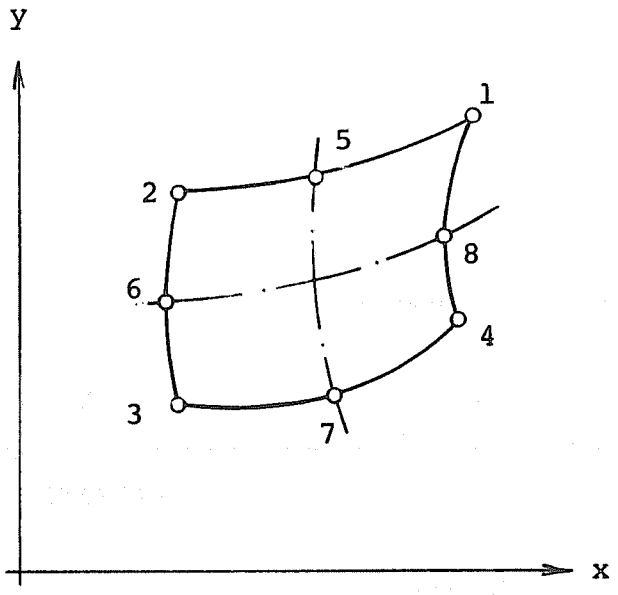

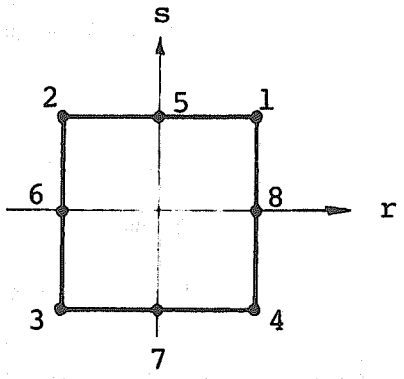

Node	r	s
1	+1	+1
2	-1	+1
3	-1	-1
4	+1	-1
5	0	+1
6	-1	0
7	0	-1
8	+1	0

1) Coordinate Interpolation Function: The natural coordinates r, s and the global coordinates x, y are related by

$$x(r, s) = \sum_{i=1}^{Q} h_i x_i$$

$$y(r, s) = \sum_{i=1}^{Q} h_i y_i \qquad \text{(A.1)}$$

where h_i are the interpolation functions, and Q is the number of nodal points ($4 \leq Q \leq 8$) describing the

quadrilateral element. Defining

$$R = 1 + r$$

$$S = 1 + s$$

$$\bar{R} = 1 - r$$

$$\bar{S} = 1 - s$$

$$R^* = 1 - r^2$$

$$S^* = 1 - s^2$$

the interpolation functions are given by

Q	4	5	6	7	8
h_1	$(1/4)\ RS$	$-(1/2)h_5$			$-(1/2)h_8$
h_2	$(1/4)\ \bar{R}S$	$-(1/2)h_5$	$-(1/2)h_6$		
h_3	$(1/4)\ \bar{R}\bar{S}$		$-(1/2)h_6$	$-(1/2)h_7$	
h_4	$(1/4)\ R\bar{S}$			$-(1/2)h_7$	$-(1/2)h_8$
h_5	$(1/2)\ R^*S$				
h_6	$(1/2)\ \bar{R}S^*$				
h_7	$(1/2)\ R^*\bar{S}$				
h_8	$(1/2)\ RS^*$				

(A.2)

Equation A.2 is written for a compete eight-node quadrilateral element. If fewer than eight nodes, but greater than or equal to four nodes are used to define the element, the corresponding interpolation function of the omitted node is deleted and the functions h_1 to h_4 are modified accordingly.

2) Displacement Functions: Denoting the components of the global displacement u_x and u_y in the x and y directions, respectively, the displacement functions also have the same interpolation functions as in the coordinate transformations

$$u_x(r, s) = \sum_{i=1}^{Q} h_i u_x^i$$

$$u_y(r, s) = \sum_{i=1}^{Q} h_i u_y^i \qquad (A.3)$$

where u_x^i and u_y^i are the global displacements at node i.

3) Strain Displacement Transformations: Let matrix B relate the strain components e to the nodal point displacements u

$$e(r, s) = B(r, s)\, u \qquad (A.4)$$

where

$$u^t = (u_x^i, u_y^i) \quad ; \quad i = 1, \ldots, Q$$

$$e^t = (e_{xx}, e_{yy}, e_{xy})$$

with

$$e_{xx}(r, s) = \sum_{i=1}^{Q} (\partial h_i/\partial x)\ u_x^i$$

$$e_{yy}(r, s) = \sum_{i=1}^{Q} (\partial h_i/\partial y)\ u_y^i$$

and

$$e_{xy}(r, s) = \frac{1}{2} \sum_{i=1}^{Q} (\partial h_i/\partial y)\ u_x^i + \frac{1}{2} \sum_{i=1}^{Q} (\partial h_i/\partial x)\ u_y^i$$

The linear strain displacement transformation matrix B can be expressed in the following form

$$B(r, s) = \begin{bmatrix} \partial H / \partial x \\ \partial H / \partial y \\ \partial H / \partial y \partial x \\ H^* \end{bmatrix} \qquad (A.5)$$

where

$$\partial H/\partial x = (\partial h_1/\partial x,\ 0,\ \partial h_2/\partial x,\ 0,\ \ldots,\ \partial h_Q / \partial x,\ 0)$$

$$\partial H/\partial y = (0,\ \partial h_1/\partial y,\ 0,\ \partial h_2/\partial y,\ \ldots,\ 0,\ \partial h_Q/\partial y)$$

$$\partial H/\partial y \partial x = (\partial h_1/\partial y,\ \partial h_1/\partial x,\ \partial h_2/\partial y,\ \partial h_2/\partial x\ \ldots\ \ldots,\ \partial h_Q/\partial y,\ \partial h_Q/\partial x)$$

$$H^* = (h_1/\bar{x},\ 0,\ h_2/\bar{x},\ 0,\ \ldots\ldots,\ h_Q/\bar{x},\ 0)$$

with

$$\bar{x}(r, s) = \sum_{i=1}^{Q} h_i x^i$$

Since the functions h_i are in terms of r and s, the chain rule is applied in order to compute the derivatives with respect to the global x-y coordinates.

$$\begin{bmatrix} \partial/\partial r \\ \partial/\partial s \end{bmatrix} = \begin{bmatrix} \partial x/\partial r & \partial y/\partial r \\ \partial x/\partial s & \partial y/\partial s \end{bmatrix} \begin{bmatrix} \partial/\partial x \\ \partial/\partial y \end{bmatrix} \tag{A.6}$$

Invert the Jacobian operator to obtain

$$\begin{bmatrix} \partial/\partial x \\ \partial/\partial y \end{bmatrix} = \frac{1}{J} \begin{bmatrix} \partial y/\partial s & -\partial y/\partial r \\ -\partial x/\partial s & \partial x/\partial r \end{bmatrix} \begin{bmatrix} \partial/\partial r \\ \partial/\partial s \end{bmatrix} \tag{A.7}$$

where J is the Jacobian determinant given by

$$J = (\partial x/\partial r)(\partial y/\partial s) - (\partial x/\partial s)(\partial y/\partial r) \tag{A.8}$$

From Eq. A.1, the derivatives of the global coordinates x and y with respect to the natural coordinates r and s can be evaluated by

$$\begin{aligned} \partial x/\partial r &= \sum_{i=1}^{Q} (\partial h_i/\partial r)\, x^i \\ \partial x/\partial s &= \sum_{i=1}^{Q} (\partial h_i/\partial x)\, x^i \\ \partial y/\partial r &= \sum_{i=1}^{Q} (\partial h_i/\partial r)\, y^i \\ \partial y/\partial s &= \sum_{i=1}^{Q} (\partial h_i/\partial s)\, y^i \end{aligned} \tag{A.9}$$

For any given values of r and s, the derivatives of the interpolation functions can now be evaluated, and then by using Eq. A.9, it is possible to compute the 2 x 2 Jacobian operator which transforms the derivatives from natural to global coordinates. The derivatives of the interpolation functions h_i with respect to global coordinates x and y can be calculated by Eq. A.7 to obtain the elements of the transformation matrix B in Eq. A.5.

4) Numerical Evaluation of Element Stiffness Matrix

For a two-dimensional body of thickness t, the element stiffness matrix k can be obtained by

$$k = \int_V B^t D B \, dv \qquad \text{(A.10)}$$

where D is the constitutive matrix and

$$\begin{aligned} dv &= t\, dx\, dy \quad \text{for plane stress} \\ dv &= dx\, dy \quad \text{for plane strain} \\ dv &= x\, dx\, dy \quad \text{for axisymmetric} \end{aligned} \qquad \text{(A.11)}$$

changing the variables of integration to r and s, and by using Eq. A.11, the element stiffness k can be written as

$$k = \int_{-1}^{1}\int_{-1}^{1} B^t(r, s) D(r, s) B(r, s) J(r, s) \eta \, dr \, ds \qquad \text{(A.12)}$$

where

for plane stress analysis $\eta = t$

for plane strain analysis $\eta = 1.0$

for axisymmetric analysis $\eta = \sum_{i=1}^{Q} h_i x^i$

The integral can be evaluated by using the two-dimensional Gauss integration formula

$$k = \sum_{j=1}^{N} \sum_{k=1}^{N} W_j W_k [B^t(r_j, s_k) D(r_j, s_k) B(r_j, s_k)] \eta(r_j, s_k) J(r_j, s_k) \tag{A.13}$$

where r_j, s_k are the natural coordinates of the integration point; W_j and W_k are the associated weights; and N is the order of integration.

I (b) Bar Element

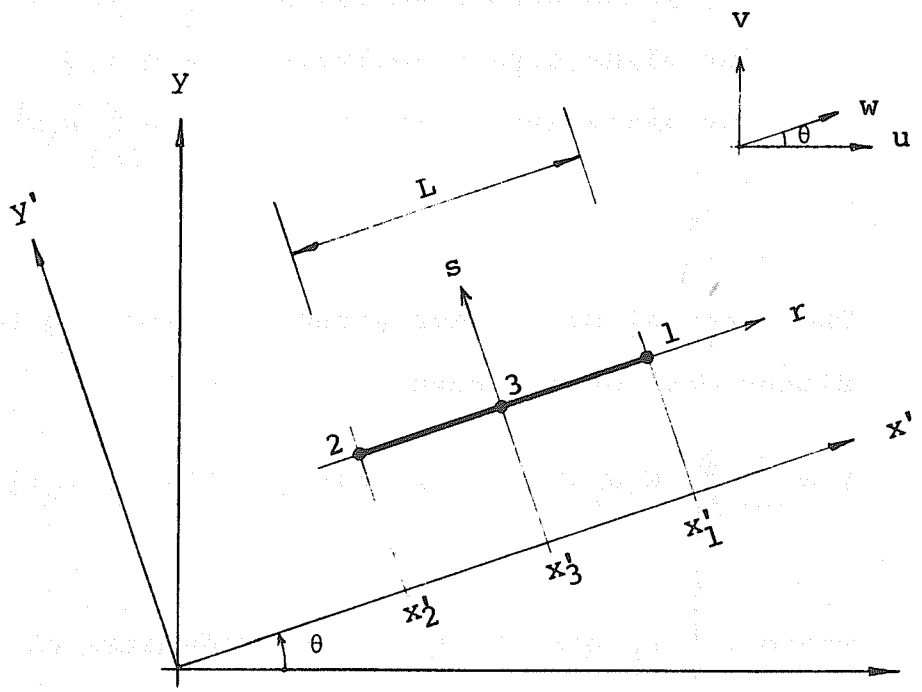

1) Shape Functions

$$h_1 = (1/2)(1 + r) - (1/2)(1 - r^2) = (r/2)(r + 1)$$

$$h_2 = (1/2)(1 - r) - (1/2)(1 - r^2) = (r/2)(r - 1)$$

$$h_3 = (1 - r^2)$$

$$(dh_1/dr) = r + 1/2 \qquad (B.1)$$

$$(dh_2/dr) = r - 1/2$$

$$(dh_3/dr) = -2r$$

2) Coordinate Interpolations

$$x'(r) = \sum_{i=1}^{Q} h_i \, x'_i \qquad (B.2)$$

3) Displacement Function

$$w(r) = \sum_{i=1}^{Q} h_i w^i \tag{B.3}$$

4) Strain Displacement Transformation

$$e'(r) = B'(r)\, w(r) \tag{B.4}$$

where

$$w^t(r) = (w_1, \ldots, w_Q)$$

$$e'(r) = (dw(r)/dx') = \sum_{i=1}^{Q} (dh_i/dx')w^i$$

Therefore, for Q = 3,

$$B'(r) = (dh_1/dx',\ dh_2/dx',\ dh_3/dx')$$

and

$$dx'/dr = [(dh_1/dr)x_1' + (dh_2/dr)x_2' + (dh_3/dr)x_3'] = J'(r) \tag{B.5}$$

Note that

$$dr/dx' = 1/J'(r)$$

also

$$dx' = J'(r)\, dr$$

$$dw(r)/dx' = (dw(r)/dr)\ (dr/dx') = dw(r)/J'(r)dr$$

Thus

$$B'(r) = (dh_1/dr,\ dh_2/dr,\ dh_3/dr)\ \frac{1}{J'(r)} \tag{B.6}$$

5) Element Stiffness in x'-y' Coordinate System

$$k' = \int_v (B')^t D (B') dv \qquad (B.7)$$

Since $D = E$

$dv = A\, dx'$

where E is the moldulus of elasticity, and A, the cross sectional area, the element stiffness becomes

$$k' = \int_{x_2}^{x_1} (B')^t E (B') A\, dx'$$

$$= \int_{-1}^{1} \begin{bmatrix} dh_1/dr \\ dh_2/dr \\ dh_3/dr \end{bmatrix} [dh_1/dr,\ dh_2/dr,\ dh_3/dr] [(AE/J(r))] dr \qquad (B.8)$$

The quantity J(r) can be evaluated as

$$J(r) = (r + 1/2)x_1' + (r - 1/2)x_2' - 2rx_3'$$

$$= r(x_1' + x_2' - 2x_3') + (1/2)(x_1' - x_2')$$

If $x_3 = (x_1' + x_2')/2$

then $J = (x_1' - x_2')/2 = \text{constant}$ (B.9)

and the element stiffness reduces to

$$k' = \int_{-1}^{1} \begin{bmatrix} r + 1/2 \\ r - 1/2 \\ -2r \end{bmatrix} [r + 1/2,\ r - 1/2,\ -2r][AE/J]\ dr$$

$$= \frac{2\ AE}{x_1' - x_2'} \begin{bmatrix} 7/6 & 1/6 & -4/3 \\ & 7/6 & -4/3 \\ \text{symm.} & & 8/3 \end{bmatrix} \qquad \text{(B.10)}$$

If the center node is omitted, it degenerates to

$$J = (x_1' - x_2')/2 = L/2$$

where L is the member length, and the element stiffness becomes the familiar

$$k' = \int_{-1}^{1} \begin{bmatrix} 1/2 \\ -1/2 \end{bmatrix} [1/2,\ -1/2]\ (2\ AE/L)\ dr$$

$$= \frac{AE}{L} \begin{bmatrix} 1 & -1 \\ -1 & 1 \end{bmatrix} \qquad \text{(B.11)}$$

6) <u>Transformation to Global x-y Coordinates</u>:

$$k = a^t\ k\ a \qquad \text{(B.12)}$$

in which a is given by

$$[a] = \begin{bmatrix} C & S & 0 & 0 & 0 & 0 \\ 0 & 0 & C & S & 0 & 0 \\ 0 & 0 & 0 & 0 & C & S \end{bmatrix}$$

where $C = \cos\theta$ and $S = \sin\theta$.

I (c) Link Element [9]

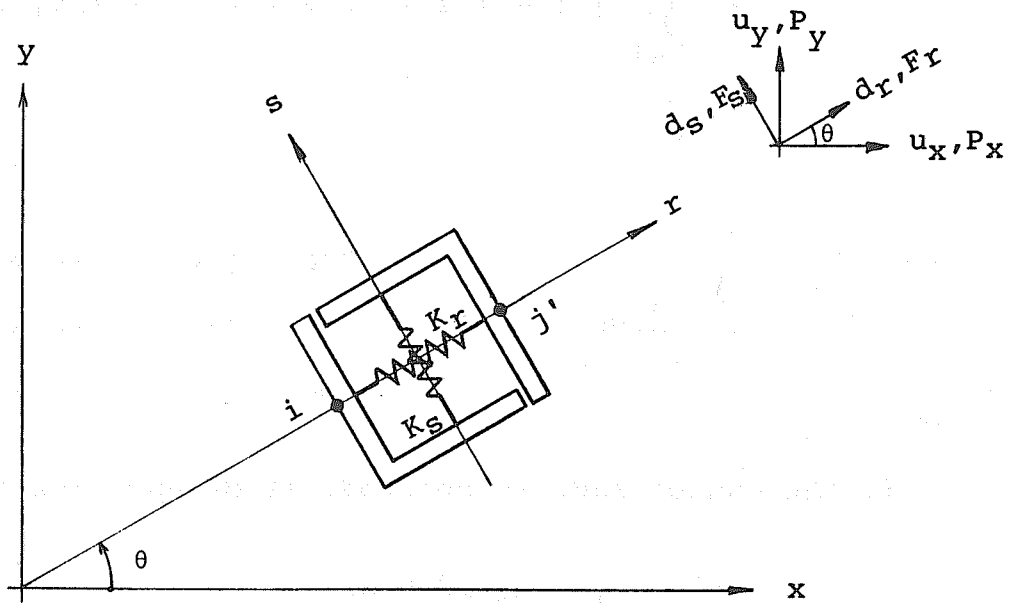

1) Forces and Displacements Relationship:

$$\begin{bmatrix} F_r \\ F_s \end{bmatrix} = \begin{bmatrix} K_r & 0 \\ 0 & K_s \end{bmatrix} \begin{bmatrix} d_r \\ d_s \end{bmatrix} \qquad (C.1)$$

or $F = \bar{k} d$

2) Displacement Transformation: Let

$C = \cos \theta$

$S = \sin \theta$

$$\begin{bmatrix} d_r \\ d_s \end{bmatrix} = \begin{bmatrix} -C & -S & C & S \\ S & -C & -S & C \end{bmatrix} \begin{bmatrix} u_{ix} \\ u_{iy} \\ u_{jx} \\ u_{jy} \end{bmatrix} \qquad (C.2)$$

or $d = a\,u$

3) Force Transformation:

$$\begin{bmatrix} P_{ix} \\ P_{iy} \\ P_{jx} \\ P_{jy} \end{bmatrix} = \begin{bmatrix} -C & S \\ -S & C \\ C & -S \\ S & C \end{bmatrix} \begin{bmatrix} F_r \\ F_s \end{bmatrix} \qquad (C.3)$$

or $P = a^t F$

4) Link Element Stiffness k : By substitution

$$P = a^t F$$
$$= a^t \bar{k}\, d$$
$$= a^t \bar{k}\, a\, u$$

it can be seen that

$$k = a^t \bar{k}\, a \qquad (C.4)$$

which can be expanded to obtain

$$k = \begin{bmatrix} K_r C^2 + K_s S^2 & K_r SC - K_s SC & -K_r C^2 - K_s S^2 & -K_r SC + K_s SC \\ & K_r S^2 + K_s C^2 & -K_r SC + K_s SC & -K_r S^2 - K_s C^2 \\ & & K_r C^2 + K_s S^2 & K_r SC - K_s SC \\ & \text{symm.} & & K_r S^2 + K_s C^2 \end{bmatrix}$$

(C.5)

I (d) Bond Element

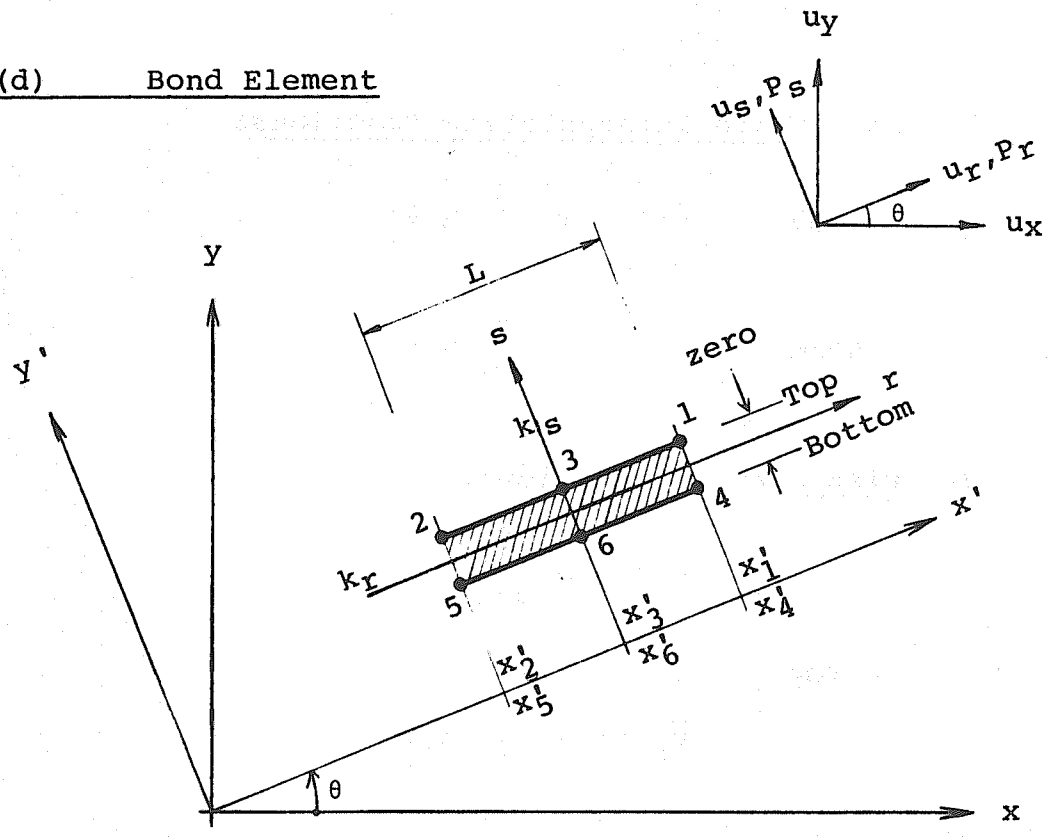

1) Shape Functions:

$$h_1 = (1 + r)/2 - (1 - r^2)/2 = (r^2 + r)/2$$

Top $$h_2 = (1 - r)/2 - (1 - r^2)/2 = (r^2 - r)/2$$

$$h_3 = (1 - r^2) \qquad \text{(D.1)}$$

$$h_4 = (1 + r)/2 - (1 - r^2)/2 = (r^2 + r)/2$$

Bottom $$h_5 = (1 - r)/2 - (1 - r^2)/2 = (r^2 + r)/2$$

$$h_6 = (1 - r^2)$$

2) Coordinate Interpolation Functions:

$$\text{Top} \qquad \bar{x}'(r) = \sum_{i=1}^{3} h_i \bar{x}'_i$$

$$\text{Bottom} \qquad \underline{x}'(r) = \sum_{i=4}^{6} h_i \underline{x}'_i \qquad \text{(D.2)}$$

3) Displacement Functions:

$$\bar{u}_r(r) = \sum_{i=1}^{3} h_i \bar{u}_r^i$$

Top

$$\bar{u}_s(r) = \sum_{i=1}^{3} h_i \bar{u}_s^i$$

$$\underline{u}_r(r) = \sum_{i=4}^{6} h_i \underline{u}_r^i \qquad \text{(D.3)}$$

Bottom

$$\underline{u}_s(r) = \sum_{i=4}^{6} h_i \underline{u}_s^i$$

4) Force and Displacement Relationship:

$$P_r(r) = k_r \, w_r(r)$$

$$P_s(r) = k_s \, w_s(r) \qquad \text{(D.4)}$$

where $$w_r(r) = \bar{u}_r(r) - \underline{u}_r(r)$$

$$= \sum_{i=1}^{3} h_i \bar{u}_r^i - \sum_{i=4}^{6} h_i \underline{u}_r^i$$

and $$w_s(r) = \bar{u}_s(r) - \underline{u}_s(r)$$

$$= \sum_{i=1}^{3} h_i \bar{u}_s^i - \sum_{i=4}^{6} h_i \underline{u}_s^i$$

5) Equivalent Nodal Forces:

Virtual Displacements $$\partial u = \sum_{i}^{Q} h_i \, \partial u^i$$

External Virtual Work $$W_e = [\partial u^i]^t F^i$$

Internal Virtual Work $$W_I = [\partial u]^t P$$

$$= [\sum_{i}^{Q} h_i \, \partial u^i]^t k_o w$$

$$W_e = W_I$$

$$[\partial u^i]^t F^i = \int_v [\sum_{i}^{Q} h_i \, \partial u^i]^t k_o w \, dv$$

$$F^i = \int_{x_2'}^{x_1'} k_o [\sum_{i}^{Q} h_i]^t w \, dx'$$

$$= \int_{x_2'}^{x_1'} k_o [\sum_{i}^{Q} h_i]^t [\sum_{i}^{QT} h_i - \sum_{i}^{QB} h_i] \, dx' \begin{bmatrix} \bar{u}_i \\ \underline{u}_i \end{bmatrix}$$

where k_o, QT, QB are the generalized stiffness, number of nodal points at top, and number of nodal points at bottom, respectively.

6) Element Stiffness k' in Local Coordinates: Note that

$$\text{Top} \quad \begin{bmatrix} \bar{F}_r^i \\ \bar{F}_s^i \end{bmatrix} = - \begin{bmatrix} F_r^i \\ F_s^i \end{bmatrix} \text{ Bottom}$$

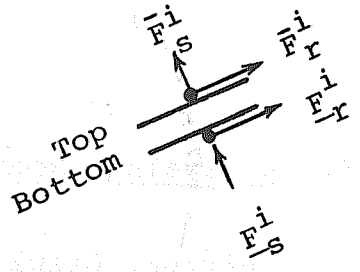

Consider the top edge (2-3-1)

$$W_e = [\partial \bar{u}_r^i]^t \, \bar{F}_r^i = [\partial \bar{u}_r^i]^t \begin{bmatrix} \bar{F}_r^1 \\ \bar{F}_r^2 \\ \bar{F}_r^3 \end{bmatrix}$$

$$\begin{bmatrix} \bar{u}^i \\ \underline{u}^i \end{bmatrix}^t = (\, u_r^1 \; u_r^2 \; u_r^3 \; u_r^4 \; u_r^5 \; u_r^6 \,)$$

$$\bar{P}_r(r) = k_r \, \bar{w}_r(r)$$

$$= k_r [\sum_{i=1}^{3} h_i \bar{u}_r^i - \sum_{i=4}^{6} h_i \underline{u}_r^i]$$

$$\doteq k_r \, (\, h_1 \; h_2 \; h_3 \; -h_4 \; -h_5 \; -h_6 \,) \begin{bmatrix} u_r^1 \\ u_r^2 \\ u_r^3 \\ u_r^4 \\ u_r^5 \\ u_r^6 \end{bmatrix}$$

$$W_I = \int_V [\partial \bar{u}_r]^t \, \bar{P}_r(r) \, dv = \int_V [\sum_{i=1}^{3} h_i \partial \bar{u}_r^i]^t \, pdv$$

or

$$W_I = [\partial \bar{u}_r^i]\ k_r \underbrace{\int_{x_2'}^{x_1'} \begin{bmatrix} h_1 \\ h_2 \\ h_3 \end{bmatrix} (h_1\ h_2\ h_3\ -h_4\ -h_5\ -h_6)\,dx'}_{[\bar{H}_r]} \begin{bmatrix} u_r^1 \\ u_r^2 \\ u_r^3 \\ u_r^4 \\ u_r^5 \\ u_r^6 \end{bmatrix}$$

Define $\bar{J}(r) = dx'/dr$

$$= (dh_1/dr)x_1' + (dh_2/dr)x_2' + (dh_3/dr)x_3'$$

$$= (r + 1/2)x_1' + (r - 1/2)x_2' - (2r)x_3'$$

$$= r(x_1' + x_2' - 2x_3') + (x_1' - x_2')/2$$

If $x_3' = (x_1' + x_2')/2$

Then $\bar{J} = (x_1' - x_2')/2 = L/2$

Similarly $\underline{J} = (x_4' - x_5') = L/2$

$$[\bar{F}_r^i] = k_r \underbrace{\int_{-1}^{1} [\bar{H}_r]\,\bar{J}\,dr}_{\bar{k}_r'} [u_r^i]$$

By the same procedure, it can be shown that

$$\bar{F}_s^i = k_s \int_{-1}^{1} [\bar{H}_s]\ \bar{J}\,dr\ u_s^i = \bar{k}_s'\ u_s^i$$

$$\underline{F}_r^i = k_r \int_{-1}^{1} [\ \underline{H}_r\ ]\ \underline{J}\ dr\ u_r^i = \underline{k}_r'\ u_r^i$$

$$\underline{F}_s^i = k_s \int_{-1}^{1} [\ \underline{H}_s\ ]\ \underline{J}\ dr\ u_s^i = \underline{k}_s'\ u_s^i$$

Note that $[\ \bar{H}_r\ ] = [\ \bar{H}_s\ ] = -[\ \underline{H}_r\ ] = -[\ \underline{H}_s\ ]$

Denote $[\ \bar{H}_r\ ] = [\ H\ ]$; $-[\ \underline{H}_r\ ] = -[\ H\ ]$

Therefore, the element stiffness k' can be written as

$$k' = \begin{bmatrix} \bar{k}_r' & 0 \\ 0 & \bar{k}_s' \\ \underline{k}_r' & 0 \\ 0 & \underline{k}_s' \end{bmatrix} = \int_{-1}^{1} \begin{bmatrix} k_r H & 0 \\ 0 & k_s H \\ -k_r H & 0 \\ 0 & -k_s H \end{bmatrix} (L/2)\,dr \qquad (D.6)$$

with

$$\int_{-1}^{1} H dr = \int_{-1}^{1} \begin{bmatrix} h_1h_1 & h_1h_2 & h_1h_3 & -h_1h_4 & -h_1h_5 & -h_1h_6 \\ h_2h_1 & h_2h_2 & h_2h_3 & -h_2h_4 & -h_2h_5 & -h_2h_6 \\ h_3h_1 & h_3h_2 & h_3h_3 & -h_3h_4 & -h_3h_5 & -h_3h_6 \end{bmatrix} dr$$

Recall that $h_1 = h_4$; $h_2 = h_5$; $h_3 = h_6$.

Only the following integration need be carried out.

$$\int_{-1}^{1} h_1h_1\ dr = \int_{-1}^{1} h_4h_4\ dr$$

$$= \int_{-1}^{1} [\ (r^2 + r)/2\ ]^2\ dr = 4/15$$

$$\int_{-1}^{1} h_1 h_2\ dr = \int_{-1}^{1} h_4 h_5\ dr$$

$$= \int_{-1}^{1} [\ (r^2 + r)(r^2 - r)/4\ ]\ dr = -1/15$$

$$\int_{-1}^{1} h_1 h_3\ dr = \int_{-1}^{1} h_4 h_6\ dr$$

$$= \int_{-1}^{1} [\ (r^2 + r)(1 - r^2)/2\ ]\ dr = 2/15$$

$$\int_{-1}^{1} h_2 h_2\ dr = \int_{-1}^{1} h_5 h_5\ dr$$

$$= \int_{-1}^{1} [\ (r^2 - r)/2\ ]^2\ dr = 4/15$$

$$\int_{-1}^{1} h_2 h_3\ dr = \int_{-1}^{1} h_5 h_6\ dr$$

$$= \int_{-1}^{1} [\ (r^2 - r)(1 - r^2)/2\ ]\ dr = 2/15$$

$$\int_{-1}^{1} h_3 h_3 \, dr = \int_{-1}^{1} h_6 h_6 \, dr$$

$$= \int_{-1}^{1} (1 - r^2)^2 \, dr = 16/15$$

Thus the element stiffness in matrix form is

$$k' = \frac{L}{2(15)} \begin{bmatrix}
4k_r & 0 & -k_r & 0 & 2k_r & 0 & -4k_r & 0 & k_r & 0 & -2k_r & 0 \\
 & 4k_s & 0 & -k_s & 0 & 2k_s & 0 & -4k_s & 0 & k_s & 0 & -2k_s \\
 & & 4k_r & 0 & 2k_r & 0 & k_r & 0 & -4k_r & 0 & -2k_r & 0 \\
 & & & 4k_s & 0 & 2k_s & 0 & k_s & 0 & -4k_s & 0 & -2k_s \\
 & & & & 16k_r & 0 & -2k_r & 0 & -2k_r & 0 & -16k_r & 0 \\
 & & & & & 16k_s & 0 & -2k_s & 0 & -2k_s & 0 & -16k_s \\
 & & & & & & 4k_r & 0 & -k_r & 0 & 2k_r & 0 \\
 & & & \text{symm.} & & & & 4k_s & 0 & -k_s & 0 & 2k_s \\
 & & & & & & & & 4k_r & 0 & 2k_r & 0 \\
 & & & & & & & & & 4k_s & 0 & 2k_s \\
 & & & & & & & & & & 16k_r & 0 \\
 & & & & & & & & & & & 16k_s
\end{bmatrix}$$

(D.7)

If the center nodes are eliminated, it degenerates to the element of Goodman, Taylor and Brekke [111].

$$J = (x_1' - x_2')/2 = L/2$$

$$\int_{-1}^{1} h_1 h_1 \, dr = \int_{-1}^{1} h_4 h_4 \, dr$$

$$= \int_{-1}^{1} [\ (1 + r)/2\ ]^2 \, dr = 2/3$$

$$\int_{-1}^{1} h_1 h_2 \, dr = \int_{-1}^{1} h_4 h_5 \, dr$$

$$= \int_{-1}^{1} [\ (1 + r)(1 - r)/4\ ] \, dr = 1/3$$

$$\int_{-1}^{1} h_2 h_2 \, dr = \int_{-1}^{1} h_5 h_5 \, dr$$

$$= \int_{-1}^{1} [\ (1 - r)/2\ ]^2 \, dr = 2/3$$

$$k' = \frac{L}{2(3)} \begin{bmatrix} 2k_r & 0 & k_r & 0 & -2k_r & 0 & -k_r & 0 \\ & 2k_s & 0 & k_s & 0 & -2k_s & 0 & -k_s \\ & & 2k_r & 0 & -k_r & 0 & -2k_r & 0 \\ & & & 2k_s & 0 & -k_s & 0 & -k_s \\ & & & & 2k_r & 0 & k_r & 0 \\ & & \text{symm.} & & & 2k_s & 0 & k_s \\ & & & & & & 2k_r & 0 \\ & & & & & & & 2k_s \end{bmatrix} \qquad (D.8)$$

7) Transformation to Global x-y Coordinates: Let

$$C = \cos\theta$$

$$S = \sin\theta$$

$$a' = \begin{bmatrix} C & S \\ -S & C \end{bmatrix}$$

$$[a] = \begin{bmatrix} a' & & & & & & & \\ & a' & & & & & & \\ & & a' & & & & & \\ & & & a' & & & & \\ & & & & a' & & & \\ & & & & & a' & & \\ & & & & & & a' & \\ & & & & & & & a' \end{bmatrix} \qquad (D.9)$$

Then the global stiffness k is simply obtained by

$$k = a^t k' a \qquad (D.10)$$

APPENDIX II

General Structure of the Computer

Program NTAFEA

II (a) Program Macro-Flow-Chart

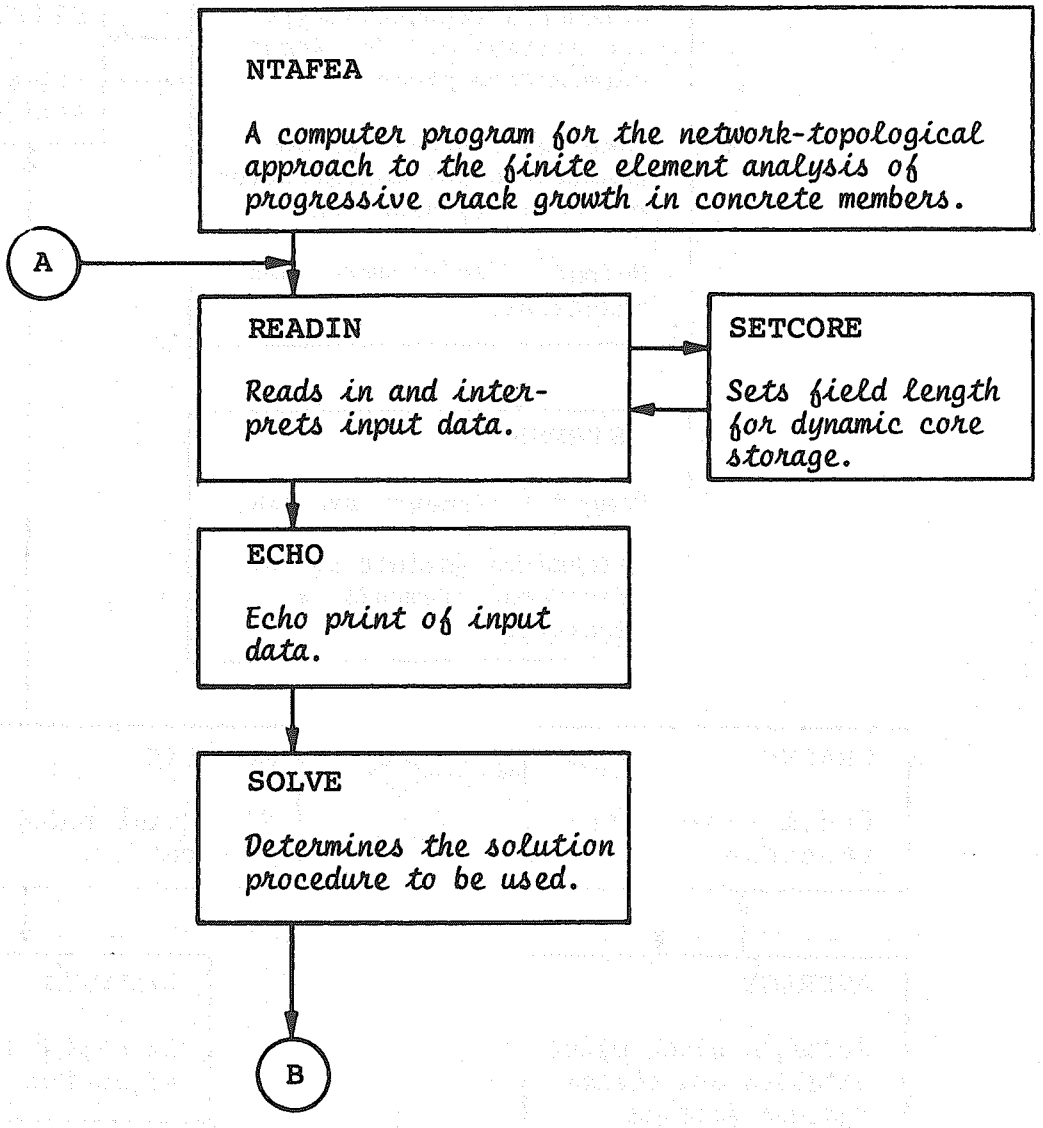

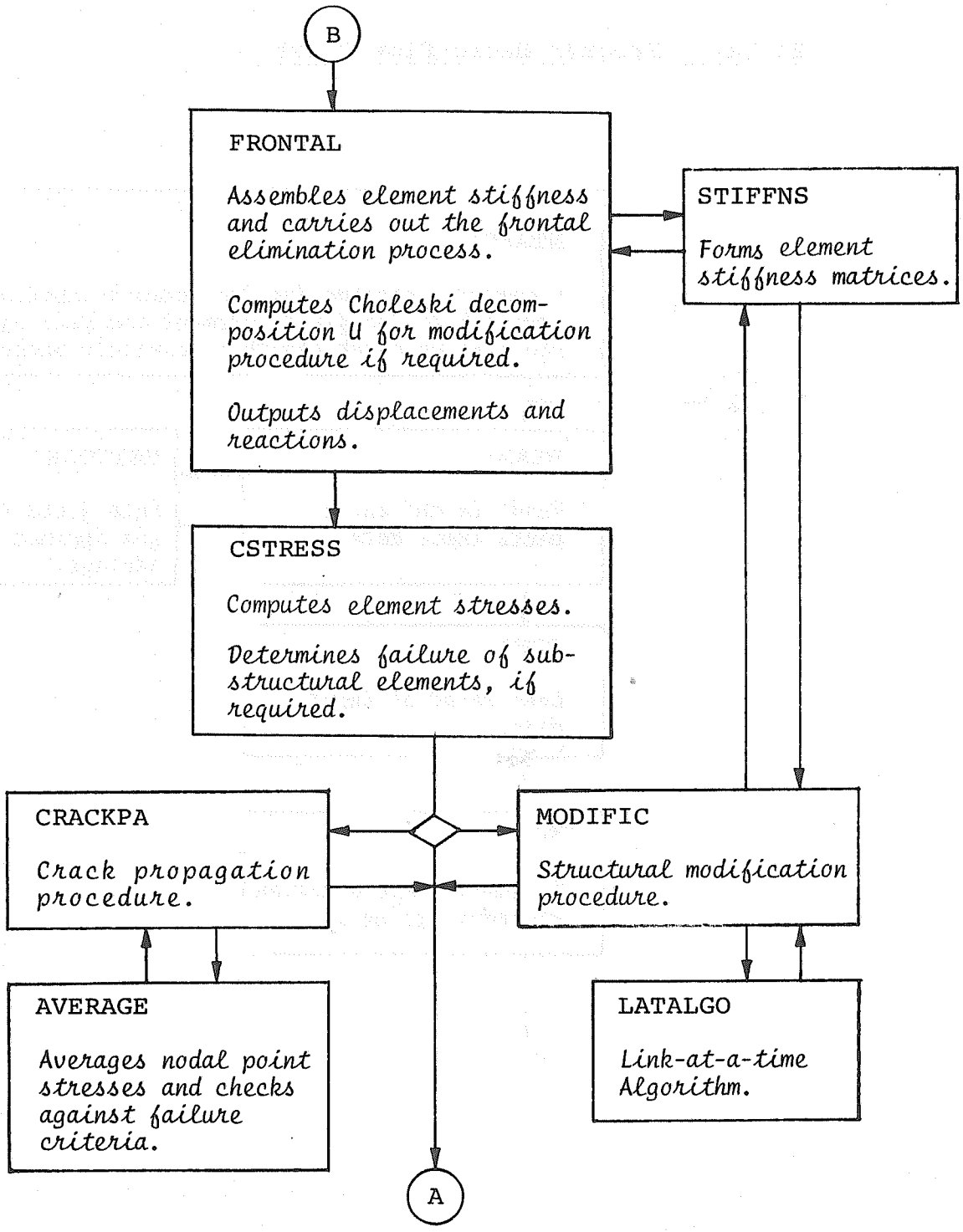
B
FRONTAL
Assembles element stiffness and carries out the frontal elimination process.
Computes Choleski decomposition U for modification procedure if required.
Outputs displacements and reactions.
STIFFNS
Forms element stiffness matrices.
CSTRESS
Computes element stresses.
Determines failure of substructural elements, if required.
CRACKPA
Crack propagation procedure.
MODIFIC
Structural modification procedure.
AVERAGE
Averages nodal point stresses and checks against failure criteria.
LATALGO
Link-at-a-time Algorithm.
A

APPENDIX III

Computer Program Input Description

III (a) General Remarks

1) The input to the computer program is basically format-free. However, for the purpose of minimizing the effort in decoding the BCD (Binary Coded Digit) and in searching for next START or STOP card, the following two restrictions are imposed:
   a) The START and STOP cards must begin at column 1.
   b) Data of coordinates, structural elements, loading conditions and boundary conditions are read in with a format either supplied by the user or by default.
2) Each word must be separated by one or more blank spaces or by a comma.
3) Blank spaces are generally ignored except within a pair of quotation marks or parentheses.
4) Any character appearing after a "/" mark is treated as comment and will not be processed by the program.
5) The program examines only the first four characters of each word. Therefore, any word which is longer than four characters can be abbreviated.
6) Each input command can continue onto a second card. A comma at the end of a string of characters on the first card will serve as a continuation mark.
7) In case of input via teletype, an equal sign at the end of a string of characters will delete the whole

string. Other input editing features follow the rules of the Remote Terminal System.

8) Execution MODE cards can be inserted anywhere within the input sequence as long as each is followed by a command card with the "$" sign.

9) The following abbreviations are reserved words:

E	*Young's Modulus*
NU	*Poisson's Ratio*
UC	*Ultimate Compressive Strength*
UT	*Ultimate Tensile Strength*
KH	*Horizontal Spring Constant*
KV	*Vertical Spring Constant*
UHC	*Ultimate Horizontal Compressive Strength*
UHT	*Ultimate Horizontal Tensile Strength*
UVC	*Ultimate Vertical Compressive Strength*
UVT	*Ultimate Vertical Tensile Strength*
MAX.	*Maximum*

10) The sequence of input is rather flexible. However, it is advisable to follow the general sequence as stipulated in the next section.

III (b) Input Commands

1) START

Signifies the start of a new problem. It must begin at column 1 and is required for every problem. ($ START is also an acceptable command, but not advisable.)

2) $ PROBLEM TITLE " *Title* "

Any acceptable FROTRAN *characters can be used as title to identify each given problem. Up to 130 characters can be enclosed within the quotation marks.*

3) $ NORMAL MODE

Normal execution mode. The program automatically assumes a normal mode if no other mode is specified.

4) $ CHECK MODE

Key parameters in the program execution will be ouput for spot checks.

5) $ DEBUG CODE

More extensive intermediate results will be output for debugging purposes.

6) $ PANIC MODE

Causes a dump of the active core at each step of computation. It is extremely time-consuming and the output is voluminous. Therefore, this mode is recommended only for very small problems.

7) $ PUNCH MODE

Causes the resulting changes in element and

nodal point data to be punched on cards which can be used as input when execution resumes.

8) $ UNPUNCH MODE

Turns off the punch mode. The program automatically assumes the unpunch mode unless a punch mode is specified.

9) $ MAXIMUM FIELD LENGTHS

Defines the field lengths for the dynamic core storage. It must be input for every problem. However, any one or all of the following input cards may be omitted, and the corresponding field length will be defined by default. The parameter n is an integer.

MAX. DIMENSION OF COORDINATES = 2	*Preset value*
MAX. DEGREES OF FREEDOM PER NODE = 2	*Preset value*
MAX. NODE NUMBERS = n	*Default = 384*
MAX. ELEMENT NUMBERS = n	*Default = 192*
MAX. MATERIAL TYPES = n	*Default = 4*
MAX. ELEMENT TYPES = n	*Default = 4*
MAX. NODES PER ELEMENT = n	*Default = 8*
MAX. DISPLACEMENT BOUNDARY POINTS = n	*Default = 32*
MAX. LOADED NODAL POINTS = n	*Default = 32*
MAX. FRONTAL SIZE = n	*Default = 32*
MAX. BUFFER SIZE = n	*Default = 1664*

10) $ ELEMENT TYPE $i = m_i$

Parameter i is the integer identifying the element type, and m_i can be one of

the following elements:

m_i { BAR, BOND, LINK, PLANE STRESS, PLANE STRAIN, AXISYMMETRIC }

11) $ MATERIAL TYPE i = m_i e_i = v_i

Parameter i is the interger identifying the material type, and m_i can be one of the materials listed below. Input the material constants e_i and their values v_i as many as required to define the material. Compressive strenth is indicated by a minus (-) sign.

m_i	e_i					
CONCRETE	E	NU	UC	UT		
STEEL	E	NU	UC	UT		
BAR	E	UC	UT			
BOND	KH	KV	UHC	UHT	UVC	UVT
LINK	KH	KV	UHC	UHT	UVC	UVT

Example: $ MATERIAL TYPE 1 = CONCRETE E = 3000000,
NU = 0.2 UCT = -3000 UT = 300

12) $ NODAL POINT COORDINATES "(*Input Format*)"

After this card, supply nodal point number, x-coordinate, y-coordinate, in that order, according to the input format specified. If the input format is omitted, the program will assume a standard format of (I5, 5X, 3F10.0).

b *A blank card to end reading of this group.*

13) $ STRUCTURAL ELEMENT DATA "(*Input Format*)"

After this card, supply the structural element data according to the input format specified, in the following order:

Element number
Element type number
Material type number
Index for crack exclusion: 1=yes; 0=no
Index for substructure: 1=yes; 0=no
Number of nodal points (max. 8)
Node I
Node J
Node K
Node L
Node M
Node N
Node O
Node P
Bar Area or Angle of link element
Pretensioned stress

If no input format is specified, the program will assume a format of (I5, 4I3, 8I5, 2F10.3)

b *A blank card to end reading of this group.*

14) $ DISPLACEMENT BOUNDARY CONDITIONS "(*Input Format*)"

After this card, supply the imposed displacement boundary conditions according to the format specified, in the following order:

Nodal point number
Known x-displacement
Known y-displacement

Known displacements are read in as alphanumeric numbers. If there is an unknown displacement in any directions, leave the space blank. If no input format is specified, the program will assume a format of (I5, 5X, 3A10).

b *A blank card to end reading of this group.*

15) $ LOADING CONDITIONS "(*Input Format*)"

After this card, supply the nodal point loads according to the format specified, in the following order:

Nodal point number
Load in x-direction
Load in y-direction

If no input format is specified, the program will assume a format of (I5, 5X, 3F10.0)

b — *A blank card to end reading of this group.*

16) $ NUMBER OF STEPS = *n*

Integer n is the number of steps in crack growth, modification or iteration.

17) $ ECHO PRINT ONLY

Causes input data to be printed out for checking purpose.

18) $ SOLVE WITH FRONTAL PROCEDURE

To obtain a solution with the frontal technique.

19) $ SOLVE WITH CRACK GROWTH PROCEDURE

To obtain a crack pattern under the given loading condition.

20) $ SOLVE WITH MODIFICATION PROCEDURE

To perform structural modification and re-analysis by the Link-at-a-Time Algorithm. Supply the following cards to define the modification process:

STAGE *i* NUMBER OF NODES INVOLVED = *n*

Parameter i is the integer identifying the stage of modification, and integer n is

the number of nodes involved in this stage of modification. This card is required for every stage of modification.

ADD NODES "(*Input Format*)"

After this card, supply the coordinates of the added nodes, same as (12). The program will assume the prevailing format defined previously either by input or by default, if no input format is specified here. Omit this card if no new nodes are to be added.

b *A blank card to end reading of this group.*

ADD ELEMENTS "(*Input Format*)"

After this card, supply the structural element data, same as (13). The program will assume the prevailing format defined previously either by input or by default, if no input format is specified here. Omit this card if no new elements are to be added.

b *A blank card to end reading of this group.*

DELETE ELEMENTS "(*Input Format*)"

After this card, supply the element number to be deleted. However, the input format should be consistant with other structural element data, i.e., the input format should be for all the items listed in (13).

b *A blank card to end reading of this group.*

21) STOP

Signifies the end of program execution. It must begin at column 1, and may appear only once at the very end of the input sequence. ($ STOP *is also an acceptable command, but not advisable.)*